UNIVERSITAT DE BARCELONA

Controls on the development of sedimentary sequences in continental basins

Examples from the Cenozoic of Iberia

Luis Valero Montesa

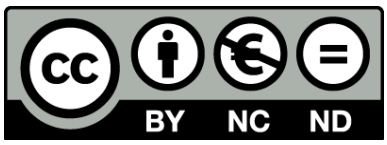

Controls on the development of sedimentary sequences in continental basins

Examples from the Cenozoic of Iberia

Departament d'Estratigrafia, Paleontologia i Geociències Marines
Universitat de Barcelona
Grup de Recerca de Geodinàmica i Anàlisi de Conques
Institut de Recerca Geomodels

Luis Valero Montesa
Memòria de Tesi Doctoral
Novembre, 2015

Departament d'Estratigrafia, Paleontologia i Geociències Marines
Universitat de Barcelona
Grup de Recerca de Geodinàmica i Anàlisi de Conques
Institut de Recerca Geomodels

Controls on the development of sedimentary sequences in continental basins. Examples from the Cenozoic of Iberia.

Memòria de Tesi Doctoral presentada per **Luis Valero Montesa**
per optar al grau de Doctor en Ciències Geològiques per la Universitat de Barcelona.
Aquesta memòria ha estat realitzada dintre del
Programa de Doctorat de "Ciències de la Terra" (RD99/2011) sota la direcció de
Dr. Miguel Garcés Crespo i el Dr. **Lluís Cabrera Pérez**

Luis Valero Montesa
Barcelona, Novembre de 2015

Dr. Miguel Garcés

Dr. Lluís Cabrera

This PhD thesis has been carried out in the *Department of Stratigraphy, Paleontology and Marine Geosciences*, the *Institute de Recerca Geomodels*, and the *Grup de Recerca de Geodinàmica i Anàlisi de Conques*. Financial support was provided by a grant *Ajuts al Personal Investigador en Formació* from the Universitat de Barcelona. (APIF-2010-2011). Paleomagnetic measurements were made in the Paleomagnetic Laboratory of Barcelona (CCiTUB-IT-JA-CSIC) and in the Paleomagnetic Laboratory Fort Hoofdijk (Utrecht).

Contents

Prologo (Preface)

Permitidme un inciso geológico para los profanos de lo que viene luego, de lo que no van a entender casi nada. Permitidme los otros algunas licencias técnicas, que luego (espero) estén resueltas en la memoria.

La estratigrafía, que es lo que yo hago, analiza los estratos que grano a grano se acumulan en las cuencas sedimentarias. En ellos se pueden archivar los cambios ambientales que modificaron las dinámicas sedimentarias. Cada estrato conforma una página, que al juntarse con otras tejen capítulos de la historia de la Tierra. En los sedimentos que conforman los estratos también pueden grabarse los cambios del campo magnético de la Tierra, por ejemplo sus inversiones. Sí, la dirección del campo magnético cambia. En esta tesis hemos cazado algunas de estas inversiones magnéticas, y puesto que sabemos cuándo se produjeron, hemos podido datar las rocas. Para mí, este es el primer hecho fascinante de mi investigación. Y todo empieza a causa de que los electrones se dispongan de una determinada manera en uno de los orbitales del átomo de hierro, hecho que desemboca en intensificar el magnetismo de una roca. Para rizar el rizo, al sedimentarse granos microscópicos de óxidos (de hierro principalmente) estos quedan orientados apuntando al Norte (o al Sur) de la Tierra como antiguas brújulas en las que su aguja del Norte se quedó encallada. Me sigue sorprendiendo, y es por lo que vale la pena el trabajo de laboratorio, ver como después de ir calentando muestras, y corregir su posición, al final la dirección obtenida indica Norte o Sur.

Con estas dataciones se pueden hacer muchas cosas. Por ejemplo calcular tasas de sedimentación, que explican el ritmo al que se depositan los sedimentos. Después de hacer esto, hemos visto que existe una relación entre las tasas y la arquitectura de los diferentes tipos de rocas sedimentarias.

También, en las rocas, pueden grabarse los cambios en la insolación que recibe la Tierra dependiendo lo lejos que este del Sol y la duración de las estaciones, ya que estos cambios producen variaciones en el clima que modifican los sedimentos que se van acumulando en las cuencas. Los movimientos complejos de los planetas, fuerzan a este *punto azul pálido* y a los otros planetas a dibujar órbitas caóticas, aunque más o menos predecibles. Y en parte de esto también trata esta tesis. En particular, nos hemos fijado en un ciclo que afecta a la excentricidad (cuán circular es) de la órbita de la Tierra cada 405 mil años (más o menos). Si vamos más allá, descubrimos que los causantes son Venus y Júpiter, quienes por su posición, tiran de la órbita de la Tierra haciéndola más o menos circular según pasa el tiempo. Y aunque no quiero extenderme, que la formación de calizas en lagos antiguos en los que hoy son los Monegros y el resto de la cuenca del Ebro, o la formación de carbón en unas minas en Galicia sea consecuencia de unas condiciones particulares de las orbitas de Venus y de Júpiter me sigue asombrando.

Solemos decir que en el pasado están las claves del futuro. Pero ha de notarse que esta historia tiene una métrica, la de los ciclos orbitales. Hoy en día, vivimos tiempos fascinantes para las geociencias porque nunca antes se supo tanto, ni hubo instrumentos tan precisos. Hay que aprovechar el tirón, cabalgar a hombros de gigantes, aguantar las embestidas y no deshacer lo hecho como si fuera sal en el océano.

Agradecimientos

Una tesis también puede plantearse como un proceso psicológico, en el que casi todos los doctorandos pasamos por las mismas fases. Es por eso, supongo, que en la etapa inicial uno se vuelve pesado por la ilusión, y en la etapa final simplemente insoportable. Mis agradecimientos sinceros a aquellos que más han aguantado mi etapa marrón. Ahora que acabo, y escribo al final el principio, me doy cuenta de la cantidad de gente que ha contribuido, activamente, pasivamente o meramente sin estorbar. Una tesis no se hace sola y por (mucha) suerte a mí me han ayudado directa o indirectamente muchas personas. Un lugar de honor es para los aquellos de los que me olvido más abajo y que merecerías estar aquí, a vosotros mi más sinceras gracias.

En segundo lugar a Miguel Garcés, mi director. Con su paciencia infinita y permitirme esa "libertad bajo control", ha ido moldeándome e instruyéndome en el oficio del paleomagnetismo, de la ciencia, y en el de ser mejor persona. Quedan lejos ahora (ocho años) los tiempos del trabajo de Fin de Licenciatura, en que empecé a aprender de verdad. Esta tesis sublima parte de este aprendizaje, y es, en mucha parte, obra suya.

A Lluís Cabrera, de quien llevo también muchos años aprendiendo, aunque aún me falten algunas clases de moderación y prudencia, claves para la sabia gestión. A pesar de su trabajo como decano, ha sabido contribuir en aspectos técnicos, así como solventar rápida y eficazmente los problemas que han ido surgiendo a lo largo de la tesis.

A Alberto Sáez codirector en la sombra, siempre disparando consejos útiles, y expresando con claridad (y sagacidad) sus pensamientos.

También a los distintos profesores que he ido teniendo a lo largo de mi educación, no pondré nombres (excepto el de Justo Jiménez) pero es obra de todos y cada uno. Gracias a los profes de Estratigrafía del departamento, con los que siempre he tenido un trato cordial y de los que, indirectamente, también contribuyeron en esta tesis: Pere Busquets, Ferran Colombo, Mariano Marzo, Emilio Ramos, Miguel López, Pau Arbués y Patricia Cabello.

A Pedro Huerta, del que he aprendido muchísimo, y que fue (co)director en Almazán. Le agradezco todo su trabajo y su paciencia. También las estancias en Ávila, con Bego y Pablo. Y también a Ildefonso Armenteros de la Universidad de Salamanca, porque el trabajo de Almazán en parte también es suyo. Y a los gemelos mecánicos de Serón de Nágima, que en un lluvioso domingo después de comer arreglaron el descalabrado diferencial de la furgoneta con golpes certeros.

A las magnetonenas y en especial a Elisenda Costa y a Bet Beamud. Elisenda fue mi rompehielos al principio y buena guía siempre, el faro de un puerto que a saber dónde me llevará. Y Bet siempre me ha ayudado, en el laboratorio, en el campo y en la redacción de artículos. Siempre dispuesta a echar una mano con paciencia y buena cara. También tengo gratitud a a Miriam Gómez por las jornadas de campo de Almazán, a Ylenia Almar y también a Ana.

A M. Carmen Rebellón y a Carles Martin Closas por el trabajo que hacen cada día en el programa de doctorado de Ciencias de la Tierra, y que casi nunca es agradecido como correspondería.

Paralelamente a la tesis he hecho mi persecución particular, en busca de Ari, que me ha llevado por varios sitios, Palma, Madrid, Granada y Wellingtón. La mayor parte del tiempo fuera lo pasé en Granada, trabajando en el Instituto Andaluz de Ciencias de la Tierra. Esto fue así gracias a Carlota Escutia, quien merece un lugar de honor en estos agradecimientos. Muchas gracias Carlota (también a Hans) por permitirme un sitio confortable y acondicionado en el que trabajar en la tesis, tus consejos siempre útiles, y estupendas cenas. En Granada, y en los otros lugares he conocido a gente fantástica. La gente del IACT y de la universidad de Granada y amigos me han hecho sentir siempre como en casa!

En el Fort Hoofdijk de Utrecht pasé las frías tardes de verano en el laboratorio analizando muestras supervi-

sado por Cor Langereis y Maxim Krasnoperov. Gracias a Tom Mullender y Mark Dekkers por las buenas charlas y también por la ayuda en el análisis de muestras. De Utrecht también aprecio los consejos de Hemmo Abels. En Estados Unidos, hice un curso de Magnetismo de Rocas en el IRM de Minnesota. Gracias a Mike Jackson y Julie Bowles y a la National Science Foundation por permitirme asistir y a los compañeros de curso, por los buenos ratos, en especial a Allison Teletzke por cuestiones de intendencia para Yellowstone, y a Violeta Riera. En el Marum de Bremen hice también un excelente curso de escalas de tiempo gracias a la European Science Foundation y a Michael Kucera, Heiko Pälike y otros organizadores. En Italia hice dos cursos en astrocronologías, el primero en Coldigioco, cerca de Ancona, del que guardo un recuerdo memorable, y donde hice buenos amigos en ciencia, que también me ayudaron en cosas de la tesis, Christian Zeeden, Mathieu Martínez, entre otros. De los profesores aprendí mucho, especialmente de Frits Hilgen, aunque también Jacques Laskar, Klaudia Kuiper, Heiko Pälike o Sandro Montanari. A Jan Smit porque me invito a un helado y me explico las vicisitudes de los Boletus italianos, y a Walter Alvarez por contarnos historias al pie de una higuera. A Frits Hilgen le agradezco también la colaboración en el tercer artículo, y la organización del otro curso de Italia junto con Diederik Liebrand y Sietske Batenburg. Gracias también a los participantes (imposibles de enumerar) por hacer sublimes esos momentos italianos, trabajando en las playas sicilianas.

Les xixes em van fer escriure aquests agraïments, gairebé en moments d'extrema-unció doctoral. Per això y per la vostra santa paciència i descansillos i Menorcas i moltes més coses esteu aquí agraïdes Judit Torner, Mercé Bermejo, Patri Povea, Oli Iglesias, María Jaume y Albert Català. A los Ovilistas les debo también un elogio, Eloi Carola, Jorge Belenguer, Adrià Guerrero, Manoel Valcarcel, Enric Pascual, Aritz Urruela, Jordi Vilà… i a la gent de la casa, especialment als de les Geosortides, tius espavileu i organitzeu sortides, que el bon geòleg es fa al camp!, a Frede Escosa, Marina Nebot, Nuria Carrera, a Pablo M. Granado, Marco Di Matteis, per tants dinars, a l'Oriol Ferrer per un EGU a Viena fantàstica, als companys de sala Xavi Rayo, Xavi Tubau, Aitor Rumín, Nicolá Grasseau y Yaniel Vázquez i la P. Povea, es veu que clarament falta intel•ligència femenina!, i a tots els de la sala marítima veïna, i als i les de les ales del costat i de baix.

Als coleguis de Barna: Dra. Berta López, Dra. Marta Ribó, Dr. Olga Margalef, Dr. Xavier Rodriguez, Dra. Jelena Barbir, (casi) Dr. Jaume Llopart, (casi) Dr. Joana Ortiz, (casi) Dr. Alvaro Sáinz, (casi) Dr. Cristina Biete, (casi) Dr. Aina Margalef, ja veieu que està ple de doctors, i això sense contar els doctors honoris causa: Martí, Carlota, Gemma, Elsa, Iñigo, Gabri, Ferran, Anna i Úrsula … Gràcies Elsa també pels consells de maquetació i per compartir tants bons temps a la Maison Parxís, juntament amb Gaël, Albert, Genís i d'altres pobladors d'aquella casa de Sant Antoni. Y Carlota y Jaume per acollir-me a Cal Guinardó els últims agònics mesos, i també a la Gemma. Al Dr. Prof. Don Tito Esteve Machache Segura, a Edu, Daisy, Oscar, i la penya de Tarraco. Als colegues de la carrera com el Lluís Guilà, Iñaki, Duye, la Geli, la Tere… la Laura Pallarés, la Tina Martinez, Esther Rodríguez y l'E. Jiménez (que ja fa vuit anys fa que vam anar a perforar a la Gronsa i a Vic amb el Miguel!!!), Jara Martí i a la Raquel Robles i tots el altres que em perdonin!

A Eduard Albert i Rubén Calvo per moltíssimes coses però sobretot perquè sorprenentment sortirem d'aquesta com a doctors.

A l'Ari per deixar-se perseguir. I per que tot es fàcil al seu costat.

A mi hermano Jaime,

y a mis padres José y Gloria, por todo y más.

Timothy looked at the deep ocean sky, trying to see Earth and the war and the ruined cities and the men killing each other since the day he was born. But he saw nothing. The war was as removed and far off as two flies battling to the death in the arch of a great high and silent cathedral. And just as senseless...

"What are you looking at so hard, Dad?"

"I was looking for Earthian logic, common sense, good government, peace, and responsibility."

"All that up there?"

"No. I didn't find it. It's not there any more. Maybe it'll never be there again. Maybe we fooled ourselves that it was ever there."

Ray Bradbury, The Million-Year Picnic, The Martian Chronicles (1946)

Una tesi no s'acaba,

es mata.

Olga Margalef

Quan et pensis que has acabat

et queda la meitat.

A mis padres, José y Gloria

Resum (en Català)

Aquest tesi te com a principal objectiu datar conques Cenozoiques clau en l'evolució geològica de la Península Ibèrica mitjançant magneto- i astrocronologies. La tesis està constituïda per una recopilació d'articles, cadascun d'ells amb el seu propi objectiu. La unió dels diferents treballs realitzats dóna lloc a uns resultats i discussió a on s'aborden les diferents camins mitjançant els quals els registres sedimentaris poden expressar litològicament els cicles de Milankovitch, claus en la generació de seqüencies sedimentaries.

En geosciènces el control del temps es quelcom bàsic, ja que de la cronologia d'un registre estratigràfic poden partir altres estudis. Tot i que s'hi ha treballat intensament, a la Península Ibèrica encara resten varies conques que o bé necessiten una cronologia o bé les cronologies existents son susceptibles de ser refinades. El principal mètode de datació continu de sèries sedimentàries es la magnetostratigrafia. Barata y relativament ràpida, la magnetostratigrafia ha tingut molt èxit i ha contribuït a construir models d'edat que han estat útils per entendre l'evolució de les estructures tectòniques, per datar esdeveniments concrets dintre de les conques sedimentàries o per datar biozones o jaciments de faunes i flores, entre d'altres usos. Per altra banda, el desenvolupament de la ciclostratigrafia, que consisteix en datar successions sedimentaries mitjançant el reconeixement dels cicles de Milankovitch, ha permès, allà on s'ha pogut implementar, cronologies més precises i robustes. Aquesta tesi té com a primer objectiu proporcionar cronologies per a conques Cenozoiques de referència de Iberia mitjançant tècniques magneto- i ciclostratigràfiques.

Quan una sèrie sedimentaria té adscrita una magnetostratigrafia o una ciclostratigrafia, i per tant un model d'edat acurat, es possible investigar a que responen els canvis sedimentaris que s'observen al llarg del registre sedimentari. D'aquesta manera s'han dut a terme tres estudis independents per a cada una de les tres conques estudiades amb diferents objectius adaptats a cada una de les conques. Les conques estudiades han estat la de l'Ebre, la d'Almazán i la d'As Pontes.

A la conca de l'Ebre, a l'àrea de Mequinensa, s'ha establert un model d'edat primer basat en la magnetostratigrafia. Les edats obtingudes son coherents amb les derivades de magnetostratigrafies veïnes prèvies, fixant el límit Oligocè-Miocè a la base de la formació Torrente de Cinca. A més, s'ha fet un estudi ciclostratigrafic basat en els canvis de facies produïts a les lleres dels antics llacs que s'havien establert en aquesta àrea de la conca durant finals de l'Oligocè i principis del Miocè. L'anàlisi espectral de la variabilitat del rang de facies mostra cicles en el domini de la precessió, de la obliqüitat i de l'excentricitat. És destacable el domini de l'excentricitat, on tant els cicles de 100-ka (kiloanys), 405-ka i 2.4-Ma (Milions d'anys) dominaren la dinàmica d'expansions i retraccions lacustres. Hem interpretat que els períodes de nivell alt d'aigua dels paleo-llacs va ser conseqüència de períodes recurrents amb balanços d'aigua positius relacionats amb cicles de precessió. A on la modulació de la precessió produïda en moments d'excentricitat màxima és responsable de la recurrència de fases de balanç d'aigua positiu, resultant en pujades del nivell dels llacs. L'estudi complet del registre continental de la conca de l'Ebre (uns 25 Ma) mostra migracions dels sistemes lacustres degut a canvis en els patrons de subsidència associats a l'evolució dels orògens circumdants. Superposat a aquesta migració, l'efecte del cicles d'excentricitat de 2.4-Ma en les grans expansions i retraccions dels antics llacs és notable. Es destacat l'efecte dels canvis climàtics en el desenvolupament de seqüencies en els depocentres lacustres, tot i tractar-se de un context amb tectònica activa als marges de conca. Proposem un desacoblament entre les seqüencies sintectòniques dels marges i les seqüencies climàtiques al centres de la conca.

A la conca d'Almazán hem construït una magnetostratigrafia que comprèn uns 2700 metres del rebliment paleogen. Gràcies a la magnetostratigrafia s'ha pogut datar l'inici de la sedimentació, que ara es situa al Lutecià dintre del cron magnètic C21. També s'han datat els límits entre les seqüencies deposicionals establertes per la conca: el límit A1-A2 és Bartonià i queda dintre del cron C18, i el límit A2-A3 es Priabonià i es situa dintre del cron C13. El límit Eocè-Oligocè es troba prop de la base de la seqüencia A3. El jaciment de vertebrats de Miñana (MP15-16) té una edat Bartoniana (cron C18), mentre que el jaciment de Deza (MP 17b) es situa al cron C15 al Priabonià mitjà. Degut a la qualitat d'afloramentdel registre hem pogut estendre la magnetostratigrafia a l'ample de la conca mitjançant nivells de correlació clau, com poden ser nivells de canals amalgamats de gresos. Aquest fet ha permès obtenir un mapa dels canvis de polaritat magnètica pel Paleogen d'Almazán. Son destacables els canvis en la potencia del registre entre la part Sud-est i la part Nord-oest, indicant canvis laterals importants en la subsidència i per tant en les taxes de sedimentació. Al superposar el mapa paleomagnetic amb la cartografia de les formacions, s'observa una correlació entre les formacions i la seva arquitectura interna, i les taxes de sedimentació. En intervals amb subministrament clàstic elevat hi predominen els sistemes fluvials i al•luvials distals. Si les taxes de sedimentació son altes, als sistemes fluvials hi dominen els canals de tipus ribbon i la preservació de les planes d'inundació juxtaposades. Als sistemes al•luvials distals hi predominen les lutites ocres-vermelloses. En intervals amb alta entrada de clàstics però amb baixes taxes de sedimentació, als sistemes fluvials hi predominen canals de tipus sheet amb força amalgamació i una pobre preservació de dipòsits fins de les planes d'inundació. A les parts al•luvials, es troben principalment lutites amb el desenvolupament d'horitzons pedogenitzats, ja siguin calcretes, dolocretes, gipscretes, o lutites amb nòduls carbonatats. Per contra, a les zones amb minsa entrada de terrígens, quan les taxes de sedimentació son més altes típicament hi predominen dipòsits lacustres, i a mesura que es redueixen les taxes de sedimentació apareixen, primer dipòsits palustres, després dipòsits palustres amb pedogènesi i finalment nivells de calcretes. Aquest estudi ha permès trobar les relacions existents en el balanç de masses de la conca, es a dir la distribució del volum de sediment en una conca i la arquitectura sedimentaria resultant. En més detall, la relació del quocient entre acomodació i entrada de sediment, que representa els balanç de masses, controla tant la arquitectura sedimentària com la distribució dels elements deposicionals en les conques sedimentàries.

A la conca d'As Pontes s'ha redefinit la magnetostratigrafia prèvia. Basant-nos en el model d'edat magnètic, hem construït una astrocronologia mitjançant l'anàlisi espectral de un rang de facies, a on s'ordenen 33 litologies en funció de la seva posició en la conca, de distal a proximal. Els resultats derivats de l'anàlisi espectral del rang de facies, mostren que l'alternança entre lignits i clàstics respon a canvis climàtics relacionats amb variacions de l'excentricitat de la Terra. Els mínims d'excentricitat es caracteritzen per un predomini de lignits, mentre que als màxims d'excentricitat hi predominen els dipòsits terrígens al•luvials. Interpretem que l'estabilitat climàtica produïda als mínims d'excentricitat genera estabilitat dels ecosistemes, i per tant una cobertora vegetal eficient, que contribueix a minimitzar la erosió i meteorització a les capçaleres i àrees font de sediments. En afegit, l'estabilitat en els gradients dels sistemes de transport de sediment durant períodes sense canvis geomorfològics notables contribueix a minimitzar la erosió i permet acumular series potents de lignits a les parts distals de la conca. Es especialment significatiu l'efecte dels mínims dels cicles d'excentricitat de 2.4-Ma en el desenvolupament de nivells de lignit. Durant aquests períodes és quan es desenvolupen i es conserven els principals nivells carbonífers, els quals foren objectius miners. La conca d'As Pontes es una conca petita i amb marges constituïts per un apilament vertical d'encavalcaments. Tot i això, l'efecte dels cicles climàtics es dominant en les part més internes de la conca.

La diferent mida, clima i règims tectònics en els quals van evolucionar les tres conques permeten extreure'n patrons de comportament comuns dels sistemes sedimentaris davant de l'impacte climàtic dels cicles orbitals. A la discussió d'aquesta tesi comparem aquests resultats amb altres conques de diferents

edats i fisonomies. Considerem que l'expressió dels cicles de Milankovitch en conques continentals té dos orígens. Per una banda cicles desenvolupats a les parts distals de la conca, deguts a canvis en l'espai d'acomodació o "dowstream cycles" i els cicles que afecten la quantitat de sediment que entra a una conca des del rerepaís o "sediment supply cycles", i que els anomenem "upstream cycles". Els primers sorgeixen fruit de quan la precipitació neta (precipitació menys evaporació) augmenta o disminueix. Aquelles conques amb un sistema lacustre (o un sistema sensible als canvis en la lamina d'aigua) experimentaran un augment o una disminució en l'espai d'acomodació degut a les pujades o baixades de la làmina d'aigua. Això propicia una retrogradació dels cinturons de facies i probablement un augment en les taxes de sedimentació terra endins. Per contra un baixada de la làmina d'aigua promourà progradació de les facies, probablement un augment relatiu de les taxes de sedimentació en les àrees submergides i un descens en les àrees emergides. Els canvis en la làmina d'aigua es produeixen immediatament en temps geològics, i per tant els temps de resposta de les conques a aquests canvi es consideren molt reduïts. Aquest fet permet que les conques sedimentaries expressin cicles d'excentricitat en tots les seves principals freqüències, i també cicles d'obliqüitat i precessió. Exemples d'aquest tipus son la Conca de l'Ebre i també les conques de Newark, de Green River (Estats Units d'Amèrica), o la Conca Orcadiana (Escòcia), essent aquestes exemple de conques amb sistemes de transferència de sediments grans o mitjans. La secció d'Orera, a la Conca de Calatayud; la secció de Cascante a la Conca de Teruel o la Conca de Ptolemais, a Grècia, son exemples de conques amb sistemes de transferència petits.

Els cicles upstream, que son aquells que s'expressen mitjançant canvis en el flux de sediment, son més complexos. La senyal climàtica (polsos) en el volum de sediment es va dispersant i esmorteint al llarg del sistemes de transport, ja sigui perquè la senyal queda estorada (o alliberada) en alguns punts de les conques o dels marges, o bé perquè hi operen amb força els processos autogenics. S'han fet estudis de modelització que han donat com a resultat respostes ambivalents per les arribades dels polsos de sediment als embornals (sinks) de les conques. Per una banda uns estudis parlen de respostes esmorteïdes i per tant indetectables, mentre que per l'altra altres estudis apunten a un paper amplificador de les senyals clàstiques per part dels rius. Aquest estudis parlen del temps de resposta de les conques, com a un fet crític en la conservació dels polsos sedimentaris. En el cas de les conques grans, es considera que l'efecte esmorteïdor (buffering effect) produït als sistemes de transferència de sediments inhibeix el desenvolupament de cicles que actuen dintre de les freqüències de Milankovitch. Per tant, les conques grans es descarten com a fonts potencials de registrar els upstream cycles. Tanmateix, l'efecte en l'acomodació que produeixen els cicles downstream en els sistemes que presentin al menys una fase que inclogui la presencia d'aigües superficials possiblement tingui un pes més gran en la conformació de cicles litològics en el registre sedimentari. Per tant, normalment qualsevol tipus de conca que presenti o bé llacs o fases aquàtiques en la seva història es poc susceptible de registrar senyals que involucrin canvis en el subministrament de sediments (probablement excepte llacs molt profunds, del tipus llac Baikal). En conseqüència, només seran susceptibles de registrar aquests cicles aquelles conques que tinguin temps de resposta relativament ràpids i que, a més, no presentin canvis litològics que involucrin canvis en la làmina d'aigua. Conques petites, amb sistemes de transferència de sediments curts i que evolucionin sota un règim tectònic estable son susceptibles de registrar cicles originats com a canvis en l'entrada de volums sedimentaris. Exemples d'aquest tipus son per exemple la conca d'As Pontes, la conca de Madrid, o la secció de Lupoaia (a la Conca d'Oltenia, Romania) o la conca de Megalòpolis a Grècia.

En conjunt tot plegat es pot interpretar com que a banda de un règim climàtic concret la morfologia i característiques de les conques sedimentaries son elements claus en quant a l'expressió dels cicles de Milankovitch. Es peculiar la diferencia entre l'expressió de intervals carbonífers a l'Ebre i a As Pontes. Mentre a l'Ebre petits intervals amb carbó i nivells alts dels llacs es donen durant períodes d'excentricitat màxima, a As Pontes els períodes carbonífers son aquells d'excentricitat mínima.

Chapter 1
Introduction

Erecting robust temporal frameworks is crucial to understand and to assess the different processes that shaped strata, and thus constitutes an essential part of modern geosciences. The most widespread technique to date continuously long continental sedimentary sequences is magnetostratigraphy. Further, the development of cyclostratigraphy has allowed an enhancement of age models for sedimentary records. This is because Milankovitch cycles show high-frequency cycles (precession and obliquity) that permit a larger number of tie-points to the astronomical solutions. In consequence, if the expression of the orbital rhythms in the stratigraphy is adequate, astronomic age models allow for more resolution than magnetostratigraphy. Combination of both methods gives rise to robust chronologies with unprecedented resolution.

Although the Cenozoic geology of the Iberian Peninsula has been intensively studied, still there are strategic locations lacking independent dating or otherwise with improvable age models. The first goal of this thesis is to provide accurate and complete age models for key basins of Iberia. In order to obtain independent chronologies, it is necessary to embrace a long and densely sampled span of record (time), which will make unequivocal the correlation of the local magnetic polarity pattern (and the sedimentary cycles) to the Geological Time Scale. The Ebro, Almazán, and As Pontes basins were chosen because of their geological importance and because long sections with overlapping ages were available.

All the studied records encompass a long time span (>7-Ma), which may be used for sedimentological and stratigraphic research in a wide range of time-scales. In particular, we focused in assessing the impact in the stratigraphy of the very long-term Milankovitch cycles (>1Ma) and their relationship in the generation of sedimentary sequences at basin scales. Disentangling such relationship may shed light into the tectonic or climatic origin of observed sedimentary sequences. In parallel, the development of age models allows for a precise quantification of sedimentation rates. The study of the sedimentation rates may help to determine the relationship between accommodation and sediment supply within a basin. The ratio between accommodation and sediment supply is indicative of the changes in the mass-balance in a sedimentary basin. Evaluating the stratigraphic response to the mass-balance changes may help to predict the basin response to climatic and tectonic forcing.

The results of this PhD project provide insights on the expression of the Milankovitch cycles in continental basins and also on the relationship between accommodation and sediment supply in the development of sedimentary sequences. Our data together with results from other case studies allows for a discussion about the pathways in which Milankovitch cycles affected the continental sedimentary records through a mass-balance approach. The way in which sediment routing systems evolve in response to climate forcing is a crucial part of the integral study of sedimentary basins.

In order to undertake these subjects, three independent studies have been carried out. The general methodology dealing with magnetostratigraphic and cyclostratigraphic age model building is explained in Chapter 2.

In Chapter 3 the different studies carried out in this thesis are summarized.

Chapter 3.1. is based on the paper: Valero, L., Garcés, M., Cabrera, L., Costa, E., Sáez, A. (2014). 20-Myr of eccentricity paced lacustrine cycles in the Cenozoic Ebro Basin. Earth and Planetary Science Letters 408, 183-193. In this paper is shown a new magnetostratigraphy performed for the Los Monegros Lacustrine system in the Mequinenza area of the Ebro Basin. In addition, a new astronomical age model was build, resembling a correlation between eccentricity maxima and lacustrine expansions. The complete

continental record of the Ebro basin was revisited and a link between the 2.4-Myr eccentricity cycles and lacustrine expansion is shown for the most of the continental record. A decoupling between (tectonic) supply-driven clastic sequences fed from basin margins and (climatic) base level-driven lacustrine sequences in active settings with medium to large sediment transfer systems is suggested.

Chapter 3.2. is based on the article: Valero, L., Huerta, P., Garcés., M., Armenteros, I., Beamud, E., Gómez-Paccard, M. (2015). Linking sedimentation rates and large-scale architecture for facies prediction in nonmarine basins (Paleogene, Almazán Basin, Spain). Basin Research. In this work a magnetostratigraphy encompassing ca. 2700 m was built. The magnetostratigraphy allowed dating the Paleogene infill of the Almazán Basin, and calibrate the biostratigraphic data. Furthermore, the timing and the different forcing of depositional sequences was evaluated. Finally, the link between sedimentation rates and the depositional elements distribution and their architecture is discussed.

In Chapter 3.3 summarizes the article: Valero, L., Cabrera, L., Sáez, A., Garcés, M. Long-period astronomically-forced terrestrial carbon sinks (submitted). This article shows a correlation of eccentricity cycles minimum and peat development in the As Pontes Basin, even at a million-year scale. The interaction between a resilient vegetal cover and graded profiles during steady climates (eccentricity minima) is suggested to decrease erosion and weathering along the sedimentary routing system, thus reducing the clastic input.

Finally, in Chapter 4, the integration between the results shown on Chapter 3 allows for a general discussion and Chapter 5 includes the conclusions of the thesis.

Chapter 2
Methods

2.1. PALEOMAGNETISM

This section includes a brief description of the fundamentals of paleomagnetism applied to dating sedimentary sequences. For further reading in detailed aspects related to magnetostratigraphic methods, a number of textbooks are recommended (Butler, 1992; Opdyke and Channell, 1996; Tauxe, 1998; Langereis et al., 2010; Garcés, 2015).

Magnetostratigraphy

Magnetic polarity stratigraphy or magnetostratigraphy relies on the ability of sedimentary rocks to acquire a remanent magnetisation when they form, which parallels the direction of the Earth's ambient magnetic field. Since the geomagnetic field has undergone multiple nonperiodic reversals through Earth history, a magnetic zonation of sedimentary sequences is feasible according to the polarity of the rock magnetization. A magnetostratigraphic zonation allows dividing the stratigraphic record into time slices which can be correlated worldwide. Magnetostratigraphic dating refers to the identification in the stratigraphic record of magnetozones, which can be correlated to age-equivalent geomagnetic chrons. The compiled absolute ages of geomagnetic chrons form the basis for the geomagnetic polarity time scale (GPTS), which is routinely revised with new radiometric or astronomic calibrations (Garcés, 2015).

Earth Magnetic Field: the Dipole

The Earth's magnetic field is originated by the convection of the iron rich material of the Earth's outer core. At the Earth's surface the geomagnetic field is approximately that of a geocentric axial dipole (GAD) (Hospers, 1954), and at timescales $>10^3$ it agrees to the field expected from a GAD during either normal- and reversed-polarity intervals (Merrill et al., 1996). The fact that the geomagnetic field can be modelled as a geocentric dipole that can switch randomly its polarity is of fundamental importance in paleomagnetic studies (Hospers, 1951; Opdyke and Channell, 1996; Langereis et al., 2010).

Assuming the GAD, the geomagnetic and geographic axes coincide, and the geomagnetic equator will coincide with the geographic equator. The geomagnetic field on any point of the Earth's surface is a vector (F). This vector displays a component in the horizontal plane (H) with an angle respect the geographical meridian (D), measured eastwards from 0° to 360°. The angle of the magnetic vector (F) with the horizontal plane is the Inclination (I), measured from downwards ranging from 90° to -90° (Fig. 2.1.1).

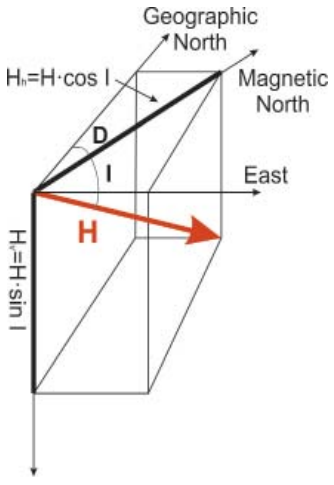

Figure 2.1.1. Description of the magnetic field. The total magnetic field vector H can be broken into a vertical component Hv, and a horizontal component Hh. The inclination I is the angle between the horizontal and H. The declination D, is the azimuthal angle between the horizontal component of H and the geographic north. Adapted from Butler (1992).

Table 2.1.1 Principal magnetic minerals of application in paleomagnetism. Tc: Curie temperature. Adapted from Evans and Heller (2003)

Mineral	Formula	T_c (ºC)
Magnetite	Fe_3O_4	580
Hematite	α-Fe_2O_3	675
Maghemite	γ-Fe_2O_3	590-675
Goethite	α -FeOOH	120
Pyrrhotite	Fe_7S_8	320
Greigite	Fe_3S_4	~330

The geomagnetic inclination (I) will vary systematically with latitude (λ) according to the formula: Tan (I) = 2 Tan (λ).

Natural Remanent Magnetisation (NRM)

Three types of solids depending on their response to a magnetic field exist: Paramagnetic, Diamagnetic and Ferromagnetic. Ferromagnetic solids have atoms with magnetic moments, in which adjacent atomic moments interact strongly (Butler, 1992). It can result in solids with parallel coupling (ferromagnetic), antiparallel coupling of their atomic magnetic moments (Antiferromagnetism). In addition, some magnetic materials display an antiparallel coupling with layers of unequal moment (ferrimagnetism and canted antiferrimagnetism) (Fig. 2.1.2). Most common magnetic minerals that exhibit spontaneous magnetization belong to the group of iron oxides and sulphides (Table 2.1.1). These minerals are capable of capture the ambient magnetic field after cooling below the Blocking temperature.

The rocks that contain magnetic minerals can lock-in and preserve a record of the geomagnetic field. To achieve the capture of the ambient magnetic field however, magnetic minerals need to occur in the appropriate amount and size range, in order to overcome too short relaxation times (or to be oriented following the magnetic field). The preservation of the direction of the magnetic field by a rock is termed Natural Remanent Magnetization (NRM). In nature, there are three main mechanisms by which the magnetic mine-

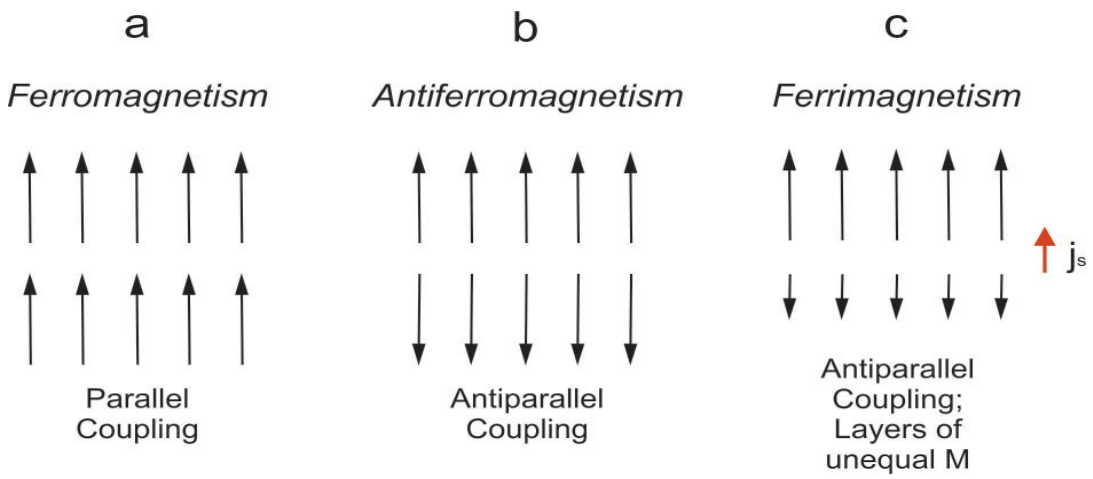

Figure 2.1.2. Exchange couplings for (a) ferromagnetic, (b) antiferromagnetic, and (c) ferrimagnetic materials. The net magnetization for ferrimagnetic material is shown at right; the net magnetization of antiferromagnetic material is zero. Adapted from Butler (1992).

rals are magnetized: Thermoremanent Magnetization (TRM), Chemical Remanent Magnetization (CRM), and Detrital Remanent Magnetization (DRM).

Thermoremanent Magnetization is NRM produced by cooling from above the Curie Temperature (Tc) in the presence of a magnetic field (Butler, 1992). The action of the magnetic field at the Blocking temperature results in the TRM, which allows the rock capturing the ambient field. TRM is the form of acquisition of most igneous rocks, which magnetic carriers are principally titanomagnetite solid solution series. TRM can be acquired even under low magnetic fields such as the Earth's magnetic field (Roberts et al., 2013), or the ancient Moon's magnetic field (Weiss & Tikoo, 2014).

Chemical Remanent Magnetization (CRM) is termed to the magnetization below the blocking temperature of ferromagnetic minerals due to changes in their chemical properties. These chemical reactions include the alteration of a pre-existing mineral to a ferromagnetic mineral or a precipitation of a ferromagnetic mineral from solution. The magnetic moments are acquired when the crystals grow through a critical state, which enables long enough relaxation times. CRM is typically acquired by sedimentary rocks during either the first phases of diagenesis or the during exhumation phases. CRM is suitable for magnetostratigraphy as long as the acquisition takes place in an early post-depositional stage (Garcés, 2015). In continental sedimentary rocks frequent carriers of CRM are cements of hematite and goethite, whereas in marine settings iron-sulfides are common.

A Detrital Remanent Magnetization (DRM) is carried by magnetic minerals, with a pre-existing TRM or CRM, incorporated into the sedimentary rock as detrital particles, either as part of the terrigenous fraction or from biogenic sources within the water column. If the magnetic grains are sufficiently small, their magnetic moments counterbalance the gravitational torques, producing a statistical particle alignment with the ambient field (Garcés, 2015). Common carriers of DRM are iron oxides hematite and magnetite, because they resist erosion and transport along the sediment transfer systems. A number of experiments have evidenced the importance of the post-depositional alignment, which together with the DRM and CRM components constitute the total magnetic remanence that a given rock accumulated during its history. The identification of the different NRM components is crucial for all the paleomagnetic studies, and this is achieved by means of diverse stepwise demagnetization techniques (Langereis et al., 1989).

The Geomagnetic Polarity Timescale and Magentostratigraphic Correlation

Matuyama's (**松山**) finding that Earth's magnetic field had undergone reversals in the past, allowed building a Global Geomagnetic Polarity Timescale or GPTS. The GPTS aims to include and date all the relevant polarity switches that the Earth's magnetic field had experienced. The pursuit of polarity reversals was principally carried out in the marine mid-oceanic ridges (Heirtzler et al. 1968). The mid-oceanic ridges include a sequence of magnetic reversals, which are mirrored in the two wings of the ridges by the remanent magnetization of the oceanic crust after cooling during the process of sea-floor spreading. The development of radioisotopic techniques allowed the construction of a first GPTS (Cox et al., 1964). The GPTS was improved as research vessels included more and progressively older magnetic anomalies and the radioisotopic techniques were refined. In the last years, the development of the astronomical dating (further explained in the next chapter), together with the synchronization of the different "geological rock clocks" has allowed a great refinement of the GTPS (Kuiper et al., 2008; Pälike et al., 2008; Gradstein et al., 2012), although the Geological Time Scale in under permanent evolution (Hilgen, 2008; De Vleeschouwer and Parnell, 2014).

Sampling and laboratory processing

Sampling is a key step in order to perform a characteristic local magnetostratigraphy. Sampling at regular intervals (if possible in time), appropriate density, and fine-grained sediments is required. To reach in-situ fresh rocks is important in order to avoid rock alterations or possible remagnetizations. A water/air cooled

portable drill is often used to take the samples. In-situ core orientation is normally achieved using adapted compasses, which allow for azimuth and dip directions calculations.

The NRM is divided into primary and secondary magnetizations. The primary is the magnetization obtained during the cooling (TRM) or during the early deposition (CRM & DRM) of a rock. The secondary magnetization is formed by all other magnetic components acquired during the rock evolution. The more important component that can be extracted from the NRM is the Characteristic Remanent Magnetization (ChRM) as is the most stable and consistent component that can be isolated. In order to identify the different NRM components, the principal techniques used are the thermal and the alternating magnetic field stepwise demagnetization processes (Langereis et al., 1989). These techniques consist in stepwise increments of temperature (thermal) or magnetic fields (alternating magnetic fields) in magnetically isolated environments. After each step the remaining magnetization of the specimen is measured. The resultant changes in the magnetic vector and the intensity are displayed and analysed. The stepwise demagnetization stops when the sample overcomes the blocking temperature (thermal) or the saturation intensities of

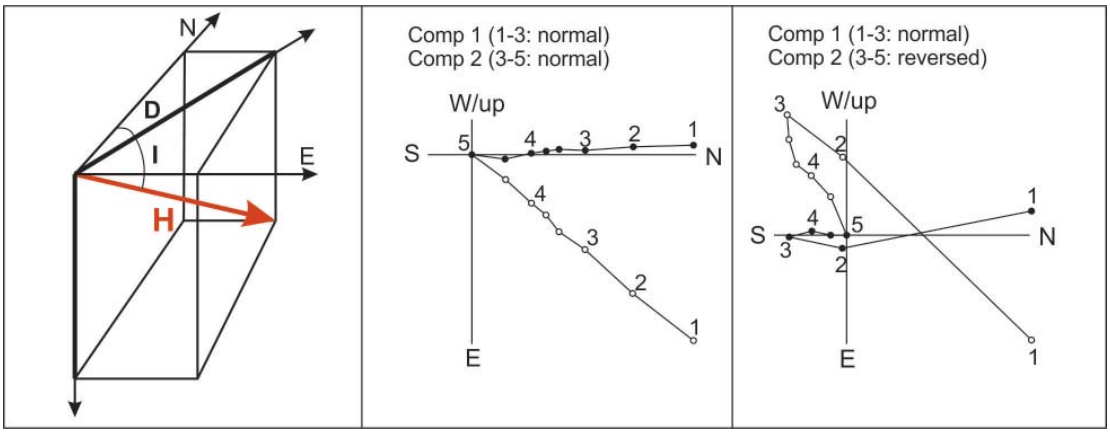

Figure 2.1.3. (A) As shown in Fig. 1, the magnetic field on any point on Earth's surface is a vector H which can be discomposed into a horizontal Hh and a vertical component Hv. The angle of Hh with the magnetic North is the Declination D. The inclination I is the angle between H and the horizontal. (B) and (C) show different Zijderveld diagrams (Zijderveld, 1967), which is the standard method for present and analyze the stepwise demagnetization results. During demagnetization process, changes in the magnetization vector affecting intensity and direction occur. The endpoint of the vector measured after each demagnetization step is projected both onto the horizontal plane (closed symbols) and onto the vertical plane (open symbols). Difference vectors (lines between end points) then show the behavior of the total vector upon stepwise removal of magnetization. (B) is an example of a normal sample, whereas (C) depicts a reversal sample. Adapted from Butler, (1992).

principal magnetic carriers (alternating magnetic fields). Usually the magnetic susceptibility of a specimen is measured at each step, this allowing for monitoring of mineralogical changes during sample demagnetization. Finally, the analysis of the track of the magnetic vectors during the demagnetization process is analysed giving rise to the identification of the different NRM components. The most common representation of results of progressive demagnetization is the orthogonal projection diagrams (Zijderveld, 1967), which allows depicting in a single diagram both the directional and the intensity information by the projection of the NRM vector into two orthogonal planes (Fig. 2.1.3). Magnetic components can be extracted from the Zidjerveld diagrams using least-square analysis (Kirchvink, 1980). Among the components, the ChRM is the most interesting component to isolate for magnetostratigraphic purposes.

The ChRM is expressed with their values of Declination and Inclination, which allow for the calculation of the Virtual Geomagnetic Pole (VGP) (Tauxe, 1998). Before, however it is required to assess the primary origin of the ChRM. This can be tackled using diverse methods such as the fold test, the consistency test,

the reversal test, or the conglomerate test (Butler 1992; Opdyle and Channell 1996; Tauxe, 1998). The fold test is positive if after the correction for the dip of the strata the ChRM directions of both flanks converge. This test demonstrates that magnetization was acquired before folding. The consistency test is positive if a polarity sequence is laterally traceable across the sedimentary record involving any independent correlation. The reversal test is positive if antipodality of the average normal and reversed paleomagnetic directions is achieved. The reversal test is not crucial for magnetostratigraphy since the magnetic polarity can be often assessed from partially overlapped paleomagnetic directions (Garcés, 2015). Finally, the conglomerate test is positive if the clasts of a conglomerate display random paleomagnetic directions.

Magnetostratigraphic correlation

The primary origin of the ChRM validates the resultant VGPs, and allows building a local magnetostratigraphy. VGPs from individual samples/horizons are compared with the overall paleomagnetic pole computed from the mean magnetization direction for the entire section. Variation in VGP in the section is then expressed as a VGP latitude, which represents the latitude of individual VGP in the coordinates of the overall paleomagnetic pole. VGP latitudes close to $+90^0$ represent normal polarity, and VGP latitudes close to

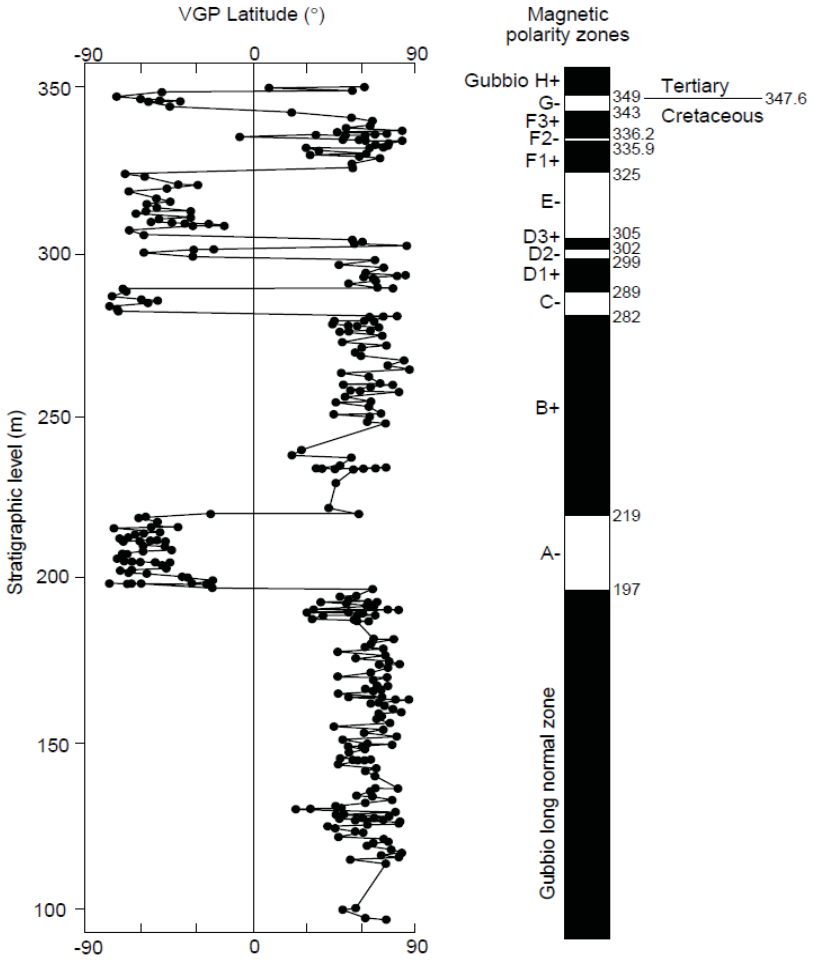

Figure 2.1.4. At the left, example of Virtual Geomagnetic Pole latitudes (VGP) from the Scaglia Rossa section in the Umbrian Apennines near Gubbio, Italy. Plotting together the VGP points allows for setting local magnetozones, where black is normal polarity and white reversed polarity. At the right picture of a sample hole within the same section.

-90^0 represent reverse polarity (Fig. 2.1.4). VGP latitudes are plotted as a function of stratigraphic position of the samples. The polarity interpretation is usually presented as black (normal) and white (reverse) bar diagrams (Opdyke and Channell, 1996).

Once a local magnetic stratigraphy is achieved it is possible to set the obtained pattern within the GTS. A

first external approach to the GPTS is usually necessary, for example, biostratigraphy it is useful to constrain the stage level or even better are radiometric ages. To make unequivocal and independent correlations it is fundamental ensure the completeness of the magnetozones in the local magnetostratigraphy and also to embrace a long span of time. A sampling including 8 samples per magnetozone and at least a stratigraphy covering more than 3 Ma (in the last 30 Ma) and more than 9 Ma (between 30 and 70 Ma) uses to be sufficient (Johnson and McGee, 1983; Garcés, 2015). Finally, a correlation between local and global timescales can be achieved by seeking the best match between scales.

References

Butler, R. F., 1992. Palaeomagnetism, magnetic domains to geologic terranes, Blackwell Scientific Publications (Boston, MA, USA), 319 pp.

Cox, A., Doell, R. R. & Dalrymple, G. B. (1964). Reversals of the Earth's magnetic field, Science 144, 1537–1543.

De Vleeschouwer, D. & Parnell, A. C. (2014). Reducing time-scale uncertainty for the Devonian by integrating astrochronology and Bayesian statistics. Geology, 42(6), 491-494.

Evans, M. & Heller, F. (2003). Environmental Magnetism: Principles and Applications of Enviromagnetics. London: Elsevier, p. 299.

Garcés, M. (2015). Magnetostratigraphic Dating. In Rink, W.J. and Thompson J.W. (eds): Encyclopedia of Scientific Dating Methods, Springer, 507-517.

Gradstein, F., Ogg, J., Schmitz, M. & Ogg, G. (2012). The Geologic Time Scale 2012. Amsterdam, the Netherlands: Elsevier.

Heirtzler, J. R., Dickson, G. O., Herron, E. M., Pitman, W. C., & Le Pichon, X. (1968). Marine magnetic anomalies, geomagnetic field reversals, and motions of the ocean floor and continents. Journal of Geophysical Research, 73(6), 2119–2136.

Hilgen, F.J. (2008). Recent progress in the standaritzation and calibration of Cenozoic Time Scale. Newsletters on Stratigraphy, 43, 15-22. doi: 10.1127/0078-0421/2008/0043-0015

Hospers, J. (1951). Remanent magnetism of rocks and the history of the geomagnetic field, Nature 168, 1111–1112

Hospers, J. (1954). Rock Magnetism and Polar Wandering. Nature, 173, 1183-1184.

Johnson, N. M. & McGee, V. E. (1983). Magnetic polarity stratigraphy: stochastic properties of data, sampling problems, and the evaluation of interpretations. Journal of Geophysical Research, 88(B2), 1213–1221.

Kirschvink, J. L. (1980). The least-squares line and plane and the analysis of palaeomagnetic data, Geophys. Journal of the Royal Astronomical Society 62, 699–718.

Kuiper, K. F., Deino, A., Hilgen, F. J., Krijgsman, W., Renne, P. R., & Wijbrans, J. R. (2008). Synchronizing rock clocks of Earth history. Science, 320(5875), 500-504.

Langereis et al., 1989. Langereis, C. G., Linssen, J. H., Mullender, T. A.T. & Zijderveld, J. D. A. (1989). Demagnetisation. In: David E. James (editor), The Encyclopedia of Solid Earth Geophysics.Van Nostrand Reinhold Company, New York, USA.

Langereis, C. G., Krijgsman, W., Muttoni, G. & Menning, M. (2010). Magnetostratigraphy –concepts, definitions, and applications. Newsletters on Stratigraphy, 43(3), 207–233.

Merrill et al., 1996 Merrill, R.T., McElhinny, M.W. & McFadden, P. L. (1996). The magnetic field of the Earth: palaeomagnetism, the core, and the deep mantle. International Geophysics Series, vol. 63, 531 pp. Academic Press, San Diego.

Opdyke, N. D., Channell, J. E.T. (1996). Magnetic stratigraphy. San Diego, USA: Academic Press, 346pp.

Pälike, H., & Hilgen, F. (2008). Rock clock synchronization. Nature Geoscience, 1(5), 282-282.

Roberts Artal, L., Biggin, A., MacNiocaill, C., de Wit, M., Langereis, C., Wilson, A., & Arndt, N. (2014). New palaeomagnetic results from outcrop and drill core samples of the 3.47 billion year old Komati Formation, Barberton Mountain Land, South Africa. In EGU General Assembly Conference Abstracts (Vol. 16, p. 6800).

Tauxe, L. (1998). Palaeomagnetic Principles and Practice, 299 pp., Kluwer Academic Publishers

Weiss, B. P., & Tikoo, S. M. (2014). The lunar dynamo. Science, 346 (6214), 1198-1198.

Zijderveld, J. D. A. (1967). AC demagnetization of rocks: analysis of results. Methods in paleomagnetism, 3, 254-286. Amsterdam, the Netherlands: Elsevier.

2.2. CYCLOSTRATIGRAPHY

Cyclostratigraphy is the branch in stratigraphy that deals with the description, analysis and interpretation of cyclic variations in the stratigraphic record and especially those that result from orbital climate forcing (Hilgen, 2010). Quasi-periodic changes in Earth's orbit produce changes in the total amount, the latitudinal and the seasonal distribution of insolation producing changes in the climate. Such climatic changes are found as cyclic changes in the sedimentary record and can be tuned to astronomical solutions that account for past insolation quantities. The astronomical parameters that affect insolation are: (1) Earth's orbital eccentricity e, which determines Earth-Sun distance, and thus total insolation; (2) Earth's axial tilt, or obliquity of the ecliptic ε, which determines the angle of incidence of insolation; and (3) the precession of Earth's rotation axis, or precession of the equinoxes, ψ which determines the timing and location of the seasons with respect to Earth's orbit (Hinnov, 2013; Fig. 2.2.1).

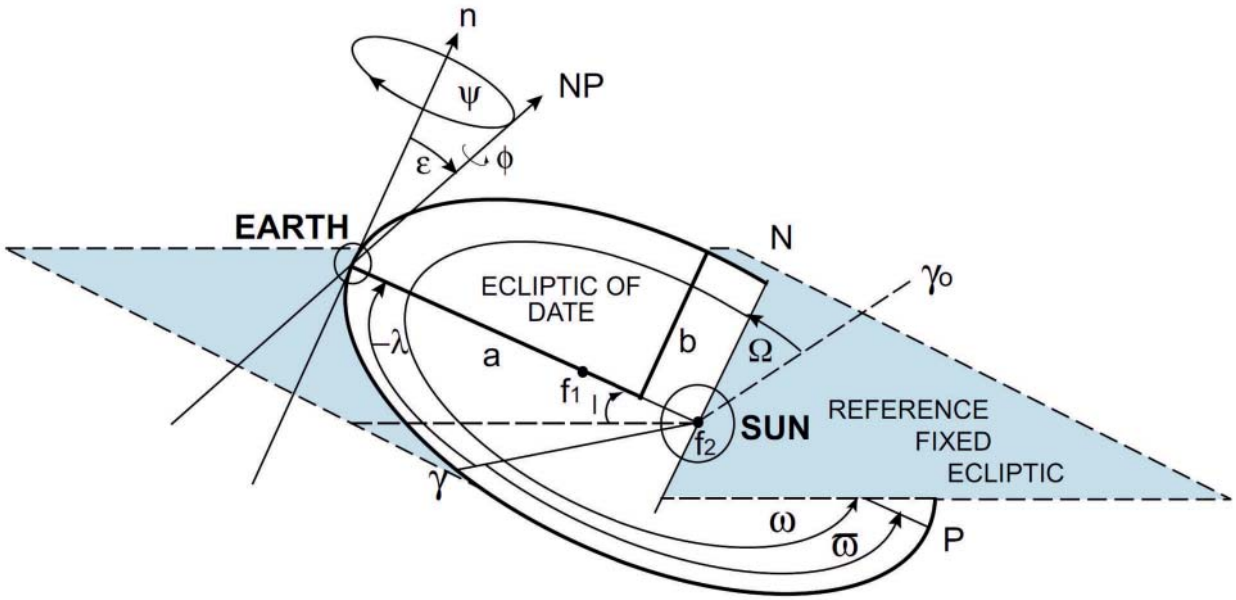

Figure 2.2.1. Earth's astronomical parameters are shown in a configuration near modern-day summer solstice, viewed from above the Northern Hemisphere. Earth's orbit is elliptical with major axis a and minor axis b. The Sun occupies one of the two foci (*f1,f2*). The orbital elements are eccentricity ($e=[a^2-b^2]^{1/2}/a$), longitude of perihelion ($\prod$), Inclination (I), and the longitude of the ascending node (Ω). The plane of Earth's orbit is the "ecliptic of date" that is inclined at an angle *I* relative to the "fixed reference ecliptic". It intersects the reference ecliptic at a longitude Ω at a point N, the ascending node, relative to a fixed vernal point γ_0. The orbital perihelion point P, measured relative to γ_0 as longitude of perihelion $\prod = \Omega + \omega$, in two planes, moves slowly counterclockwise. The argument of the perihelion ωmeasures the angular distance between P and N. The angle $\varpi = \prod + \psi$ tracks the moving vernal point γ relative to P, which moves clockwise along measured in the clockwise direction i.e., in the direction of Earth's path; here for clarity it is drawn in the opposite direction. Earth has a counterclockwise rotation rate ϕ and an obliquity of the ecliptic ε that precesses clockwise at rate ψ, NP is Earth's rotation axis ("North Pole"), and n is the normal to the ecliptic of date. Extracted from Hinnov (2013).

The Orbital Motions: a secular solution for insolation quantities.

Laplace (1973) and Lagrange (1776) provided the first secular calculations, which have been routinely improved until recent times, with the inclusion in the solutions of the outer planets and major asteroids,

and the relativistic effects (Varadi et al.2003; Laskar et al., 2004a; Laskar et al., 2011). The present long-term solution for the orbital and precessional elements (Laskar et al., 2004a; Laskar et al., 2011) uses an integration of the gravitational equations, the dissipative contributions, in particular in the evolution of the Earth-Moon system, and is presumably reliable over the last 40-50 million years (Laskar et al., 2004a; Laskar et al., 2011a). Such solutions provide precise calculations of the insolation quantities of the Earth, which are crucial for paleoclimatic studies and constitute an independent dating tool.

The principal periodicities of the present astronomical solutions for the most of the Cenozoic are: (1) the long and short eccentricity cycles, 405-kyr and ~100-kyr respectively, and the very long eccentricity cycle, 2.37-Myr; (2) obliquity that has a principal cycle of 41-kyr (39.8-kyr between 30-40Ma) with a large-amplitude modulation period of 1.2-Myr; (3) and the precession index ($e \sin \varpi$), which produces a signal strongly modulated by eccentricity, and presents a multiple-component variation that affects climate with major periods at 24-kyr, 22-kyr, and 19-kyr. Among these cycles the long eccentricity cycle (405-kyr) is considered the most stable of the prominent cycles, and is typically referred as the "405-kyr Metronome". The 405-kyr cycle is consequence of the orbital perihelia of Venus and Jupiter (g2-g5, Laskar et al., 2004a), which due to the large mass of Jupiter guaranties robust modeling of this cycle over many hundreds of million years (Laskar et al., 2011; Hinnov, 2013).

Geology and astronomical cycles

Astronomical tuning developed in consequence of the astronomical theory of ice-ages (Herschel, 1832; Adhemár, 1842; Croll, 1864; Hilgen, 2010). Milankovitch (1941) established his theory of the Earth's insolation parameters and hypothesized that glaciations occurred when Northern Hemisphere summer insolation was lowest. The development of accurate dating tools, mainly radioisotopic (Arnold and Libby, 1949) and paleomagnetic methods (Harrison and Funnell, 1965) together with the development of reliable proxies for paleoclimatic studies (Emiliani, 1955) allowed for independent tests of Milankovitch theory, finally firmly established after Hays et al., (1976). Today, the Geologic Time Scale 2012 (Gradstein et al., 2012) utilizes an absolute astronomical time scale (ATS) to calibrate much of Cenozoic time, and numerous multimillion-year-long "floating" ATS intervals in the Mesozoic time scale (Hinnov and Hilgen, 2012; Hinnov, 2013)

Tuning sedimentary records to the astronomical solutions

In order to perform astrochronologic correlations it is necessary to extract the climatic signal from the sedimentary record. This is carried out by means of proxy variables, which descript target variables (parameters) such as temperature, carbon concentration, or paleoenvironment. A reliable proxy, for example, is $\delta 18O$, which reflects paleotemperatures and ice volumes (Bintanja and van de Wal, 2008). In this thesis, we use the stratigraphic variations in lithology in order to assess paleoenvironmental changes driven by orbital forcing. With this aim we performed ranks of sedimentary facies as a function of their paleoposition (paleoenvironment) within the basin. This is a qualitative distinction that may underestimate high-frequency variations. Despite this, the ranks of facies integrate most of the changes occurred in a record including the lateral changes, and for long or very long records filters stochastic noisy signals. The sampling density is required to be higher than the Nyquist frequency (1/2 x sample interval), which is the limit to the highest frequency information that can be obtained from real data. In depth domain (stratigraphic thickness) the sampling density relies on the assessment of sedimentary rates. We oversampled most of the studied intervals in order to detect frequencies >10-kyr, where the primary temporal control was provided by magnetostratigraphy.

Once the proxy is extracted from the bulk record, it is necessary to search for recurrent frequencies by means a statistical assessment to know whether they are driven or not by the orbital oscillations. This is carried out using different methods for time-series analysis. Spectral analysis is performed by means

of the Fourier series analysis, currently FFT (fast calculation methods). A number of programs perform spectral analysis, many of them including different methods. We normally made spectral analysis in depth domain (thickness) using the Analyseries and later the Redfit programs (Paillard et al., 1996; Schulz and Mudelsee, 2000). In Analyseries we preferently used the Blackman method, which allows good accuracy, and later, the Redfit analysis that permits an accurate estimate of red noise, which is basic for assessing the reliability of the lower frequencies.

The correlation of sedimentary cycles to the astronomical solutions is typically performed with the Analyseries software. By selecting an astronomical target and a stratigraphic data file, and using the Linage (Splinage) tool, Analyseries permits to visualize and correlate the two together. After this step, it is necessary to establish a statistical assessment of whether the correlation is actually appropriate (Hinnov, 2013). A number of procedures to test the reliability of the tuning exist. The "minimal tuning" method (Muller and MacDonald, 2000; Machlus et al., 2008) have been widely used with success. We princi-

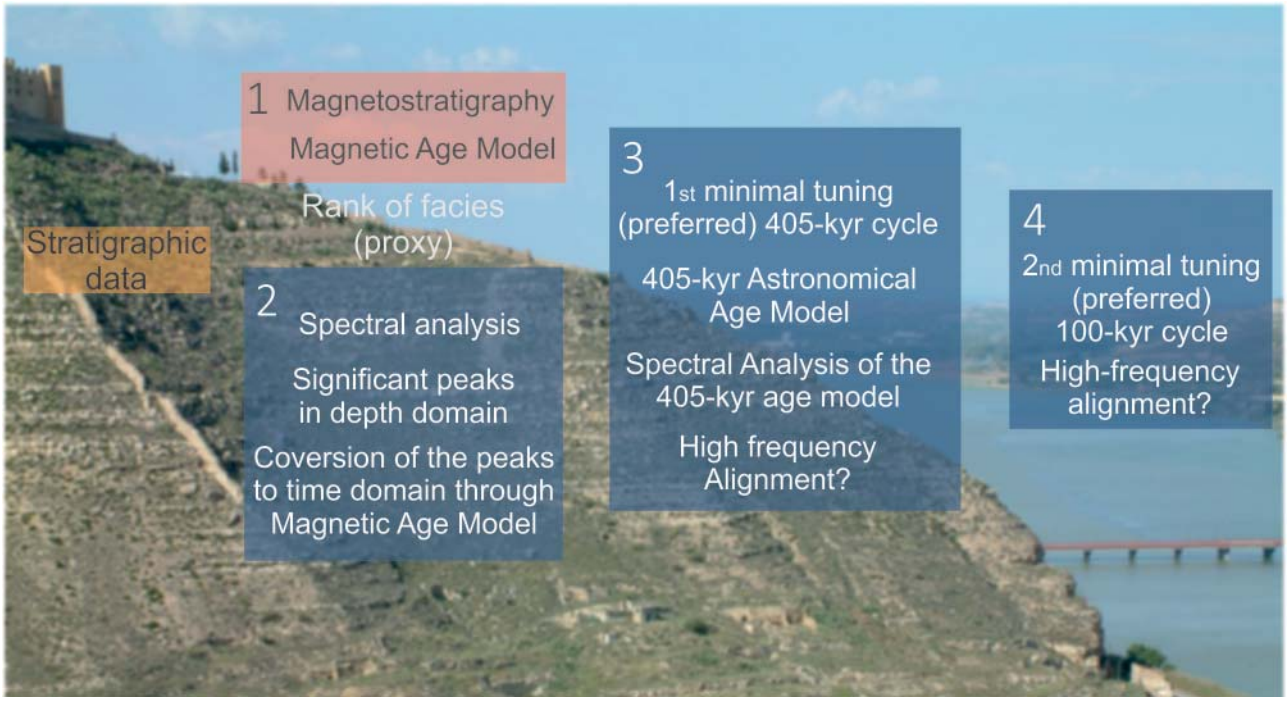

Figure 2.2.2 Summary of the methods used to obtain astronomical age models for the studied basins. Principally, this workflow is a variation of the "minimal tuning" method (Muller and MacDonald, 2000) using magnetochronological constraints.

pally used this method, which consists into tune data to a single astronomical frequency, and assess the success or failure of the tuning to realign other astronomical terms. We identified and converted to time domain the significant (>90/95/99% confidence) spectral peaks in the depth domain (thickness) by means of magnetostratigraphic age models. Subsequently, a tuning to the orbital solution was achieved by means of the 405-kyr cycle, because of its spectral power, stability through time, and because is an order the magnitude above the minimal resolution of magnetostratigraphy (10^3 yr). Finally, a positive realignment of higher-frequency cycles such as the short eccentricity, obliquity or precession, indicates an improvement of the age model, and thus a successful astrochronology (Fig. 2.2.2).

Other statistical methods are (1) the "average spectral misfit" (Meyers and Sageman, 2007; Meyers, 2008; Meyers et al., 2012) that evaluates the fit of stratigraphic data to an astronomical target spectrum while comprehensively evaluating a range of plausible sedimentation rates; (2) the "Bayesian Monte Carlo" method (Malinverno et al., 2010), which is used to search for the sedimentation rate that maximizes

spectral power at the astronomical frequencies; (3) Depth-derived time scale modeling (Huybers and Wunsh, 2004; Huybers, 2007; Aswasereelert et al., 2013), relies upon cyclostratigraphic data series collected from different sections of a given time interval, and the availability of independent time control (Hinnov, 2013).

References

Adhémar, J.A. (1842). Révolutions de la mer, déluges périodiques. Private edition, Paris.

Arnold, J.R. & Libby, W.F. (1949). Age determinations by radiocarbon content: checks with samples of known age. Science, 110, 678–680.

Aswasereelert, W., Meyers, S. R., Carroll, A. R., Peters, S. E., Smith, M. E., & Feigl, K. L. (2013). Basin-scale cyclostratigraphy of the Green River Formation, Wyoming. Geological Society of America Bulletin, 125(1-2), 216-228.

Bintanja, R., & Van de Wal, R. S. W. (2008). North American ice-sheet dynamics and the onset of 100,000-year glacial cycles. Nature, 454(7206), 869-872.

Croll, J. (1864). XIII. On the physical cause of the change of climate during geological epochs. The London, Edinburgh, and Dublin Philosophical Magazine and Journal of Science, 28(187), 121-137.

Emiliani, C. (1955). Pleistocene temperatures. The Journal of Geology, 538-578.

Gradstein, F., Ogg, J.G., Schmitz, M.D., & Ogg, G.M. (2012). The Geologic Time Scale 2012: Amsterdam, Elsevier, 1144 p.

Harrison, C.G.A. & Funnell, B.M. (1964). Relationship of paleomagnetic reversals and micropaleontology in two late Cenozoic cores from the Pacific Ocean. Nature, 204, 566.

Hays, J.D., Imbrie, J., Shackleton, N.J. (1976). Variations in the Earth's orbit: pacemaker of the ice ages. Science 194, 1121–1132.

Herschel, J. F. W. (1832). XVII.—On the Astronomical Causes which may influence Geological Phænomena. Transactions of the Geological Society of London, (2), 293-300.

Hilgen, F. J. (2010). Astronomical dating in the 19th century. Earth-Science Reviews, 98(1), 65-80.

Hinnov, L.A., and Hilgen, F.J. (2012). Chapter 4: Cyclostratigraphy and astrochronology, in Gradstein, F., Ogg, J., Ogg, G., and Smith, D., eds., A Geologic Time Scale 2012: Amsterdam, Elsevier, p. 63–83.

Hinnov, L. A. (2013). Cyclostratigraphy and its revolutionizing applications in the earth and planetary sciences. Geological Society of America Bulletin, 125(11-12), 1703-1734.

Huybers, P., & Wunsch, C. (2005). Obliquity pacing of the late Pleistocene glacial terminations. Nature, 434(7032), 491-494.

Huybers, P. (2007). Glacial variability over the last two million years: an extended depth-derived agemodel, continuous obliquity pacing, and the Pleistocene progression. Quaternary Science Reviews, 26(1), 37-55.

Lagrange, J. L. (1776). Oeuvres complètes, t. IV, Gauthier-Villars, Paris, France, 1869, 255

Laplace, P. S. (1773–1776). Oeuvres complètes, t. VIII, Gauthier-Villars, Paris, France, 1891, 199.

Laskar, J., Robutel, P., Joutel, J., Gastineau, M., Correia, A.C.M. & Levrard, B. (2004a). A numerical solution for the insolation quantities of the Earth: Astronomy & Astrophysics, v. 428, p. 261–285, doi:10.1051/0004-6361:20041335.

Laskar, J., Fienga, A., Gastineau, M. & Manche, H. (2011a). La2010: A new orbital solution for the long-term motion of the Earth: Astronomy and Astrophysics, v. 532, A89, doi:10.1051/0004-6361/201116836

Machlus, M. L., Olsen, P. E., Christie-Blick, N., & Hemming, S. R. (2008). Spectral analysis of the lower Eocene Wilkins Peak Member, Green River Formation, Wyoming: Support for Milankovitch cyclicity. Earth and Planetary Science Letters, 268(1), 64-75.

Malinverno, A., Erba, E., & Herbert, T. D. (2010). Orbital tuning as an inverse problem: Chronology of the early Aptian oceanic anoxic event 1a (Selli Level) in the Cismon APTICORE. Paleoceanography, 25(2).

Meyers, S. R., & Sageman, B. B. (2007). Quantification of deep-time orbital forcing by average spectral misfit. American Journal of Science, 307(5), 773-792.

Meyers, S. R. (2008). Resolving Milankovitchian conztroversies: The Triassic Latemar Limestone and the Eocene Green River Formation. Geology, 36(4), 319-322.

Meyers, S. R., Siewert, S. E., Singer, B. S., Sageman,

B. B., Condon, D. J., Obradovich, J. D., Jicha, B. R., & Sawyer, D. A. (2012). Intercalibration of radioisotopic and astrochronologic time scales for the Cenomanian-Turonian boundary interval, Western Interior Basin, USA. Geology, 40(1), 7-10.

Milankovitch, M. (1941). Kanon der Erdbestrahlung und seine Anwendung auf das Eiszeitenproblem: Royal Serbian Academy, Section of Mathematical and Natural Sciences, Belgrade, 633 p. (and 1998 reissue in English: Canon of Insolation and the Ice-Age Problem: Belgrade, Serbian Academy of Sciences and Arts, Section of Mathematical and Natural Sciences, 634 p.).

Muller, R.A., & MacDonald, G.J. (2000), Ice Ages and Astronomical Causes: Data, Spectral Analysis, and Mechanisms: London, UK. Springer-Praxis, 318 p.

Newton, I. (1687). Philosophiæ Naturalis Principia Mathematica. Jussu Societatis Regiæ, London, UK.

Paillard, D., Labeyrie, L., & Yiou, P. (1996). MacIntosh program performs time series analysis: Eos [Transactions, American Geophysical Union], v. 77, p. 379.

Schulz, M., & Mudelsee, M. (2002). REDFIT: estimating red-noise spectra directly from unevenly spaced paleoclimatic time series. Computers & Geosciences, 28(3), 421-426.

Varadi, F., Bunnegar, B. & Ghil, M. (2003). Successive refinements in long-term integrations of planetary orbits. Astrophysical Journal 592, 620-630.

Weedon, G. P. (2003). Time-series analysis and cyclostratigraphy: examining stratigraphic records of environmental cycles. Cambridge University Press.

Chapter 3
Results

3.1. LONG-PERIOD ASTRONOMICAL FORCING IMPACT ON SEQUENCE GENERATION IN A FORELAND BASIN.

The Oligocene-Miocene sedimentary sequences of the Ebro Basin record the evolution of lacustrine systems during the late filling stages of the southern Pyrenean foreland. These lacustrine deposits show rhythmic lithological variations at different scales. Our aim was to test whether this sedimentary rhythmicity bears a causal relationship with the quasi-periodic Earth's orbital oscillations. We coupled a facies rank division, based on sedimentary models, and a magnetostratigraphy-based age model to build numerical time series that represents sedimentary sequences. Subsequently, we carried out a cyclostratigraphic analysis in order to unravel the peak frequencies that are represented in the sedimentary record.

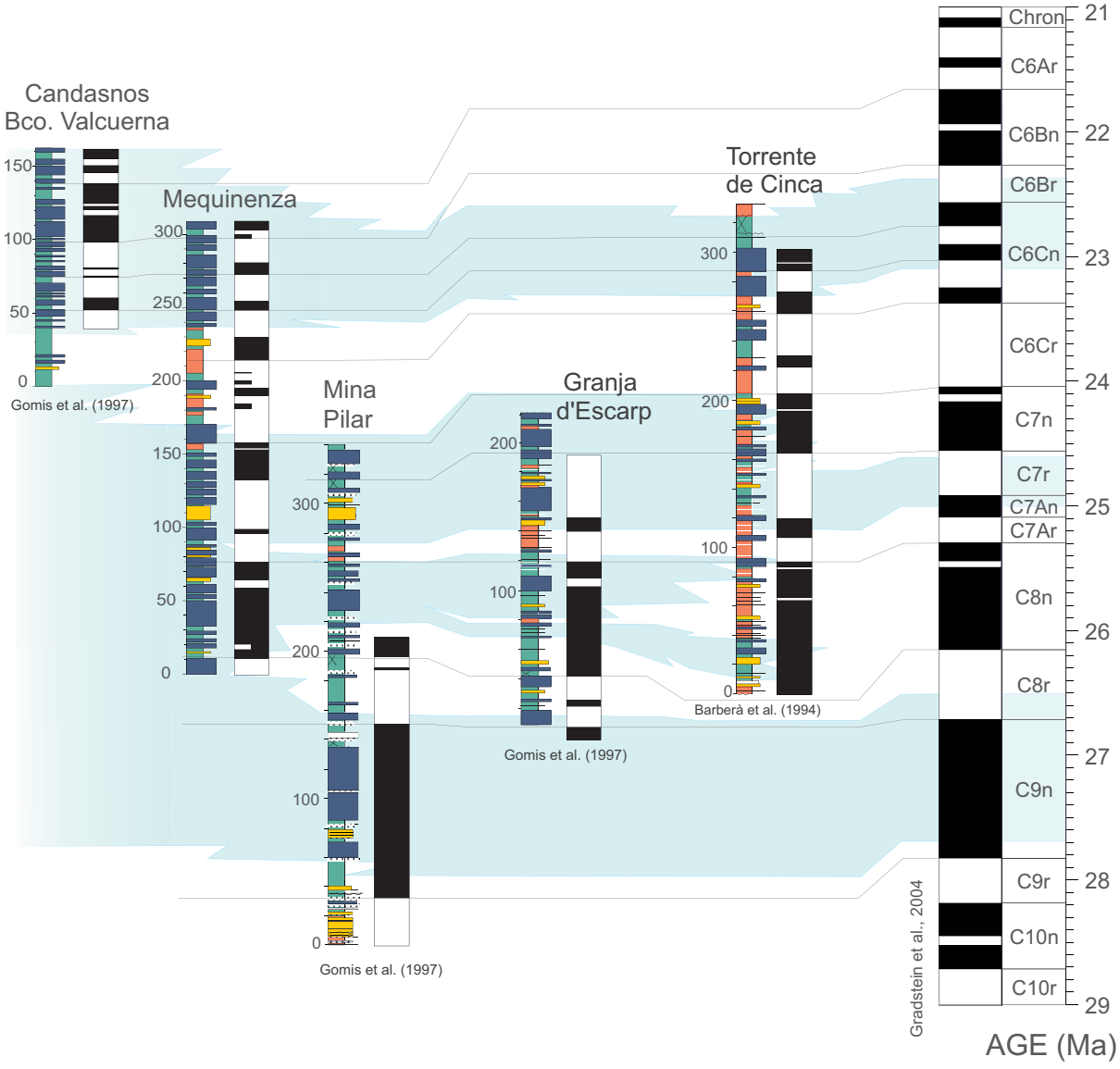

Figure 3.1.1. Integrated magnetostratigraphy of the MLS sequence in the Mequinenza area based on earlier works (Gomis et al., 1997; Barberà et al., 2001) and the present study. Multiple overlapping magnetostratigraphic sections allow an identification of a sequence of reversals that can be traced laterally, thus giving strong evidence of a primary magnetization. The blue-shade bands mark the lacustrine facies.

The facies rank division was performed after characterization of facies and facies associations following the depositional models of Cabrera (1983). The resulting depth rank time series is taken as a close representation of the evolution of the water volume of the overall lake system. High-frequency oscillations of the lake levels are thought to be caused by variations in the precipitation/evaporation ratios, and therefore can be used as a climatic proxy.

A magnetostratigraphy was built in order to obtain an age model for the Mequinenza section. To achieve this, the local magnetostratigraphy was correlated with earlier magnetostratigraphic results spanning the complete Mequinenza and Torrente de Cinca Formations (Barberà et al., 2001; Gomis et al., 1997). The resulting composite section was correlated to the Geomagnetic Polarity Time Scale (Fig. 3.1.1; Gradstein 2004; Gradstein 2012).

Spectral analyses in the depth (thickness) domain of the depth-rank time series revealed principal peaks matching the ratios of the principal components of the Milankovitch periodicities. After calibration with the magnetostratigraphic age model, spectral analysis in time domain revealed a principal component around 405-kyr, which we associate with the Earth's long eccentricity cycle (Laskar et al, 2004). A Gaussian band-pass filter of periods shorter than 20 m was applied to the time series in the stratigraphic domain in order to enhance the signal of the 405-kyr cycle. This periodicity was then tuned to the 405-kyr component of the eccentricity solution (Fig. 3.1.2; Laskar et al., 2004). The tuning was achieved by correlating the lacustrine maxima to the maxima of the eccentricity, which was the best solution according to the magnetostratigraphic constraints.

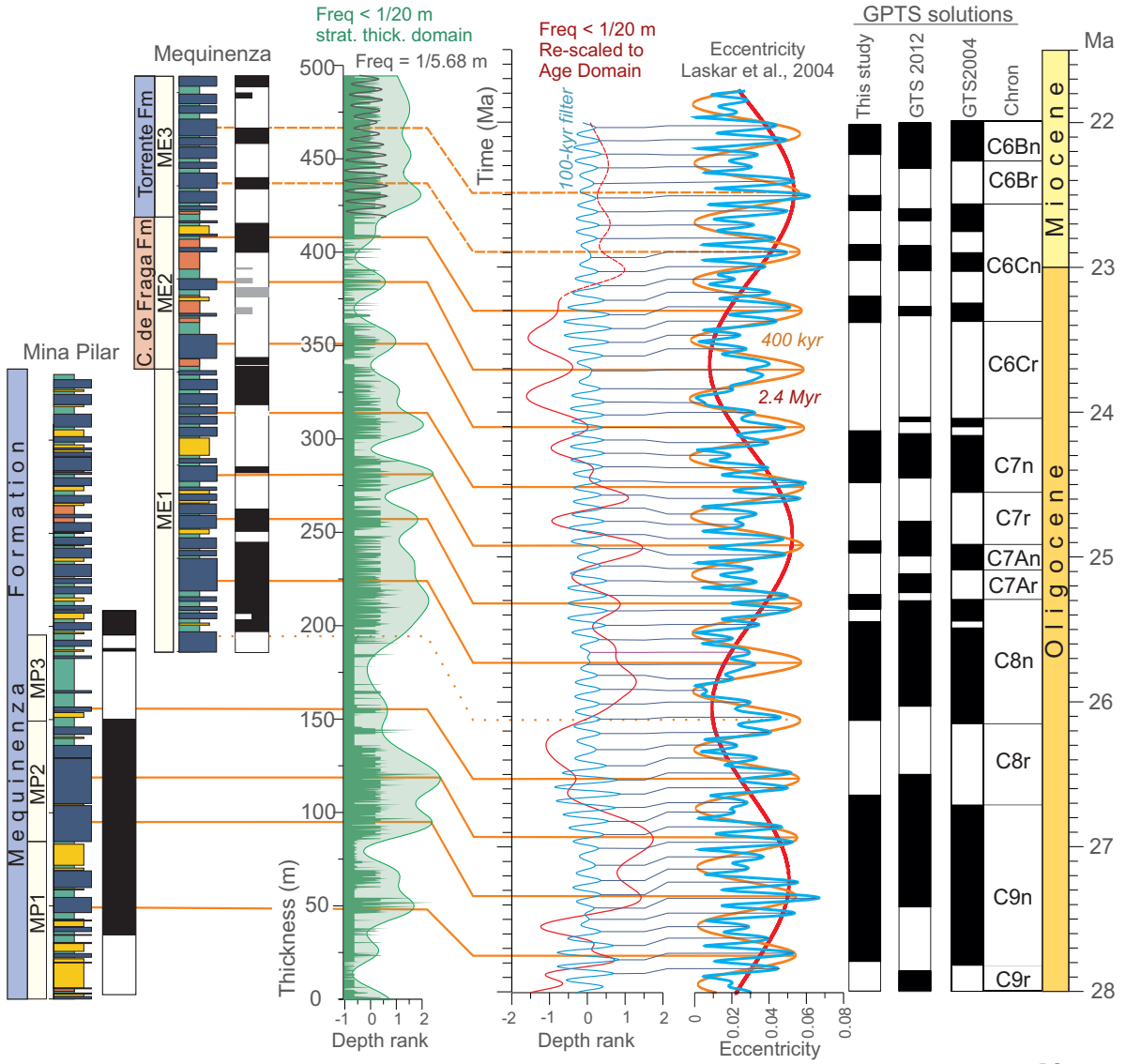

Figure 3.1.2. Astrochronology of the MLS stratigraphic sequence. In the left, the stratigraphic logs are divided into 6 intervals according to the lithology. In green, the inferred bathymetry of the lake with an envelope, which removes frequencies <20m. The filtered signal revealed a long-wavelength oscillation associated to the 2.4-Myr eccentricity cycle, where eccentricity maxima correlate to peaks of lake expansion. Superposed to this trend, a higher frequency signal is interpreted as the expression of the 400-kyr eccentricity cycle. Analyseries software (Paillard et al., 1996) was used to link the filtered paleobathymetry series with the 400-kyr eccentricity cycle of the astronomical solution (Laskar et al., 2004). In the middle, the resulting time series was rescaled into age domain (red line) and a Gaussian filter centered at 100 kyr (bandwidth 0.00165) was applied. The output (blue) was linked to the 100-kyr eccentricity term of the astronomical solution. In the right, the age of geomagnetic reversals that results from this analysis is compared with most recent calibrations of the time scale (Gradstein et al., 2004; 2012).

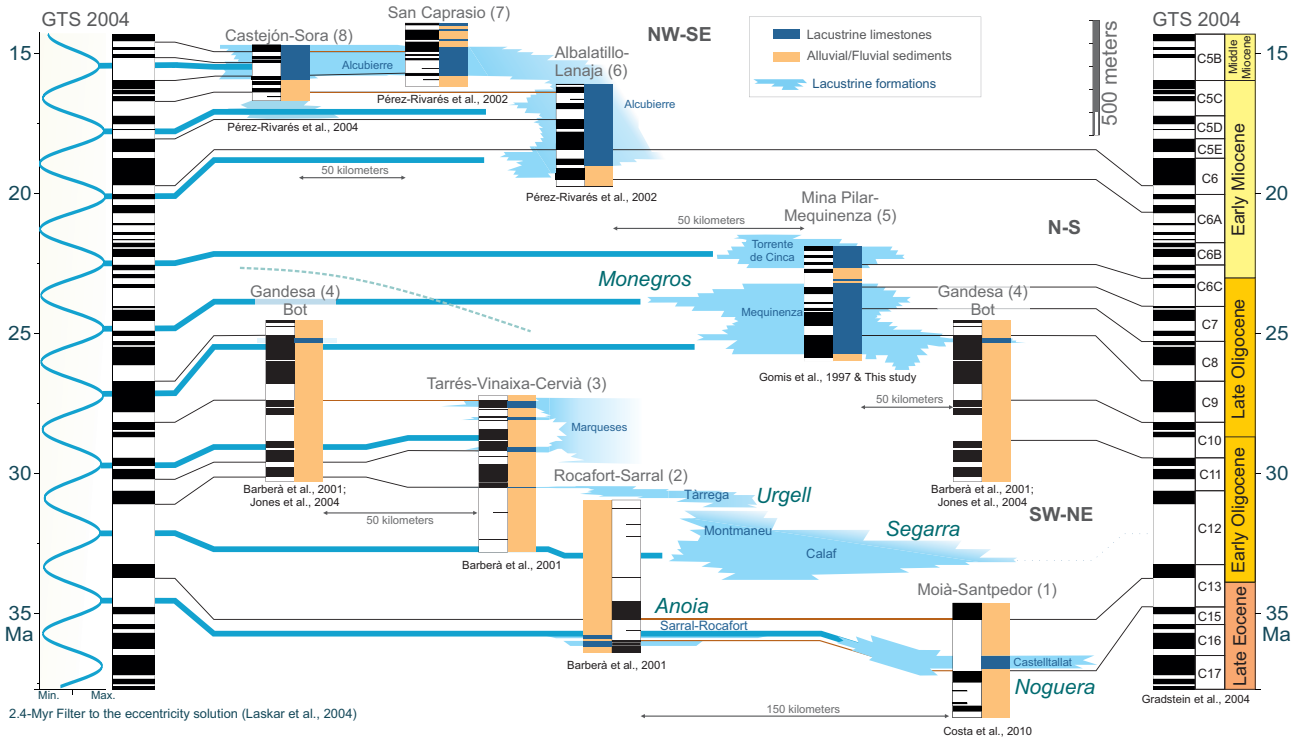

Figure 3.1.3. A magnetostratigraphy-based chronostratigraphy of the continental record of the eastern (bottom panel) to central (top panel) Ebro foreland basin. In the left, a 2.4-Myr band-pass filter of the eccentricity solution (Laskar et al., 2004) and the GPTS (Gradstein et al., 2004). Blue lines mark peaks of 2.4-Myr eccentricity maxima. In the middle, magnetostratigraphy and synthetic lithostratigraphy of key-sections, with indication of lacustrine (dark blue) and alluvial/fluvial sediments (brown). The lateral extent of lacustrine formations (light blue) is based on field correlations (Anadón et al., 1989; Arenas and Pardo, 1999; Barberà et al., 2001), and are faded out to mark the end of lateral control.

Spectral analyses of the time series after tuning with 405-kyr eccentricity age model showed an enhanced alignment of peaks near the 100-kyr band. Such alignment suggests than an improvement in the age model after astronomical tuning, which confirms the astronomical forcing hypothesis. In some intervals, especially those embracing the lacustrine facies, the impact of the obliquity and precession was also revealed.

Apart from the 100-kyr and 400-kyr cyclicity, the band pass-filter in the depth domain also revealed a lower frequency component, which was identified as the 2.4-Myr eccentricity cycle. The maxima of 2.4-Myr eccentricity cycles are associated to major expansions of the lacustrine system, whereas major lacustrine retractions occurred during minima of the 2.4-Myr eccentricity cycle.

A magnetostratigraphic age control is available for the complete continental Ebro record which permitted to examine the impact of the 2.4-Myr eccentricity cycle in the sedimentation. All available data were integrated into a single stratigraphic panel (Fig. 3.1.3). In this panel a progressive southwards migration of the

lacustrine systems is observed, as a consequence of the evolution of south-Pyrenean orogenic wedge and its control on sediment supply and subsidence. Added to this long-term subsidence-driven trend, rhythmic expansions of the lacustrine systems correlate with maxima of the 2.4-Myr eccentricity cycle (Fig. 3.1.3).

Despite the important paleogeographic rearrangements in the Mediterranean region and the high-amplitude global climate shifts during the Oligocene and Miocene, in the Ebro Basin, lake environments remained paced by the orbital eccentricity. Times of lake expansion representing relatively wet periods are correlated to eccentricity maxima. This phase-relationship is shared with most of Neogene Mediterranean basins. These conclusions are reached in the context of a foreland basin, where million-year scale sedimentary sequences are often interpreted as of tectonic origin. Discerning between long-period orbital cycles and tectonic-driven sequences is revealed as a fundamental issue in interpreting the large-scale stratigraphic architecture in foreland systems. A decoupling between tectonically-forced clastic sequences and climate-forced lacustrine sequences arises as a plausible scenario.

References

Anadón, P., Cabrera, L., Colldeforns, B., & Sáez, A. (1989). Los sistemas lacustres del Eoceno superior y Oligoceno del sector oriental de la Cuenca del Ebro. Acta Geologica Hispanica, 1989, vol. 24, num. 3-4, p. 205-230.

Arenas, C., & Pardo, G. (1999). Latest Oligocene–Late Miocene lacustrine systems of the north-central part of the Ebro Basin (Spain): sedimentary facies model and palaeogeographic synthesis. Palaeogeography, Palaeoclimatology, Palaeoecology, 151(1), 127-148.

Barberà, X., Cabrera, L., Marzo, M., Parés, J. M., & Agustí, J. (2001). A complete terrestrial Oligocene magnetobiostratigraphy from the Ebro Basin, Spain. Earth and Planetary Science Letters, 187(1), 1-16.

Cabrera, L., 1983. Estratigrafía y Sedimentología de las formaciones lacustres del tránsito Oligoceno–Mioceno del SE de la cuenca del Ebro. PhD Thesis. Univ. de Barcelona, Barcelona.

Gomis, E., Parés, J.M., Cabrera, L., 1997. Nuevos datos magnetoestratigráficos del tránsito Oligoceno–Mioceno en el sector SE de la Cuenca del Ebro (provincias de Lleida, Zaragoza y Huesca, NE de España). Acta Geol. Hisp.32, 185–199.

Gradstein, F.M., Ogg, J.G., Smith, A.G., 2004. A Geologic Time Scale 2004. Cambridge University Press, Cambridge, UK.

Gradstein, F.M., Ogg, J.G., Schmitz, M., Ogg, G., 2012. The Geologic Time Scale 2012 2-Volume Set. Elsevier

Laskar, J., Robutel, P., Joutel, F., Gastineau, M., Correia, A.C.M., Levrard, B., 2004. A long-term numerical solution for the insolation. Astron. Astrophys.285, 261–285.

Paillard, D., Labeyrie, L., Yiou, P., 1996. Macintosh program performs time-series analysis. Eos Trans. AGU77, 379.

3.2. LINKING SEDIMENTATION RATES AND LARGE-SCALE ARCHITECTURE FOR FACIES PREDICTION IN NONMARINE BASINS

The Almazán Basin is located in the north central Spain, amidst the Duero and the Ebro basins. The basin presents an outstanding exposure of the alluvial, fluvial and lacustrine sediments of Paleogene age. Existing chronostratigraphic constrains were limited to a reduced number of mammal fossil sites which indicate a middle-late Eocene age for the older units. Our aim was to obtain a chronologic framework for the complete Paleogene record of the basin by means of magnetostratigraphy. Subsequently, we focused on understanding the relationships between sedimentation rates and the large-scale architecture of the depositional elements. We collected samples from 269 sites through the alluvial Almazul, lacustrine Mazaterón and fluvial Gómara formations, comprising a total thickness of 2700 m. A local magnetostratigraphy was built and subsequently correlated to the GPTS (Fig. 3.2.1; Gradstein et al., 2012).

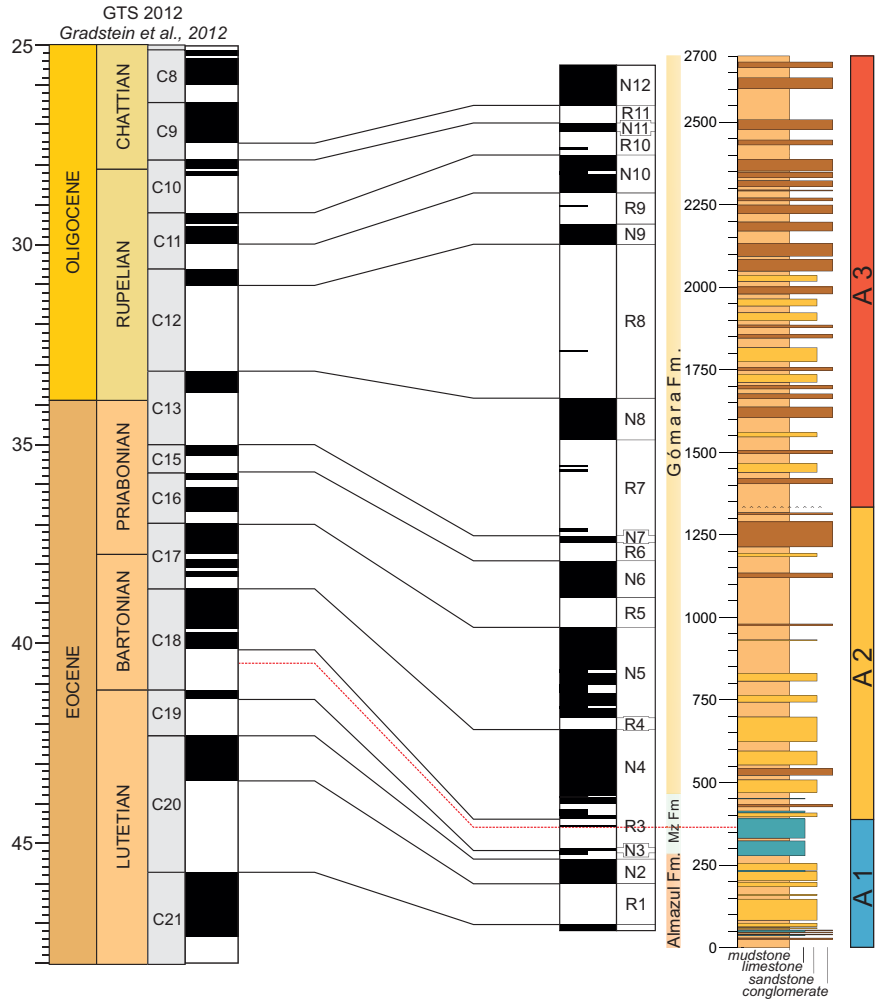

Figure 3.2.1. Correlation between the local magnetostratigraphic section of Almazán to the GPTS (Gradstein et al., 2012), including the formations and the depositional sequences of the Almazán Basin. The red line indicates the location of Miñana fossil site and its correlation with the GPTS.

The excellent lateral exposure of strata and the occurrence of remarkable key beds allowed for correlation of geomagnetic reversals across the basin and the mapping of derived isochrons (Fig. 3.2.2). The magnetostratigraphic map provides a robust temporal framework for all the features included in the map, as the Depositional Sequence division of the Almazán Basin. The results indicate that the Depositional Sequence A1 encompass from chron C21n to C18r, lasting ca. 5 Myr. Depositional Sequence A2 comprises from

chron C18r to chron C13r, with duration of 5.8 Myr, and including most of the Bartonian and Priabonian Stages. Depositional Sequence A3 lasts 6.6 Myr, from chron C13r to chron C9n, comprising the end of Priabonian, Rupelian and part of the Chattian. The Eocene/Oligocene boundary is placed near the base of A3. In addition, the fossil sites located in the basin were dated. The Mazaterón mammal fossil locality (MP 15-16, Cuesta & Jiménez, 1994), in the lower part of the Mazaterón Formation, correlates to chron C18r (Lower Bartonian), in agreement with previous biochronological interpretations (Cuesta & Jiménez, 1994). The mammal fossil locality of Deza 2 (MP 17b, Badiola et al., 2009) is correlated with Chron C15r, at

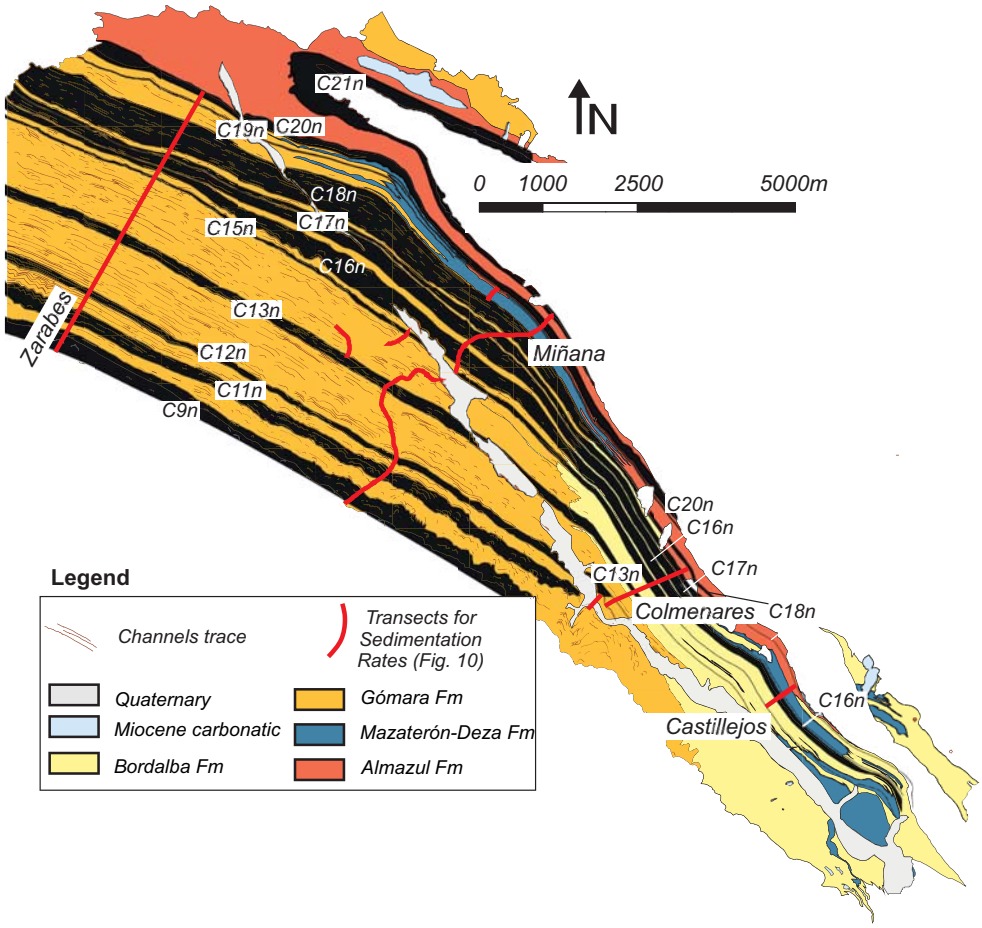

Figure 3.2.2. Magnetostratigraphic map of the Gómara monocline. Magnetic reversals had been extended through the monocline following traceable levels. Black bands mark the normal magnetic polarity intervals. The magnetostratigraphic sampling track has been marked and corresponds to the Almazul and Mazaterón sections, unified as Miñana transect in this figure. The other sections shown correspond to the ones where sedimentation rates were calculated (Fig. 3.2.3). Geological formations are included. A widening of the magnetic reversals towards the NW, where clastic formations dominate can be distinguished.

mid-Priabonian. A significant wedging of the units is observed southeastwards. The wedging represents changes in the sedimentation rates, and is mainly associated to changes in the subsidence patterns.

Earlier sedimentological analysis (Huerta et al., 2011) allowed for a classification of the different sedimentary systems in function of their large-scale architecture. In the fluvial system sand bodies range from ribbon-shaped channel fills with low interconnectivity to sheet-like channel fills with high interconnectivity. In the alluvial plains we recognized mudstones and evaporitic mudstones, and in the distal zones lacustrine/palustrine limestones and stacked calcretes. When the magnetostratigraphic results are combined with the large-scale architectural classification a relationship between sedimentation rates and the large-scale architecture is evidenced (Fig. 3.2.3).

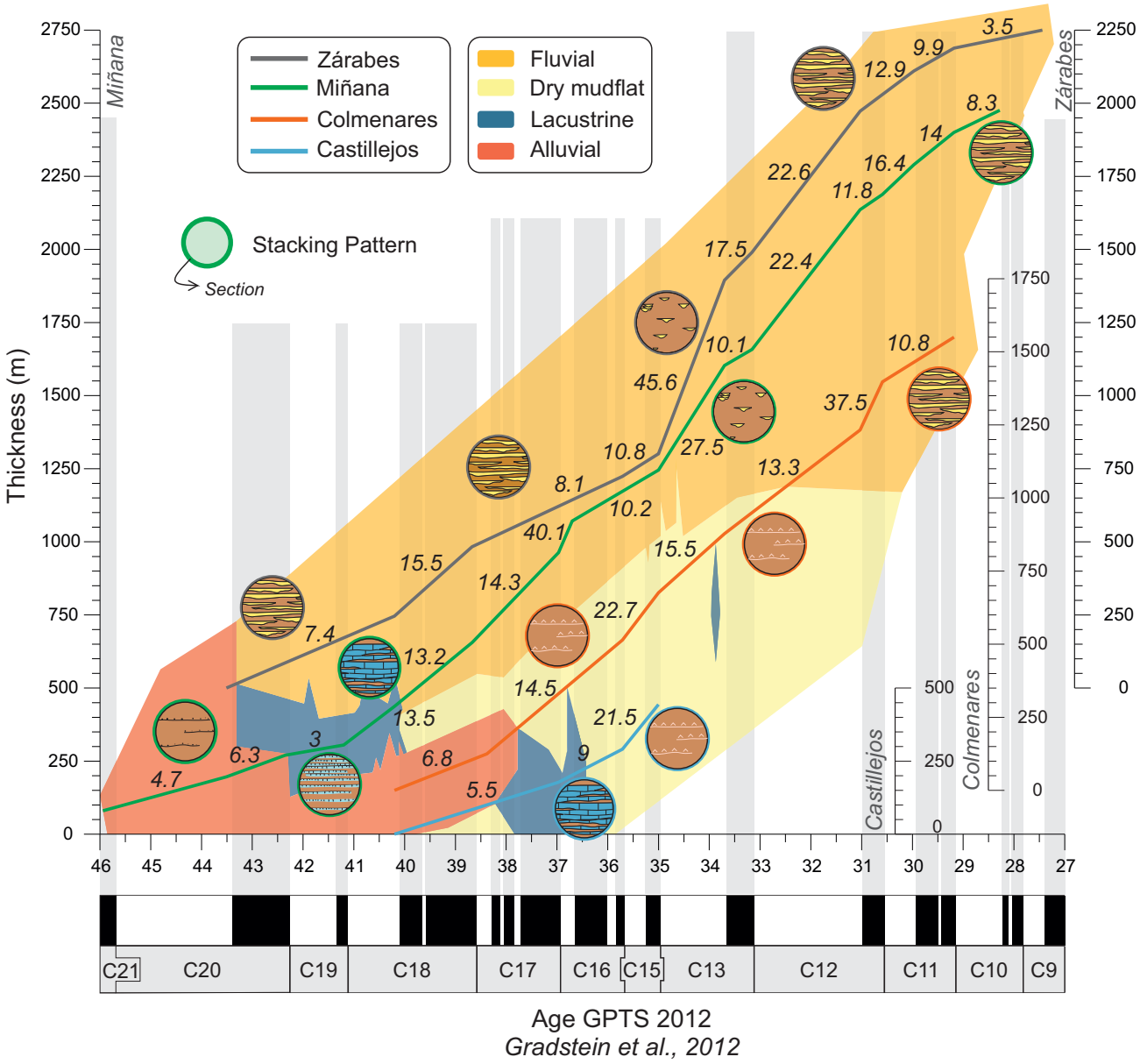

Figure 3.2.3. Sedimentation rates resulting from plotting stratigraphic thicknesses against magnetostratigraphic ages for four key transects (location in Fig. 3.2.2). These sections encompass the most characteristic formations and large-scale architectures of the Almazán Basin. Polygons indicate the sedimentary environments, which nearly coincide with the formations. The stacking pattern is drawn in circles, and its perimeter colour indicates the section. The numbers refer to Sedimentation Rates, (in cm/kyr), and are calculated within magnetic reversals, which are the vertical underlying white or grey stripes. Each section has its own thickness coordinates origin, only for representative purposes.

The integration of all the results allows for a better understanding of the sedimentary evolution of the basin and its relation with the tectonics (Fig. 3.2.4). The principal controls on accommodation are related to the emplacement or evolution of structures both in the margins and within the basin. These structures controlled the subsidence patterns, and the paleocurrent distribution. The architecture of the large-scale depositional elements is determined by the ratio between accommodation and sediment supply, which can be seen as a marker of the mass-balance state in the basin. Changes in the mass-balance resulted into changes of the depositional elements. Locations developed under with high rates of sediment supply are characterized by fluvial to alluvial sedimentation. In this context, if accommodation is high, ribbon shaped channels with profuse fluvial flood plains with fine-grained sediments will occur. If accommodation is low,

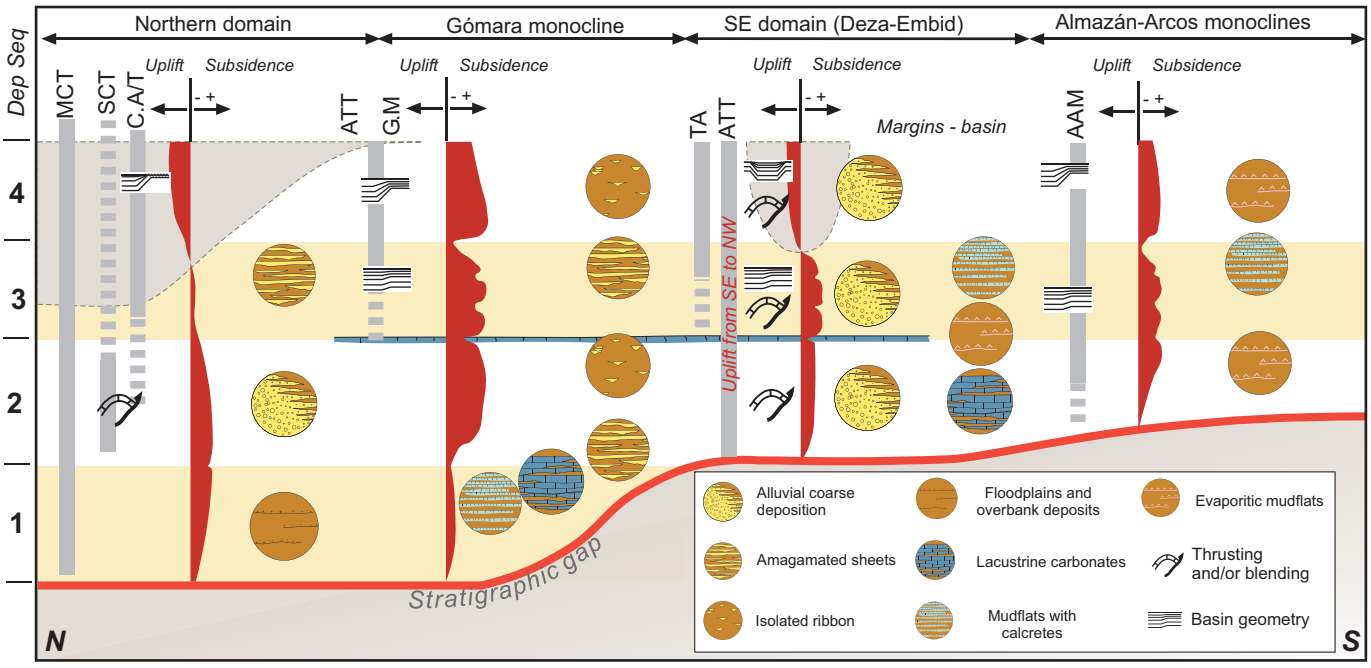

Figure 3.2.4. Summary of the evolution of tectonic uplift and subsidence for the four Paleogene tectonic domains during the four depositional sequences (right). Subsidence and uplift are estimated from the architectural arrangement. The syn-sedimentary styles and the development of alluvial fans as consequence of the uplift of nearby structures are shown. MCT, Main Cameros Thrust; SCT, South Cameros Thrust; CA/T, Cardejón Anticline/Thrust; ATT, La Alameda-Tapiela Thrust; GM, Gómara Monocline; TA, Torlengua Anticline; AAM, Almazán-Arcos Monoclines.

sheet-like amalgamated channels are frequent while preservation of flood plain deposits is low. On the other hand, in the context of low sediment supply, a range of large scale elements grading from lacustrine to palustrine and finally calcretes occur as accommodation decreases. Between these two contexts of high and low sediment supply areas, alluvial mudflats occur. Depending on the equilibrium of the accommodation space and sediment supply these areas vary between clayed mudflats to evaporitic mudflat.

References

Badiola, A., Hooker, J. J., Quer, R., Checa, L., Astibia Ayera, H., & Cuesta Ruiz-Colmenares, M. Á. (2009). The role of new Iberian finds in understanding European Eocene mammalian paleobiogeography. Geologica Acta, 7, 243-258.

Cuesta, M.Á. & Jiménez, E. (1994). Síntesis del Paleógeno del borde oriental de la cuenca de Almazán (Soria): vertebrados de Mazaterón. Stud. Geol. Salmatic., XXIX, 157–170.

Gradstein, F.M., Ogg, J.G., Schmitz, M., Ogg, G., 2012. The Geologic Time Scale 2012 2-Volume Set. Elsevier

Huerta, P., Armenteros, I., & Silva, P. G. (2011). Large-scale architecture in non-marine basins: the response to the interplay between accommodation space and sediment supply. Sedimentology, 58(7), 1716-1736.

3.3. LONG-PERIOD ASTRONOMICALLY-FORCED CARBON SINKS

The As Pontes Basin evolved in a transpressive tectonic context, in response to a NW-SE-oriented dextral strike-slip fault in NW Spain. The record shows an alternation between clayish coal levels and terrigenous sediments. A previous magnetostratigraphic study revealed a Late Oligocene to Early Miocene age for the complete sedimentary basin infill (Huerta et al., 1997). Our aim was to test astronomical forcing of the recurrent occurrence of the coal levels along the stratigraphic sequence. The As Pontes Basin and the Mequinenza area in the Ebro Basin contain sediments of same age which were deposited within the same climatic belt. Therefore, in the case that As Pontes coals were astronomically forced it would allow for a comparison with the Ebro Basin sedimentation trends. In addition, the As Pontes Basin represents an opportunity for understanding the effects of climate-driven sediment pulses in the sediment routing systems.

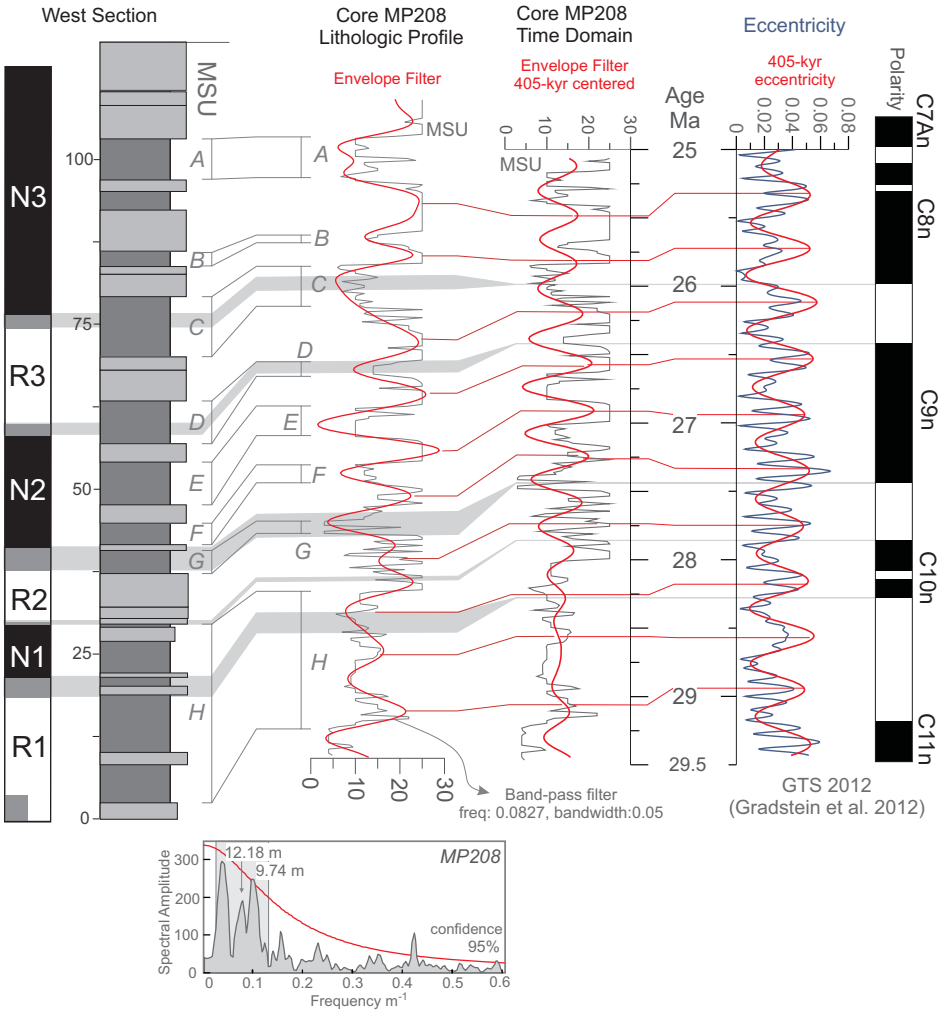

Figure 3.3.1. Phase relationship determination. At the left, the local magnetostratigraphy and the lithological log is shown. In the middle left, the facies record of Core MP208 is shown in the stratigraphic domain with the Gaussian band-pass filtered component in red superimposed (freq: 0.0827 cycles/m; bandwidth: 0.05). In the middle right, the borehole facies data of MP208 are shown in the time domain, using the magnetostratigraphic age model for conversion. Again the Gaussian band-pass filtered component of the 405-kyr cycle is shown. At the right, the eccentricity target curve (Laskar et al., 2004) is shown together with the filtered component isolating the 405-kyr eccentricity term. Red lines represent correlation lines that match maxima of the core data in the stratigraphic domain and maxima of the core data in the time domain, which are associated with clastic sediments, with successive 405-kyr eccentricity maxima. This is the unique correlation supported by the magnetochronologic age constraints.

Our first step was to review the previous magnetostratigraphic study (Huerta et al., 1997), whose main conclusions were here assumed except for the lowermost part of the section. We propose a new correlation of the lower part of the section around chron C10r. The new correlation to the GPTS 2012 (Gradstein et al., 2012) yields steadier and reliable sedimentation rates and better agrees with the existing biochronological constraints. The new chronological framework allows performing a cyclostratigraphic analysis.

A core database that includes core lithological descriptions from mining prospects is available. We classified these data as a function of their paleoenvironment interpretation using the criteria of Sáez et al., (2002; 2003). We selected 6 cores located in a central position in the basin in order to reduce the influence of tectonics and autogenic processes associated to the sediment transfer system. A lithologic correlation between the cores and the magnetostratigraphically dated section provided constrains for an integrated age model. Derived sedimentation rates show variable results depending on lithology, typically higher for the clastic intervals than for the coal-rich intervals. Despite the changes in sedimentation rates, spectral analyses in thickness domain revealed significant peaks for all the cores around 12 m. These peaks however, present a high dispersion and usually range from 20 to 8 m. Assuming the sedimentation rates from magnetostratigraphy, which oscillate between ca. 2.5 and 3.5 cm/kyr, these peaks fall within the range of the long orbital eccentricity cycle of 405-kyr.

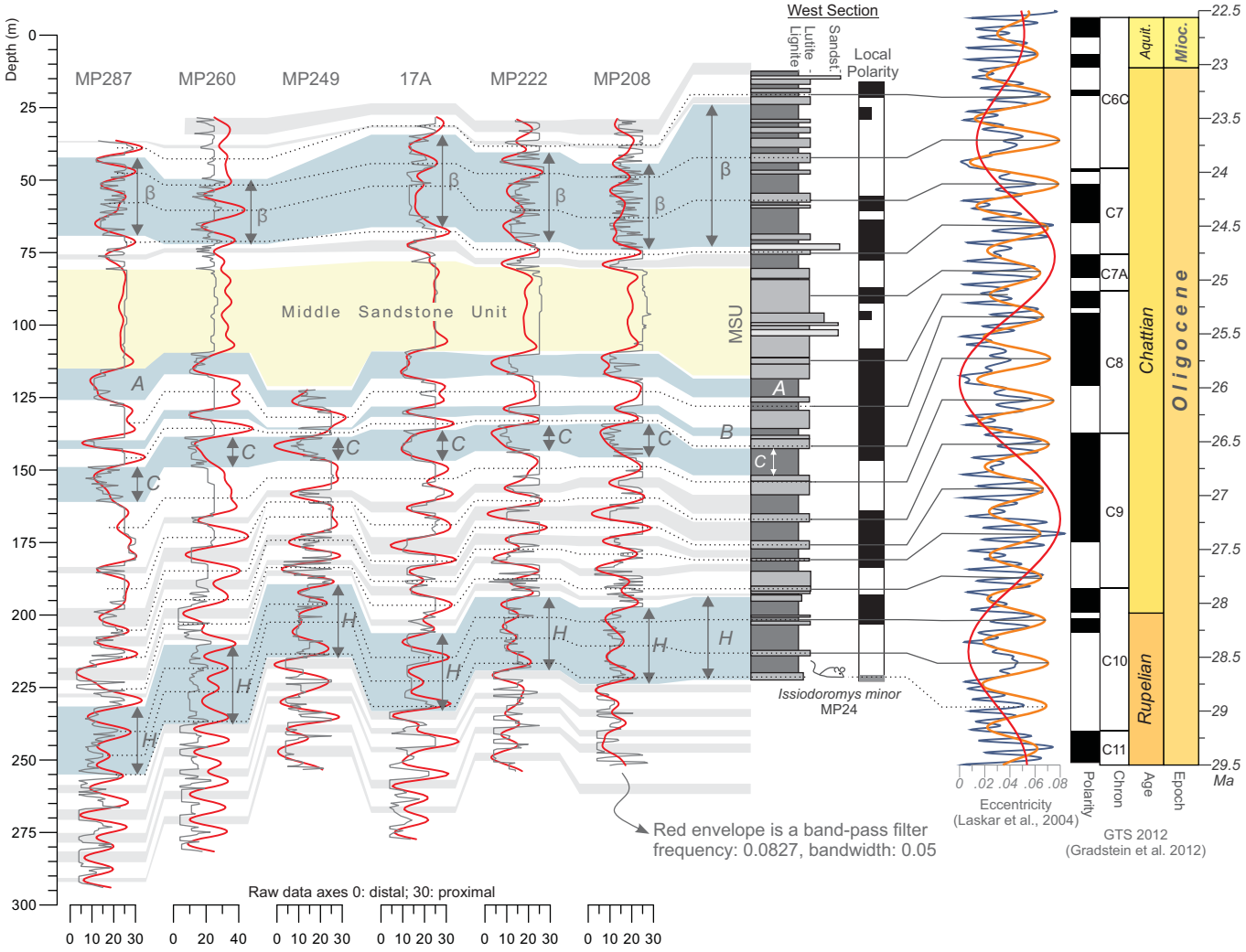

Figure 3.3.2. The six cores used for the cyclostratigraphic analysis are shown from left to right. The facies variability is shown per core as thin black lines below the core headings. The lithology and polarity data is adapted from Huerta et al. (1997). Superimposed on these lines, the red curves mark the bandpass-filtered component centred at 12.07 m, with a bandwidth of 0.05 m-1. The shifts from proximal to distal facies are correlated between all the cores, and finally to the West section. By means of magnetostratigraphy and the biochronological constraints, the West section is correlated to the GPTS of Gradstein et al. (2012). Horizontal (dashed) black lines indicate clastic pulses, which following the magnetostratigraphic age constraints are correlated to successive 405-kyr eccentricity maxima (Laskar et al., 2004). Horizontal grey shading indicates the extension of the distal facies from the cores to the West section. These coal-bearing seams are correlated to 405-kyr eccentricity minima. Bluish shading marks the stratigraphic intervals of the coal pits used with industrial purposes. These intervals correspond to 405-kyr eccentricity minima, within 2.4-Myr eccentricity minima.

We isolated these peaks by means of a wide Gaussian band-pass filter for the core MP 208. This filter was tuned to the 405-kyr cycle of the orbital solution (Laskar et al., 2004). Only the tuning of the coaly beds to the 405-kyr eccentricity minima and the terrigenous intervals to the maxima of the 405-kyr eccentricity cycle respects the magnetostratigraphic constraints (Fig. 3.3.1). The tuning provides an astronomical age model for the As Pontes Basin at a 405-kyr scale. In order to verify independently such age model we applied the Gaussian band-pass filter to all the cores (Fig. 3.3.2), and later we performed spectral analyses in the time domain for all the cores. The spectral analyses show an alignment of the peaks in the 100-kyr band for the most of the cores, which independently verifies the 405-kyr tuning. Apart of the 405-kyr cycles, the correlation shows that the principal coal levels correspond to maxima of the 2.4-Myr eccentricity cycles. The 2.4-Myr eccentricity cycle is a modulator of the 405-kyr eccentricity cycle and, principally, of the 100-kyr cycle. During a 2.4-Myr eccentricity minima, the amplitude range of the 100-kyr cycles reduces, which in turn also decreases the amplitude of precession, and thus insolation changes.

Prolonged periods marked by low-amplitude insolation changes during combined eccentricity minima cycles of the minima of 100-kyr and 405-kyr cycles span several tenths of thousands of years, and sustain relatively stable climatic periods that avoid extreme seasonal signals. We propose that these stable climatic conditions during eccentricity minima promoted that peatlands and their adjacent ecosystems fixed soils efficiently, thereby decreasing erosion of the surrounding reliefs (Corenblit et al., 2011). In turn, the resultant reduction in clastic sediment supply favoured peatland expansion in the basin. Conversely, during eccentricity maxima, and therefore high-amplitude precession, extreme maxima changes in seasonality during precession minima (for the Northern Hemisphere), will lead to the shrinking and fall of ecosystems and peatland decline.

Under stable climatic conditions and enhanced vegetation cover, the basin slope tends to approximate dynamic equilibrium, particularly in a very low-gradient continental basin. Geomorphologic stability also contributes to reduce erosional rates, and subsequently sediment input (Whipple, 2001; Castelltort and Van Der Driessche, 2003). These periods of stability are more pronounced during the 2.4-Myr eccentricity minima when such minima are combined, with minimum eccentricity associated with the 405-kyr, and 100-kyr cycles. During these orbital configurations, climatic stability can persist for about 50-60-kyr. The astronomical correlation shows that it is during these periods that the thicker peat layers that cover almost the entire basin accumulated.

Orbital forcing in the coal-bearing As Pontes basin is demonstrated by the correlation between coal-alluvial sequences and the eccentricity cycles of 405-kyr and 2.4-Myr. Orbital rhythms were transmitted to the sediment record by the coupling between stable and favourable climatic conditions, landscapes in equilibrium, and enhanced vegetation cover resilience. This suggests that even in small-sized tectonically active settings, the climatic signature can be found, and not necessarily driven by changes in the water balance. If the relationship between peatlands and long-term orbital forcing is shared with other mid-latitude basins,

a wide-range of sensitive environments needs to be considered as potential carbon reservoirs. The overall response of basins to climatic changes may constitute an important long-term agent of global cooling.

References

Castelltort, S., & Van Den Driessche, J., (2003). How plausible are high-frequency sediment supply-driven cycles in the stratigraphic record?: Sedimentary Geology, v. 157, p. 3–13, doi: 10.1016/S0037-0738(03)00066-6.

Corenblit, D., Baas, A.C.W., Bornette, G., Darrozes, J., Delmotte, S., Francis, R. a., Gurnell, A.M., Julien, F., Naiman, R.J., & Steiger, J., (2011). Feedbacks between geomorphology and biota controlling Earth surface processes and landforms: A review of foundation concepts and current understandings: Earth-Science Reviews, v. 106, no. 3-4, p. 307–331, doi: 10.1016/j.earscirev.2011.03.002.

Gradstein, F.M., Ogg, J.G., Schmitz, M., Ogg, G., 2012. The Geologic Time Scale 2012 2-Volume Set. Elsevier

Huerta, Á., Parés, J. M., Cabrera, L., Ferrús i Pinyol, B., & Sáez, A. (1997). Magnetocronología de las sucesiones cenozoicas de la cuenca de As Pontes (La Coruña, Noroeste de España). Acta geológica hispánica, 32(3-4), 127-145.

Laskar, J., Robutel, P., Joutel, F., Gastineau, M., Correia, A.C.M.& Levrard, B. (2004). A long-term numerical solution for the insolation. Astron. Astrophys.285, 261–285.

Sáez, A., & Cabrera, L., (2002). Sedimentological and palaeohydrological responses to tectonics and climate in a small, closed, lacustrine system: Oligocene As Pontes Basin (Spain): Sedimentology, v. 49, p. 1073–1094, doi: 10.1046/j.1365-3091.2002.00490.x.

Sáez, A., Inglès, M., Cabrera, L., & de las Heras, A. (2003), Tectonic-palaeoenvironmental forcing of clay-mineral assemblages in nonmarine settings: The Oligocene-Miocene As Pontes Basin (Spain): Sedimentary Geology, v. 159, p. 305–324, doi: 10.1016/S0037-0738(02)00333-0.

Whipple, K.X., 2001, Fluvial landscape response time: How plausible is steady-state denudation? American Journal of Science, v. 301, no. May, p. 313–325, doi: 10.2475/ajs.301.4-5.313.

Chapter 4
Discussion

THE UPSTREAM AND DOWNSTREAM IMPACT OF MILANKOVITCH CYCLES IN CONTINENTAL NONMARINE SEDIMENTARY RECORDS.

Researchers have acquired a high comprehension of the sedimentary systems dynamics by means of field data and analogical and numerical modelling. In recent times, an especial emphasis has been given to the understanding of the full itinerary of the sediments from source to sink. This is principally motivated by the fact that sinks are witnesses of the processes involved in the evolution of the catchments and transfer areas (Romans et al., 2015). Studies of historical ($<10^3$) sedimentary records aim at explaining the processes acting at short temporal scales. However, a longer temporal perspective is needed to have a full comprehension of the dynamics of sedimentary systems. Long-term processes (10^3-10^6) are fundamental as are the principal carver of the sedimentary record. Continental basins, especially lacustrine records, are considered reliable archives of Earth's orbit oscillations. Conciliation between the state of the art of the different disciplines is required in order to understand the different processes involved in the expression of the Milankovitch cycles in the sedimentary records. At the same time, the characterization of the processes through which climate affects the sedimentary systems behaviour is a necessary part of the source to sink studies. In this section, the significance of the results obtained in this thesis are combined and compared to other records. Finally, a discussion about the different possible pathways in which Milankovitch cycles can be displayed in the lithological cycles of endorheic records is presented.

Summary of the results of the Ebro and As Pontes basins

In the Ebro Basin (Valero et al., 2014), the location of the lacustrine depocenters was conditioned by the migration of the subsidence distribution due to the thrust-belt structuring and the subsequent foreland evolution. Despite tectonics, the superimposed signal of climate was found to be the main cause of lake level variation. Times of orbital eccentricity maxima are associated to lake level highstands, indicating a positive water balance. Intervals with high-amplitude precession cycles, due to eccentricity modulation, are seen as the drivers of water recharge. The buffering effect of the transfer system (Castelltort and Van Der Driesche, 2003) is invoked to explain the lack of a clear expression of tectonic events propagated basinwards. Likewise, changes in the source areas driven by climatic shifts were damped downstream, and blurred towards the distal parts of the basin.

Oppositely to the Ebro Basin, the As Pontes Basin is a small basin that lacked a central lake system during the studied interval. Without the buffering effect of a lengthy sediment transfer system, any change in the source areas can be readily transmitted downstream. The occurrence of peatlands in the distal parts, made the system very sensitive to shifts in the terrigenous input. In As Pontes, it has been shown that climatic stability at times of eccentricity minima appears associated to peat development and burial. This is likely more linked to resilient vegetation cover and equilibrium geomorphologic profiles, which reduced the sediment supply (Valero et al., submitted). The cyclic arrangement in the depocenters was shaped by changes in the sediment supply, which may increase, and dilute the accumulation of organic matter, rather than by variable lake level. Despite there is not enough resolution as to test for precession or obliquity, the stacking pattern shows no evidence of these higher frequency orbital cycles. It suggests a control of eccentricity on the expression of orbital forcing in a clastic-dominated system.

The upstream and downstream transmission of tectonics and climate to sedimentary records

The analysis carried out in the Almazán Basin (Valero et al., 2015) illustrates how the distribution of the depositional elements, their internal architecture, and the sedimentation rates are consequence of variations in the AS/SS ratio (Accommodation/Sediment supply; Strong et al., 2005). This makes the AS/SS ratio an excellent marker for the mass balance variations, the distribution of the total volume of sediment along a basin, allowing for a quantification of the response of a basin to extrinsic changes, which are mainly climate and tectonics. Although if a single depositional element is analysed at short time scales, the ratio also may include the autogenic variations.

Tectonic influence in the AS/SS ratio

Despite the occurrence of discrete thrust-sheet emplacement events, the orogenic shortening and loading are thought to be continuous on time, as might be predicted from the general steadiness of plate convergence velocities and from critical taper theories of orogenic wedges (DeCelles and Giles, 1996). Hence, tectonics is principally significant in the generation of basin sequences at a million year range (Petersen et al., 2010; Miall et al., 2014), and at shorter time scales in proximal settings in which the variable slip rates of individual thrusts or faults can affect available space for sedimentation (Densmore et al., 2007; Ezquerro et al., 2014). In practice, a differential tectonic movement between basin and source area(s) produces changes in the areal extent of the drainage areas, the gradients of the landscape profile, and have a direct influence in the subsidence patterns by the overall redistribution of orogenic loading (Catuneanu et al., 2009). Changes in the drainage network influence the rate and the amount of sediment delivered to the basin, whereas changes in the slope, condition the diffusivity of fluvial systems by means of the fluvial style and the availability for floodplain storage. These two factors exert a prime influence in sediment supply. On the other hand, the subsidence patterns modify the distribution of potential accommodation through space and time. This is important as the balance between accommodation and water and sediment supply leads to different basin filling trends, see overfilled, balanced and underfilled (Carroll and Bohacs, 1999).

Climatic influence in the AS/SS ratio

Climate controls the fluvial discharge, the vegetation cover, the sediment load and the location of the buttress point (basin base level) if water reservoirs installed in the basin. The fluvial discharge has a direct influence in the magnitude and grain-size characteristics of the sediment supply (Allen et al., 2013), and depends both upon the total amount and the annual distribution of water discharge, and the weathering and erosion rate, which at the same time are reliant on the density and type of vegetation (Corenblit et al., 2011). The sediment load has an impact in the accommodation space, and in the proximal settings may influence the tectonic style of the frontal wedge structures. The buttress point exerts a direct control in the accommodation (Holbrook et al., 2006). Despite in low gradient basins the influence of a lacustrine transgression may not be significant in the architectural arrangement of the medial and proximal fluvial deposits (Blum and Törnqvist, 2000; Sáez et al., 2007), such shifts may embrace an important extent of a basin, conditioning the transition point between confined and unconfined siliciclastic systems. It would account for the diffusivity of the sedimentary systems by changes in the basin profiles, and also it may lead to significant shifts in the location of the depositional elements. The total amount and annual distribution of precipitation and evaporation, together with the transmissivity of the underlying rocks accounting for groundwater feeding are the key factors that produce shifts in the water volume of reservoirs. The relationship of water bodies with vegetation might be complex. Although most of the studies point to a denser canopy in relation to higher net precipitation, it is known that the vegetal cover is responsible of the higher percentage of evapotranspiration (Good et al., 2015), and thus lower lake levels may show a linkage with enhanced vegetation cover. Finally, climate is also claimed to influence the erosion rates producing transient

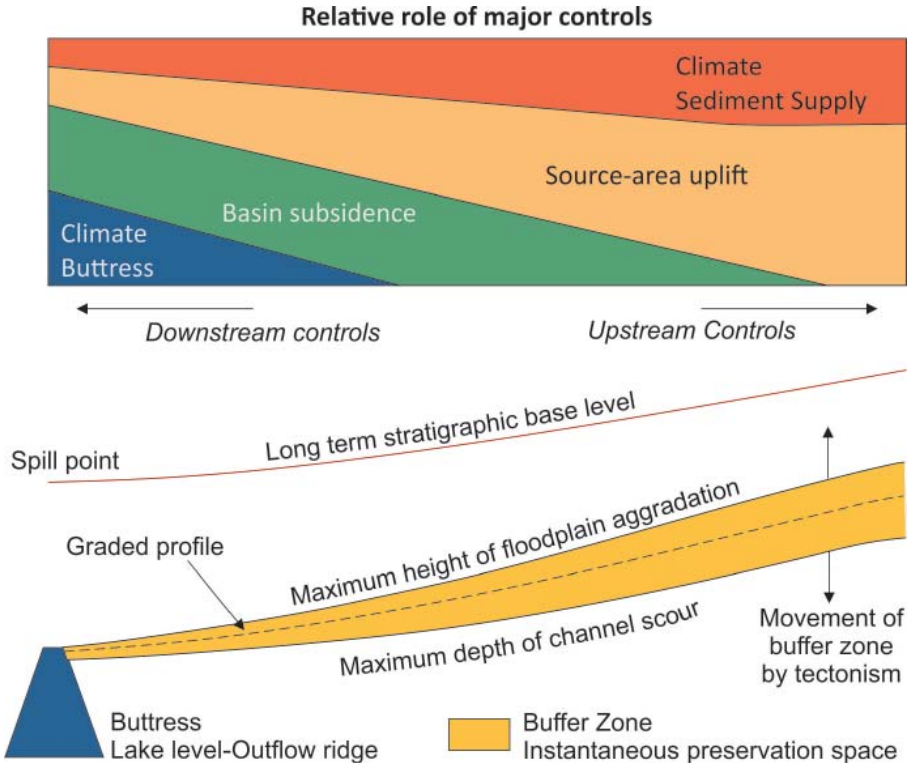

Figure 4.1. Allogenic controls on alluvial sedimentation. Modified after Holbrook et al., (2006); Fisher and Nichols (2013); and Miall (2014). The diagram shows a qualitative approach of the different allogenic controls upstream and downstream. The buffer and the buttress concept (Holbrook et al., 2006) and the maximum long term aggradation limit and spill point (Fisher and Nichols, 2013) are also included. Milankovitch cycles involve the two extremes of the upwards diagram, in one hand affecting the sediment supply, whereas in the other hand the vertical and lateral shifts of the buttress point by means of lake (base) level.

slopes during unsteady climates (Whipple, 2001).

The effects of accommodation and/or sediment supply in the continental stratigraphy can be classified into downstream and upstream controls (Shanley and McCabe, 1994). As seen above, climate shifts affect the sedimentary record by means of several processes which may act upstream or downstream (Fig. 4.1).

Climatic downstream controls

In relation to climate, the principal factor that affects sedimentary records downstream is the level oscillations of the water bodies. Noteworthy, this only will be expressed in the cases that the topography intersects the phreatic level, resulting in aerial water storage. It is known that shear stress may produce erosion below the water surface and that unconfined flows above the water shore can occur. In spite of this, the lake level can be assimilated as the basin base level (buttress) in non-marine basins (Holbrook et al., 2006). As lake level marks the base of rivers, the effects of a rise or fall of the water level may propagate rangewards along the overall sediment routing systems. Shifts in the water level contribute to create or destroy accommodation. In addition, the location of depositional elements within a basin is tightly related to the shore position. In consequence, water level oscillations may yield significant shifts of the different facies belts, and also changes in the architectural style of the large-scale depositional elements.

Most of the Milankovitch cycles expressed in continental basins are related to changes in the water supply affecting the (ground) waters level. This type of forcing is detected throughout the Phanerozoic under a wide range of climates, with examples found in the Devonian Orcadian Basin (Andrews and Hartley, 2015), the Triassic-Jurassic Newark Supergroup (Olsen and Kent, 1999), or the Eocene Green River Formation (Smith et al., 2008). In the Wilkins Peak Member of the Green River Basin, precession cycles

are recorded as yielders of different rock oil values (Machlus et al., 2008). Oil shale is thought to reflect generally fresher lake water and higher lake stands enabling O2 depletion in bottom waters (Smith et al., 2014). Persistent lacustrine intervals are recorded during 405-kyr eccentricity maxima intervals, whereas alluvial facies denoting lake low-stand occurred during 405-kyr eccentricity minima times (Smith et al., 2014). It suggests that, likewise the Ebro Basin, lacustrine expansions in the Wilkins Peak member were related to the occurrence high amplitude precession cycles modulated by eccentricity. Similarly, Olsen and Kent, (1996) attributed a precessional forcing to the cyclical lacustrine strata of the Newark Basin. These

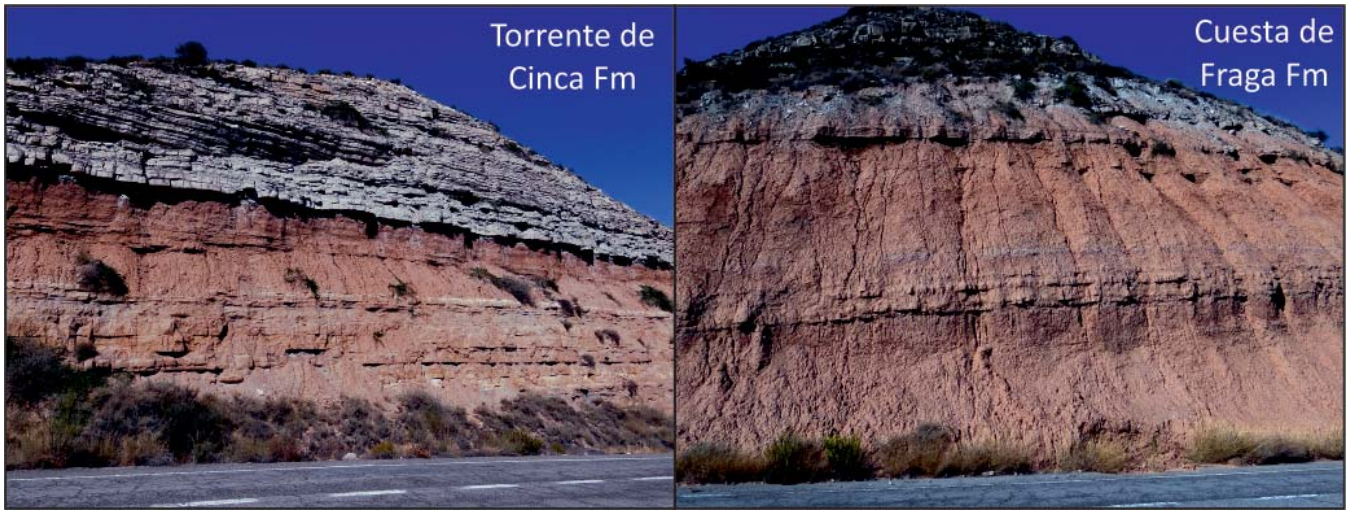

Figure 4.2. Differences in the expression of orbital cycles between dominant lacustrine (left) and distal alluvial (right) paleoenvironments in the Cuesta de Fraga/Torrente de Cinca Formations of the Ebro Basin. Lacustrine/palustrine environments are sensitive to minimal shifts in the precipitation/evaporation ratio responding strongly responding to such changes. On the contrary, only major water level shifts reach the alluvial plains allowing to different facies deposition.

basic cycles are grouped into a hierarchy of larger cycles expressing short and long eccentricity, which modulate the precession cycles (Olsen & Kent, 1999). In the Ebro Basin it is noteworthy the expression of precession as lithological cycles only when lacustrine facies occur (Fig. 4.2). In spite of this, precession cycles in non-lacustrine sequences may be preserved as changes in other more specific rock properties and, marginwards, as changes of fluvial architecture.

The examples given above correspond to cases that concern large basins. However, most of the distinct Milankovitch forcing in continental basins has been reported in small basins. Such basins use to display a cyclicity that involves, at least at some part of the cycle, changes in the water table. These cycles are typically expressed by the development of different carbonate facies deposits at some phase of the cycle, depending on the paleoenvironmental conditions. Among this sort of small basins, in which a lacustrine phase is present, the Ptolemais Formation in Greece and the Orera section in Spain are archetypes.

The Lower Pliocene Ptolemais Formation has a stratigraphy showing a remarkable alternation between lignites and marls. Van Vugt et al., (1998) linked the occurrence of lignites to a minimum in insolation, which represents relatively cold and generally arid summers. During precession minima (maxima insolation) carbonate-rich marls suggest increased precipitation, likely during winter (Steenbrink et al., 2006). The imprint of the 100-kyr eccentricity is not apparent in the Ptolemais Fm. However, other intervals in the Ptolemais Basin, like the Vegora and Prosilio sections express 405-kyr eccentricity cycles, and less apparently the 100-kyr eccentricity cycle. The Prosilio member includes continental aerobic clastic elements, principally sands and conglomerates, alternating with pebbly siltstones and clays, the latter corresponding

to eccentricity maxima cycles (Steenbrink et al., 2006). In the Ptolemais Formation, the cyclic lithological changes are interpreted as a domination of precipitation and related run-off over evaporation in controlling lake level (Van Vugt et al., 1998).

The Orera composite section is located in the intramontane Calatayud Basin, in North-central Spain. The basin encompasses a middle Miocene record that displays an outstanding alternation between mudstone and carbonate beds (Abdul-Aziz et al., 2000). Cyclostatigraphic analysis of the Orera section discloses a dominant control of precession (Abdul-Aziz et al., 2003), while 405-kyr eccentricity cycles are expressed by the occurrence of carbonate-poor intervals, suggesting prolonged drier conditions at times of eccentricity minima. On the contrary, the 100-kyr eccentricity cycle is not very distinct. The Orera lithological cycles are suggested to be controlled in a way similar to the Ptolemais record, where changes in the water budget allowed expansion or shrinking of the shallow lacustrine systems. However, in Orera the evaporation rate seems to be more important than in Ptolemais (Abdul-Aziz et al., 2003). In addition, the more arid conditions prevailing during the sedimentation of the Orera Basin prevented the formation of lignite during the dry phase of the cycle.

Other records expressing variations in the lake level in relation to orbital forcing exist. In Spain, in the Teruel Basin some sections display records shaped by orbital forcing. The Cañizar, Cascante, and Prado sections show a distinct alternation of mudstones and white carbonates in their lower part. In the Cascante section, Abels et al., (2009) analysed the microfacies, allowing for a refined environmental interpretation. During the lower term of the section, prior to cycle 26, the carbonates are mostly related to shallow and transient lake facies (Abels et al., 2009a). Spectral analysis revealed a principal control of precession in the development of the cycles, albeit obliquity and 100-kyr eccentricity cycles are also present (Abdul Aziz et al., 2004). Abels et al., (2009) pointed out that a positive water budget leading to lake-level rise during precession minima was the cause of the development of carbonate beds. Carbonate beds representing stable lacustrine conditions are correlated with eccentricity maxima, while unstable and shallow transient lacustrine facies correlate with eccentricity minima, suggesting precession-driven water fill.

In these basins, cyclicity is recorded as an alternation between an arid and a wet phase, and high-frequency cycles are prone to be expressed. Likely, this is enabled because these settings are sensitive to minor oscillations in the water budget, which responds readily to changes in insolation and precipitation. Cycles normally consist in precession and obliquity, the latter typically expressed during eccentricity minima. The occurrence of upstream variations in such settings may be obscured in the lithological record because of the stronger impact in the stratigraphy of lacustrine base level shifts. Changes in the sediment fluxes are likely held in the rock composition, for example changes in the clay fraction due to different weathering products. Such changes can be depicted by means of appropriate techniques like XRF analyses (Weber et al., 2010), or by means of the study of the rock magnetic properties.

Climatic upstream controls

The mass-balance of a basin can also be altered by changes of sediment supply (SS), and thus the AS/SS ratio. The sediment supply variations are rooted in changes in erosion and weathering in the source area, and in the transfer systems by changes in the streams advection capacity. These factors are tightly linked to vegetation, and bedrock characteristics. Prospective supply-driven orbital cycles can be disrupted by intrinsic factors. In fact, autogenic processes are thought to be responsible of the lack of sedimentary records governed by orbitally forced changes in the sediment fluxes (Armitage et al., 2013), especially in large basins (Castelltort and Van Der Driessche, 2003). In particular, the climate signal along the sediment routing systems is potentially hampered by alluvial autocylicity (Kim and Paola, 2007; Hajek et al., 2012), intrinsic dynamics of the drainage network (Viaplana et al., 2014), and the buffering effect of the transfer systems (Castelltort and Van Der Driessche, 2003). The potential distortion by autocyclicity increases as larger is the itinerary of a sedimentary pulse towards the sink.

In recent years, modelling studies aiming to disentangle the effects of high frequency variations in the sedimentary records aroused. However, altogether their results in relation to Milankovitch cycles are ambivalent. Armitage et al., (2011; 2013) argued that the response time of landscapes is in the order of 10^6 yr, clearly surpassing the precession, obliquity and short and long eccentricity frequencies. They stated that it is likely that climate-driven perturbation of upland catchments will be strongly damped by transient landscape behaviour. Their results agree with Densmore et al., (2007), which showed that the response time to a new equilibrium state ranges between ~0.5 to 2-Myr. On the other hand, Simpson and Castelltort (2012) showed that river transport strongly amplifies high-frequency sediment flux variations arising from changing water discharge, due to positive feedback between discharge and the channel gradient. The amplification of sedimentary pulses makes cycles very likely in the (marine) sedimentary record.

As these models are not designed to explain changes in endorheic systems, the response to accommodation changes due to changes in net precipitation (water level rise or fall) is not included. Neither are included the effects of floodplain storage, nor wind-recycled material, which may play an important control.

Despite the referred hurdles, some case studies exist, i.e. the As Pontes Basin, in which Milankovitch cycles are seen as drivers of sediment supply dominated cycles. Among these, little is reported about high-frequency cycles. A discussion on this was already offered by van Vugt et al., (2001), who stated that siliciclastic dominated (endorheic) basins were prone to express eccentricity, whereas carbonate basins were dominantly shaped by precession. One explanation for this was that the modulating effect of the 2.4-Myr very long-term eccentricity in the 100-kyr eccentricity cycles may have obscured the expression of the latter (van Vugt et al., 2001). Alternatively, they proposed that carbonate basins responded more linearly to insolation changes than siliciclastic basins, where the effects of non-linear processes resulted into a lack of high-frequency lithological cycles. They studied the Lupoaia section of the Oltenia Basin in Rumania and the Megalopolis Basin in Greece.

Similarly to the As Pontes Basin, the middle Pleistocene Megalopolis section shows an alternation between thick lignite seams and siliciclastics. Van Vugt (2000) presented a correlation with astronomical curves guided by magnetostratigraphic and radiometric data. Their results show a correspondence of lignite layers with the 100-kyr eccentricity maxima, whereas siliciclastics occur at times of 100-kyr eccentricity minima. Shorter cycles are not well expressed and are suggested to be originated by changes in the water budget due to changes in the insolation. The pollen content suggests a positive relationship between Artemisia abundance and the amount of siliciclastics (Okuda et al., 2002). Cycles alternating between intervals with Artemisia and intervals with deciduous forests likely suggest a control of vegetation in the depositional patterns or at least, a coeval response of landscapes and vegetation cover.

In the Lupoaia section, an alternation of lignite seams and intervals of clay, silt and sand were deposited during the Gilbert magnetic chron (Lower Pliocene). Their magnetostratigraphic age model shows a match between lignite seams and maxima of the eccentricity cycles, whereas the siliciclastics are related to periods of eccentricity minima. Less developed shorter scale cycles are also found at some intervals. In Lupoaia, the average sedimentation rates are about 17.5 cm/kyr, with higher values occurring during siliciclastic intervals. The origin of the cycles is thought to be changes in the climate that altered the vegetation cover (van Vugt et al., 2001). At times of eccentricity minima, climate limited the vegetal cover enhancing the erosion, and thus increasing the sediment input. On the other hand, during eccentricity maxima times, a denser vegetal cover produced sediment input reduction and peat accumulation. The Lupoaia system is likely a system dominated by changes in the sediment supply with a climatic origin. However, changes in the water budget seem to be responsible of some

higher-frequency variations in both the sedimentary record and vegetation cover. Vegetation in turn controlled the sediment available at short eccentricity time-scales.

There are sections lacking a lignite phase which also display a dominance of eccentricity probably controlled by shifts in the sediment supply. For example, the Armantes section, in the Calatayud Basin displays a cyclic pattern represented by an alternation between calcretes (caliches) and red beds. 27 cycles were found in a middle Miocene section recording ca. 3 Ma (Krijgsman et al., 1994; under the CK92 time scale, Cande & Kent, 1995). It represents a cyclicity of 111-kyr, suggesting an eccentricity-dominated stratigraphy, although shorter cycles are also present. The environmental interpretation of the calcretes suggests horizons that formed under very low sedimentation rates in times of semiarid climate (Alonso-Zarza, 2003), whereas red beds suggest periods with ephemeral flooding, and subsequent deposition of suspended load. This marks a sequential arrangement dominated by changes in the sediment supply, expressed at a 100-kyr scale. On the other hand, some observed shorter climatically-driven oscillations suggest variable shifts in the net precipitation budget.

The Madrid Basin constitutes another example. This basin evolved under semi-arid conditions during mid-Miocene times in central Spain. In the distal parts of the basin, pond-palustrine environments with carbonate deposition and starved areas with calcrete accumulation alternated with red beds representing alluvial plains. Spectral analysis of the Valdearenas and Muruex composite section reveals a significant power at the frequencies of short and long eccentricity (100-kyr and 405-kyr) in addition, a 2.4-Myr cycle was also found (Abels et al., 2010). The Carbonate-rich interval, which consists of 40 m of dominant carbonated facies, occurred after maxima of a 405-kyr eccentricty cycle in concomitant minima of 100-kyr, 405-kyr, and 2.4-Myr eccentricity cycles. The clastic sedimentation resumed after several consequent 405-kyr eccentricity maxima cycles within a maxima of the 2.4-Myr eccentricity cycle. The lack of high-frequency cycles suggests that the net precipitation is not the carrier of the cycles. A possible explanation is that water level was controlled by the sedimentary filling state, resulting from the ratio between subsidence-driven accommodation and supply (Armenteros and Huerta, 2006) with origin in climatically-driven sedimentary pulses.

Sediment supply-driven cycles and accommodation-driven cycles

Despite some models predict a precluded response of the sedimentary archives to changes in the sediment supply at Milankovitch time scales, it is shown that there are basins expressing lithological cycles at such scales. Basins with lacustrine (water bodies) phases are very sensitive to changes in the water supply or water geochemistry. Thus these basins tend to respond readily to insolation changes, being excellent archives for precession and obliquity. A complementary explanation is that in these settings, accommodation is promptly changed due to climatically-induced buttress vertical shifts.

On the other hand, basins with an outweighed clastic signal, in which cycles involve shifts in the sediment supply, are less sensitive to direct insolation changes. This is what van Vugt et al., (2001) called non-linear responses. All the cases recording upstream cycles occur in small basins, with small sediment transfer systems, i.e reactive basins (Allen, 2008b; Covault et al., 2011). In these basins the response times are reduced, and the buffering effect circumvented. This allows these settings to express climate cycles as changes in the sediment fluxes. However, the cycles expressed are typically $\geq$100-kyr eccentricity cycles. The response time of these small reactive basins, which is the time in which clastic signal is propagated basinwards, is suggested to be below 100-kyr, whereas the lack of a clear expression of obliquity or precession suggest a response time above 40-kyr.

Particularly interesting are those basins that show accommodation-driven and supply-driven cycles in different periods of their sedimentation, or at same time but different locations. The Ptolemais Basin, for example, shows (water level) accommodation-driven cycles recording precession in the Ptolemais mem-

ber, but supply-driven cycles in the Prosilio member. The Teruel Basin shows a similar pattern of cyclicity in the lower part of the Prado and Cascante sections. But, after a shift in the sediment patterns, likely due

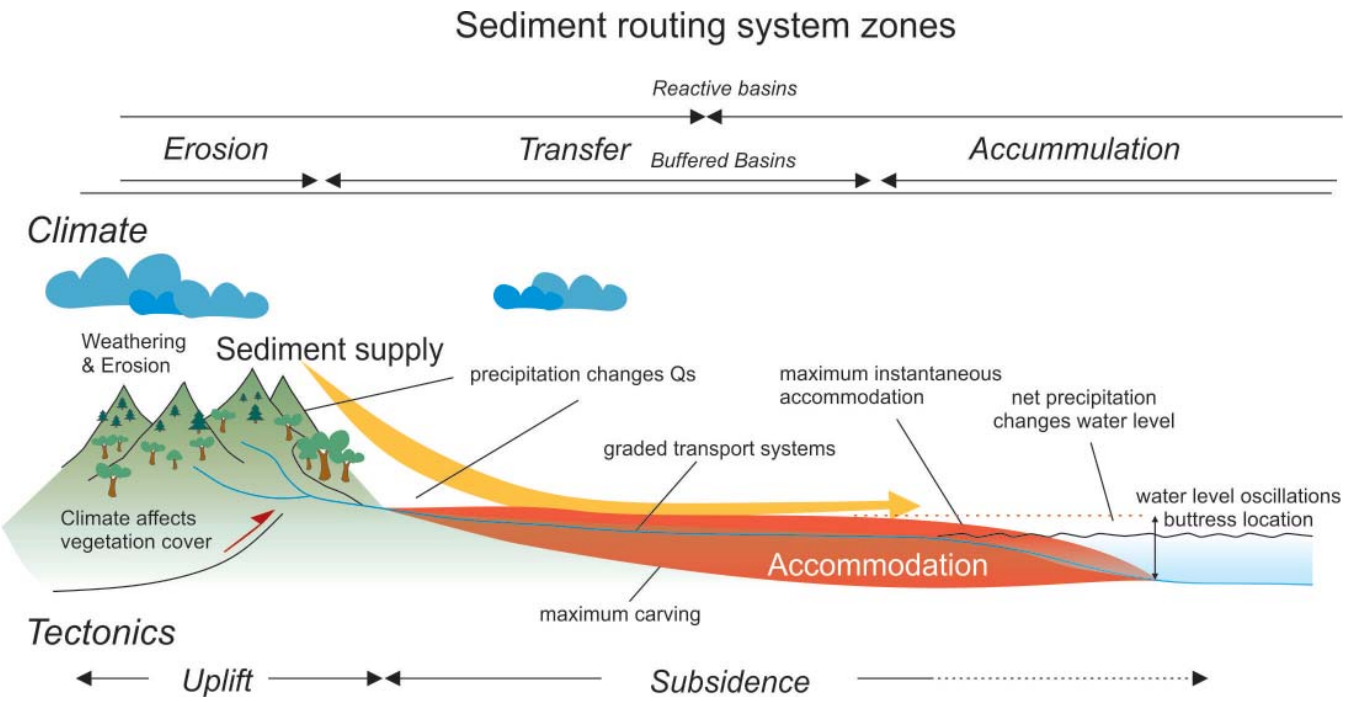

Figure 4.3. Summary of the principal controls on the lithological expression of Milankovitch cycles in continental endorheic basins. Accommodation-forced cycles are prone to dominate the distal areas within the influence of water reservoirs. Sediment supply cycles only will be expressed in the basins lacking central lacustrine/palustrine systems, and with rapid response times. Modified after Romans et al., 2015.

to tectonic causes occurring at circa 9.4 Ma, the expression of the lithological cycles between sections differs. It is likely that the Cascante section still displays accommodation-dominated lacustrine cycles, whereas the Prado section records a shift towards alluvial facies under increased clastic supply. The different expression of orbital oscillations within the same basin during the same time interval is an important area to explore, principally because of its consequences for lithological correlation based on orbital cycles.

In summary, basins involving lacustrine, palustrine, or other environmental facies sensitive to superficial waters storage are much more sensitive to net precipitation variations. It modifies the AS/SS ratio sufficiently as to obscure possible sediment flux variations associated to the changed discharge. Basins without a lacustrine (palustrine or susceptible to water level changes) phase, and thus lacking climatically-driven accommodation changes, are more sensitive to archive sediment pulses with a climatic origin. Small basins, with small transfer systems and lacking carbonate facies are the ideal candidates to archive the impact of orbital forcing in the landscapes (Fig. 4.3). Sedimentation models that include the relationship between accommodation and sediment supply, the effects of different density and type of vegetation, and its coupled response with climate are needed to enhance their reliability.

Long term orbital forcing

Both the As Pontes and the Ebro Basin depict 2.4-Myr eccentricity cycles. Although there are differences in the pathways in which the long term cycles are expressed. In As Pontes, long-term cycles are likely expressed by means of stable and graded profiles during climatic stability. The origin of the As Pontes cycles is therefore found upstream. On the other hand, the Ebro Basin presents a filling of the water reservoirs during eccentricity maxima times, due to the long-term persistence of high-amplitude precession cycles. Reservoir filling, although the discharge mainly is originated upstream, affects the sedimentary record downstream. Overall, it is suggested that independently of the origin of climatic forcing, the development

of very long-period eccentricity cycles is clearly above the response times of the basins. Likely, the most important is to study records developed under the same tectonic conditions, which allows for a stability of the depositional environments. If the depositional elements are stable, changes in the climate will alter easily the mass-balance of a basin. Eventually, if the basin involves lacustrine systems, a range of cycles from precession to long term eccentricity can be expected if the preserved record is sufficiently long (>7-Myr).

The different transmission mechanisms from the orbital oscillations to the sedimentary record may produce a contrasting expression of the orbital cycles in the record. The As Pontes Basin and the Mequinenza section formed coevally (Late Oligocene) within the same climatic belt. Nevertheless, their different features, such as catchment area and sediment transfer systems longitude, are responsible of their different expression of orbital cycles. In As Pontes Basin the deposition of coal is associated to eccentricity minima times, in contrast minor coal seams and thick lacustrine carbonate in Mequinenza are found during eccentricity maxima times. Coal accumulation and lacustrine carbonate sedimentation are the principal carbon sinks in continental environments, being significant contributors to the carbon cycle. The study of the type of basin, sedimentation mechanisms and time in which the carbon is stored may provide insights on the carbon cycle and global climate in relation to non-marine carbon sinks. It is remarkable the antiphase behaviour of times of enhanced carbon storage between As Pontes Basin and the Ebro Basin. Calculation of the rates and volumes of carbon burial of both basins may reveal possible disequilibria or buffering in the continental carbon storage between eccentricity minima and maxima intervals. This may be substantial during intervals of very long-eccentricity maxima and minima times in which the expression of cycles are amplified due to the modulation of shorter eccentricity terms. Accordingly, it reveals the importance of the physiognomy of the basins, which may be more important than climate itself, in carbon storage.

References

Aziz, H. A., Hilgen, F., Krijgsman, W., Sanz, E. & Calvo, J. P. (2000). Astronomical forcing of sedimentary cycles in the middle to late Miocene continental Calatayud Basin (NE Spain). Earth and Planetary Science Letters, 177(1), 9-22.

Abdul Aziz, H., Krijgsman, W., Hilgen, F., Wilson, D. & Calvo, J.P. (2003). An astronomical polarity timescale for the late middle Miocene based on cyclic continental sequences. Journal Geophysical Research, 108 (B3).

Aziz, H. A., van Dam, J., Hilgen, F. J., & Krijgsman, W. (2004). Astronomical forcing in Upper Miocene continental sequences: implications for the Geomagnetic Polarity Time Scale. Earth and Planetary Science Letters, 222(1), 243-258.

Abels, H.A., Abdul Aziz, H., Calvo, J.P. & Tuenter, E. (2009). Shallow lacustrine carbonate microfacies document orbitally paced lake-level history in the Miocene Teruel Basin (North–East Spain). Sedimentology, 56, 399–419.

Abels, H.A., Aziz, H.A., Krijgsman, W., Smeets, S.J.B. & Hilgen, F.J. (2010). Long-period eccentricity control on sedimentary sequences in the continental Madrid Basin (mi ddle Miocene, Spain). Earth and Planetary Science Letters, 289, 220–231.

Allen, P. A. (2008). Time scales of tectonic landscapes and their sediment routing systems. Geological Society, London, Special Publications, 296(1), 7-28.

Allen, P. A., Armitage, J. J., Carter, A., Duller, R. A., Michael, N. A., Sinclair, H. D., Whitchurch, A. L. & Whittaker, A. C. (2013). The Qs problem: sediment volumetric balance of proximal foreland basin systems. Sedimentology, 60(1), 102-130.

Alonso-Zarza, A.M. (2003). Palaeoenvironmental significance of palustrine carbonates and calcretes in the geological record. Earth Sciences Reviews, 60, 261–298. http://dx.doi.org/10.1016/S0012-8252(02)00106-X.

Andrews, S. D. & Hartley, A. J. (2015). The response of lake margin sedimentary systems to climatically driven lake level fluctuations: Middle Devonian, Orcadian Basin, Scotland. Sedimentology. doi: 10.1111/sed.12200

Armenteros, I. & Huerta, P. (2006). The role of clastic sediment influx in the formation of calcrete and palustrine facies: a response to paleographic and climatic con-ditions in the Southeastern Tertiary Duero basin (northern Spain). In: Alonso-Zarza, Eds A.M., Tanner, L.H. (Eds.), Paleoenvironmental Record and Applications of Calcretes and Palus-

trine Carbonates. In: Spec. Pap., Geol. Soc. Am., vol.416, pp.119–132.

Armitage, J. J., Duller, R. A., Whittaker, A. C., & Allen, P. A. (2011). Transformation of tectonic and climatic signals from source to sedimentary archive. Nature Geoscience, 4(4), 231-235.

Armitage, J.J., Dunkley Jones, T., Duller, R. A., Whittaker, A.C & Allen, P. A. (2013), Temporal buffering of climate-driven sediment flux cycles by transient catchment response: Earth and Planetary Science Letters, v. 369-370, p. 200–210, doi: 10.1016/j.epsl.2013.03.020

Blum, M. D. & Törnqvist, T. E. (2000). Fluvial responses to climate and sea-level change: a review and look forward. Sedimentology, 47(s1), 2-48.

Cande, S. C. & Kent, D. V. (1995). Revised calibration of the geomagnetic polarity timescale for the Late Cretaceous and Cenozoic. Journal of geophysical research, 100(B4), 6093-6095.

Carroll, A. R., & Bohacs, K. M. (1999). Stratigraphic classification of ancient lakes: Balancing tectonic and climatic controls. Geology, 27(2), 99-102.

Castelltort, S., & Van Den Driessche, J. (2003), How plausible are high-frequency sediment supply-driven cycles in the stratigraphic record?: Sedimentary Geology, v. 157, p. 3–13. doi: 10.1016/S0037-0738(03)00066-6.Catuneanu et al., 2009

Corenblit, D., Baas, A.C.W., Bornette, G., Darrozes, J., Delmotte, S., Francis, R. A., Gurnell, A.M., Julien, F., Naiman, R.J., & Steiger, J. (2011). Feedbacks between geomorphology and biota controlling Earth surface processes and landforms: A review of foundation concepts and current understandings: Earth-Science Reviews, v. 106, no. 3-4, p. 307–331, doi: 10.1016/j.earscirev.2011.03.002.

Covault, J. A., Romans, B. W., Graham, S. A., Fildani, A., & Hilley, G. E. (2011). Terrestrial source to deep-sea sink sediment budgets at high and low sea levels: Insights from tectonically active Southern California. Geology, 39(7), 619-622.

DeCelles, P.G. & Giles, K.A. (1996). Foreland basin systems. Basin Research, 8, 105–123.

Densmore, A. L., Allen, P. A., & Simpson, G. (2007). Development and response of a coupled catchment fan system under changing tectonic and climatic forcing. Journal of Geophysical Research: Earth Surface (2003–2012), 112(F1).

Ezquerro, L., Luzón, A., Navarro, M., Liesa, C. L., & Simón, J. L. (2014). Climatic vs. tectonic signals in a continental extensional basin (Teruel, NE Spain) from stable isotope (δ18O) and sequence stratigraphical evolution. Terra Nova, 26(5), 337-346.

Good, S. P., Noone, D., & Bowen, G. (2015). Hydrologic connectivity constrains partitioning of global terrestrial water fluxes. Science, 349(6244), 175-177.

Holbrook, J., Scott, R. W., & Oboh-Ikuenobe, F. E. (2006). Base-level buffers and buttresses: a model for upstream versus downstream control on fluvial geometry and architecture within sequences. Journal of Sedimentary Research, 76(1), 162-174.

Kim, W., & Paola, C. (2007). Long-period cyclic sedimentation with constant tectonic forcing in an experimental relay ramp. Geology, 35(4), 331-334.

Krijgsman, W., Langereis, C. G., Daams, R., & Van der Meulen, A. J. (1994). Magnetostratigraphic dating of the middle Miocene climate change in the continental deposits of the Aragonian type area in the Calatayud-Teruel basin (Central Spain). Earth and Planetary Science Letters, 128(3), 513-526.

Machlus, M.L., Olsen, P.E., Christie-Blick, N. & Hemming, S.R. (2008). Spectral analysis of the lower Eocene Wilkins Peak Member, Green River Formation, Wyoming: Support for Milankovitch cyclicity: Earth and Planetary Science Letters, v. 268, no. 1-2, p. 64–75, doi: 10.1016/j.epsl.2007.12.024.

Miall, A. D. (2014), Fluvial Depositional Systems: New York, Springer, doi: 10.1007/978-3-319-006666

Okuda, M., Van Vugt, N., Nakagawa, T., Ikeya, M., Hayashida, A., Yasuda, Y., & Setoguchi, T. (2002). Palynological evidence for the astronomical origin of lignite–detritus sequence in the Middle Pleistocene Marathousa Member, Megalopolis, SW Greece. Earth and Planetary Science Letters, 201(1), 143-157.

Olsen, P. E., & Kent, D. V. (1996). Milankovitch climate forcing in the tropics of Pangaea during the Late Triassic. Palaeogeography, Palaeoclimatology, Palaeoecology, 122(1), 1-26.

Olsen, P.E., & Kent, D. V. (1999). Long-period Milankovitch cycles from the Late Triassic and Early Jurassic of eastern North America and their implications for the calibration of the Early Mesozoic time-scale and the long-term behaviour of the planets: Philosophical Transactions of the Royal Society A: Mathematical, Physical and Engineering Sciences, v. 357, no. 1757, p. 1761–1786, doi: 10.1098/rsta.1999.0400.

Petersen, K.D., Nielsen, S.B., Clausen, O.R., Stephenson, R. & Gerya, T. (2010). Small-scale mantle convection produces stratigraphic sequences in sedimentary basins. Science 329, 827–830.

Romans, B. W., Castelltort, S., Covault, J. A., Fildani, A.,

& Walsh, J. P. (2015). Environmental signal propagation in sedimentary systems across timescales. Earth-Science Reviews.

Shanley, K.W. & McCabe, P.J. (1994). Perspectives on the sequence stratigraphy of continental strata: American Association Petroleum Geologists Bulletin, v.78, p. 544–568

Simpson, G., & Castelltort, S. (2012). Model shows that rivers transmit high-frequency climate cycles to the sedimentary record. Geology, 40(12), 1131-1134.

Smith, M. E., Carroll, A. R., & Singer, B. S. (2008). Synoptic reconstruction of a major ancient lake system: Eocene Green River Formation, western United States. Geological Society of America Bulletin, 120(1-2), 54-84.

Smith, M. E., Carroll, A. R., Scott, J. J., & Singer, B. S. (2014). Early Eocene carbon isotope excursions and landscape destabilization at eccentricity minima: Green River Formation of Wyoming. Earth and Planetary Science Letters, 403, 393-406.

Steenbrink, J., Hilgen, F. J., Krijgsman, W., Wijbrans, J. R., & Meulenkamp, J. E. (2006). Late Miocene to Early Pliocene depositional history of the intramontane Florina–Ptolemais–Servia Basin, NW Greece: Interplay between orbital forcing and tectonics. Palaeogeography, Palaeoclimatology, Palaeoecology, 238(1), 151-178.

Strong, N., Sheets, B., Hickson, T., & Paola, C. (2005). A mass-balance framework for quantifying downstream changes in fluvial architecture. Fluvial Sedimentology VII, Special Publication, International Association of Sedimentologists, 35, 243-253.

Valero, L., Garcés, M., Cabrera, L., Costa, E., & Sáez, A. (2014). 20 Myr of eccentricity paced lacustrine cycles in the Cenozoic Ebro Basin. Earth and Planetary Science Letters, 408, 183-193.

Valero, L., Huerta, P., Garcés, M., Armenteros, I., Beamud, E., & Gómez-Paccard, M. (2015). Linking sedimentation rates and large-scale architecture for facies prediction in nonmarine basins (Paleogene, Almazán Basin, Spain). Basin Research. doi: 10.1111/bre.12145

Valero, L., Cabrera, L., Sáez, A., Garcés, M. Long-term astronomically-forced terrestrial carbon sinks (submitted).

Viaplana, M., Babault, J., Van Den Driessche, J., Dominguez, S., & Legrand, X. (2014).Drainage network dynamics in an accretionary wedge: an experimental approach. AAPG, European Regional Conference and Exhibition, Barcelona, Spain.

Van Vugt, N. (2000). Orbital forcing in late Neogene lacustrine basins from the Mediterranean. A magnetostratigraphic and cyclostratigraphic study. PhD thesis, Utrecht University, Geologica Ultraiectina, 189, 167 pp.

Van Vugt, N., Steenbrink, J., Langereis, C.G., Hilgen, F.J. & Meulenkamp, J.E. (1998). Magnetostratigraphy-based astronomical tuning of the early Pliocene lacustrine sediments of Ptolemais (NW Greece) and bed-to-bed correlation with the marine record: Earth and Planetary Science Letters, v. 164, no. 3-4, p. 535–551, doi: 10.1016/S0012-821X(98)00236-2.

van Vugt, N., Langereis, C.G., & Hilgen, F.J. (2001). Orbital forcing in Pliocene–Pleistocene Mediterranean lacustrine deposits: dominant expression of eccentricity versus precession: Palaeogeography, Palaeoclimatology, Palaeoecology, v. 172, no. 3-4, p. 193–205, doi: 10.1016/S0031-0182(01)00270-X.

Weber, M. E., Tougiannidis, N., Kleineder, M., Bertram, N., Ricken, W., Rolf, C., Reinsch, T. & Antoniadis, P. (2010). Lacustrine sediments document millennial-scale climate variability in northern Greece prior to the onset of the northern hemisphere glaciation. Palaeogeography, Palaeoclimatology, Palaeoecology, 291(3), 360-370.

Whipple, K.X. (2001). Fluvial landscape response time: How plausible is steady-state denudation? American Journal of Science, v. 301, no. May, p. 313–325, doi: 10.2475/ajs.301.4-5.313.

Chapter 5
Conclusions

5.1. TEMPORAL FRAMEWORKS

A refined high-resolution chronology has been obtained for key basins of the Iberian Peninsula by means of combined magnetostratigraphic and astronomical dating. In the As Pontes Basin the age model is based on cyclostratigraphic analysis and astronomical tuning of a previous magnetochronology. The overall sequence is dated between around 30.8 (base) and 21.7 Ma (top sediments in the Eastern sub-basin). Resulting sedimentation rates for the As Pontes Basin are typically low. In the West Section average sedimentation rates including the middle sandstone unit are around 3.9 cm/kyr. Excluding this unit from calculation, sedimentation rates are around 3 cm/kyr.

In the Ebro Basin, the magnetostratigraphic data of the Mequinenza area agrees with the results of Barberà et al., (2001). The base of the Mequinenza composite section is dated to around 28.1 Ma, and the top of the section, within the Torrente de Cinca Fm., has an Aquitanian age, around 22 Ma. Average sedimentation rates for carbonated intervals are around 6-7 cm kyr^{-1}, whereas in red beds sedimentation rates are typically between 7-10 cm kyr^{-1}. The astronomical ages reinforce the view that lacustrine and perilacustrine environments of the Ebro Basin were very sensitive to orbital forcing, with a clear expression of eccentricity cycles. The impact of the 2.4-Myr cycles has been demonstrated fundamental in the development of lacustrine units throughout most of the continental Ebro Basin infill.

In the Almazán Basin a magnetostratigraphy encompassing *ca.* 2700 m was built which includes the complete Paleogene infill. The results show that sedimentation began at mid-Lutetian times (Eocene). Most of the record was affected by folding and thrusting both within the basin and its margins, which generated depositional sequences that have been successfully dated. The top depositional sequence (A4) yields a Rupelian age.

5.2. RELATIONSHIPS BETWEEN THE LOCATION OF DEPOSITIONAL ELEMENTS AND THEIR INTERNAL ARCHITECTURE AND SEDIMENTATION RATES (SR)

The excellent outcrop conditions allowed for mapping the magnetic reversals of across the Almazán Basin. The paleomagnetic map together with previous mapping of geological units and their sedimentological analysis permitted a quantification of sedimentation rates for the most of the Paleogene infill of the basin. Relative changes in SR show a correspondence with the large-scale sedimentary architecture. In areas with high sediment supply, higher SR (30–40 cm kyr^{-1}) are related to ribbon-shaped isolated channel fills and predominance of floodplain fine grained deposits. On the other hand, lower SR ($<$10 cm kyr^{-1}) correspond to laterally extensive sheet-like interconnected channel fills and an increase in the average grain size. In basin sectors with low sediment input, the predominance of fine sediments, mudstones and evaporitic mudstones reveals a slight decrease in sedimentation rates (SR around 15–20 cm kyr^{-1}) with respect to the areas with high sediment supply (fluvial system). Palustrine/lacustrine limestone units occur in areas of very low sediment input and low sedimentation rates (SR around 9 cm kyr^{-1}) which are reflecting the carbonate production. Stacked calcrete profiles develop in areas with low sediment supply and very low sedimentation rates (SR around 3 cm kyr^{-1}) related to distal alluvial or distal floodplain areas.

5.3. MASS-BALANCE CONTRIBUTION TO BASIN INFILL ARCHITECTURE

The tight relationship between the sedimentation rates and the location of the depositional elements supports the idea that the distribution of depositional elements and their internal arrangement is a function of the mass-balance of the basin. The mass-balance in turn, is controlled by the shifts in the accommodation and sediment supply. Therefore, a relationship between sedimentation rates, the rate of sediment extracted of the routing system, and the final stratigraphy can be established. (Fig. 5.1).

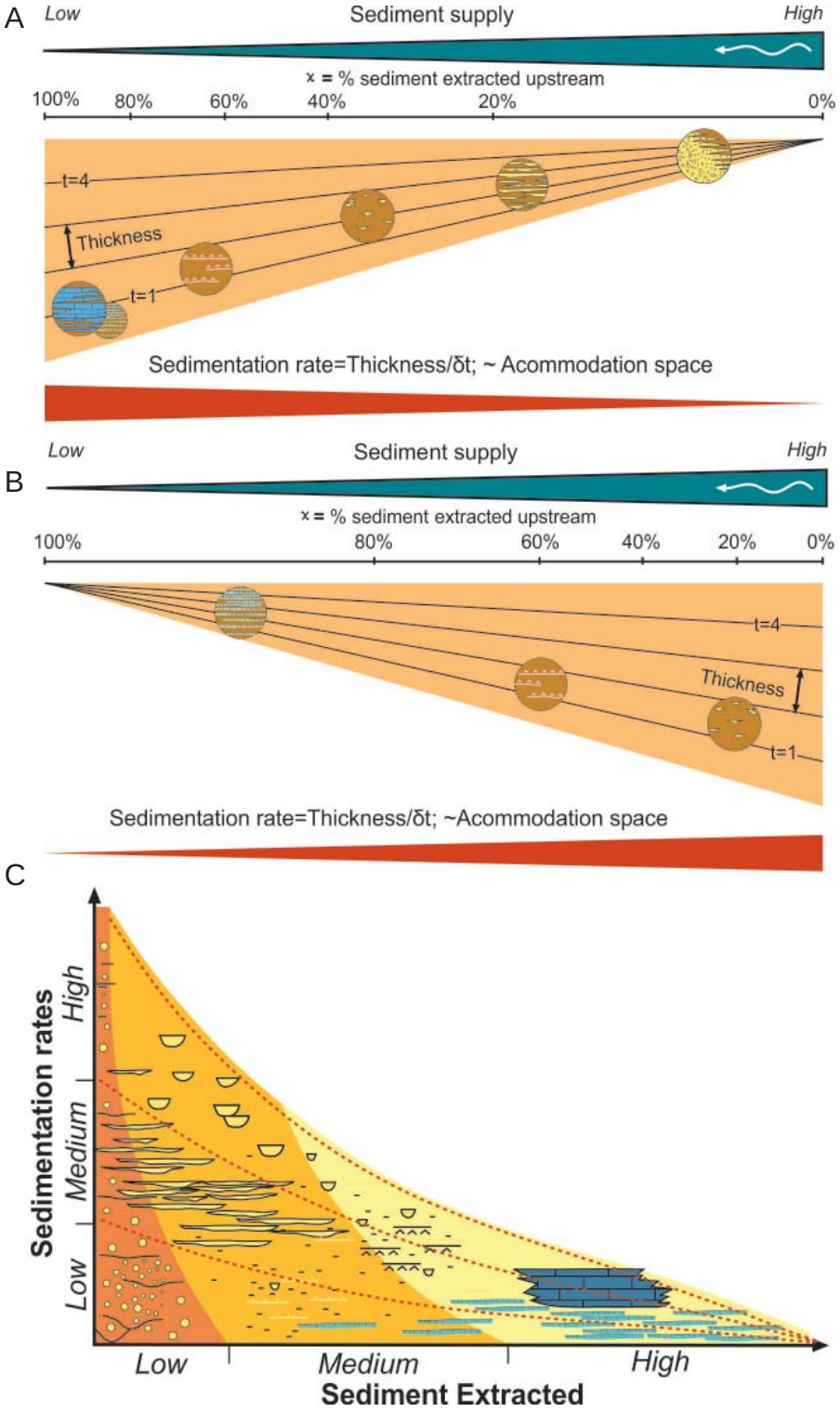

Figure 5.1. A: Relationship of accommodation and sediment supply (mass-balance) with the basin depositional and architectural elements. B: Comparison of the distribution of the sediments and depositional elements in foretilted and backtilted basins. C: Relationship between sedimentation rates and the sediment extracted along a basin (χ) is summarized.

5.4. ASTRONOMICAL CYCLES IN TECTONICALLY ACTIVE SETTINGS

The Mequinenza section, like most of the Ebro Basin record, and the As Pontes Basin were developed coevally to the development of structures in the margins of the basin. Despite these potential perturbations, the orbital oscillations are expressed in the record as lithological cycles. This implies that the characterization of basin depositional sequences solely based on unconformities in the basin margins might be inaccurate. On the contrary, a scenario in which the tectonic sequences in the margin are decoupled with the climatically-driven sequences in the lacustrine depocenters seems plausible.

5.5. THE IMPACT OF MILANKOVITCH CYCLES IN CONTINENTAL BASINS. INFLUENCE OF THE SEDIMENT TRANSPORT SYSTEMS IN THE EXPRESSION OF THE CYCLES.

Regarding the sediment routing systems, non-marine basins are approximately closed systems. It has been shown that orbital cycles can be expressed as lithological cycles in two ways. Downstream cycles that affect the sedimentation by means of the changes in the base level (lacustrine level), thus promoting changes in the accommodation, and are characteristic of basin sustaining water reservoirs. On the other hand, upstream cycles, with origin in the changes in the sediment supplied to the basin, are found in small basins lacking water reservoirs. Sediment supply climatically-driven cycles are typically obscured by the buffering effect of large to medium sediment transfer systems, and also by changes in the base level in settings with lacustrine environments. Upstream cycles are usually affected by strong changes in the sedimentation rates. This conceals these basins to exhibit the typical bundling or arrangement of strata shaped by orbital rhythms.

Appendix 1

20 Myr of eccentricity paced lacustrine cycles in the Cenozoic Ebro Basin

Earth and Planetary Science Letters 408 (2014) 183–193

Contents lists available at ScienceDirect

Earth and Planetary Science Letters

www.elsevier.com/locate/epsl

20 Myr of eccentricity paced lacustrine cycles in the Cenozoic Ebro Basin

Luis Valero [a,*], Miguel Garcés [a], Lluís Cabrera [a], Elisenda Costa [b], Alberto Sáez [a]

[a] Institut de Recerca GEOMODELS, Departament d'Estratigrafia, Paleontologia i Geociències Marines, Facultat de Geologia, Universitat de Barcelona, Martí i Franquès s/n, 08028 Barcelona, Spain
[b] Departament de Geodinàmica i Geofísica, Facultat de Geologia, Universitat de Barcelona, Martí i Franquès s/n, 08028 Barcelona, Spain

ARTICLE INFO

Article history:
Received 20 February 2014
Received in revised form 26 September 2014
Accepted 3 October 2014
Available online 29 October 2014
Editor: G.M. Henderson

Keywords:
long term astronomical forcing
Eocene
Oligocene
Miocene
continental paleoenvironments
Ebro Basin

ABSTRACT

Long-period orbital forcing is a crucial component of the major global climate shifts during the Cenozoic as revealed in marine pelagic records. A complementary regional perspective of climate change can be assessed from internally drained lake basins, which are directly affected by insolation and precipitation balance. The Ebro Basin in northeastern Iberia embraces a 20 Myr long continuous sedimentary record where recurrent expansions and retractions of the central lacustrine system suggest periodic shifts of water balance due to orbital oscillations. In order to test climatic (orbital) forcing a key-piece of the basin, the Los Monegros lacustrine system, has been analyzed in detail. The cyclostratigraphic analysis points to orbital eccentricity as pacemaker of short to long-term lacustrine sequences, and reveals a correlation of maxima of the 100-kyr, 400-kyr and 2.4-Myr eccentricity cycles with periods of lake expansion. A magnetostratigraphy-based chronostratigraphy of the complete continental record allows further assessing long-period orbital forcing at basin scale, a view that challenges alternate scenarios where the stratigraphic architecture in foreland systems is preferably associated to tectonic processes. We conclude that while the location of lacustrine depocenters reacted to the long-term tectonic-driven accommodation changes, shorter wavelenght oscillations of lake environments, still million-year scale, claims for a dominance of orbital forcing. We suggest a decoupling between (tectonic) supply-driven clastic sequences fed from basin margins and (climatic) base level-driven lacustrine sequences in active settings with medium to large sediment transfer systems.

1. Introduction

Astronomically-tuned oceanic sedimentary records show that certain rare orbital configurations were favorable to polar ice-sheet expansions, thus controlling global climate trends (Lourens and Hilgen, 1997). Internally drained basins may be particularly sensitive to climate change because lake-level oscillations readily account for the balance between precipitation and evaporation. Unfortunately, closed drainage conditions rarely persist for long because erosion and fluvial capture operate at shorter, million-year time-scales (García-Castellanos et al., 2003). Outstanding exceptions are found in Neogene to recent sediments of Lake Baikal (Kashiwaya et al., 2001) and the Triassic–Jurassic Rift System of Newark Supergroup of eastern North America (Olsen 1986; Olsen and Kent, 1999), where lacustrine sequences record long-period orbital forcing.

Assessing the climatic origin of large-scale sedimentary cycles is often controversial because internally driven geodynamic forces typically operate at 10^6–10^7 yr time scales (Petersen et al., 2010), a range which overlaps with the known orbital cycles of the very long period eccentricity (0.97-Myr and 2.4-Myr) and obliquity amplitude (obliquity nodes at average 1.2-Myr) for the last 50 Ma. In the context of endorheic foreland systems causal relationships link the million-year scale clastic sequences with tectonic uplift and erosion along the margins. Plus, despite large sediment transfer systems have a buffer effect on supply-driven sequences (Castelltort and Van Den Driessche, 2003), the signature of high-amplitude long-wavelength tectonic pulses can be transmitted at long distances within the sedimentary basin as subsidence or/and supply-driven sequences (Paola et al., 1992; DeCelles and Giles, 1996).

The Paleogene–Neogene Ebro Basin in NE Spain is a peculiar case among the circum-Mediterranean foreland basins because plate convergence and collision sustained a land-locked basin configuration since its seaway closure in the Late Eocene (Costa et al., 2010) until its river capture in the middle–late

* Corresponding author. Tel.: +34 934034888.
E-mail addresses: luisvalero@ub.edu (L. Valero), mgarces@ub.edu (M. Garcés).

http://dx.doi.org/10.1016/j.epsl.2014.10.007

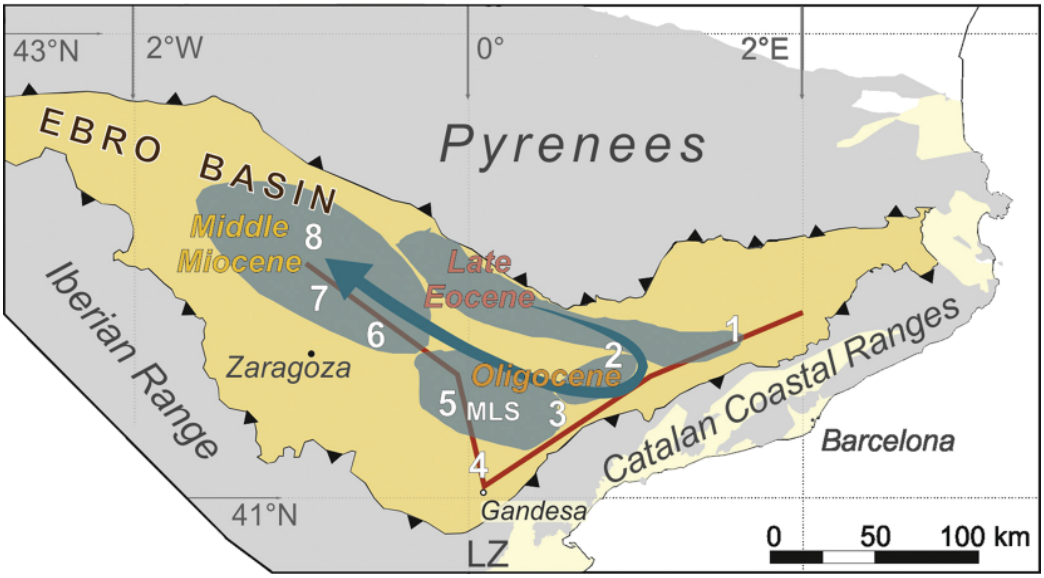

Fig. 1. Map of the Ebro Basin with location of lacustrine systems (blue-shaded areas) from late Eocene to Middle Miocene. Blue arrow marks the track of lacustrine shifting. Numbers indicate the location of sections discussed: 1. Moià-Santpedor; 2. Rocafort-Sarral; 3. Tarrés-Cervià; 4. Gandesa-Bot; 5. Mina Pilar-Mequinenza; 6. Albalatillo-Lanaja; 7. San Caprasio; 8. Castejón-Sora. Red lines indicate the location chronostratigraphic panels of Fig. 8.

Miocene. The internally drained Ebro Basin underwent continuous and steady aggradation of terrigenous sediments fed from the active margins, grading into lacustrine sediments towards the inner basin areas. The progradational and retrogradational trends of the alluvial-lacustrine systems were used in the past for a chronostratigraphic subdivision based on the tectonosedimentary unit concept (Alonso-Zarza et al., 2002) or as tectonically-driven sequences (Anadón et al., 1989). The length and completeness of this record is most suitable for an independent, high-resolution magnetostratigraphic dating, which can provide a robust age model; a basic requirement for assessing the origin of sedimentary cycles.

In this paper we aim at exploring the tectonic and climatic (orbital) signatures in the recurrent expansion and retraction of the lake systems of the Eastern–Central Ebro Basin. To achieve this, a cyclostratigraphic study of the Late Oligocene–Early Miocene sequence of Los Monegros Lacustrine System (MLS) was carried out (Fig. 1). The MLS sequence is well suited for this study because the nearly three-dimensional outcrop exposures in the area of Mequinenza allow the precise identification of a thick (*ca.* 500 m) and continuous stack of successive lacustrine cycles. In addition, the magnetostratigraphy of these sequences can be used to construct an age model for astronomical tuning, as astronomical ages of geomagnetic reversals around the Oligocene–Miocene boundary are well constrained (Shackleton et al., 1999; Liebrand et al., 2011). To further test if the observed cyclicity is forced by long-period orbital oscillations, an integration of the complete late Eocene to middle Miocene succession of the Eastern and Central Ebro Basin is examined.

2. The Los Monegros Lacustrine System

The MLS sequence (Fig. 1, Supplementary Fig. A1) consists in shallow lacustrine limestone successions, grading laterally and vertically into mudflats and terminal lobes and small deltas formed by red mudstones and sandstones. The very low depositional gradient made this system very sensitive to water balance, where small changes of lake level affected large basin areas (Anadón et al., 1989; Arenas and Pardo, 1999; Sáez et al., 2007). Lake level changes (Fig. 2) controlled the sequential arrangement of the lacustrine and alluvial-lacustrine sedimentary units, which exhibit a hierarchical architecture. In the inner lacustrine sectors, within the carbonate dominated successions, a basic 1.5 to 3 m thick (para)sequence occurs. This sequence displays a shallowing upwards trend, which includes from bottom to top: subaqueous coal deposits and/or calcisiltites (offshore facies), near-shore facies composed by gastropod and ostracode bearing micritic limestones and thin palustrine limestones overlain by greenish to gray mudstones (Cabrera and Sáez, 1987; Cabrera et al., 2002). The proportion of siliciclastic deposits (gray, variegated and red mudstones and sandstones) increases towards the marginal lacustrine zones, where thin limestone beds grade into red mudstones and thin sandstones.

The basic sequences can be grouped into 6–8 m thick carbonate dominated composite sequences in the lake depocenters. In the near-shore areas, composite sequences consist in 8–12 m thick mudstone dominated intervals with thin limestones interbeded. Carbonate-rich composite sequences are grouped into 25 to 35 m thick clusters, separated by thinner siliciclastic intervals which represent periods of major lake contraction. In its turn, in the mudstone dominated marginal lacustrine zones these clusters consist of limestone bed bundles interbedded with gray and variegated to red mudstone intervals. Finally, these clusters are grouped into thick limestone packages which correspond to the formal lithostratigraphic units of the Mequinenza and Torrente de Cinca carbonate-dominated units, and the alluvial Cuesta de Fraga Formation (Cabrera, 1983).

3. Magnetostratigraphy

A magnetostratigraphic study was carried out in order to provide an age model for the MLS sedimentary sequence. Two overlapping sections (PA and ME) were logged and later merged into a 307 m thick Mequinenza composite section (Fig. 3). Lithostratigraphic correlation between the PA and ME sections was feasible from field observations and later adjusted using magnetostratigraphic data (Fig. 3).

The Mequinenza section was sampled at 2 m stratigraphic intervals with a total number of 171 oriented paleomagnetic drill cores. Sampled lithologies included limestones, red to brown–grey silts and marls and, occasionally, fine-grained sandstones. Earlier magnetostratigraphic studies on the same stratigraphic units (Gomis et al., 1997; Barberà et al., 2001) showed that sediments retain

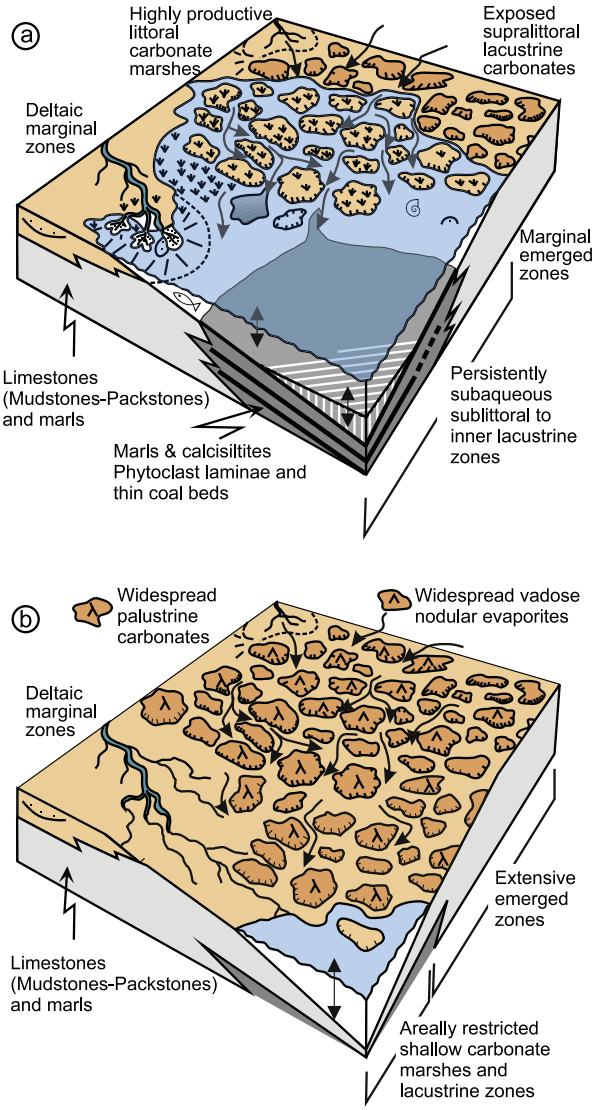

Fig. 2. Sedimentary model for the Mequinenza lacustrine sequences, modified after Cabrera et al. (2002). A) High-stand stage with coal deposits accumulated in the deepest parts. Laminated limestones grade into rooted mudstone, white, grey and greenish mudstone towards the lake margins. Red mudstone and sandstone occurred onshore. B) Low-stand stage with a detrital facies belt prograding basinwards.

a stable Characteristic Remanent Magnetization (ChRM) carried by either magnetite (limestones and marls) or hematite (red beds).

In order to isolate the ChRM, samples were stepwise thermally demagnetized at 50 °C temperature increments up to 300 °C and, thereafter at increments of 20 °C up to complete demagnetization of the NRM. Measurements were carried out in the laboratory of Paleomagnetism "Jaume Almera" (CCiTUB-CSIC) in Barcelona using a three axis superconducting rock magnetometer (2G-SRM750). Magnetic susceptibility was measured at each demagnetization step with a KLY-2 susceptibility bridge (Geofyzika Brno) in order to monitor mineralogical changes upon heating. The results from most of samples reveal the presence of two magnetic components (Fig. 4). A low-temperature, possibly viscous, component is removed after heating to 220 °C to 350 °C. Above this temperature a characteristic component is found with maximum unblocking temperatures ranging from 450 °C (limestones and grey silts) to 650 °C (red mudstones), interpreted as carried by the iron oxides magnetite and hematite, respectively. Substantial increases of magnetic susceptibility often occurred upon heating to temperatures above 400 °C, thus possibly indicating the formation of magnetic minerals during demagnetization.

The ChRM components were picked after visual inspection of Zijderveld plots in 112 samples (65% of the total number of samples) and directions were calculated by means of principal components analysis (Kirschvink, 1980) (Fig. 4). Fisherian means of the normal and reversed polarity directions pass the reversal test, although the reversed polarity mean clearly presents an anomalous shallow inclination. This deviation from expected values could be explained as the result of partial overlap of a normal polarity viscous component. Both normal and reversed polarity means present a clockwise departure of 9.6° (normal) and 13.3° (reversal) from GAD. The large dispersion of directional data, however, does not give statistical significance to these differences.

The Virtual Geomagnetic Pole (VGP) latitude was calculated at sample level and plotted against thickness in order to establish a Local Magnetic Polarity Stratigraphy (Fig. 3), where magnetozones represented by only one site were not considered as reliable features for correlation. A correlation of the Local Magnetostratigraphy with the Geomagnetic Polarity Time Scale (GPTS 2004, Gradstein et al., 2004) was feasible after integration with biostratigraphic (fossil rodents), magnetostratigraphic and litostratigraphic data from other sections in the region (Gomis et al., 1997; Barberà et al., 2001) (Fig. 5). The lower normal magnetozone in the Mequinenza section was consistently traced in the field and cross-checked with multiple magnetostratigraphic sections (Fig. 5), thus supporting a primary (synsedimentary) origin of the magnetization. The base of this magnetozone is taken as the key horizon for correlation with the Mina Pilar section. Best match of the composite sequence with the GPTS confirms earlier calibration results (Barberà et al., 2001). Correlation of a short magnetozone in Mequinenza (N5 in Fig. 3) with Torrente de Cinca section further suggests the existence of a brief normal geomagnetic event within C6Cr (referred to as cryptochron C6r-1 in the CK95 GPTS, Cande and Kent, 1995). This short chron is also found in high resolution magnetostratigraphic records in deep sea sediments (Lanci et al., 2005), although not recognized in the most recent time scale compilations (Gradstein et al., 2004, 2012).

The resulting correlation allows constructing a robust age calibration of the MLS sequence extending between 28.5 Ma and 21.5 Ma (Fig. 5), placing the Oligocene–Miocene boundary near the base of the Torrente de Cinca Formation in this area. The average sedimentation derived from magnetostratigraphy reflects an overall trend of steadily decreasing rates, higher rates being recorded in lower units of Mina Pilar section (*ca.* 13 cm/kyr), and lower rates in the upper part of the Mequinenza section (*ca.* 6 cm/kyr). In addition to this regional trend, variations in sedimentation rate occur in relation to shifts in the sedimentary environment. As observed in the Miocene sequences of the central Ebro Basin (Pérez-Rivarés et al., 2004), lacustrine limestone units yielded accumulation rates (*ca.* 6 cm/kyr), lower than the average 9 cm/kyr of the distal alluvial redbed sediments of the Cuesta de Fraga Fm (Supplementary Fig. A2).

4. Cyclostratigraphic analysis

Previous cyclostratigraphic analysis (Luzón et al., 2002; Barberà, 1999) revealed high frequency precession-related orbital forcing in specific limestone-dominated short intervals. But medium to low frequency (>100-kyr) cyclicity was undetermined because the studied time range were in all cases shorter than 1 Myr. In order to better examine the longer period cyclicity, a 500 m-thick composite sequence is studied here (Fig. 1, Fig. 3).

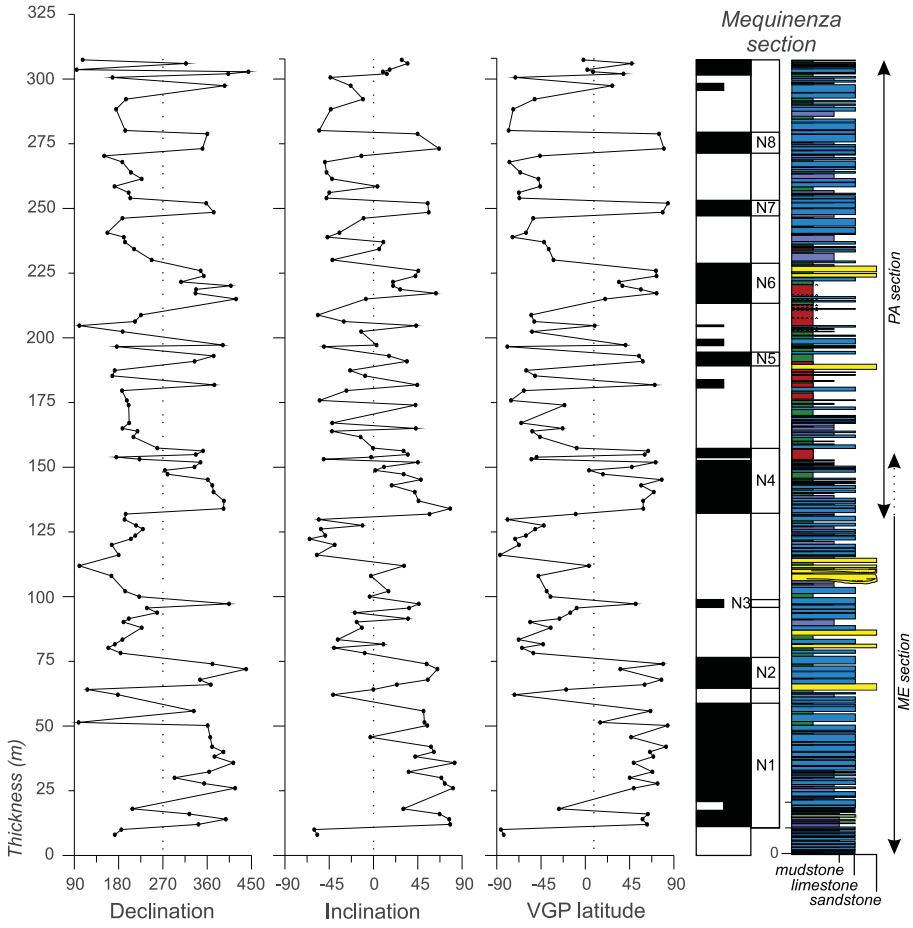

Fig. 3. Litho- and magnetostratigraphy of the Mequinenza composite section. (For interpretation of the references to color in this figure, the reader is referred to the web version of this article.)

4.1. Depth rank

For the cyclostratigraphic analysis, a time series which represents relative lake-level oscillations was built on the basis of sedimentary facies. We assumed that shifting lacustrine facies responded basically to water-depth changes, these being controlled by climatically driven changes in the water budget (Freytet and Plaziat, 1982; Olsen and Kent, 1996, 1999; Luzón et al., 2002; Alonso-Zarza, 2003). A rank of facies which can be ordered from shallow to deep lake conditions was characterized, obtaining an inferred relative paleobathymetry for the lacustrine system (Olsen and Kent, 1996). To build a time series, depth values were taken through the section at constant stratigraphic intervals of 40 cm, corresponding to a time resolution of 4 to 7 kyr (described in detail in Supplementary Table A1 and Supplementary Material).

4.2. Spectral analysis

Spectral analysis was done by REDFIT software (Schulz and Mudelsee, 2002) with a Rectangular/Blackman-Harris window and 2000 simulations. This method allowed estimating the red noise addition during data interpolation. Evolutionary wavelet spectra were obtained by the MATLAB script provided in Torrence and Compo (1998).

The MLS sequence encompasses several facies associations of varying clastic contribution which produced changes in sedimentation rate related to sedimentary environment, a source of noise in the spectral analysis (Machlus et al., 2008). To minimize distortions of the time series related to unsteady sedimentation, the sequence was split into 6 intervals according to the lithology (Fig. 6). Spectral analysis in the depth (thickness) domain was carried out in all 6 intervals, yielding significant peaks at frequencies whose ratios reproduce the ratios of eccentricity of 400-kyr and 100-kyr, 41-kyr obliquity and precession (Table 1). A preliminary age model constrained by magnetostratigraphy confirms that the lower frequency and most ubiquitous spectral peak of 25–30 m yields an average period of 400-kyr (Fig. 7). Thus, the 400-kyr cycle was selected for tuning because of its stability, both in our data and in the astronomical solution. To facilitate this task, the 400-kyr cycle was isolated from higher frequency signals by applying a bandpass filter below 20 m (which would correspond to 334-kyr in the lowest sedimentation rate interval) (green curve in Fig. 6). The filtered signal reveals, superposed on the 400-kyr beat, a long-wavelength oscillation which we associate to the 2.4-Myr eccentricity cycle, with eccentricity maxima correlated to times of lake expansion and eccentricity minima to lake low-stands (Fig. 6).

Linkage of the time series with the 400-kyr term of the orbital eccentricity (Laskar et al., 2004) was completed with the Analyseries 2.0.4 software (Paillard et al., 1996). The 400-kyr cycle at the base of the Mequinenza section was found poorly represented in the filtered signal possibly because of an edge effect (the correlation between the Mequinenza and Mina Pilar sections represents a lateral shift of 5 km, Supplementary Material), but reasonably identifiable from the lithostratigraphic log. Two 400-kyr cycles at the top of the section are also obscured due to the lack of facies contrast at times of persistent high lake levels. Assuming the current astronomical calibration of the GPTS at the Oligocene–

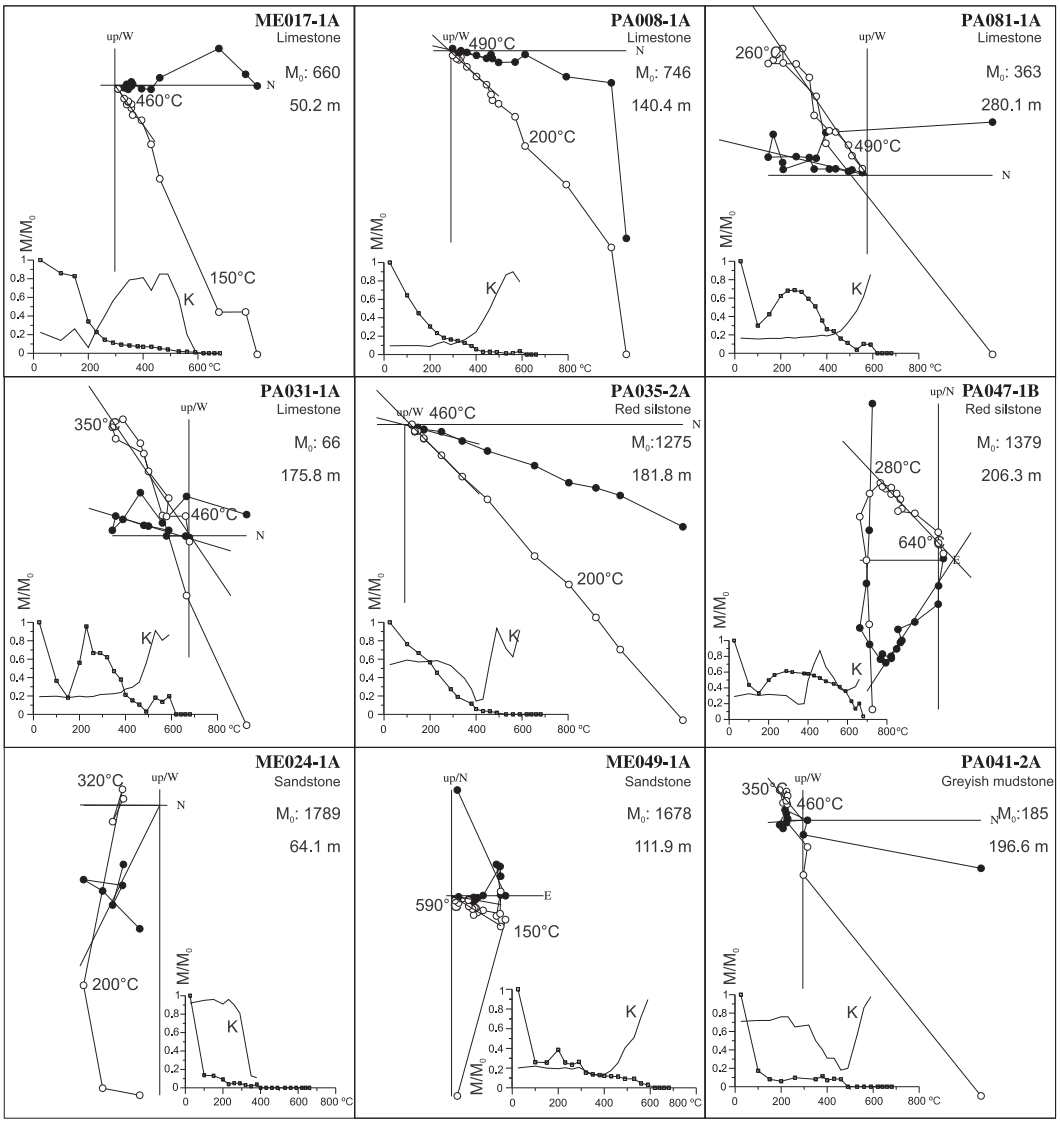

Polarity	N	Dec	Inc	k	α_{95}
Reverse	59	193.3	-25.1	4.4	10
Normal	53	9.6	49.8	4.6	10.3

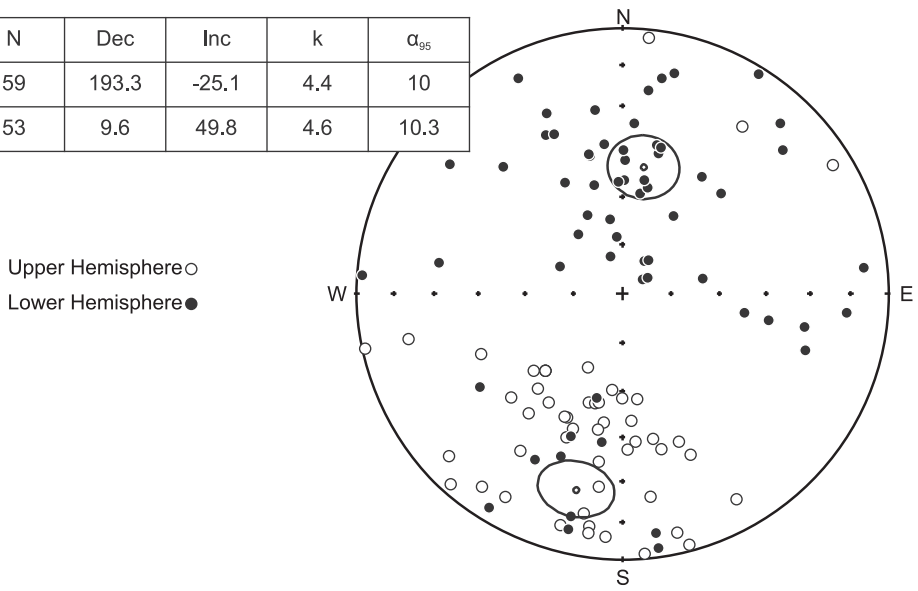

Fig. 4. Stepwise NRM thermal demagnetization (Zijderveld plots) of representative lithologies and normalized NRM and magnetic susceptibility changes upon heating. M_0: Initial NRM in 10^{-6} A/m. Sample stratigraphic position in meters referred to Fig. 3. Below, stereonet projection of paleomagnetic directions and their associated normal and reversed mean directions.

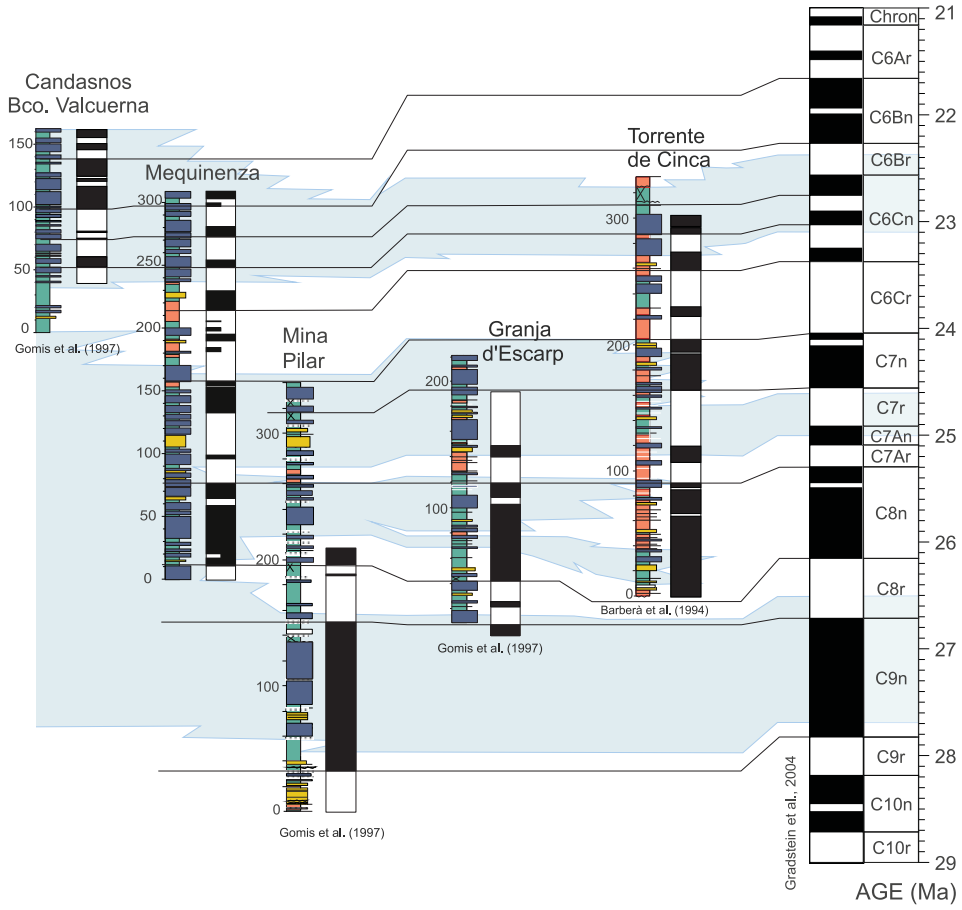

Fig. 5. Integrated magnetostratigraphy of the MLS sequence in the Mequinenza area based on earlier works (Gomis et al., 1997; Barberà et al., 2001) and the present study. Multiple overlapping magnetostratigraphic sections allow an identification of a sequence of reversals that can be traced laterally, thus giving strong evidence of a primary magnetization. The blue-shade bands mark the lacustrine facies.

Table 1
Significant periodicities of paleobathimetry time series of the MLS sequence obtained from spectral analysis in depth domain (REDFIT software, Schulz and Mudelsee, 2002). The confidence of the peaks is shown with % of significance between brackets. The correspondence in time domain of each peak is calculated assumed a period of 405 kyr (interval MP2, ME1, ME2 and ME3) or 100 kyr (interval MP1 and MP3) for the longest cycle identified at each stratigraphic interval.

Section	Interval	405 (kyr)	100 (kyr)	41 (kyr)	23 (kyr)	19 (kyr)
Mequinenza	ME3	24.23 m (95%)	5.74 m (90%) 95.94 kyr	2.67 m (99%) 44.62 kyr		1.23 m (95%) 20.55 kyr
	ME2	28.79 m (99%)	7.03 m (95%) 98.89 kyr	3.55 m (90%) 49.93 kyr	1.66 m (95%) 23.35 kyr	1.379 m (95%) 19.39 kyr
	ME1	26.7 m (99%)	6.92 m (95%) 115.76 kyr	2.25 m (90%) 37.62 kyr	1.48 m (95%) 24.74 kyr	
Mina Pilar	MP3		10.40 m (90%)	3.24 m (90%) 31.15 kyr		
	MP2	28.35 m (95%)	7.73 m (90%) 110.42 kyr			1.31 m (95%) 18.71 kyr
	MP1		14.26 m (99%)			

Miocene transition (Shackleton et al., 1999; Liebrand et al., 2011; Gradstein et al., 2012), magnetic reversals bounding this age were taken as a constraint for tuning. The resulting time series was rescaled into age domain (red). A new spectral analysis of the resulting 400-kyr tuned time series revealed increasing power of the 100-kyr peak, and an alignment of the 100-kyr peaks in the evolutionary wavelet spectra (Fig. 7). These results allow to tune with the eccentricity solution (Laskar et al., 2004) after applying a band-pass filter centered at the 100-kyr (bandwidth 0.00165, blue filter in Fig. 6).

The new age model derived from astronomical tuning allows comparing ages of geomagnetic reversals with the recent calibrations of the time scale (Pälike et al., 2006; Gradstein et al., 2004, 2012). Agreement within the resolution of the eccentricity cycle is found with GTS2004 (Gradstein et al., 2004). On the contrary, a mismatch with GTS2012 (Gradstein et al., 2012) is noticed for ages older than 25 Ma, reaching a maximum discrepancy of 400 kyr at the base of chron C9n. Noteworthy the GTS2012, which for this interval relies on astronomical tuning (Gradstein et al., 2012), has an unsolved discrepancy of same order with the radiometric time scales (Gradstein et al., 2012).

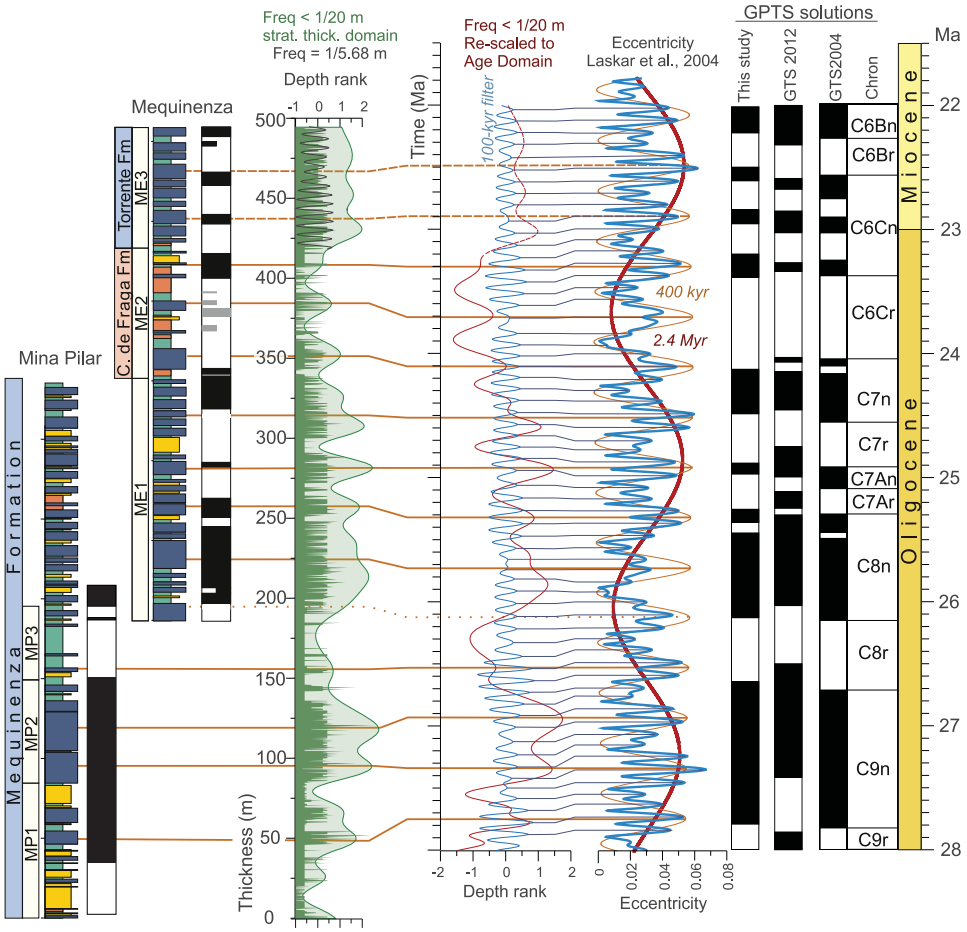

Fig. 6. Astrochronology of the MLS stratigraphic sequence. In the left, the stratigraphic logs are divided into 6 intervals according to the lithology. In green, the inferred bathymetry of the lake with an envelope which removes frequencies <20 m. The filtered signal revealed a long-wavelength oscillation which is associated to the 2.4-Myr eccentricity cycle, where eccentricity maxima correlates to peaks of lake expansion. Superposed to this trend, a higher frequency signal is interpreted as the expression of the 400-kyr eccentricity cycle. Analyseries software (Paillard et al., 1996) was used to link the filtered paleobathymetry series with the 400-kyr eccentricity cycle of the astronomical solution (Laskar et al., 2004). In the middle, the resulting time series was rescaled into age domain (red line) and a Gaussian filter centered at 100 kyr (bandwidth 0.00165) was applied. The output (blue) was linked to the 100-kyr eccentricity term of the astronomical solution. In the right, the age of geomagnetic reversals that results from this analysis is compared with most recent calibrations of the time scale (Gradstein et al., 2004, 2012).

5. Long-period orbital forcing of lacustrine sequences

The derived chronology of the MLS sequence reveals that three major phases of lacustrine expansion correlate to consecutive periods of maxima of the 2.4-Myr eccentricity cycle (Fig. 5, Fig. 6), thus suggesting long-period orbital forcing. Furthermore, the MLS sequence is integrated in a 20 Myr long sedimentary record which includes a succession of limestone formations representing shallow fresh-water perennial lakes. Some of these units extended over areas of up to 3000 km^2 at periods of lake high-stand (Anadón et al., 1989). Alternating with these relatively wet periods, nearly complete drying of the basin occurred at times of low-stand levels. A magnetochronological framework is available for the complete sequence of the eastern and central Ebro Basin after the work of Barberà et al. (2001), Gomis et al. (1997), Costa et al. (2010, 2011) and Pérez-Rivarés et al. (2002, 2004). These studies provide a time framework to test long-period orbital forcing of lacustrine sedimentation in the Eastern Ebro Basin (Fig. 8).

Succeeding basin continentalization the earliest lacustrine units in the East Ebro Basin were deposited adjacent to the South-Pyrenean Front. A first phase of evaporite deposition was followed by the fresh-water lacustrine limestones of the Castelltallat Fm, which extended over 100 km along an E–W elongated belt and reached maximum thickness of 200 m at its depocenter. Magnetostratigraphy of the Santpedor-Moià composite section (Costa et al., 2011) allows a precise correlation of this phase of lacustrine expansion to the lower part of chron C13r (Fig. 8), while by the end of the Eocene lake environments shrink and practically disappeared from the eastern Ebro Basin. During this period, the E/O boundary is marked by a distinct progradation of an amalgamated sandstone unit, interpreted as the response of the fluvial fan system to a transient lake level lowstand (Costa et al., 2011).

A renewed expansion of lake environments occurred during the early Oligocene, its maximum expansion being represented by the coal-bearing limestones of the Calaf Fm (Fig. 8). Despite lacking direct magnetostratigraphy, the Calaf Fm grades laterally into alluvial sequences which are correlated to chron C12r (Costa et al., 2010). Sedimentation during this phase was characterized by a progressive southwards migration and retraction of lake environments (Montmaneu and Tàrrega Fms., Fig. 8). Lacustrine sedimentation was eventually interrupted after deposition of the Tàrrega Fm, when an important progradation of alluvial systems occurred.

The late Early Oligocene is characterized by a rapid westward shift of lacustrine environments to the area of Mequinenza (Fig. 1), where the MLS depocenter remained stable for the rest of the Oligocene. The basal lacustrine units of the MLS do not outcrop on surface, but their approximate limits and thickness are known from exploration boreholes (Cabrera et al., 2002). Proximal equivalents

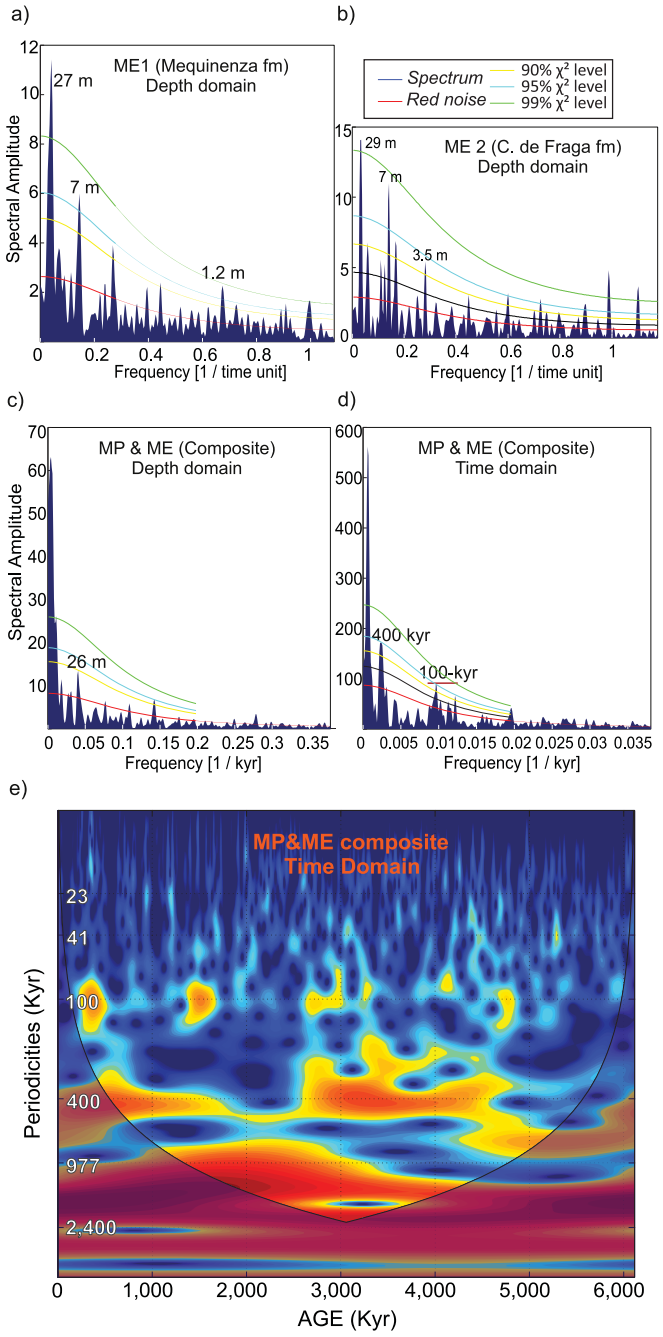

Fig. 7. Spectral analysis (Redfit, Schulz and Mudelsee, 2002) and wavelet analysis (Torrence and Compo, 1998) of the bathymetry time series of the MLS sequence. Spectral analysis in depth domain shows significant peaks at characteristics frequencies in each interval (A, B), while the entire section only reveals a significant peak near 26 m (C). It is interpreted that peaks at high frequencies are obscured by changes of sedimentary rates. Conversion into time domain after tuning with the 400-kyr eccentricity cycle increases notably the spectral power corresponding to the 100-kyr cycle (D). 400-kyr and 100-kyr cycles can be observed in wavelet analysis (E).

of these units are the mixed alluvial/lacustrine Marqueses Fm (Fig. 8), but its limited exposure on surface prevents further analysis on its stacking pattern.

As shown above, three major phases of lacustrine expansion were observed during the deposition of the MLS sequence. The first expansion includes the coal-bearing carbonate sequences of the lower Mequinenza Fm, dated to within chron C9n (Gomis et al., 1997). At this time, lacustrine facies spread to nearly reach the basin margins in the Gandesa area (Barberà et al., 2001; Jones et al., 2004). The second lacustrine expansion within the Mequinenza Fm is traced along the Cinca River valley, where lacustrine limestones spread northwards over more than 10 km on top of distal alluvial red mudstones of Pyrenean source (Fig. 5). The Mequinenza depocenter experienced a sharp and temporary disappearance of lacustrine environments during the latest Oligocene, followed by a new last expansion during the earliest Miocene (Torrente de Cinca limestone Fm, Fig. 5).

After deposition of the Torrente de Cinca Fm, lacustrine environments migrated westwards to the central parts of Ebro Basin. A shallow-lake carbonate belt (Alcubierre Fm, Fig. 8) graded laterally into a thick evaporitic sequence which accumulated in the basin center since the Oligocene. First expansion of the carbonates of the Alcubierre Fm is dated in the Albalatillo section to within chron C6An.1n (Pérez-Rivarés et al., 2002). In the Sierra de Alcubierre a second cycle peaks within chron C5Dn (Pérez-Rivarés et al., 2002), followed at the Early/Middle Miocene transition by the most pronounced lake expansion of the whole record (Pérez-Rivarés et al., 2004). A sharp basin-wide transition from the salt to fresh water lake environments (Arenas and Pardo, 1999) indicates an important rise of water balance, in coincidence with the warm phase of the middle Miocene Climate Optimum (Holbourn et al., 2007).

The spatial and temporal distribution of sedimentary environments in the Ebro Basin reveals a long-term migration of lake depocenters, a process in first place controlled by the patterns of tectonic thrust sheet loading, crustal subsidence and uplift. During the Late Eocene, the location of earliest lake environments was determined by the foredeep flexure adjacent to the South-Pyrenean Front (Anadón et al., 1989). In the Early Oligocene the cratonwards shift of the flexural subsidence (Vergés et al., 2002), coupled with the progradation of the clastic wedge caused a southwards migration of the lake environments. Finally, by the late Oligocene the East Iberian margin was involved in the rifting of the western Mediterranean region (Gaspar-Escribano et al., 2004). This new geodynamic regime caused uplift in the eastern Ebro Basin and, consequently, a westward migration of the sedimentary depocenters.

In addition to the long-term migration of lacustrine depocenters, shorter wavelenght oscillations in the size of lake environments occurs at a mean period of 2.4-Myr. Discerning between both is not straightforward and requires a three-dimensional view of the sedimentary stacking pattern. However, some lake expansion pulses were of such amplitude that led to their identification at distances over 100 km. Shrink and disappearance of lake environments also occurred at key intervals such as the Eocene/Oligocene and the Oligocene/Miocene transitions.

The magnetostratigraphy-based chronology of the continental Ebro Basin infill supports a correlation of periods of maximum expansion of lake environments with maxima of the 2.4 Myr eccentricity cycle, thus suggesting orbital forcing. It is noteworthy that this view challenges earlier interpretations, which associate the formation-scale stratigraphic architecture in foreland systems with tectonic processes (Alonso-Zarza et al., 2002; Miall, 2014). It is suggested that sensitivity to climate change of the lake systems in the Ebro Basin was possibly facilitated by the buffer effect of the sediment transfer systems, large enough to attenuate the supply-driven tectonic signal that propagated from active margins (Castelltort and Van Den Driessche, 2003; Armitage et al., 2013).

6. Eccentricity paced climates in the circum-Mediterranean area

The astronomical tuning of the MLS sequence shows that periods of lacustrine expansions are associated with times of eccentricity maxima of the 100-kyr, 400-kyr and 2.4-Myr cycle (Fig. 2),

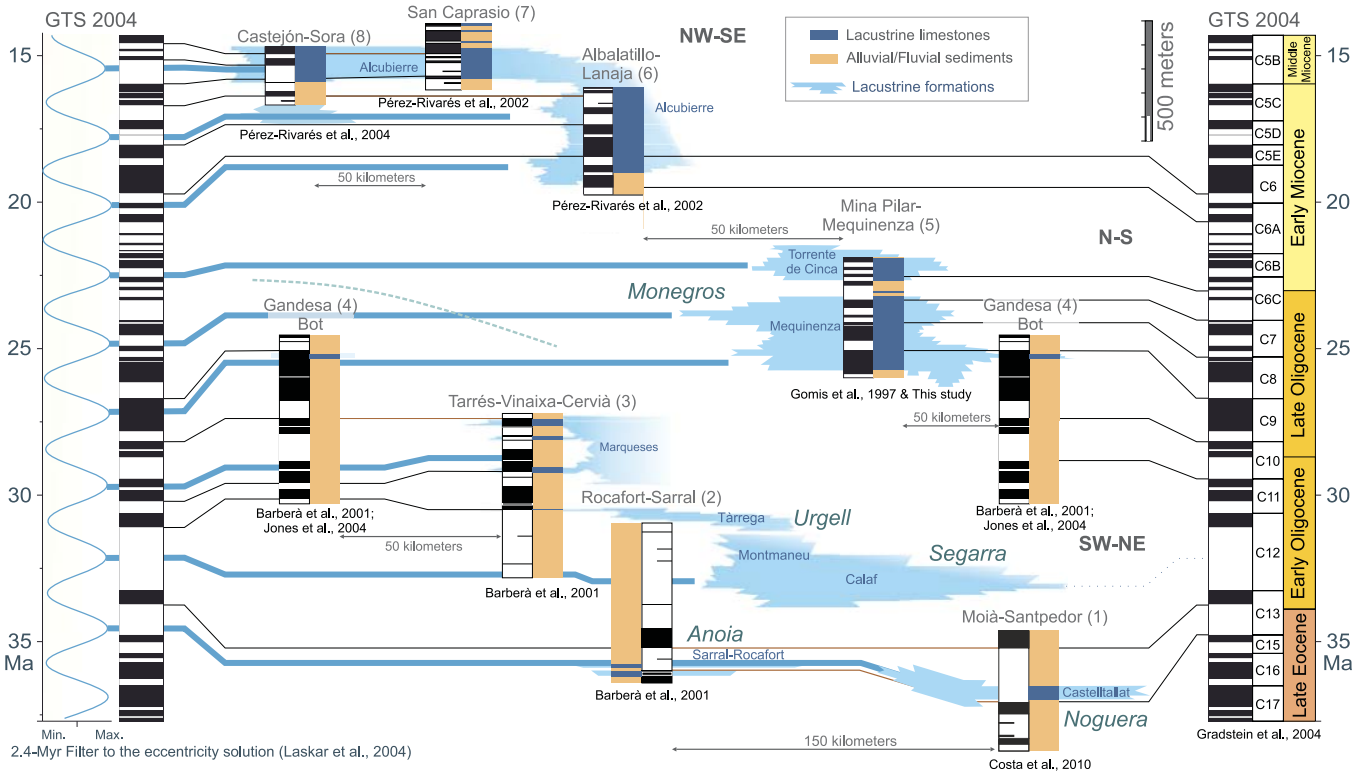

Fig. 8. A magnetostratigraphy-based chronostratigraphy of the continental record of the eastern (bottom panel) to central (top panel) Ebro foreland basin (see location of panels in Fig. 1). In the left, a 2.4-Myr band-pass filter of the eccentricity solution (Laskar et al., 2004) and the GPTS (Gradstein et al., 2004). Blue lines mark peaks of 2.4-Myr eccentricity maxima. In the middle, magnetostratigraphy and synthetic lithostratigraphy of key-sections (see location in Fig. 1), with indication of lacustrine (dark blue) and alluvial/fluvial sediments (brown). The lateral extent of lacustrine formations (light blue) is based on field correlations (Anadón et al., 1989; Arenas and Pardo, 1999; Barberà et al., 2001), and are faded out to mark the end of lateral control.

whereas times of eccentricity minima are marked by shrinking of lake environments. These results are in agreement with earlier studies in the Mediterranean region (Lourens et al., 2004) and other perimediterranean Neogene records (van Vugt et al., 2001; Abdul Aziz et al., 2003; Abels et al., 2009) which concluded that the 100-kyr and 400-kyr eccentricity minima and maxima were related to periods of low- and high-average precipitation respectively. Since the contribution of the 2.4-Myr cycle to the insolation spectra is very low (Laskar et al., 2004), it is inferred that long-period orbital forcing is transmitted through modulation of the shorter eccentricity cycles of 400-kyr and (specially) 100-kyr and, consequently, by the amplitude of the precession cycle. It has been suggested that an important moisture source in the northern Mediterranean borderland regions could be the North Atlantic cyclones, with prevailing southern trajectories at times of precession minima (Tuenter et al., 2004; Kutzbach et al., 2014). It is plausible then that the Iberian plate, situated along the track of the north Atlantic depressions entering the Mediterranean region, was receptive to this orbital forcing, as shown in the Pliocene sediments of the Guadalquivir Basin (Sierro et al., 2000).

The continuous record of sapropels in the Mediterranean basin suggests that coupling between precession and atmospheric circulation predicted for recent times extended into the Miocene (Tuenter et al., 2004; Abels et al., 2009; Mourik et al., 2010). Likewise, the long continuous eccentricity-paced record of wet/dry periods in the Ebro Basin suggests that a similar coupling extended into Paleogene climates of southwestern Europe. During this period, substantial paleogeographic transformations occurred, which include the progressive closing of the Atlantic–Indian connection through the Tethys Ocean, and the opening of the western Mediterranean during the Neogene. At global scale, major changes in atmospheric and the oceanic thermohaline circulation are associated with the stepwise growth of Antarctic ice cap and Arctic glaciations (Zachos et al., 2001). It is remarkable that the imprint of long-period eccentricity cycles is not obscured by these large magnitude rearrangements, emphasizing the role of mid-latitude atmospheric circulation in Mediterranean climates.

Long-period orbital forcing related to the 2.4-Myr cycle was already pointed out in earlier studies in the Neogene continental basins of Central Spain (Abels et al., 2009, 2010; van Dam et al., 2006). However, they suggest a phase-relationship of the 2.4-Myr cycle which is opposite to our results from the Ebro basin. Particularly intriguing is the small mammal record, showing abundance of wet-adapted assemblages at times of 2.4-Myr and 0.97-Myr eccentricity minima (van Dam et al., 2006). In the Madrid Basin, the occurrence of carbonate intervals at times of 2.4-Myr eccentricity minima was attributed to a prolonged absence of relatively dry and evaporative conditions during eccentricity minima (Abels et al., 2010). But, it must be noted that carbonate formations in the Neogene basins of Central Spain basins often formed from amalgamation of palustrine calcretes and carbonate paleosoils. These carbonate units were formed in poorly drained marginal areas, under very low terrigenous supply (Alonso-Zarza, 2003; Armenteros and Huerta, 2006), not necessarily linked to wetter climate conditions. On the other hand, the role that local factors (basin shape and size, relief and drainage area) exert in the link between climate and sedimentation needs to be considered. Further research is required to constrain the basin characteristics that influence the evaporation/precipitation ratios and control the diverse sedimentary responses to orbital forcing.

7. Conclusions

The stratigraphic architecture of the late stages (Late Eocene to Middle Miocene) of the eastern Ebro Basin shows a punctuated migration of the lacustrine systems as a response to the balance between sediment supply and subsidence (Fig. 1). Superposed to this trend of shifting depocenters, the periodic expansion and retraction of the successive lake units indicates that orbital forcing is expressed over a wide range of frequencies, included the million-year scale. Spectral analysis reveals significant power at 100-kyr and 400-kyr linked to the short- and long-eccentricity cycles. In addition, a magnetochronological framework which embraces a 20 Myr long record has allowed identifying very-long period oscillations of the lake system associated to the 2.4-Myr eccentricity cycle.

Despite the important paleogeographic rearrangements in the Mediterranean region and the high-amplitude global climate shifts during the Oligocene and Miocene, lake environments remained paced by the orbital eccentricity. Times of lake expansion representing relatively wet periods are correlated to eccentricity maxima. This is a phase-relationship which is shared with most of Neogene Mediterranean basins.

It is worth noting that these conclusions are reached in the context of a foreland basin, where million-year scale sedimentary sequences are often interpreted as of tectonic origin. Discerning between long-period orbital cycles and tectonic-driven sequences is revealed as a fundamental issue in interpreting the large-scale stratigraphic architecture in foreland systems. A decoupling between tectonically-forced clastic sequences and climate-forced lacustrine sequences arises as a plausible scenario.

Acknowledgements

This research was funded by the Spanish project COFORSED (CGL2010-17479) and the Research Group of “Geodinàmica i Anàlisi de Conques” (2009GGR 1198). LV acknowledges the University of Barcelona for financial support (APIF-UB). We thank Bet Beamud and Núria Carrera for paleomagnetic sampling assistance. Thanks to the Laboratory of Paleomagnetism of Barcelona (CCiTUB-ICTJA CSIC). This is a contribution to the ESF Research Networking programme EARTHTIME-EU. Hemmo Abels and two anonymous reviewers are thanked for their thorough reviews that contributed to improve the manuscript. Sébastien Castelltort is thanked for a previous revision of the manuscript.

Appendix A. Supplementary material

Supplementary material related to this article can be found online at http://dx.doi.org/10.1016/j.epsl.2014.10.007.

References

Abdul Aziz, H., Krijgsman, W., Hilgen, F., Wilson, D., Calvo, J.P., 2003. An astronomical polarity timescale for the late middle Miocene based on cyclic continental sequences. J. Geophys. Res. 108 (B3).

Abels, H.A., Abdul Aziz, H., Calvo, J.P., Tuenter, E., 2009. Shallow lacustrine carbonate microfacies document orbitally paced lake-level history in the Miocene Teruel Basin (North–East Spain). Sedimentology 56, 399–419.

Abels, H.A., Aziz, H.A., Krijgsman, W., Smeets, S.J.B., Hilgen, F.J., 2010. Long-period eccentricity control on sedimentary sequences in the continental Madrid Basin (middle Miocene, Spain). Earth Planet. Sci. Lett. 289, 220–231.

Alonso-Zarza, A.M., 2003. Palaeoenvironmental significance of palustrine carbonates and calcretes in the geological record. Earth-Sci. Rev. 60, 261–298. http://dx.doi.org/10.1016/S0012-8252(02)00106-X.

Alonso-Zarza, A.M., et al., 2002. Tertiary. In: Gibbons, W., Moreno, T. (Eds.), The Geology of Spain. Geological Society, London, pp. 293–334.

Anadón, P., Cabrera, L., Colldeforns, B., Sáez, A., 1989. Los sistemas lacustres del Eoceno superior y Oligoceno del sector oriental de la Cuenca del Ebro. Acta Geol. Hisp. 24, 205–230.

Arenas, C., Pardo, G., 1999. Latest Oligocene–Late Miocene lacustrine systems of the north–central part of the Ebro Basin (Spain): sedimentary facies model and palaeogeographic synthesis. Palaeogeogr. Palaeoclimatol. Palaeoecol. 151, 127–148.

Armenteros, I., Huerta, P., 2006. The role of clastic sediment influx in the formation of calcrete and palustrine facies: a response to paleographic and climatic conditions in the Southeastern Tertiary Duero basin (northern Spain). In: Alonso-Zarza, Eds A.M., Tanner, L.H. (Eds.), Paleoenvironmental Record and Applications of Calcretes and Palustrine Carbonates. In: Spec. Pap., Geol. Soc. Am., vol. 416, pp. 119–132.

Armitage, J.J., Dunkley Jones, T., Duller, R.A., Whittaker, A.C., Allen, P.A., 2013. Temporal buffering of climate-driven sediment flux cycles by transient catchment response. Earth Planet. Sci. Lett. 369–370, 200–210.

Barberà, X., 1999. Magnetostratigrafia de l'Oligocè del sector sud-oriental de la Conca de l'Ebre: implicacions magnetobiocronològiques i seqüencials. PhD Thesis. Publications Univ. de Barcelona, Barcelona.

Barberà, X., Cabrera, L., Marzo, M., Parés, J.M., Agustí, J., 2001. A complete terrestrial Oligocene magnetobiostratigraphy from the Ebro Basin, Spain. Earth Planet. Sci. Lett. 187, 1–16.

Cabrera, L., 1983. Estratigrafía y Sedimentología de las formaciones lacustres del tránsito Oligoceno–Mioceno del SE de la cuenca del Ebro. PhD Thesis. Univ. de Barcelona, Barcelona.

Cabrera, L., Sáez, A., 1987. Coal deposition in carbonate-rich shallow lacustrine systems: the Calaf and Mequinenza sequences (Oligocene, eastern Ebro Basin, NE Spain). J. Geol. Soc. 144, 451–461.

Cabrera, L., Cabrera, M., Gorchs, R., de las Heras, F.X., 2002. Lacustrine basin dynamics and organosulphur compound origin in a carbonate-rich lacustrine system (Late Oligocene Mequinenza Formation, SE Ebro Basin, NE Spain). Sediment. Geol. 148, 289–317.

Cande, S.C., Kent, D.V., 1995. Revised calibration of the geomagnetic polarity timescale for the Late Cretaceous and Cenozoic. J. Geophys. Res. 100, 6093–6095.

Castelltort, S., van Den Driessche, J., 2003. How plausible are high-frequency sediment supply-driven cycles in the stratigraphic record? Sediment. Geol. 157, 3–13.

Costa, E., Garcés, M., López-Blanco, M., Beamud, E., Gómez-Paccard, M., Larrasoaña, J.C., 2010. Closing and continentalization of the South Pyrenean foreland basin (NE Spain): magnetochronological constraints. Basin Res. 22, 904–917.

Costa, E., Garcés, M., Sáez, A., Cabrera, L., López-Blanco, M., 2011. The age of the “Grande Coupure” mammal turnover: new constraints from the Eocene–Oligocene record of the Eastern Ebro Basin (NE Spain). Palaeogeogr. Palaeoclimatol. Palaeoecol. 301, 97–107.

van Dam, J.A., Abdul Aziz, H., Alvarez Sierra, M.A., Hilgen, F.J., van den Hoek Ostende, L.W., Lourens, L.J., Mein, P., van der Meulen, A.J., Pelaez-Campomanes, P., 2006. Long-period astronomical forcing of mammal turnover. Nature 443, 687–691.

DeCelles, P.G., Giles, K.A., 1996. Foreland basin systems. Basin Res. 8, 105–123.

Freytet, P., Plaziat, J.C., 1982. Continental carbonate sedimentation and pedogenesis-Late Cretaceous and Early Tertiary of southern France. In: Purser, B.H. (Ed.), Contrib. to Sedimentology, vol. 12. Schweizerbart'sche Verlag, Stuttgart. 217 pp.

García-Castellanos, D., Vergés, J., Gaspar-Escribano, J., Cloetingh, S., 2003. Interplay between tectonics, climate, and fluvial transport during the Cenozoic evolution of the Ebro Basin (NE Iberia). J. Geophys. Res. 108, B7.

Gaspar-Escribano, J., García-Castellanos, D., Roca, E., Cloetingh, S., 2004. Cenozoic vertical motions of the Catalan Coastal Ranges (NE Spain): the role of tectonics, isostasy and surface transport. Tectonics 23 (1).

Gomis, E., Parés, J.M., Cabrera, L., 1997. Nuevos datos magnetoestratigráficos del tránsito Oligoceno–Mioceno en el sector SE de la Cuenca del Ebro (provincias de Lleida, Zaragoza y Huesca, NE de España). Acta Geol. Hisp. 32, 185–199.

Gradstein, F.M., Ogg, J.G., Smith, A.G., 2004. A Geologic Time Scale 2004. Cambridge University Press, Cambridge, UK.

Gradstein, F.M., Ogg, J.G., Schmitz, M., Ogg, G., 2012. The Geologic Time Scale 2012 2-Volume Set. Elsevier.

Holbourn, A., Kuhnt, W., Schulz, M., Flores, J.-A., Andersen, N., 2007. Orbitally-paced climate evolution during the middle Miocene “Monterey” carbon–isotope excursion. Earth Planet. Sci. Lett. 261, 534–550.

Jones, M.A., Heller, P.L., Roca, E., Garcés, M., Cabrera, L., 2004. Time lag of syntectonic sedimentation across an alluvial basin: theory and example from the Ebro Basin, Spain. Basin Res. 16, 467–488.

Kashiwaya, K., Ochiai, S., Sakai, H., Kawai, T., 2001. Orbit-related long-term climate cycles revealed in a 12-Myr continental record from Lake Baikal. Nature 410, 71–73.

Kirschvink, J.L., 1980. The least-squares line and plane and the analysis of palaeomagnetic data. Geophys. J. Int. 62, 699–718.

Kutzbach, J.E., Chen, G., Cheng, H., Edwards, R.L., Liu, Z., 2014. Potential role of winter rainfall in explaining increased moisture in the Mediterranean and Middle East during periods of maximum orbitally-forced insolation seasonality. Clim. Dyn. 42 (3–4), 1079–1095. http://dx.doi.org/10.1007/s00382-013-1692-1.

Lanci, L., Parés, J.M., Channell, J.E.T., Kent, D.V., 2005. Oligocene magnetostratigraphy from Equatorial Pacific sediments (ODP Sites 1218 and 1219, Leg 199). Earth Planet. Sci. Lett. 237, 617–634.

Laskar, J., Robutel, P., Joutel, F., Gastineau, M., Correia, A.C.M., Levrard, B., 2004. A long-term numerical solution for the insolation. Astron. Astrophys. 285, 261–285.
Liebrand, D., Lourens, L.J., Hodell, D.A., de Boer, B., van de Wal, R.S.W., Pälike, H., 2011. Antarctic ice sheet and oceanographic response to eccentricity forcing during the early Miocene. Clim. Past 7, 869–880.
Lourens, L., Hilgen, F., 1997. Long-periodic variations in the earth's obliquity and their relation to third-order eustatic cycles and late Neogene glaciations. Quat. Int. 40, 43–52.
Lourens, L.J., Hilgen, F.J., Shackleton, N.J., Laskar, J., Wilson, D.S., 2004. The Neogene Period. In: Gradstein, F.M., Ogg, J.G., Smith, A. (Eds.), A Geologic Time Scale 2004. Cambridge University Press, Cambridge, pp. 405–440.
Luzón, A., González, A., Muñoz, A., Sánchez-Valverde, B., 2002. Upper Oligocene–Lower Miocene shallowing-upward lacustrine sequences controlled by periodic and non-periodic processes (Ebro Basin, northeastern Spain). J. Paleolimnol. 28, 441–456.
Machlus, M.L., Olsen, P.E., Christie-Blick, N., Hemming, S.R., 2008. Spectral analysis of the lower Eocene Wilkins Peak Member, Green River Formation, Wyoming: support for Milankovitch cyclicity. Earth Planet. Sci. Lett. 268, 64–75.
Miall, A.D., 2014. Fluvial Depositional Systems. Springer, New York, USA.
Mourik, A.A., Bijkerk, J.F., Cascella, A., Hüsing, S.K., Hilgen, F.J., Lourens, L.J., Turco, E., 2010. Astronomical tuning of the La Vedova High Cliff section (Ancona, Italy) – implications of the Middle Miocene climate transition for Mediterranean sapropel formation. Earth Planet. Sci. Lett. 297, 249–261.
Olsen, P.E., 1986. A 40-million-year lake record of early Mesozoic orbital climatic forcing. Science 234, 842–848.
Olsen, P.E., Kent, D.V., 1996. Milankovitch climate forcing in the tropics of Pangaea during the Late Triassic. Palaeogeogr. Palaeoclimatol. Palaeoecol. 122, 1–26.
Olsen, P.E., Kent, D.V., 1999. Long-period Milankovitch cycles from the Late Triassic and Early Jurassic of eastern North America and their implications for the calibration of the Early Mesozoic time-scale and the long-term behaviour of the planets. Philos. Trans. Math. Phys. Eng. Sci. 357, 1761–1786.
Paillard, D., Labeyrie, L., Yiou, P., 1996. Macintosh program performs time-series analysis. Eos Trans. AGU 77, 379.
Pälike, H., Norris, R.D., Herrle, J.O., Wilson, P.A., Coxall, H.K., Lear, C.H., Shackleton, N.J., Tripati, A.K., Wade, B.S., 2006. The heartbeat of the Oligocene climate system. Science 314, 1894–1898.
Paola, C., Heller, P.L., Angevine, C.L., 1992. The large-scale dynamics of grain size variation in alluvial basins, 1: theory. Basin Res. 4, 73–90.
Pérez-Rivarés, F., Garcés, M., Arenas, C., Pardo, G., 2002. Magnetocronología de la sucesión miocena de la Sierra de Alcubierre (sector central de la cuenca del Ebro). Rev. Soc. Geol. Esp. 15, 217–231.
Pérez-Rivarés, F., Garcés, M., Arenas, C., Pardo, G., 2004. Magnetostratigraphy of the Miocene continental deposits of the Montes de Castejón (central Ebro basin, Spain): geochronological and paleoenvironmental implications. Geol. Acta 2, 221–234.
Petersen, K.D., Nielsen, S.B., Clausen, O.R., Stephenson, R., Gerya, T., 2010. Small-scale mantle convection produces stratigraphic sequences in sedimentary basins. Science 329, 827–830.
Sáez, A., Anadón, P., Herrero, M.J., Moscariello, A., 2007. Variable style of transition between Palaeogene fluvial fan and lacustrine systems, southern Pyrenean foreland, NE Spain. Sedimentology 54, 367–390.
Schulz, M., Mudelsee, M., 2002. REDFIT: estimating red-noise spectra directly from unevenly spaced paleoclimatic time series. Comput. Geosci. 28, 421–426.
Shackleton, N.J., Crowhurst, S.J., Weedon, G.P., Laskar, J., 1999. Astronomical calibration of Oligocene–Miocene time. Philos. Trans. Math. Phys. Eng. Sci. 357, 1907–1929.
Sierro, F.J., Ledesma, S., Flores, J.A., Torrescusa, S., Martínez del Olmo, W., 2000. Sonic and gamma-ray astrochronology: cycle to cycle calibration of Atlantic climatic records to Mediterranean sapropels and astronomical oscillations. Geology 4, 695–698.
Torrence, C., Compo, G.P., 1998. A practical guide to wavelet analysis. Bull. Am. Meteorol. Soc. 79, 61–78.
Tuenter, E., Weber, S.L., Hilgen, F.J., Lourens, L.J., Ganopolski, A., 2004. Simulation of climate phase lags in response to precession and obliquity forcing and the role of vegetation. Clim. Dyn. 24, 279–295.
Vergés, J., Fernàndez, M., Martínez, A., 2002. The Pyrenean orogen: pre-, syn-, and post-collisional evolution. J. Virtual Explorer 8, 57–76.
van Vugt, N., Langereis, C.G., Hilgen, F.J., 2001. Orbital forcing in Pliocene–Pleistocene Mediterranean lacustrine deposits: dominant expression of eccentricity versus precession. Palaeogeogr. Palaeoclimatol. Palaeoecol. 172, 193–205.
Zachos, J., Pagani, M., Sloan, L., Thomas, E., Billups, K., 2001. Trends, rhythms, and aberrations in global climate 65 Ma to present. Science 292, 686–693.

Appendix 2

Linking sedimentation rates and large-scale architecture for facies prediction in nonmarine basins (Paleogene, Almazan Basin,Spain)

Basin Research

IAS EAGE

Basin Research (2015) 1–20, doi: 10.1111/bre.12145

Linking sedimentation rates and large-scale architecture for facies prediction in nonmarine basins (Paleogene, Almazán Basin, Spain)

Luis Valero,* Pedro Huerta,† Miguel Garcés,* Ildefonso Armenteros,‡ Elisabet Beamud§ and Miriam Gómez-Paccard¶

*Dept. d'Estratigrafia, Paleontologia i Geociencies Marines, Facultat de Geologia, Universitat de Barcelona, Barcelona, Spain

†Dept. Geología, Universidad de Salamanca, Escuela Politécnica Superior de Ávila, Ávila, Spain

‡Dept. Geología, Facultad de Ciencias, Universidad de Salamanca, Salamanca, Spain

§Laboratori de Paleomagnetisme CCiTUB-ICTJA CSIC, Barcelona, Spain

¶Géosciences-Rennes, UMR 6118, Université de Rennes 1, Rennes, France

ABSTRACT

This article focuses on the relationships between the large-scale stratigraphic architecture of the Almazán basin infill and the sedimentation rates (SR) calculated for precise time intervals. Our aim was to improve the understanding of the timing and causes of the architectural changes, their significance in terms of accommodation space and sediment supply and their relationship with climate and tectonics. The study area includes the Gómara fluvial fan, the main sediment transfer system of the Almazán basin during Paleogene times. Its large-scale architecture shifted through time between a stacking pattern of low density ribbon-like and high density sheet-like channel fills. Laterally to the fluvial system, mudstone and evaporitic mudstone units represented evaporitic mudflats which passed laterally into palustrine/lacustrine limestone units interpreted as lakes and ponds. Stacked calcretes occurred in distal alluvial and distal floodplain settings. A magnetostratigraphy encompassing 2600 m guided by available fossil mammal biochronology has provided a temporal framework that spans the complete Paleogene infill of the basin, from Late Lutetian to Late Oligocene, filling a gap in the Cenozoic chronostratigraphy of Spanish basins. This permits to constrain the kinematics of the structures both in the basin and in its margins, and to provide the timing for the depositional sequences. These data, combined with a magnetostratigraphic map, where magnetic reversals were traced through the Gómara monocline, allow a detailed analysis of the SR variability across the fluvial system and its adjacent depositional environments. The results show that high sedimentation rates (around 30–40 cm kyr^{-1}) are related to fluvial environments with low density ribbon-shaped channels, while low SR (around or below 10 cm kyr^{-1}) are related to high density sheet-like channels. Laterally, mud dominated environments with high SR (15–20 cm kyr^{-1}) grade into palustrine/lacustrine carbonated environments with low SR (around 9 cm ky^{-1}). The lowest SR (about 3 cm kyr^{-1}) are related to the development of stacked calcrete profiles in distal floodplain and in the connection of distal alluvial and palustrine/lacustrine units.

INTRODUCTION

The development of sequence stratigraphy has provided a framework for basin-wide correlations, interpretation and prediction of sedimentary facies and environments (Mitchum *et al.*, 1977; Vail & Mitchum, 1977; Posamentier & Vail, 1988; Van Wagoner *et al.*, 1988; Catuneanu, 2006). A large number of studies have focused on the variations of large-scale architecture of fluvial systems to understand why, where and when highly interconnected fluvial channels occur (Bridge & Leeder, 1979; Shanley & McCabe, 1991; Wright & Marriott, 1993; Mackey & Bridge, 1995; Legarreta & Uliana, 1998; Sheets *et al.*, 2002; Hickson *et al.*, 2005).

The architectural arrangement of the sedimentary record in non-marine basins is the response to the interplay between accommodation space and sediment supply (Catuneanu *et al.*, 2009). The main allogenic factors driving changes in accommodation space and sediment supply are tectonics and climate, which also modify the slope of the system (Catuneanu & Elango, 2001), the avulsion rate (Bryant *et al.*, 1995; Heller & Paola, 1996), the bypass

Correspondence: Luis Valero, Dept. d'Estratigrafia, Paleontologia i Geociencies Marines, Facultat de Geologia, Universitat de Barcelona, 08028 Barcelona, Spain. E-mail: luisvalero@ub.edu.

ratio, and the amount of sediment extracted along the sediment transport system (Strong *et al.*, 2005; Paola & Martin, 2012; Michael *et al.*, 2014). Here, we hypothesize that the characterization of the large-scale architectural arrangement together with quantification of sedimentary rates can help assessing the relative role of accommodation and sediment supply in basin infill history.

Understanding the main controls on the occurrence of highly interconnected sheet like channels is highly important for oil industry, groundwater exploration, and for CO_2 storage in non-marine basins because it could help reservoir prediction (Huerta *et al.*, 2011). This article is focused on the calculation of sedimentation rates and the subsequent comparison with the large-scale architectural elements of the Almazán Basin, including fluvial, mudflat, palustrine and lacustrine sedimentary systems. The Paleogene record of the Almazán Basin is particularly suitable to perform this analysis because it integrates most of the continental environments with well-exposed vertical and lateral relationships. The basin shows an outstanding outcrop exposure, which permits three-dimensional reconstructions. To undertake these objectives, the alluvial-lacustrine and fluvial succession (*ca.* 2700 m) in the Gómara monocline has been dated by means of magnetostratigraphy. Magnetic polarity reversals have been mapped along the monocline, and sedimentation rates have been calculated for four key transects to assess their lateral changes in relation to different sedimentary environments and basin settings. The new chronostratigraphy of the basin infill can be used to derive a robust time frame for biostratigraphic calibration, and to analyse the tectonosedimentary relationships and the uplift history of the basin.

BACKGROUND

Sedimentary architecture and sedimentation rates

The architectural changes in both the fluvial systems and their lateral equivalents are often interpreted in terms of changes in the accommodation or in the ratio between accommodation and sediment supply (Muto & Steel, 1997; Carroll & Bohacs, 1999; Bohacs *et al.*, 2000; Huerta *et al.*, 2011). This is a basic assumption of sequence stratigraphy, which contributed to an efficient interpretation of the evolution of depositional systems (Catuneanu *et al.*, 2009). We took the definition of accommodation provided in Muto & Steel (2000) in which accommodation is seen as 'the thickness, measured at a specified site and time, of a space which becomes filled with sediments during a specified time interval'. This definition is practical to quantify because it is equivalent to sedimentation rates. Sediment supply is considered to be the volume of sediment delivered to a certain place of the basin in a given time (sediment deposited + sediment bypassed). This value is difficult to estimate from field data in ancient sedimentary systems. We use the classification of high- and low- sediment supply areas provided in Huerta *et al.* (2011).

Changes in the large-scale architecture of depositional systems are usually associated to changes in accommodation. Spatial and temporal variability in accommodation leads to a complex interaction throughout sediment distributive systems, affecting the localization of sedimentary environments, the bypass rate, the avulsion frequency and the slope in clastic systems, which also modify the sediment supply. To correctly understand the triggers of changes in large-scale architecture it is therefore needed to identify the accommodation and sediment supply interplay. The ratio between accommodation space and sediment supply (AS/SS) is, however, relative, because field estimations of sediment supply are hardly quantifiable. Relativeness of the AS/SS ratio can be reduced pinning accommodation between intervals sharing sedimentation rates. This allows observing the influence of sediment supply variations in both the large-scale architectural arrangement and the shifts between depositional environments. The LAB models (Leeder-Allen-Bridge; Allen, 1978; Bridge & Leeder, 1979) and most studies in ancient sedimentary records show that an increase in accommodation in fluvial settings is related to prevalence of isolated and narrow channels. There are, however, other factors such as the avulsion frequency that should be taken into account. If the avulsion frequency grows faster than sediment accumulation, it can produce high channel interconnection (Heller & Paola, 1996). In addition, some field studies disagree about the inverse relationship between channel density and accommodation space (Törnqvist, 1994; Colombera *et al.*, 2015). Beyond accommodation, we consider the ratio AS/SS, to assess the relative influence of sediment supply in the architectural changes.

The external causes affecting the ratio AS/SS in internally drained non-marine basins are climate and tectonics. Climate forcing can be assessed by means of identification of Milankovitch cycles (Hilgen *et al.*, 2014). However, orbital cycles might not be expressed in the sedimentary record if the environment is not sensitive enough or if the tectonic signal is outweighed. Alternatively, another option is to discriminate the slight differences between climate and tectonics in the sedimentary record. Climate, by means of precipitation and evaporation changes, leads to lateral and longitudinal variations of the sediment grain size (Armitage *et al.*, 2011). On the other hand, tectonics can directly affect accommodation space (AS). Models show that an increase of AS results into coarser grain size accumulation in the proximal sites, followed by a reduction in grain size in distal locations (Armitage *et al.*, 2011; Paola & Martin, 2012). However, in non-marine basins, changes in precipitation and or evaporation may modify the accommodation by base level rise or fall. In parallel, tectonics may change SS by promoting uplift and drainage changes in the catchment areas.

Geological setting

The Almazán Basin in north-central Spain is a thick-skinned piggy-back basin bounded by the Cameros Massif and the Aragonian and Castilian branches of the Iberian Chain (Fig. 1a). It developed on the hanging wall of the Cameros thrust, which moved northwards over the Cenozoic deposits of the Ebro Basin, producing the uplift of the Cameros Massif and the Iberian Chain during the Alpine orogeny (Casas, 1990; Casas-Sainz, 1993; Muñoz-Jiménez & Casas-Sainz, 1997). The Cameros massif is mainly composed by Upper Jurassic-Lower Cretaceous siliciclastics and carbonates, and the Aragonian branch of the Iberian Chain by Mesozoic carbonates and minor evaporites, with a metamorphic Paleozoic basement. Most of the sediment was delivered from these areas, while the Castilian branch of the Iberian Chain only supplied minor amounts of sediment (Huerta, 2007). During the Paleogene, the Almazán Basin was a non-marine isolated basin, which connected towards the west with the Duero Basin during Neogene times through the Aranda-Burgo de Osma corridor (Armenteros & Huerta, 2006).

The Almazán Basin has a flat-bottomed syncline geometry filled by Paleogene and Neogene non-marine deposits, reaching a maximum total thickness of more than 3500 m at its depocentre (Fig. 1b). The depocentre is bounded by the Almazán and Arcos monoclines towards the south, and the Gómara monocline and the Aragonian branch of the Iberian Chain towards the north (Casas-Sainz *et al.*, 2000). The activity of these structures was synchronous to sedimentation, controlling the distribution and thickness of the stratigraphic units that filled the basin.

Sequence stratigraphy

Detailed mapping (scale 1 : 25 000), stratigraphic correlations and seismic interpretation in the Almazán Basin were carried out in earlier studies (Huerta, 2007). Further detailed sedimentological, mineralogical and geochemical analyses were performed in the fluvial, lacustrine and playa-lake systems (Huerta *et al.*, 2010, 2011). On the basis of these studies the complete Paleogene basin infill is divided into four Depositional Sequences (A1 to A4 in Fig. 1). These sequences overlie an unconformity characterized by a hiatus that encompasses from Upper Cretaceous to lower Bartonian, and minor erosion of the Upper Cretaceous marine limestones.

Depositional Sequence A1 crops out close to the northern and eastern basin margins. It reaches a maximum thickness of 400 m, which gradually reduces towards the south and southeast. This sequence denotes a retrogradation from conglomeratic alluvial deposits passing into distal alluvial plains dominated by calcretes and shallow carbonate-precipitating lakes. The Mazaterón mammal fossil site (MP 15-16, Cuesta & Jiménez 1994) is located at the top of this sequence.

Depositional Sequence A2 crops out principally in the northern domain of the basin, with a maximum thickness of 900 m that wedges out towards the south. The base of the sequence is marked by a change in the sedimentation trend from retrogradational to progradational. A2 expanded southwards on Upper Cretaceous basement rocks, reaching the opposite basin margin.

Depositional Sequence A3 can be observed in the Gómara monocline and in the Torlengua anticline (Fig. 1). It reaches a thickness of 1100 m, wedging out towards the south and southeast, and displaying a progradational trend. The base of the sequence consists of an unconformity, which changes basinwards into a correlative conformity marked by calcretes and gypcretes, indicating a retrogradational trend of the fluvial system. Close to the Aragonian branch, in the Southeast domain (Deza-Embid), its lower boundary consists of an unconformity covering A2 and Upper Cretaceous limestones. Its thickness is notably reduced towards the upper limb of the Gómara monocline (Northern Domain) and on the upper limb of the Almazán monocline at the south of the basin.

Depositional Sequence A4 is covered by undeformed Neogene units, with the exception of few outcrops along the Gómara monocline. In contrast to older Paleogene depositional sequences, it becomes thicker southwards and displays syntectonic unconformities at the basin margins. This sequence is articulated in the Gómara monocline and records the exhumation of the northern domain, evidenced by the occurrence of Paleogene clasts.

Tectonic domains

The structural framework of the Almazán Basin is divided into five principal tectonic domains (Fig. 1): (i) the northern domain; (ii) the Almazán and Arcos monoclines; (iii) the south-eastern domain; (iv) the Gómara monocline; and (v) the basin depocentre. A description of the tectonic domains and their structures is provided, except for the basin depocentre, which steadily subsided during all the Paleogene and Neogene history.

The northern domain of the basin (i) records the maximum thickness of A1 and A2. A3 is only preserved in the core of two synclines, and A4 is absent (Huerta *et al.*, 2011). This domain is bounded by the Sierra de la Pica Thrust or South Cameros Thrust (Navarro Váquez, 1991; Guimerà *et al.*, 1995) towards the North, and the Gómara monocline towards the South (Fig. 1). It is affected by NW-SE trending folds plunging towards the NW, which at the same time were affected by perpendicular minor folds. The NW-SE anticlines are bounded by thrusts towards the north, along the Aragonian branch of the Iberian Range.

The Almazán and Arcos monoclines (ii) are located in the southern part of the basin, and are only recognizable in subsurface (Casas-Sainz *et al.*, 2002). These monoclines are WNW-ESE oriented, are related to faults affecting the Paleozoic basement, and dip 15° to 45° northwards. Folding started during A3 (adapting the

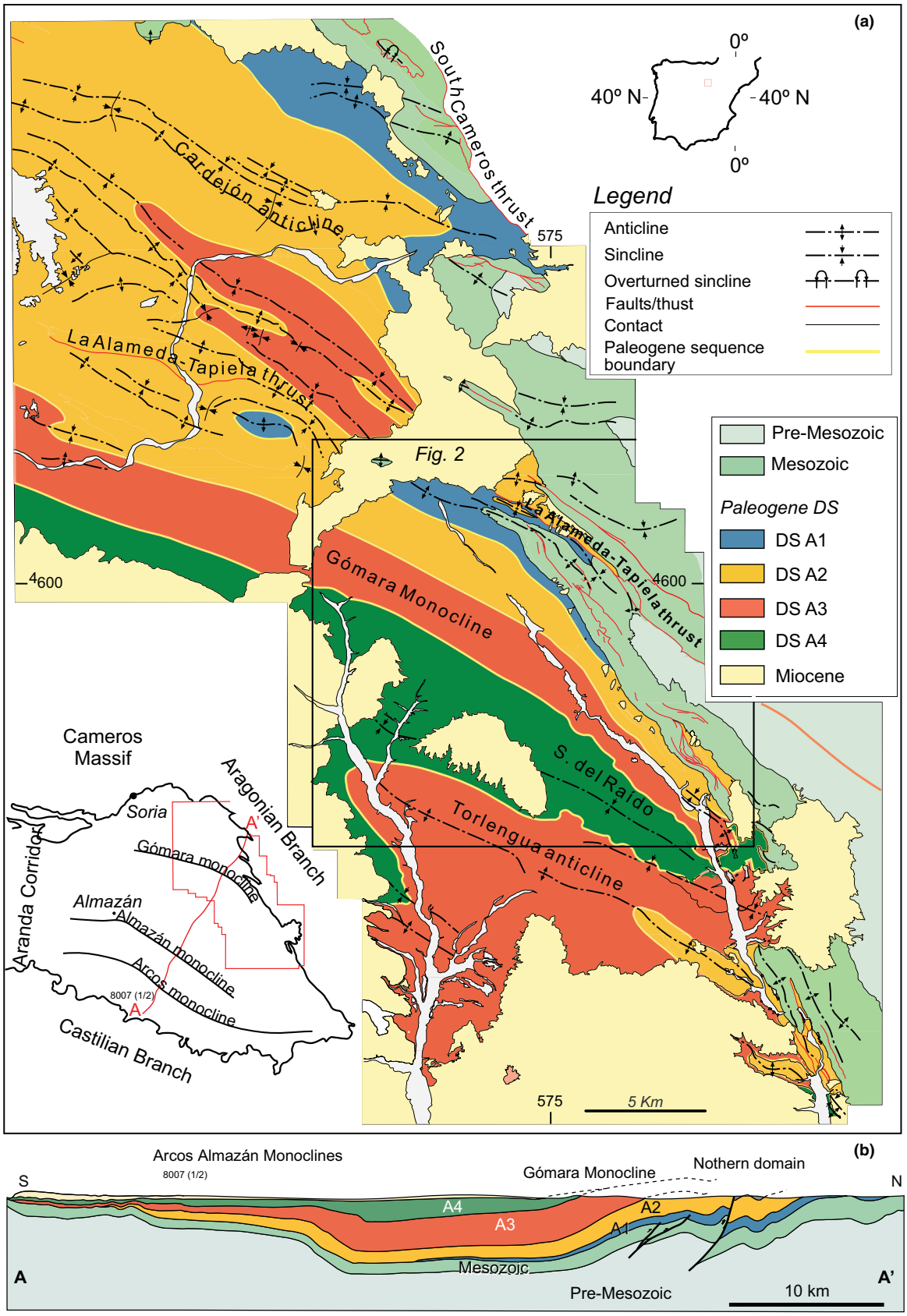

Fig. 1. (a) Tectonic map of the Northeastern domain of the Almazán basin, where the depositional sequences are shown, after Huerta *et al.* (2011). The main tectonic structures are also indicated. Squared in the centre is indicated the location of Fig. 2. (b) Cross-section oriented SSE-NNW, which location is shown above at the left. The depositional sequences and the tectonic domains of the basin are indicated.

Casas-Sainz *et al.*, 2002 unit boundaries to our sequence stratigraphic framework), producing a structural relief of about 2000 m in the case of the Almazán monocline (Casas-Sainz *et al.*, 2002). During the initial stages of the monocline development, limb rotation occurred, this evidenced by thickness reduction towards the upper limb. During A3 and A4 deposition, the monoclines developed by kink band migration showing excellently preserved growth strata (Casas-Sainz *et al.*, 2002), displaying important thickness reduction in their upper limb.

The south-eastern domain (iii) is characterized by a thickness decrease in the Paleogene succession with respect to the Gómara monocline. The A2/A3 and A3/A4 boundaries are marked by unconformities, and important local alluvial fan deposits occur in every depositional sequence boundary in this domain. The La Alameda-Tapiela anticline/thrust (this nomenclature is used for folds that in some parts evolved into thrusts) supplied with sediments the local alluvial fan systems. Southwards, the development of the Torlengua anticline folded the A4 sequence in its northern limb.

The Gómara monocline (iv) was generated in response to the development of the La Alameda-Tapiela anticline/thrust. It connects the northern domain with the basin depocentre. It has NW-SE trend, dips 30° southwards, and generated a structural relief of about 2500 m. Towards the SE, around the Deza area (Figs 1 and 2), the monocline evolved into a succession of folds. As a consequence, all the Paleogene depositional sequences (A1–A4) were folded, and also a thickness reduction in A3 towards

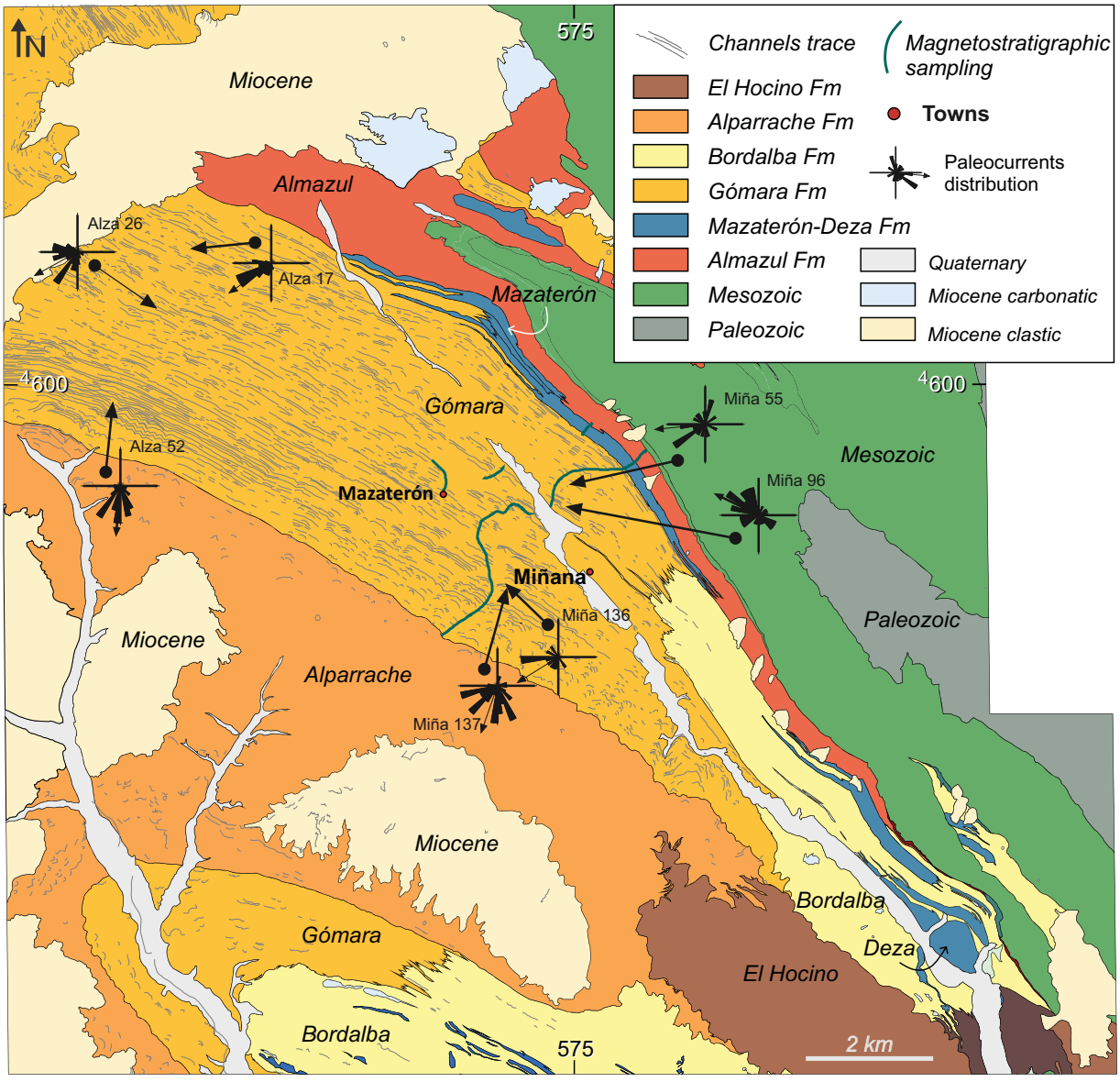

Fig. 2. Detailed map of the lithostratigraphic formations cropping out along the Gómara monocline (see location in Fig. 1). In grey, the trace of fluvial channels is marked. Dark green line shows the magnetostratigraphic sampling track.

the upper limb of the monocline is observed. A4 has a wedge shape that articulated in this monocline, opening southwards. The outcrops of this structure show a cross-section perpendicular to the main drainage system of the basin.

METHODS

Channel density calculations

The channel interconnection or channel density has been quantified mapping the channel fills and the overbank deposits in outcrops of the Gómara monocline. The Channel density is taken as the percentage of the surface in a fluvial succession occupied by channel fills. Eight representative boxes or rectangles of 0.350 km^2 were drawn in a GIS with its long side parallel to stratification (Figs 3 and 4). The size of the boxes was in the large-scale size of the fluvial architecture in the sense of Leeder (1993) and Jo & Chough (2001). Four were drawn on the Depositional Sequence A2 and four in A3, to have a representation of the channel density of the end-members identified in the fluvial succession. The results are represented in the Table 1 (The mapped boxes are available as Figures S1 and S2).

Magnetostratigraphy

Paleomagnetic sampling was performed with an electrical portable drill along the two overlapping Almazul and Mazaterón sections (Fig. 2), encompassing a total thickness of 2670 m. The sampled interval included the alluvial Almazul Fm., the lacustrine/palustrine Mazaterón Fm., and the fluvial Gómara Fm. (Fig. 2). Representative sampled lithologies included red and orange mudstones (mainly), very fine sandstones, limestones and marls (occasionally). An optimal sampling transect was chosen to include the most expanded sections with higher abundance of fine grained lithologies, the best outcrop exposures, and stratigraphic continuity. Two cores per site were drilled with an average spacing of 10 m per site, collecting a total of 269 sites.

Samples were analysed in the paleomagnetic laboratories of Fort Hoofdijk (Utrecht University) and the Institute of Earth Sciences Jaume Almera (CCiTUB-ICTJA CSIC). The Natural Remanent Magnetisation (NRM) was measured on DC SQUID superconducting rock magnetometers (2G Enterprises Ltd). Stepwise thermal increments were of 50 °C up to 350 °C, and of 30 °C up to the maximum unblocking temperature of samples. Magnetic susceptibility was measured with a KLY-2 susceptibility

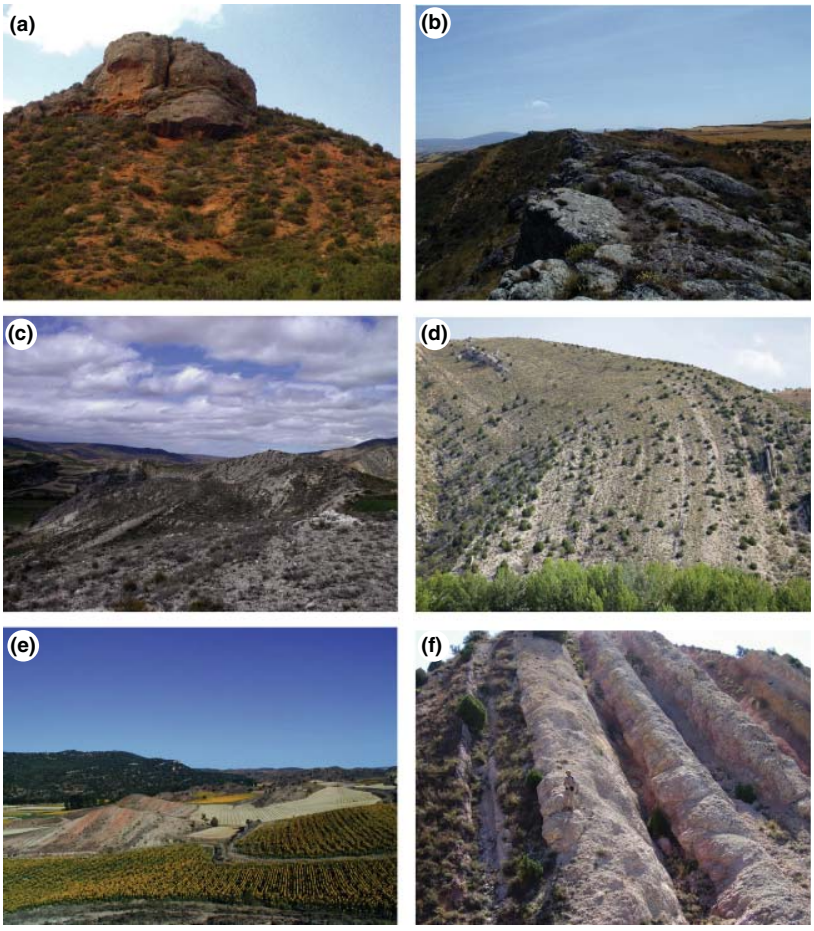

Fig. 3. Field photographs of the main large-scale architectural elements identified in the Paleogene succession of the Almazán Basin. (a) Low interconnected ribbon-shaped channel fills (Alparrache Formation). (b) Highly interconnected sheet-like channel fills (Upper part of the Gómara Formation). (c, d) Shallow water lacustrine carbonates of the Deza Formation, (d) an almost complete view of the carbonate deposits (about 200 m) is shown. (e) Mudflat deposits of the Bordalba Formation (close to the Colmenares section). (f) Stacked calcretes at the base of the Mazaterón Formation, which top is at the right of the picture.

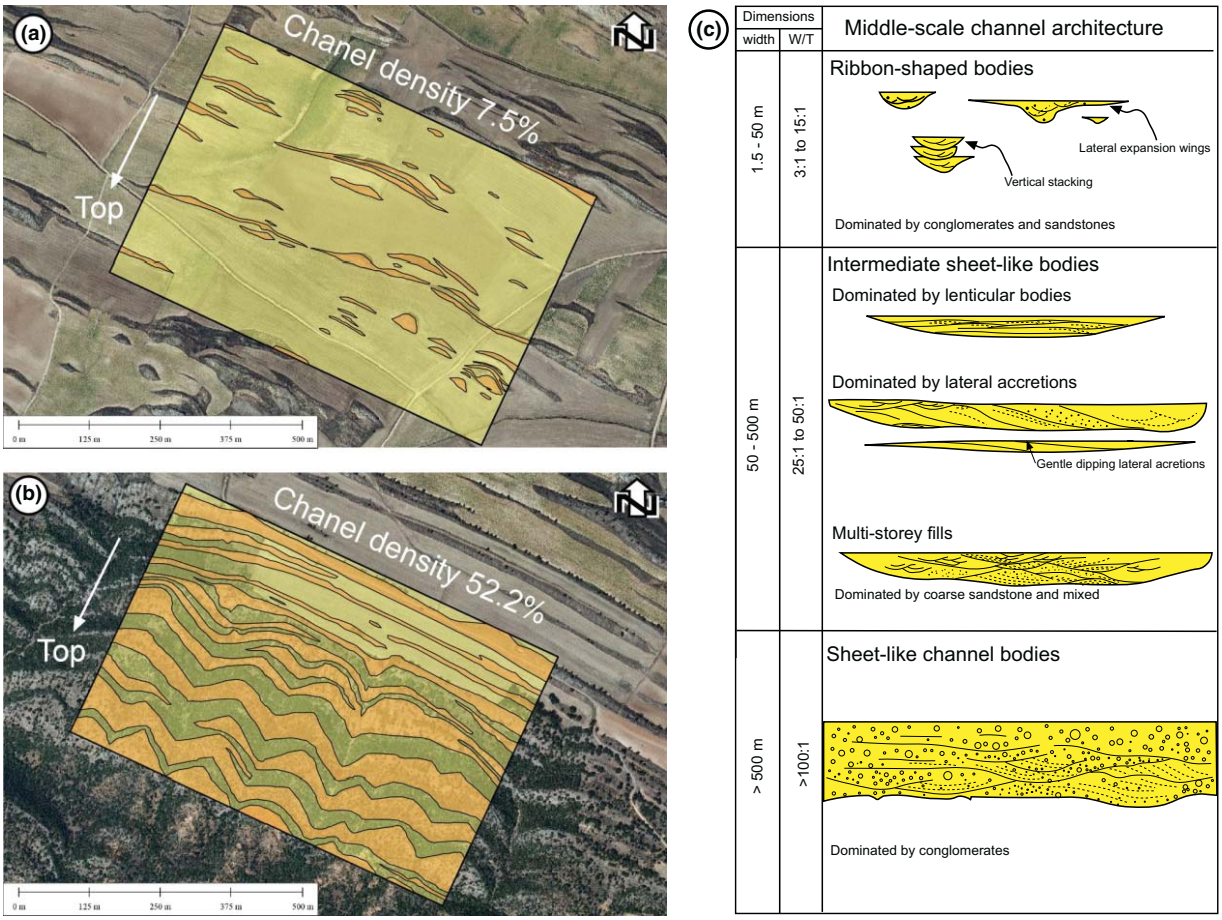

Fig. 4. Changes in the interconnectivity of channels due to variations in fluvial regime are recorded several times in the Gómara Formation. (a) Example of low density of fluvial channels areas, which mainly bear ribbon-like channel fills with low W/T ratios. (b) High density of channels. Sheet-like channel fills, with high W/T ratios. In this case, located in the top of A3, W/T ratios overcome 100. (c) Middle-scale channel internal architecture.

Table 1. Channel density calculated for eight boxes. 4 in DS A2 and 4 in DS A3

# Box	Depositional sequence	Box area (km^2)	∑Channel fill area (km^2)	Channel density (%)
1	A2	0.35	0.020	5.64
2	A2	0.35	0.022	6.40
3	A2	0.35	0.026	7.52
4	A2	0.35	0.015	4.42
5	A3	0.35	0.155	44.40
6	A3	0.35	0.116	33.23
7	A3	0.35	0.183	52.22
8	A3	0.35	0.077	22.04

bridge (Agico) at each demagnetization step to monitor mineralogical changes during heating.

Isochrons map and SR calculations

Magnetostratigraphy provided the location of magnetic reversals for the sampled section. Prominent and laterally continuous beds can be interpreted as isochrones within the magnetostratigraphic temporal resolution. The lateral extension of the reversals was inferred by means of key beds (Fig. 2), which allowed mapping the reversals along the study area. When channels are wide and interconnected or when continuous limestone beds crop out, the mapping results straightforward. However, within mudflats deposits the precision of the correlation decreases. In spite of this, the correlation was possible for the most of the monocline, allowing a fine evaluation of stratigraphic thickness variations across the Paleogene record of the Gómara monocline.

Mapping of the magnetic reversals allows the quantification of Sedimentation Rates (SR) for different time intervals (Johnson *et al.*, 1988). Direct measurements were performed along the Miñana section, which is representative of the fluvial system. In this case, the ratio between sediment accumulated and time directly gives SR. Additionally, SR were estimated in three other key transects to assess the SR variability related to sedimentary environments and basin locations. For these sections, SR were estimated after geometrical calculation of thicknesses between magnetic reversals. Thicknesses were later verified with adjacent stratigraphic logs (Huerta, 2007), and finally plotted against magnetic reversal ages

Table 2. Sedimentation rates values for different intervals within the Gómara Monocline

Interval	Initial age (Ma)	Final age (Ma)	Thickness increase (m)	Acummulated thickness (m)	Age increase (Ma)	Sedimentation rate (cm kyr^{-1})	Dip direction	Dip
Zárabes section								
1	43.51	40.2	245.73	245.73	3.31	7.42	206	25
2	40.2	38.67	237.47	483.2	1.53	15.52	200	30
3	38.67	35.71	240.65	723.85	2.96	8.13	203	35
4	35.71	35	77.3	801.15	0.71	10.89	206	35
5	35	33.7	593.63	1394.78	1.3	45.66	206	35
6	33.7	33.16	94.96	1489.74	0.54	17.59	206	35
7	33.16	31.03	483.14	1972.88	2.13	22.68	208	30
8	31.03	29.97	137.44	2110.32	1.06	12.97	208	25
9	29.97	29.18	78.24	2188.56	0.79	9.90	209	20
10	29.18	27.44	61.58	2250.14	1.74	3.54	208	20
Colmenares section								
1	40.2	38.38	124.98	124.98	1.82	6.87	55	60
2	38.38	35.71	389.19	514.17	2.67	14.58	55	75
3	35.71	35	161.73	675.9	0.71	22.78	55	85
4	35	33.7	201.79	877.69	1.3	15.52	55	90
5	33.7	31.03	354.73	1232.42	2.67	13.29	233	82
6	31.03	30.59	164.99	1397.41	0.44	37.50	232	79
7	30.59	29.18	152.57	1549.98	1.41	10.82	232	45
Castillejos section								
1	40.2	36.97	177.54	177.54	3.23	5.50	233	61
2	36.97	35.71	113.23	290.77	1.26	8.99	233	61
3	35.71	35	152.75	443.52	0.71	21.51	233	61

(Table 2). Some restrictions to the SR calculation are that: (i) sedimentation rates are inferred for intervals bounded by polarity reversals, and therefore represent average rates, and (ii) for short intervals the age uncertainty associated to the chron boundaries may lead to significant errors in the inferred SR. This allowed the assessment of SR for all the depositional systems in the monocline. Fluvial system is best represented in the Zárabes transect, mudflats and saline mudflats in the Colmenares transect, and lacustrine–palustrine systems in the Castillejos transect.

RESULTS

Large-scale architecture

The Gómara monocline (Fig. 1) accommodates up to 2500 m of sediments comprising Depositional Sequences A1 to A3. The main large-scale architectural elements (LAE) defined are: (i) Ribbon-shaped channel fills with low interconnectivity (Fig. 3a); (ii) Sheet-like channel fills with high interconnectivity (Fig. 3b); (iii) Palustrine/lacustrine Limestone units (Fig. 3c and d); (iv) Mudstone and evaporitic mudstone units (Fig. 3e); and (v) stacked calcretes (Fig. 3f). These LAE pass gradually, vertically and laterally, from one into another. Frequent transitions from ribbon-shaped channel fills with low interconnectivity to sheet-like channel fills with high interconnectivity occur gradually by means of intermediate stacking patterns.

Ribbon-shaped channel fills with low interconnectivity

This LAE is constituted by sandy ribbon-shaped channel fills and red mudstones, with a density of the channel bodies lower than 10% (Table 1; Fig. 4). It is most common in A2, especially in the middle of the sequence, and during A4 (Fig. 2). The channel and channel belt fills never exceed 50 m wide, being their common thickness around 2 m (Fig. 4a). The width/thickness (w/t) ratios typically range from 3 : 1 to 15 : 1, although in A4 some channel fills are vertically stacked (multi-storey) forming bodies with 1 : 3 w/t ratios. These channels are isolated within red mudstones. Middle-scale and simple architectural members are described in Huerta (2007); Huerta *et al.* (2011).

Sheet-like channel fills with high interconnectivity

It is constituted by sheet-like conglomerate and sandstone channel fills and red mudstones. Occasionally, calcrete beds are intercalated within the mudstones. The density of the channels is high and ranges from the 20% to 52% (Table 2; Fig. 4). It is most frequent in the upper part of A3, where channels are thicker, and wider (Fig. 4b). The channel and channel belts are wider than 500 m, some exceeding 3000 m. Common thickness is around 5 m, although thicker conglomerate beds (15–35 m) are recorded in the upper part of A3. W/t ratios are higher than 100 and there are no evidences of vertical and lateral accretion. These channels and channel belts are

dominated by conglomerates, which in the upper part of A3 contain clasts that can reach up to 70 cm. Laterally, to these channel fills calcretes are common. Middle-scale and simple architectural members are described in Huerta (2007); Huerta *et al.* (2011).

Palustrine/lacustrine Limestones

This unit consist of limestones, dolostones and marls which contain limnic fossils like gastropods, ostracods and charophytes. Reptile and mammal fossils have been occasionally found associated to these units. Carbonate facies have the classical exposition features defined in palustrine deposits, similar to those described by Alonso-Zarza *et al.* (1992); Armenteros *et al.* (1997); Alonso-Zarza (2003); Huerta & Armenteros (2005); Alonso-Zarza *et al.* (2006). Calcretes and dolocretes are common in the transitional areas between the limestone and the clastic units (Huerta & Armenteros, 2004). The thickness of the palustrine/lacustrine limestones is about 200 m although it can reach a total thickness of 450 m (Deza Fm.) These units are preferentially found in A1/A2 boundary and in A2 (Fig. 2) and occurs in areas close to the basin margin, passing towards distal positions into an evaporitic mudflat. Simple elements and facies of the palustrine/lacustrine units are described in Huerta & Armenteros (2004); Armenteros *et al.* (2006).

Mudstones and evaporitic mudstones

This unit consist of mudstones and mudstones with interstitial gypsum intercalated with tabular fine-sandstone beds and gypcretes (gypsum crusts). Sandstone channel fills are rare. It crops out in A2 and A3 in the southeastern part of the Gómara monocline and passes laterally into palustrine/lacustrine limestone units and ribbon-shaped channel fills with low interconnectivity. Simple elements and facies of this LAE are described in Huerta *et al.* (2010) which also describes the playa-lake system containing these deposits.

Stacked calcretes

This unit is constituted by several metre-scale calcrete profiles stacked vertically. The calcretes ranges from nodular or prismatic at the base to massive at the top. The massive top of a profile is overlapped by the nodular or prismatic horizon of the next profile. In some cases, the superposition of the calcrete profiles blurs the nodular or prismatic structure. In other cases, the calcretes are separated by powdery carbonate or by red mudstones. The calcretes are constituted by a microsparitic mosaic with disperse quartz grains and show oxide staining patches and mudstone relics which become smaller towards the upper parts of the profile. This LAE occurs mainly in A3, laterally to the sheet-like channel fills with high interconnectivity. The calcretes and stacked calcretes related to the connection between palustrine/lacustrine units and the clastic units (A1/A2) are similar to those described here but the latter can pass upwards into dolocretes and palustrine/lacustrine limestones (Huerta & Armenteros, 2004). The textural and structural features of the stacked calcretes are described in Huerta (2007) and Huerta *et al.* (2011).

Sedimentology

Previous sedimentological analysis of simple and medium architectural elements present in the i, ii, and v LAEs, interpret these deposits as parts of a distributive fluvial system with carbonate soils in distal floodplains (Huerta, 2007; Huerta *et al.*, 2011). Ribbon-shaped channels have been interpreted as low sinuosity channels with minor lateral movement some of them showing anastomosis. Sheet-like channels have been interpreted as lateral-stacked channel belts with great mobility across the floodplain and a braided channel pattern. The stacked calcretes are interpreted as distal flooplain areas with important pedogenesis favoured by the low sediment accumulation (Huerta, 2007; Huerta *et al.*, 2011). The LAEs identified in the vertical stacking pattern of fluvial system were laterally related, being the sheet-like channels with high interconnection upstream sections of the ribbon-shaped channels with low interconnection.

The mudstones and evaporitic mudstones have been interpreted as dry mudflats dominated by gypsum precipitation which passed southwards into saline mudflats and constituted a playa-lake system lateral to the main fluvial system (Huerta, 2007; Huerta *et al.*, 2010).

The dry mudflat passes laterally into limestones and marls with gastropods, ostracods and charophytes. Some beds show exposure features, gypsum pseudomorphs and silica nodules. These carbonates have been interpreted as carbonate precipitating lakes or ponds with low gradient margins which connects with the clastic systems through carbonate soil fringes (calcretes/dolocretes) (Huerta, 2007).

Alluvial fan sediments fringing the northern margin of the basin are not described here because they are not represented in the Gómara monocline. Only distal alluvial deposits are recorded in A1 (Miñana section).

Magnetostratigraphic results

Orange to reddish mudstones yielded unblocking temperatures circa 650 °C, suggesting that hematite is the principal magnetic carrier. Carbonate rocks yielded unblocking temperatures in general below 600 °C, suggesting that magnetite is more dominant in these lithologies. Most of the samples showed a low-temperature component, which is removed after 250 °C. The direction of this component in geographic coordinates usually parallels the drilling direction (Fig. 5a, sample MZ236), most likely related to recent viscous acquisition. A high temperature, Characteristic Remanent Magnetisation (ChRM) ranging from 350° to the maximum unblocking temperature is found in most of samples and yields both normal and reversed polarity directions. ChRM

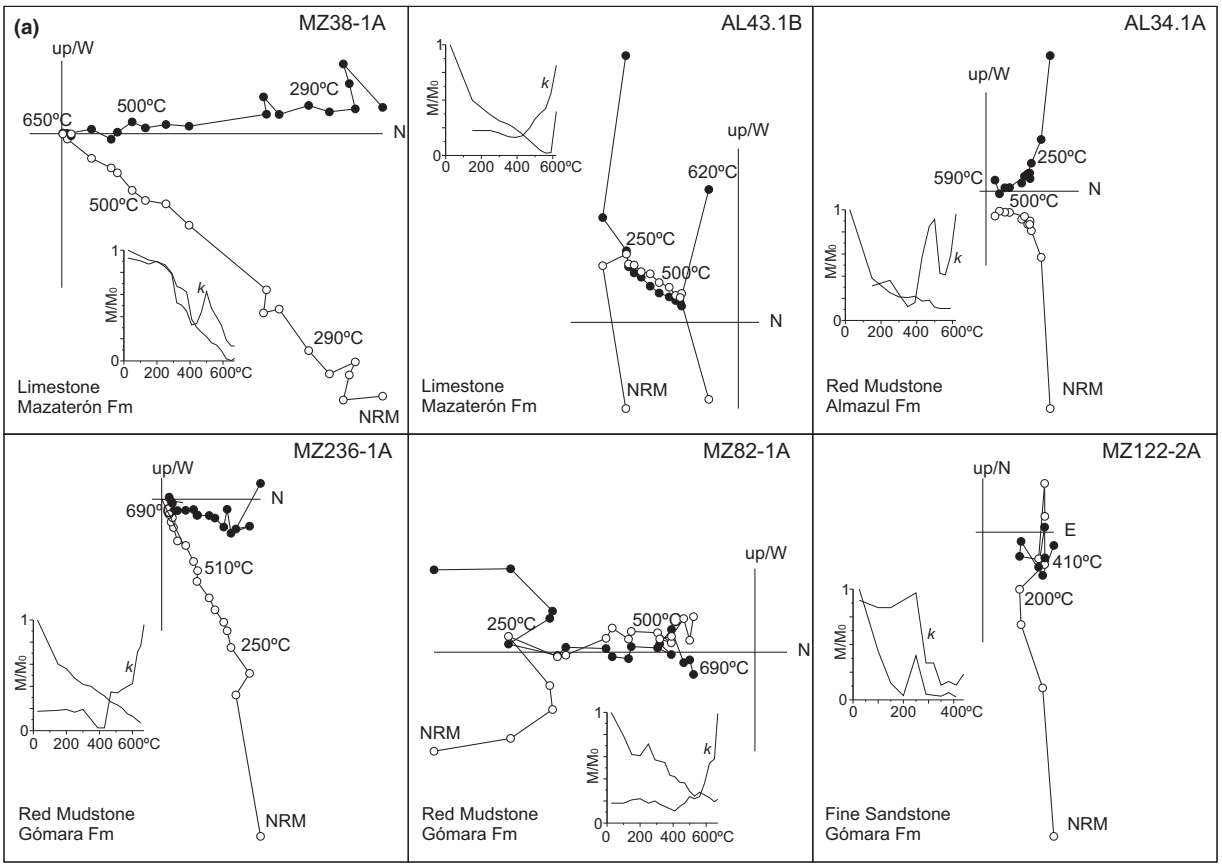

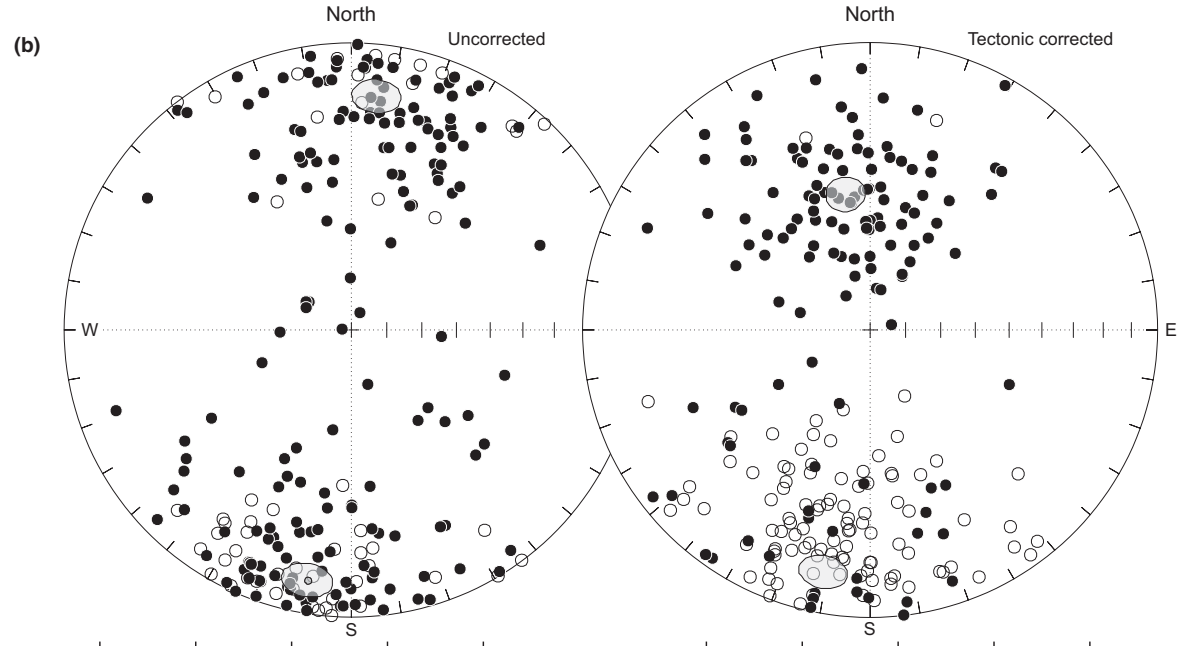

Polarity	N	Dec	Inc	Ks	α95
Normal	104	6.3	21.2	7.1	5.6
Reverse	130	190.0	15.0	5.7	5.7

Polarity	N	Dec	Inc	Ks	α95
Normal	104	349.9	50.8	8.3	5.1
Reverse	130	191.0	–18.1	6.1	5.5

Fig. 5. (a) Stepwise NRM thermal demagnetization (Zijderveld plots) of representative lithologies and normalized NRM and magnetic susceptibility changes upon heating from the Almazul and Mazaterón sections. M0: Initial NRM in 10^{-6} A/m. (b) Stereographic projection of the ChRM directions before and after tectonic correction and their associated normal and reversed mean directions by means of Fisherian statistics.

components were determined after inspection of Zijderveld plots in 234 samples (86.9% of total), and directions were calculated by means of principal component analysis (Kirschvink, 1980) (Fig. 5a).

The stereographic plot of paleomagnetic data in geographic coordinates shows a distribution of normal and reversed polarity directions with low average inclinations (Fig. 5b). Tilt correction for the southwestwards dip of beds yielded steeper mean inclination values, which are more coherent with the Paleogene Iberian plate paleolatitude (Rosenbaum *et al.*, 2002). Antipodality of the mean normal and reversed direction was not achieved, and low inclination values of the reverse samples may be related to partial overlap with a downwards-dipping low-temperature secondary component (Fig. 5). Westwards deviation of both normal and reverse mean directions could also be related to a partial overlap with drill-induced viscous magnetization. We interpret the low values of the precision parameter (k) as caused by this overlap with secondary components (Fig. 5).

The paleolatitude of the Virtual Geomagnetic Pole (VGP) was calculated at a sample level and plotted against thickness to establish a Local Magnetic Polarity Stratigraphy (LMPS, Fig. 6). Positive paleolatitudes were computed as normal polarities, while negative ones were interpreted as reversed polarities. Normal and reversed magnetozones were defined by at least two adjacent samples of the same polarity. Single-site reversals are depicted as half bar magnetozones in the LMPS plot, and are not considered for magnetostratigraphic correlation purposes. Correlation of the LMPS with the Global Polarity Time Scale (GPTS) was firstly based on biochronological data from the Mazaterón and Deza fossil mammal localities (Badiola *et al.*, 2009), which suggest upper Eocene age. Guided by these constraints, a best correlation of the LMPS to the GPTS 2012 (Gradstein *et al.*, 2012) was obtained by linking the very long reversed magnetozone R8 (Fig. 7) with chron C12R, the characteristic long reversed chron of the early Oligocene. A remarkable positive correlation results for most of the polarity sequence (Fig. 7). Solely, the correlation of the normal magnetozone N3 presented some uncertainties. The proposed correlation of N3 with chron C19n yields significantly lower sedimentation rates than average. However, a significant lithology contrast takes place during this interval, with occurrence of calcretes indicating pedogenetic processes and environments with low sediment supply. This correlation is also supported by high-resolution magnetostratigraphic studies (Edgar *et al.*, 2010) that find a new normal event within chron C18r which would correlate with the short normal magnetozone within R3 in the Mazaterón Formation (Fig. 7).

Age of depositional sequences and biostratigraphic calibration

The most remarkable pattern shown by the isochrons map (Fig. 8) was the thicknesses variations, showing a wedging towards the East. This wedging is associated with an eastern gradual reduction in clastic sedimentation. In addition, the map reveals that variable widths between isochrones can be significant between adjacent areas, and that this relationship may change throughout time. The map also provides information for dating the depositional sequences boundaries across the basin, and the fossil sites located within the sequences.

The magnetostratigraphic study presented here provides a robust temporal framework for the Depositional Sequences of the Almazán Basin (Fig. 7). Depositional Sequence A1 is found to encompass from chron C21n to C18r, lasting *ca.* 5 Myr (Fig. 7). Depositional Sequence A2 encompasses from chron C18r to chron C13r, with duration of 5.8 Myr, and including most of the Bartonian and Priabonian Stages. Depositional Sequence A3 lasts 6.6 Myr, from chron C13r to chron C9n, comprising the end of Priabonian, Rupelian and part of the Chattian. The Eocene/Oligocene boundary is placed near the base of A3 (Fig. 7). Magnetostratigraphic data are not available for Depositional Sequence A4 because this unit remains buried in the Gómara monocline, and ages can only be interpolated by means of seismic profiles.

The Mazaterón mammal fossil locality (MP 15-16, Cuesta & Jiménez, 1994), in the lower part of the Mazaterón Formation (Fig. 7), correlates to chron C18r (Lower Bartonian), in agreement with previous biochronological interpretations (Cuesta & Jiménez, 1994). The isochrons map allows dating the mammal fossil locality of Deza 2 (MP 17b, Badiola *et al.*, 2009), yielding a correlation with Chron C15r, at mid-Priabonian (Fig. 8).

Sedimentation rates

To assess the variabilitiy of SR both in time and space, the combined isochron map and bedding orientation data were used for calculation of SR along the different sections within the Gómara monocline. The results are shown in Fig. 9, where SR data are provided for every time-slice given by magnetostratigraphic reversals.

The general trend of SR shows pronounced shifts which are coincident with sequence boundaries. Both the A1/A2 and the A2/A3 boundaries are marked by increases of SR. Lateral changes in SR are associated to gradual changes of the depositional systems, which can be tentatively ordered from higher to lower SR. Although some exceptions exist, higher SR occur in fluvial systems, and gradually decrease in mudflat to lacustrine and finally palustrine settings with aerial exposition features. The principal exceptions occur in the mudflats or lacustrine systems which may present higher rates than certain fluvial intervals.

Within the fluvial system, highest SR are related to more isolated ribbon-like channels, while lowest SR are related to intervals of more amalgamated and wider

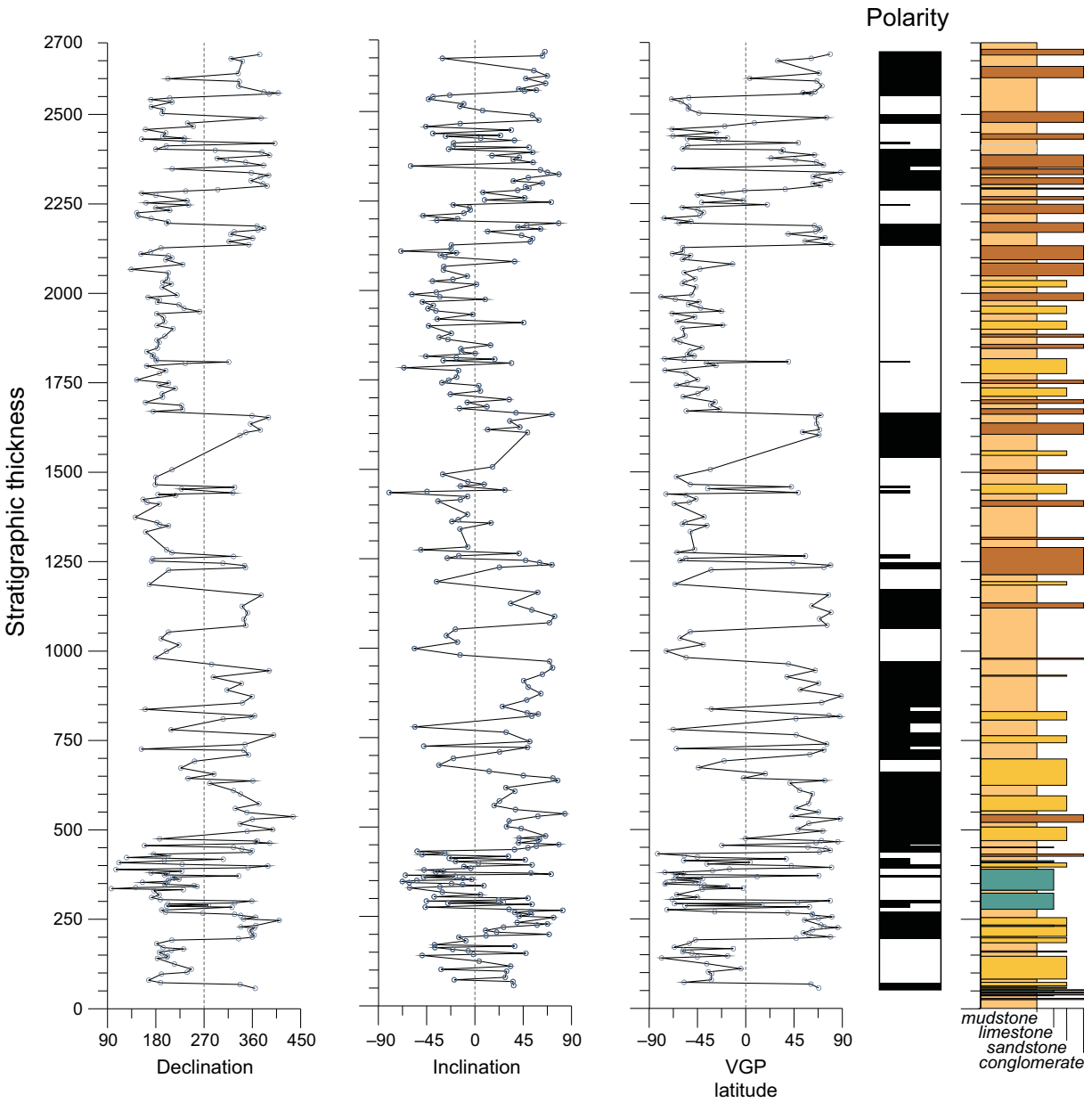

Fig. 6. Local litho- and magnetostratigraphic composite section. From left to right, changes in declination, inclination and Virtual Geomagnetic Pole (VGP) paleolatitudes. The correlation between Almazul and Mazaterón sections was performed by means of magnetostratigraphy. Stable magnetozones were defined by at least two adjacent palaeomagnetic sites of the same polarity. Normal magnetozones are represented in black and reversed magnetozones are represented in white. Single site reversals are represented by half bar magnetozones

channels. Ribbon-like channels develop when rates are above 25 cm kyr^{-1}, and amalgamated sheets occur when rates are below 12 cm kyr^{-1}. Between these values mixed architectures develop. Adjacent to the fluvial system, the mudflats yield SR which increase with the mud proportion and typically fluctuate between 14 to 23 cm kyr^{-1}. Finally, lacustrine systems lacking features indicating aerial exposure yield SR close to 9 cm kyr^{-1}, whereas the intervals dominated by calcrete accumulation record 3 cm kyr^{-1}. This indicates that net calcrete accumulation is below 3 cm kyr^{-1} because the averaged intervals include other deposits apart from calcretes.

DISCUSSION

Basin fill and tectonic history

Depositional sequence A1

Deposition in A1 begins as accommodation is created due to the Cameros thrust emplacement. The sedimentation grades upwards from distal alluvial to a calcrete fringe and palustrine-lacustrine environments. The average SR in the Miñana section (Figs 8 and 9) show a change from 4.7 to 6.3 cm kyr^{-1} in the alluvial deposits. A decrease to

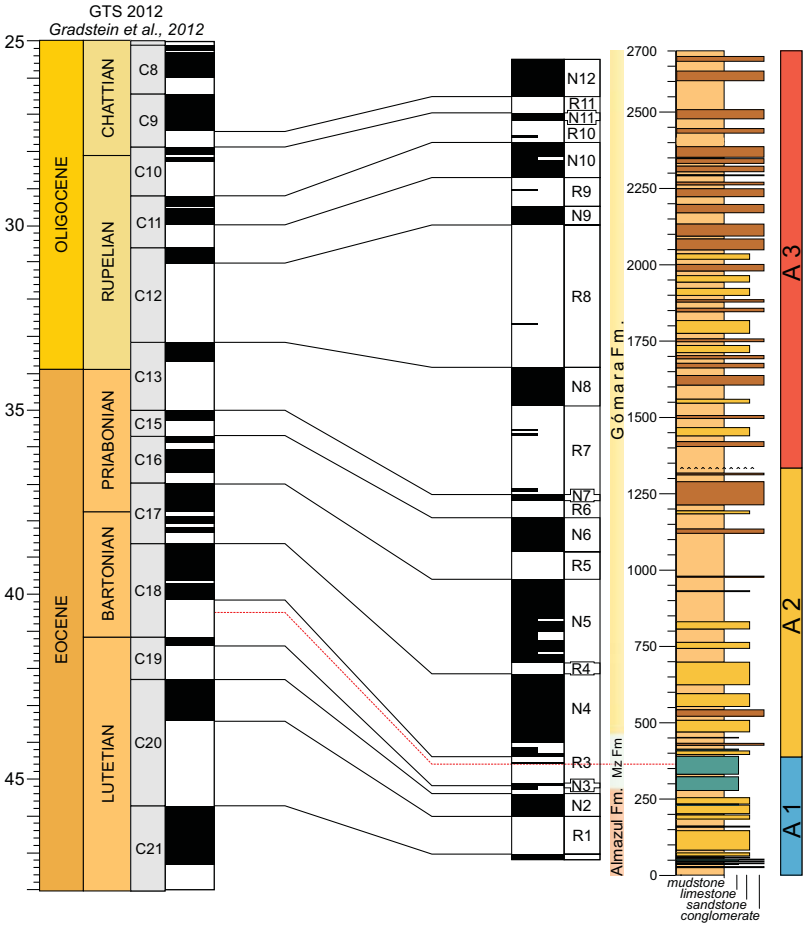

Fig. 7. Correlation between the local magnetostratigraphic section of Almazán to the GPTS (Gradstein *et al.*, 2012), including the formations and the depositional sequences of the Almazán basin. The red line indicates the location of Miñana fossil site and its correlation with the GPTS.

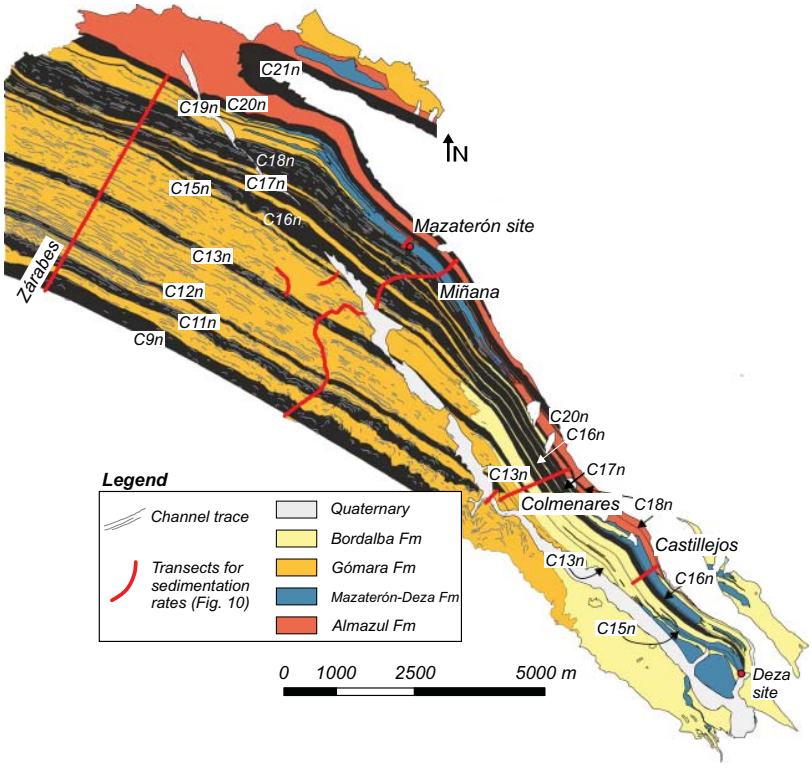

Fig. 8. Magnetostratigraphic map of the Gómara monocline. Magnetic reversals had been extended through the monocline following traceable levels. Black bands mark the normal magnetic polarity intervals. The magnetostratigraphic sampling track has been marked and corresponds to the Almazul and Mazaterón sections, unified as Miñana transect in this figure. The other sections shown correspond to the ones where sedimentation rates were calculated (Fig. 9). Geological formations are included. A widening of the magnetic reversals towards the NW, where clastic formations dominate can be distinguished.

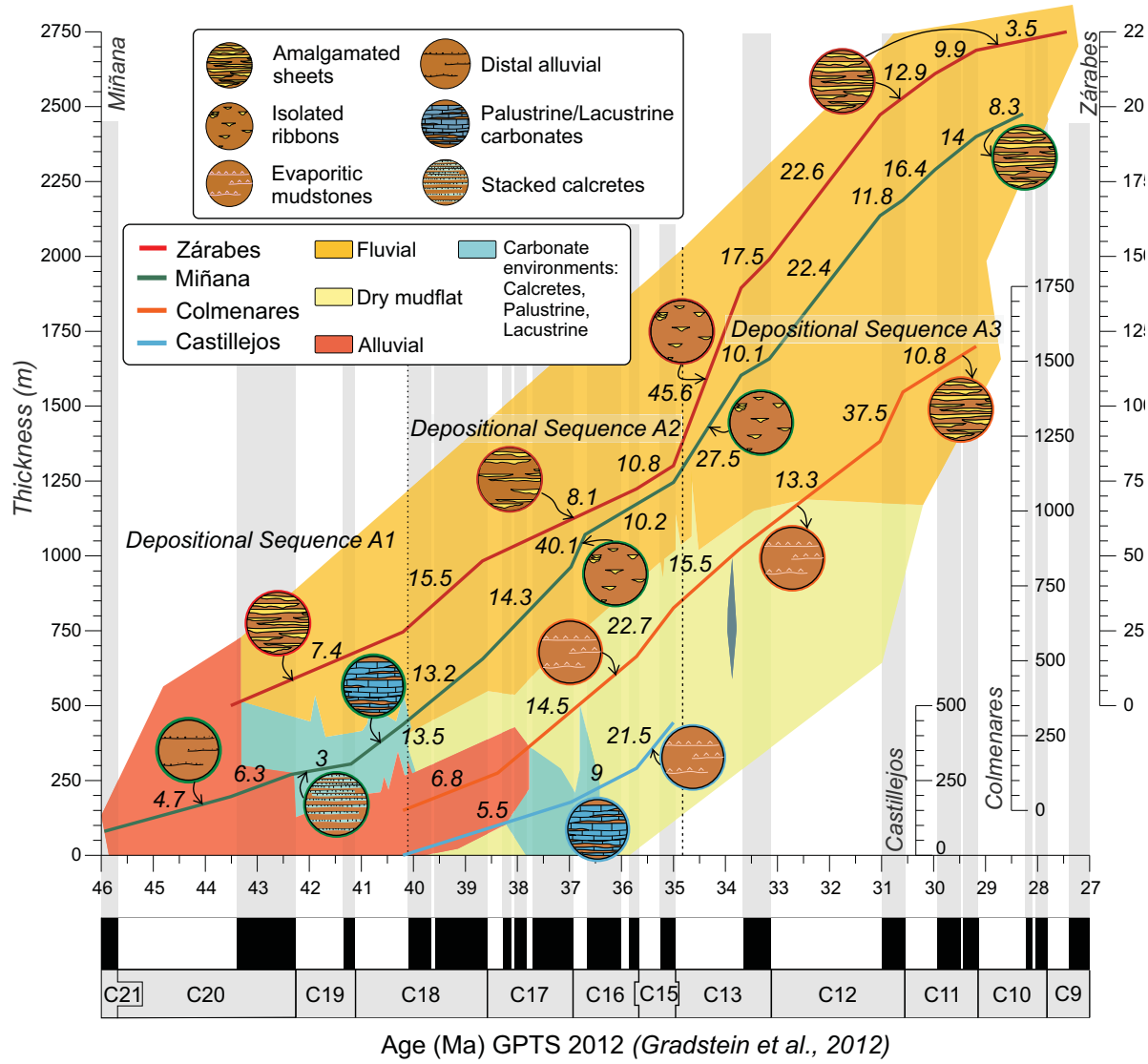

Fig. 9. Sedimentation rates resulting from plotting stratigraphic thicknesses against magnetostratigraphic ages for four key transect (location in Fig. 8). These sections encompass the most characteristic formations and large-scale architectures of the Almazán Basin Polygons indicate the sedimentary environments, which nearly coincide with the formations. The stacking pattern is drawn in circle and its perimeter colour indicates the section. The numbers refer to Sedimentation Rates, (in cm/kyr), and are calculated within ma netic reversals, which are the vertical underlying white or grey stripes. Each section has its own thickness coordinates origin, only fo representative purposes.

3 cm kyr^{-1} is related to the occurrence of stacked calcretes and palustrine/lacustrine limestones representing the carbonate soil fringe in the connection between the distal alluvial and the carbonate precipitating lake/pond. The increase in the SR recorded in the carbonates from Miñana section (13.5 cm kyr^{-1}) is related to an increase in the palustrine/lacustrine facies at the upper part of A1. This is interpreted as the beginning of a period with increasing AS which consolidates during A2.

Laterally, towards the Zárabes section (Fig. 8), the palustrine and lacustrine facies pass into fluvial deposits with wide and lateral amalgamated channels. SR of the fluvial deposits show an average of 7.4 cm kyr^{-1}. Similar SR values in the Zárabes and Miñana sections suggest that AS in the fluvial system is similar to the latera related palustrine/lacustrine environments, but the sec mentary supply in the fluvial system hinders the expa sion of the lake.

The beginning in AS creation around A1/A2 bounda and the increase in SS recorded by the development the Gómara fluvial sytem is likely linked to an increase the uplift in the Cameros Massif, which underwent ma mum uplift rates at around 40 Ma as indicated by fissi track data (Del Rio *et al.*, 2009). The uplift was trar ferred to the Almazán Basin by the activity of t Cameros thrust and, principally, by the inception of t South Cameros Thrust (SCT), and La Alameda Thru (ATT; Fig. 10; Fig. 1 for location).

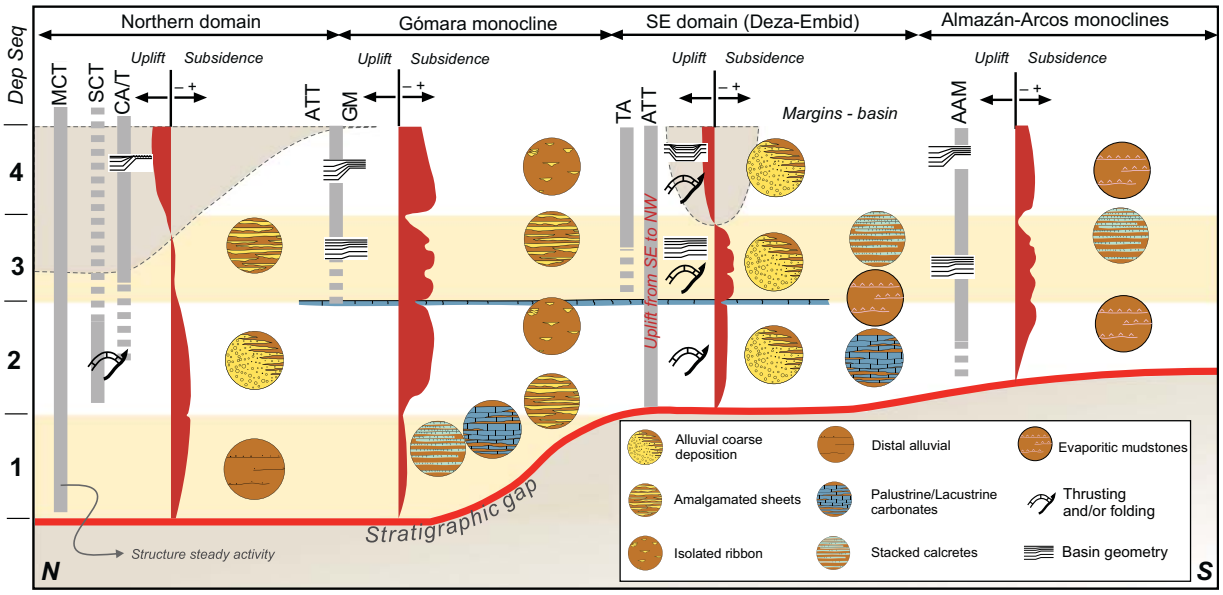

Fig. 10. Summary of the evolution of tectonic uplift and subsidence for the four Paleogene tectonic domains during the four depositional sequences (right). Subsidence and uplift are estimated from the architectural arrangement. The syn-sedimentary styles and the development of alluvial fans as consequence of the uplift of nearby structures are shown. MCT, Main Cameros Thrust; SCT, South Cameros Thrust; C A/T, Cardejón Anticline/Thrust; ATT, La Alameda-Tapiela Thrust; GM, Gómara Monocline; TA, Torlengua Anticline; AAM, Almazán-Arcos Monoclines (see Fig. 1 for location).

Depositional sequence A2

The sedimentation in A2 shows a broadening of the deposition areas towards the South and East (Fig. 10). The development of SCT and ATT provided additional accommodation space and an increase of sediment supply. The fluvial systems (Zárabes area) reflect an increase of SR to 15.5 cm kyr^{-1}, whereas the lacustrine environments of the Miñana section gradually shifted to fluvial deposits with rates slightly lower than in Zárabes (Fig. 9). In mid A2, the area experiencing more accommodation was Miñana instead of Zárabes. This is reflected in both sedimentation rates and in the Large-scale architectural pattern. The Miñana section show a sharp SR increase up to 40.1 cm kyr^{-1} and ribbon-shaped channels with low interconnection. Contrastingly, the Zárabes section yields SR of 8.1 cm kyr^{-1}, at this interval characterized by a higher channel density and width.

Towards the SE the fluvial deposits pass into a dry mudflat formed by mudstones and evaporitic mudstones (Colmenares section). In the mudflat SR were slightly lower than in the fluvial system, suggesting that the change in the architectural pattern, with the absence of channel fills, is driven by a lateral reduction in clastic supply. Further east, palustrine/lacustrine limestone units (Deza deposits) reveal a extreme reduction in sediment supply allowing the development of lakes and ponds (Huerta *et al.*, 2011) that are filled by bio-chemical precipitation (SR of 9 cm kyr^{-1}, Castillejos section). The overall decrease in the sediment supply towards the East occurred during A2, in synchrony with fold growth in the Aragonian branch. Relief generation in this basinal domain controlled the main fluvial transfer system, and sheltered the eastern sectors from receiving significant clastic contributions. Towards the top of A2, a general reduction in accommodation is deduced from the decreasing SR in all the sections (Fig. 9). This trend caused channel amalgamation in fluvial units and calcrete occurrence in their lateral mudflat deposits.

Depositional sequence A3

The A2/A3 boundary correlates with the activity of existing and newly formed tectonic structures (Fig. 10), giving rise to unconformities at the basin margins. During A3 the Gómara monocline was active, generating large AS in the lower limb and reducing AS in the upper limb. SR strongly responded to these changes, increasing to 45.6 cm kyr^{-1} in the Zárabes section, and 27.5 cm kyr^{-1} in the Miñana section. This stage is marked by ribbon-shaped channel fills with low interconnection in the Zárabes section that laterally became wider and more amalgamated towards the Miñana section. Their lateral equivalent mudflat sediments yield lower SR values (15.5 cm kyr^{-1}). The southeastwards decrease in SR is interpreted as driven by accommodation changes related to the position relative to the monocline limbs, the Zárabes section closer to the lower limb, and the Miñana and Colmenares sections closer to the upper limb. Neither the sediment supply pattern nor the distribution of the paleocurrents shows any significant change during this period.

A metre-thick fossil-rich calcrete yields interbeded within the A3 fluvial sequence in the Miñana section (near the Mazaterón village, Fig. 2). The occurrence of this layer could record a decrease in sediment supply

following the ideas of Carroll & Bohacs (1999); Bohacs *et al.* (2000); Huerta *et al.* (2011). Since magnetostratigraphic correlation brings this bed at near the Eocene-Oligocene boundary, it is plausible that it represents a transient climatically forced reduction in the sediment input. We note, however, that long-term architectural trends remain, with no sights of irreversible changes related to the transition into the icehouse world.

Towards the upper part of A3, a significant reduction in SR is observed in all the sections (Fig. 10). SR gradually decrease in the Zárabes section from values around 20 cm kyr^{-1} to below 10 cm kyr^{-1} (Fig. 9). Same trend, but delayed with respect to Zárabes, is observed in the Miñana section, decreasing from 20 to 10 cm kyr^{-1}. The reduction is SR is associated to the occurrence of the sheet-like channel fills with high interconnection. This is interpreted as a reduction in AS produced by the uplift of the Gómara monocline in its upper limb. The reduction in AS favours the lateral expansion of the fluvial system which is recorded in the Colmenares section and the migration of the fluvial depocentre southwards towards the basin centre (See Fig. 1B).

Depositional sequence A4

Previous studies (Huerta, 2007; Huerta *et al.*, 2011) showed that A4 (Chattian to Miocene) records the uplift and erosion of the northern domain of the basin, and coarse alluvial fan deposits with internal unconformities occur at the southeast domain (Deza-Embid area). A4 articulates in the Gómara monocline displaying syntectonic unconformities and becoming thicker southwards. This stratal pattern, the occurrence of ribbon-shaped channel fills with low interconnection, and the unroofing of the northern domain suggest that although sedimentation rates have not been calculated for this depositional sequence, both AS and SS were relatively high.

Accommodation, sediment supply, and large-scale architecture

Sedimentation rates reflect the accommodation space for a specific site and time interval, following Muto & Steel (2000). The SR calculated in the Gómara monocline (Almazán Basin) help us assessing the relationship between the large-scale sedimentary architecture and the accommodation space and sediment supply.

As seen above, sheet-like channel fills with high interconnectivity LAE occur at times of lower accommodation space (see upper part of the A3 with SR around or below 10 cm kyr^{-1}) than the ribbon-shaped channel fills with low interconnectivity (see A2 with SR around 30–40 cm kyr^{-1}) (Fig. 9). In this scenario, low SR reflect the low aggradation of the floodplains favouring lateral mobility and an increase in channel density, while high SR reflect an important aggradation of the floodplain which favoured avulsion and predominance of isolated channels (Bryant *et al.*, 1995). This is consistent with data from experimental models which indicate that the higher SR are recorded in floodplains while channels only act as conduits for sediment bypass (Sheets *et al.*, 2002). It is important to note that the two LAE discussed above develop in high sediment supply conditions as revealed by the clast size and the sedimentary system arrangement.

The distal and lateral reductions in SS are evidenced by the grain-size finning trend from the fluvial system to the mudflats and lacustrine environments. The AS in the palustrine/lacustrine limestone units (SR around 9 cm ky^{-1}) is lower than in the correlative mudflats mudstones (SR around 15–20 cm kyr^{-1}), and these lower than in the correlative ribbon-shaped channel fills with low interconnection. This lateral/distal reduction in AS is associated to a reduction in the SS.

Stacked calcretes reflect the lowest AS (SR around 3 cm kyr^{-1}) and low sediment supply as deduced from their location in the distal floodplain, distal alluvial and dry mudflats equivalent to sheet-like channels with high interconnections. This is in agreement with the occurrence of calcretes in low deposition settings (Tandon *et al.*, 1998; Alonso-Zarza, 2003), sheltered (Armenteros & Huerta, 2006) or uplifting regions (Alonso-Zarza *et al.*, 1999).

The study of ancient fluvial systems shows marked differences in sedimentation rates, these ranging over two orders of magnitude. When fluvial systems are analysed in the long term (SRS 9-10 of Miall, 2014), most of the data fall within the range given in the compilation work of Colombera *et al.* (2015), with sedimentation rates between 55 to 60 cm kyr^{-1} and 1 cm kyr^{-1}. For example, SR for the Siwalik sections in Pakistan average 12 cm kyr^{-1} (Johnson *et al.*, 1988) and the fluvial deposits of the Junggar Basin (China) around 24.5 cm kyr^{-1} (Ji *et al.*, 2008). The overbank and paleosol alternation of the Bighorn Basin (Wyoming) show that average rates are in the range between 40 and 28.8 cm kyr^{-1} (Abels *et al.*, 2013). Similarly, sedimentation in mudflat deposits yields values that easily overcome one order of magnitude. Abels *et al.* (2011), in the Tibetan Plateau, show SR of about 4.6 cm kyr^{-1} in mudflat environments, down to 2.1 cm kyr^{-1} in gypsiferous mudflats. In the Calatayud-Daroca basin (central Spain) mudflat-dominated deposits record SR rates of about 5 cm kyr^{-1} (Abdul-Aziz *et al.*, 2000). In lacustrine settings SR vary over a narrower range, from 10 cm kyr^{-1} in the Green River Basin (Smith *et al.*, 2008), to 6–10 cm kyr^{-1} in the Oligocene fresh water lacustrine deposits of the Ebro Basin (Valero *et al.*, 2014), and 6.5 cm kyr^{-1} in the Junggar Basin (Ji *et al.*, 2008). Variations in lacustrine settings depend on the local subsidence, source area, paleoproductivity and the over- or underfilling state of the basin (Carroll & Bohacs, 1999). Finally, the calcretes are suggested to form when pedogenesis overcome sedimentation rates (Machette, 1985) and Daniels (2003) stated that 0.5 cm kyr^{-1} is the threshold rate of pedogenic assimilation. The rate of local subsidence and the type of calcretes may increase this range as fine interbedding with

other deposits is common. SR for calcretes are thought to be in a range between <3 cm kyr^{-1} and punctual negative sedimentation.

The balance between AS and SS represents the response of the basin to external forcing. Size, slope, tectonic evolution and the nature of the source areas are specific of each basin. Thus it may be inaccurate to extrapolate absolute rates to other basins. However, the relative vertical and lateral variations and their relationship with the balance between accommodation and sediment supply may be shared with other sedimentary records.

Climate and tectonics

Lateral changes in accommodation space and sediment supply in the Almazán Basin are mainly driven by the tectonic uplift of the Cameros Massif and the Iberian Chain. This is supported by the sequence stratigraphy of the basin, and the documented relationship between sedimentary unconformities and tectonic structures. Palaeocurrents, clast composition and clay mineralogy analyses were carried out to identify the role of tectonics during basin filling (Huerta, 2007). Thrusting and folding along the margins provided the basin with sediments and the regional flexural subsidence that supports long-term accommodation. On the other hand, intrabasinal thrusting modified the sediment routing system and contributed to the localized generation or destruction of accommodation space.

Despite the buffering of the upstream signal in large to medium drainage systems (Castelltort & Van Der Driessche, 2003), it has been shown that fluvial deposits can record climatic oscillations (Abels *et al.*, 2013). Recent studies in the Teruel Basin suggest that the superimposition of climate and tectonics exerts an important control on lacustrine sedimentation an in the expansion and retraction of the lake deposits (Alonso-Zarza *et al.*, 2012; Ezquerro *et al.*, 2014). In other basins of the Iberian Chain, the main sedimentary ruptures are not found to correlate with climate change (López Martínez *et al.*, 1987; Calvo *et al.*, 1993; Muñoz-Jiménez & Casas-Sainz, 1997). Added to this complexity, it has been shown that the autogenic response of the sedimentary systems can produce organized stratal patterns with no need of external control (Hajek *et al.*, 2012).

In the Almazán basin, well defined large-scale architectural trends occur at basin scale, thus indicating external forcing. No evidence of climate forcing, such as recognition of orbital cyclicity or correlation with global events, is found at this scale. The singularity of a calcrete bed at near the Eocene-Oligocene boundary could represent a climatically driven transient decrease in the sediment input, but no remarkable shift in the overall sedimentary stacking pattern can be associated to this global scale climate transition. Thus, the occurrence of long-term orbital cycles in the Paleogene fluvial record of the Almazán basin remains not demonstrated. Further research focussed on the evaporitic mudflats and lacustrine/palustrine limestones could provide useful information on this issue.

CONCLUSIONS

The magnetostratigraphy for the Paleogene continental record of the Almazán Basin allows filling a gap of the Cenozoic chronostratigraphy of the Spanish basins. This work permits settling ages of the fossil mammal sites and the depositional sequence boundaries of the basin. In addition, the new ages provide the resolution needed to quantify of sedimentary rates throughout the Gómara Monocline. The combined evolution of depositional sequences, the architectural shifts, and the variations of sedimentation rates are interpreted in terms of accommodation and sediment supply changes.

The magnetostratigraphic results reveal that the first depositional sequence A1 started in mid-Lutetian times (chron C21n) in relation to the emplacement of the Cameros Main thrust. The development of the South Cameros Thrust started in early Bartonian (chron C18r), synchronously to deposition of A2. Close to the Eocene/Oligocene transition sedimentation of A3 starts, coeval to the growth of the Gómara, Almazán and the Arcos monoclines, and associated structures, producing differential changes in accommodation space. Since middle Chattian (chron C9n.1n), A4 records the increase in the tectonic activity. The uplift of the Gómara monocline produced the erosion of the northern domain and created growth strata that articulated in the Gómara monocline.

Relative changes in SR show a correspondence with the large-scale sedimentary architecture, and relative changes in the AS/SS ratio reveal useful for stratal pattern prediction. In areas with high sediment supply, higher SR (30–40 cm kyr^{-1}) are related to ribbon-shaped isolated channel fills (channel density <10%) and predominance of floodplain fine grained deposits. On the other hand, lower SR (<10 cm kyr^{-1}) correspond to laterally extensive sheet-like interconnected channel fills (channel density from 20% to 50%) and an increase in the average grain size.

In basin sectors with low sediment input, the predominance of fine sediments, mudstones and evaporitic mudstones reveals a slight decrease in sedimentation rates (SR around 15–20 cm kyr^{-1}) with respect to the areas with high sediment supply (fluvial system). Palustrine/lacustrine limestone units occur in areas of very low sediment input and low sedimentation rates (SR around 9 cm ky^{-1}) which are reflecting the carbonate production. Stacked calcrete profiles develop in areas with low sediment supply and very low sedimentation rates (SR around 3 cm kyr^{-1}) related to distal alluvial or distal floodplain areas.

ACKNOWLEDGEMENTS

This research was funded by the Spanish projects COFORSED (CGL2010-17479) and SEROS (CGL2014-55900-P), and the Research Group of 'Geodinàmica i Anàlisi de Conques' (2014SGR467). LV acknowledges the University of Barcelona for financial

support (APIF-UB). Thanks to Cor Langereis, Tom Mullender and Maxim Krasnoperov from the Fort Hoofdijk Paleomagnetic Laboratory (Utrecht University), and to the Barcelona Paleomagnetic Laboratory (CCiTUB-ICTJA CSIC). We are very grateful to the Editor Sébastien Castelltort, and to Liz Hajek, Ana Alonso-Zarza and an anonymous reviewer for their valuable comments on the manuscript. This is a contribution to the ESF Research Networking Programme EARTHTIME-EU (08-RNP-017) and the Geomodels Institute (Universitat de Barcelona).

CONFLICT OF INTEREST

No conflict of interest declared.

SUPPORTING INFORMATION

Additional Supporting Information may be found in the online version of this article:

Figure S1. Detailed sampling location..
Figure S2. Detailed sampling location (continuation).

REFERENCES

Abdul-Aziz, H., Hilgen, F., Krijgsman, W., Sanz, E. & Calvo, J.P. (2000) Astronomical forcing of sedimentary cycles in the middle to late Miocene continental Calatayud Basin (NE Spain). *Earth Planet. Sci. Lett.*, **177**, 9–22.

Abels, H.A., Dupont-Nivet, G., Xiao, G.Q., Bosboom, R. & Krijgsman, W. (2011) Step-wise change of Asian interior climate preceeding the Eocene-Oligocene Transition (EOT). *Paleogeogr. Paleoclimatol. Palaeocol.*, **299**, 399–412.

Abels, H.A., Kraus, M.J. & Gingerich, P.D. (2013) Precession-scale cyclicity in the fluvial lower Eocene Willwood Formation of the Bighorn Basin, Wyoming (USA). *Sedimentology*, **60**, 1467–1483.

Allen, J.R.L. (1978) Studies in fluviatile sedimentation: an exploratory quantitative model for the architecture of avulsion-controlled alluvial suites. *Sediment. Geol.*, **21**, 129–147.

Alonso-Zarza, A.M. (2003) Palaeoenvironmental significance of palustrine carbonates and calcretes in the geological record. *Earth-Sci. Rev.*, **60**, 261–298.

Alonso-Zarza, A.M., Calvo, J.P. & García Del Cura, M.A. (1992) Palustrine sedimentation and associated features - grainification and pseudo-microkarst- in the Middle Miocene (Intermediate Unit) of the Madrid Basin, Spain. *Sediment. Geol.*, **76**, 43–61.

Alonso-Zarza, A.M., Sopeña, A. & Sanchez-Moya, Y. (1999) Contrasting palaeosol development in two different tectonic settings: the Upper Buntsandstein of the Western Iberian Ranges, Central Spain. *Terra Nova*, **11**, 23–29.

Alonso-Zarza, A.M., Dorado-Valiño, M., Valdeolmillos-Rodríguez, A. & Ruiz-Zapata, M.B. (2006) A recent analogue for palustrine carbonate environments: the Quaternary deposits of Las Tablas de Daimiel wetlands, Ciudad Real, Spain. In: *Paleoenvironmental Record and Applications of Calcretes and Palustrine Carbonates* (Ed. by Alonso-Zarza A.M. & Tanner L.H.) *Geol. Soc. London. Spec. Publ.*, **416**, 153–168.

Alonso-Zarza, A., Meléndez, A., Martín-García, R., Herrero, M.J. & Martín-Pérez, A. (2012) Discriminating between tectonism and climate signatures in palustrine deposits: lessons from the Miocene of the Teruel Graben, NE Spain. *Earth-Sci. Rev.*, **113**, 141–160.

Armenteros, I. & Huerta, P. (2006) The role of clastic sediment influx in the formation of calcrete and palustrine facies: a response to paleographic and climatic conditions in the southeastern Tertiary Duero basin (northern Spain). *Geol. Soc. Am. Spec.*, **416**, 119–132.

Armenteros, I., Daley, B. & Garcia, E. (1997) Lacustrine and palustrine facies in the Bembridge Limestone (late Eocene, Hampshire Basin) of the Isle of Wight, southern England. *Palaeogeogr. Palaeoclimatol. Palaeoecol.*, **128**, 111–132.

Armenteros, I., Bustillo, M.A. & Huerta, P. (2006) Ciclos climáticos en un sistema lacustre marginal perenne carbonatado-evaporítico. Formación Deza, Eoceno superior, cuenca de Almazán. *Geo-temas*, **9**, 25–30.

Armitage, J.J., Duller, R.A., Whittaker, A.C. & Allen, P. (2011) Transformation of tectonic and climatic signals from source to sedimentary archive. *Nat. Geosci.*, 1–5, doi: 10.1038/NGEO1087.

Badiola, A., Checa, L., Cuesta, M.A., Quer, R., Hooker, J.J., Astibia, H., Natural, T. & Museum, H. (2009) The role of new Iberian finds in understanding European Eocene mammalian paleobiogeography. *Geol. Acta*, **7**, 243–258.

Bohacs, K.M., Carroll, A.R., Nede, J.E. & Mankirowicz, P.J. (2000) Lake-Basin type, source potential and hydrocarbon character: An integrated sequence-stratigraphic-geochemical framework. In: *Lake Basins through Space and Time* (Ed. by E.H. Gierlowski-Kordesch & K.R. Kelts) *Aapg Stud. Geol.*, **46**, 3–33. American Association of Petroleum Geologists, Tulsa, OK, U.S.A.

Bridge, J.S. & Leeder, M.R. (1979) A simulation model of alluvial stratigraphy. *Sedimentology*, **26**, 617–644.

Bryant, M., Falk, P. & Paola, C. (1995) Experimental study of avulsion frequency and rate of deposition. *Geology*, **23**, 365–368.

Calvo, J.P., Daams, R., Morales, J., López Martínez, N., Agustí, J., Anadón, P., Armenteros, I., Cabrera, L., Civis, J., Corrochano, A., Díaz Molina, M., Elizaga, E., Hoyos, M., Martín-Suárez, E., Martínez, J., Moissenet, E., Muñoz, A. & Pérez García, A. (1993) Up-to-date Spanish continental neogene synthesis and paleoclimatic interpretation. *Revista de la Sociedad Geológica de España*, **6**, 29–40.

Carroll, A.R. & Bohacs, K.M. (1999) Stratigraphic classification of ancient lakes: balancing tectonic and climatic controls. *Geology*, **27**, 99–102.

Casas, A.M. (1990) El frente Norte de la Sierra de Cameros: Estructuras cabalgantes y campo de esfuerzos. PhD Thesis, Universidad de Zaragoza, Zaragoza.

Casas-Sainz, A.M. (1993) Oblique tectonic inversion and basement thrusting in the Cameros Massif (Northern Spain). *Geodin. Acta*, **6**, 202–216.

Casas-Sainz, A.M., Cortés-García, A.L. & Maestro-González, A. (2000) Intraplate deformation and basin formation during the Tertiary within the northern Iberian plate: origin and evolution of the Almazán basin. *Tectonics*, **19**, 258–289.

Casas-Sainz, A.M., Cortés, A.L. & Maestro, A. (2002) Sequential limb rotation and kink-band migration recorded by growth strata, Almazán Basin, North Spain. *Sediment. Geol.*, **146**, 25–45.

Castelltort, S. & Van Der Driessche, J. (2003) How plausible are high-frequency sediment supply-driven cycles in the stratigraphic record? *Sediment. Geol.*, **157**, 3–13.

Catuneanu, O. (2006) *Principles of Sequence Stratigraphy*. Elsevier, Amsterdam.

Catuneanu, O. & Elango, H.N. (2001) Tectonic control on fluvial styles: the Balfour formation of the Karoo Basin, South Africa. *Sediment. Geol.*, **140**, 291–313.

Catuneanu, O., Abreu, V., Bhattacharya, J.P., Blum, M.D., Dalrymple, R.W., Eriksson, G., Fielding, C.R., Fisher, W.L., Galloway, W.E., Gibling, M.R., Giles, K.A., Holbrookl, J.M., Jordan, R., Kendall, C.G.S.T.C., Macurda, B., Martinsen, O.J., Miall, A.D., Neal, J.E., Nummedal, D., Pomar, L., Posamentier, H.W., Pratt, B.R., Sarg, J.F., Shanley, K.W., Steel, R.J., Strasser, A., Tucker, M.E. & Winker, C. (2009) Towards the standardization of sequence stratigraphy. *Earth Sci. Rev.*, **92**, 1–33.

Colombera, L., Mountney, N.P. & Mccaffrey, W.D. (2015) A meta-study of relationships between fluvial channel-body stacking pattern and aggradation rate: implications for sequence stratigraphy. *Geology*, **43** (4), 283–286.

Cuesta, M.A. & Jiménez, E. (1994) Síntesis del Paleógeno del borde oriental de la cuenca de Almazán (Soria): Vertebrados de Mazaterón. *Stud. Geol. Salmatic.*, **XXIX**, 157–170.

Daniels, J.M. (2003) Floodplain aggradation and pedogenesis in a semiarid environment. *Geomorphology*, **56**, 2252242.

Del Rio, P., Barbero, L. & Stuart, F.M. (2009) Exhumation of the Sierra de Cameros (Iberian Range, Spain): constraints from low-temperature thermochronology. *Geol. Soc. London. Spec. Publ.*, **324**, 153–166.

Edgar, K.M., Wilson, P.A., Sexton, P.F., Gibbs, S.J., Roberts, A.P. & Norris, R.D. (2010) New biostratigraphic, magnetostratigraphic and isotopic insights into the Middle Eocene Climatic Optimum in low latitudes. *Palaeogeogr. Palaeoclimatol. Palaeoecol.*, **297**, 670–682.

Ezquerro, L., Luzón, A., Navarro, M., Liesa, C.L. & Simón, J.L. (2014) Climatic vs. tectonic signals in a continental extensional basin (Teruel, Ne Spain) from stable isotope (δ18O) and sequence stratigraphical evolution. *Terra Nova*, **26**, 337–346.

Gradstein, F.M., Ogg, J.G., Schmitz, M. & Ogg, G. (2012) *The Geologic Time Scale 2012*. Elsevier, Cambridge University Press, Cambridge.

Guimerà, J., Alonso, A. & Mas, R. (1995) Inversion of an Extensional Ramp Basin by a Neoformed thrust: the Cameros Basin (N Spain). In: *Basin Inversion* (Ed. by Buchanan J.G. & Buchanan P.G.) *Geol. Soc. Spec. Pub.*, **88**, 433–453.

Hajek, E.A., Heller, P.L. & Schur, E.L. (2012) Field test of autogenic control on alluvial stratigraphy (Ferris Formation, Upper Cretaceous-Paleogene, Wyoming). *Geol. Soc. Am. Bull.*, **124**, 1898–1912.

Heller, P.L. & Paola, C. (1996) Downstream changes in alluvial architecture: an exploration of controls on channel-stacking patterns. *J. Sediment. Res.*, **66**, 297–306.

Hickson, T.A., Sheets, B.A., Paola, C. & Kelberer, M. (2005) Experimental test of tectonic controls on three-dimensional alluvial facies architecture. *J. Sediment. Res.*, **75**, 710–722.

Hilgen, F.J., Hinnov, L.A., Abdul Aziz, H., Abels, H.A., Batenburg, S., Bosmans, J.H.C., De Boer, B., Hüsing, S.K., Kuiper, K.F., Lourens, L.J., Rivera, T., Tuenter, E., Van De Wal, R.S.W., Wotzlaw, J.-F. & Zeeden, C. (2014) Stratigraphic continuity and fragmentary sedimentation: the success of cyclostratigraphy as part of integrated stratigraphy. In: *Strata and Time: Probing the Gaps in Our Understanding* (Ed. by Smith D.G., Bailey R.J., Burgess P.M. & Fraser A.J.) *Geol. Soc. London. Spec. Publ.*, **404**. doi: 10.1144/SP404.12.

Huerta, P. (2007) El Paleógeno de la cuenca de Almazán. Relleno de una cuenca piggyback. PhD Thesis, Universidad de Salamanca, Salamanca, Spain.

Huerta, P. & Armenteros, I. (2004) Asociaciones de carbonatos continentales en el Eoceno de la Cuenca de Almazán. *Geotemas*, **6**, 75–78.

Huerta, P. & Armenteros, I. (2005) Calcrete and palustrine assemblages on a distal alluvial-floodplain: a response to local subsidence (Miocene of the Duero basin, Spain). *Sediment. Geol.*, **177**, 253–270.

Huerta, P., Armenteros, I., Recio, C. & Blanco, J.A. (2010) Palaeogroundwater evolution in playa–lake environments. Sedimentary facies and stable isotope record (Palaeogene, Almazán basin, Spain). *Palaeogeogr. Palaeoclimatol. Palaeoecol.*, **286**, 135–148.

Huerta, P., Armenteros, I. & Silva, P.G. (2011) Large-scale architecture in non-marine basins: the response to the interplay between accommodation space and sediment supply. *Sedimentology*, **58**, 1716–1736.

Ji, J., Luo, P., White, P., Jiang, H., Gao, L. & Ding, Z. (2008) Episodic uplift of the Tianshan Mountains sice the Late Oligocene constrained by magnetostratigraphy of the Jingou River section, in the southern margin of the Junggar Basin, China. *J. Geophys. Res.*, **113**, B05102.

Jo, H.R. & Chough, S.K. (2001) Architectural analysis of fluvial sequences in the northwestern part of Kyongsang Basin (Early Cretaceous), SE Korea. *Sed. Geol.*, **144**, 307–334.

Johnson, N.M., Sheikh, K.A., Dawson-Saunders, E. & Mcrae, L.E. (1988) The use of magnetic-reversal time lines in stratigraphic analysis: a case study in measuring variability in sedimentation rates. In: *New Perspectives in Basin Analysis* (Ed. by K.L. Kleinspehn & C. Paola), pp. 189–200. Springer-Verlag, New York.

Kirschvink, J.L. (1980) The least-squares line and plane and the analysis of palaeomagnetic data. *Geophys. J. Int.*, **62**, 699–718.

Leeder, M.R. (1993) Tectonic controls upon drainage basin development, river channel migration and alluvial architecture: implications for hydrocarbon reservoir development characterization. In: *Characterization of Fluvial and Aeolian Reservoirs* (Ed. by North Colin P. & Prosser D.J.) *Geol. Soc. Spec. Pub.*, **73**, 7–22. Geological Society of London, London.

Legarreta, L. & Uliana, M.A. (1998) Anatomy of hinterland depositional sequences: upper Cretaceous fluvial strata, Neuquén basin, west-central Argentina. In: *Relative role of Eustasy, Climate, Tectonism in Continental Rocks* (Ed. by K.W. Shanley & P.J. McCabe) *SEPM Spec. Publ.*, **59**, 83–92. Society of Economic Paleontologists and Mineralogists, Tulsa, OK, USA.

López Martínez, N., Agustí, J., Cabrera, L., Calvo, J.P., Civis, J., Corrochano, A., Daams, R., Díaz, M., Elízaga, E., Hoyos, M., Martínez, J., Morales, J., Portero, J., Robles, F., Santisteban, C. & Torres, T. (1987) Approach to the

Spanish continental neogene synthesis and paleoclimatic interpretation. *Ann. Inst. Geol. Public. Hung.*, **70**, 383–391.

Machette, M.N. (1985) Calcic soils of southwestern United States. In: *Soil and Quaternary Geology of the Southwestern United States* (Ed. by Weide D.L.) *Geol. Soc. Am. Spec.*, **203**, 1221.

Mackey, S.D. & Bridge, J.S. (1995) Three-dimensional model of alluvial stratigraphy: theory and application. *J. Sediment. Res.*, **65**, 7–31.

Miall, A.D. (2014) *Fluvial Depositional Systems*. Springer, New York.

Michael, N.A., Whittaker, A.C., Carter, A. & Allen, P.A. (2014) Volumetric budget and grain-size fractionation of a geological sediment routing system: Eocene Escanilla Formation, south-central Pyrenees. *Geol. Soc. Am. Bull.*, **126**, 585–599.

Mitchum, R.M. Jr, Vail, P.R. & Thompson, S. III (1977) Seismic stratigraphy and global changes of sea level. Part 2: The depositional sequence as a basic unit for stratigraphic analysis. In: *Seismic Stratigraphy; Applications to Hydrocarbon Exploration* (Ed. by C.E. Payton) *AAPG Mem.*, **26**, 53–62. American Association of Petroleum Geologists, Tulsa, OK.

Muñoz-Jiménez, A. & Casas-Sainz, A.M. (1997) The Rioja Trough (N Spain): Tectosedimentary Evolution of a Symmetric Foreland Basin. *Basin Res.*, **9**, 65–85.

Muto, T. & Steel, R.J. (1997) Principles of regression and transgression: the nature of the interplay between accommodation and sediment supply. *J. Sediment. Res.*, **67**, 994–1000.

Muto, T. & Steel, R.J. (2000) The accommodation concept in sequence stratigraphy: some dimensional problems and possible redefinition. *Sediment. Geol.*, **130**, 1–10.

Navarro Váquez, D. (1991.Mapa Geológico de España 1:50000, Hoja 350 (Soria), ITGE. Madrid.

Paola, C. & Martin, J.M. (2012) Mass-balance effects in depositional systems. *J. Sediment. Res.*, **82**, 435–450.

Posamentier, H.W. & Vail, P.R. (1988) Eustatic controls on clastic deposition. II: Sequence and systems tract models. In: *Sea-Level Changes-An Integrated Approach* (Ed. by C.K. Wilgus, B.S. Hastings, C.S.C. Kendall, H.W. Posamentier, C.A. Ross & J.C. Van Wagoner) *SEPM*, **42**, 125–154. OK, USA.

Rosenbaum, G., Lister, G.S. & Duboz, C. (2002) Relative motions of Africa, Iberia and Europe during Alpine orogeny. *Tectonophysics*, **359**, 117–129.

Shanley, K.W. & McCabe, P.J. (1991) Predicting facies architecture through sequence stratigraphy -an example from the Kaiparowits Plateau, Utah. *Geology*, **19**, 742–745.

Sheets, B.A., Hickson, T.A. & Paola, C. (2002) Assembling the stratigraphic record: depositional paterns and time-scales in an experimental alluvial basin. *Basin Res.*, **14**, 287–301.

Smith, M.E., Carroll, A.R. & Singer, B.S. (2008) Synoptic reconstruction of a major Ancient Lake System: Eocene Green River Formation Western United States. *Geol. Soc. Am. Bull.*, **120**, 54–84.

Strong, N., Sheets, B.A., Hickson, T.A. & Paola, C. (2005) A mass-balance framework for quantifying downstream changes in fluvial architecture. In: *Fluvial Sedimentology VII* (Ed. by Blum M.D., Marriott S.B. & Leclair S.) *Int. As. Sed.*, **35**, 243–253. Blackwell.

Tandon, S.K., Andrews, J.E., Sood, A. & Mittal, S. (1998) Shrinkage and sediment supply control on multiple calcrete profile development: a case study from the Maastrichtian of Central India. *Sediment. Geol.*, **119**, 25–45.

Törnqvist, T.E. (1994) Middle and late Holocene avulsion history of the River Rhine (Rhine-Meuse delta, Netherlands). *Geology*, **22**, 711–714.

Vail, P.R. & Mitchum, R.M. Jr (1977) Seismic Stratigraphy and global changes of sea level. Part 1: Overview. In: *Seismic Stratigraphy - Applications to Hydrocarbon Exploration* (Ed. by C.E. Payton) *AAPG Mem.*, **26**, 51–52. American Association of Petroleum Geologists, Tulsa, OK.

Valero, L., Garcés, M., Cabrera, L., Costa, E. & Sáez, A. (2014) 20 Myr of eccentricity paced lacustrine cycles in the Cenozoic Ebro Basin. *Earth Planet. Sci. Lett.*, **408**, 183–193.

Van Wagoner, J.C., Posamentier, H.W., Mitchum, R.M. Jr, Vail, P.R., Sarg, J.F., Loutit, T.S. & Hardenbol, J. (1988) An overview of the fundamentals of sequence stratigraphy and key definitions. In: *Sea-Level Changes-An Integrated Approach* (Ed. by C.K. Wilgus, B.S. Hastings, C.S.C. Kendall, H.W. Posamentier, C.A. Ross & J.C. Van Wagoner) *SEPM*, **42**, 39–45. OK, USA.

Wright, V.P. & Marriott, S.B. (1993) The sequence stratigraphy of fluvial depositional systems: the role of floodplain sediment storage. *Sediment. Geol.*, **86**, 203–210.

Manuscript received 13 November 2014; In revised form 18 May 2015; Manuscript accepted 14 June 2015.

Appendix 3
Long-period Astronomically-forced Terrestrial Carbon Sinks (Submitted)

Long-period Astronomically-forced Terrestrial Carbon Sinks.

Luis Valero[1], Lluís Cabrera[1], Alberto Sáez[1], Frits Hilgen[2], Miguel Garcés[1]

1. *GEOMODELS Institute, Departament d'Estratigrafia, Paleontologia i Geociències Marines, Facultat de Geologia, Universitat de Barcelona, Martí i Franquès s/n, 08028 Barcelona, Spain.*
2. *Department of Earth Sciences, Utrecht University, Heidelberglaan 2, 3584 CD Utrecht, The Netherlands*

Abstract

Sequestration of organic matter by peat accumulation constitutes a primary sink for carbon in the global carbon cycle. Assessing the processes that control the formation and storage of peat at geological time scales is a non-solved issue of fundamental importance for understanding the global climate system. We analyzed a 7 million years long terrestrial record of Late Oligocene age from the As Pontes Basin in Northern Spain, which demonstrates that minima in the 405-kyr and 2.4-Myr eccentricity cycles play a key role in peat formation. Such nodes exhibit reduced precession amplitudes, thus avoiding extremes in seasons and seasonal contrast for a prolonged period of time. In the As Pontes Basin, this orbital configuration is associated with a decrease in siliciclastic sedimentation and enhanced peat formation. Feedbacks between equilibrium landscapes and ecosystem stability will lead to a deceleration of weathering and erosion rates in catchment areas and to minimize and stabilize the sediment flux along the sediment routing system. Mid-latitude peat burial could contribute to disturb the carbon cycle by removing (atmospheric) carbon at times of minimum eccentricity.

Introduction

Very long-term orbital oscillations (>1Myr) play an important role as triggers of irreversible changes of past climates (Zachos et al., 2001). Studies of long-period cycles as recorded in

continental sediments are essential to disentangle the local, regional and global importance of the associated climate changes (e.g. Abels et al., 2012). The search of these cycles in continental basins is, however, particularly challenging because of their inferred low preservation potential. Basic requirements for their development and study are stability of the basin depositional setting, sensitivity of the sedimentary environment to climate variations, and the preservation of a long stratigraphic record that preferably spans several cycles. A limited number of case studies exist that fully document long-period cyclicity in lacustrine systems (Olsen and Kent, 1999; Kashiwaya et al., 2001, Abels et al., 2010a; Valero et al., 2014). However, recent studies show that these cycles can also be recognized in apparently less favourable continental settings such as fluvial systems (Abels et al., 2013; Hilgen et al., 2014), and that million-year scale climatic cycles can occur superimposed on the longterm tectonic signature of foreland basins (Valero et al., 2014). These results should stimulate debate on the various forcing factors that control sedimentation in different continental basins (Shanley and McCabe, 1994) and on different timescales at which they operate (Miall, 2014).

Available numerical climate models help to understand the sedimentary system response to climate change related to the short-period cycles of precession and obliquity (e.g., Bosmans et al., 2014). However, considerable uncertainty remains on the forcing mechanisms at million-year time scales such as that of the very long-period eccentricity cycle. Agreement exists in that the alteration of the hydrological cycle, summarized as the balance between precipitation and evaporation must exert a prime control on sedimentary cyclicity. Nevertheless, climate can affect depositional settings through other processes, namely via their impact on vegetation cover, sediment production and (ground) water chemistry. In addition, sedimentary facies distribution is sensitive to erosional patterns in the catchment basin and the dynamics of sediment transfer systems, both intimately linked to vegetation cover and the morphology of the basin.

To understand how climate, by means of the million year-scale orbital oscillations, affects the sediment routing system and sedimentary facies distribution, we focused on a long coal-bearing stratigraphic record. Increase of clastic supply can lead to shrinking and obliteration of peatlands, thus making these systems excellent indicators of changes in vegetation and erosion in the catchment basin. Precession, obliquity and short eccentricity-related orbital forcing of coal-bearing sequences has already been documented (van Vugt et al., 2001; Large et al., 2003; Large et al., 2004; Briggs et al., 2007), and further correlated to marine climatic records (van Vugt et al., 1998). However, compelling evidence for a relationship between coal formation in mid-latitude swampy environments and long-period Milankovitch cycles has not yet been found. As peatlands are significant contributors to the carbon cycle (Large et al., 2004), understanding the climatic controls on coal formation is critical to better understand forcing and feedbacks in Earth's climate system.

In this paper, a cyclostratigraphic analysis of the Upper Oligocene coal-bearing sequence of the As Pontes Basin in NW Spain is carried out. The long time span of *ca.* 7 Myr of this record was essential for the investigation of recurrent basin-wide coal expansions. Magnetostratigraphic data from earlier studies (Huerta et al., 1997) were revised and integrated in this study in order to provide the necessary temporal framework. Spectral analysis was applied on selected borehole data with the aim to statistically test the orbital forcing hypothesis of the sedimentary cyclicity, before comparing the cycle record with orbital target curves. The significance of the cyclicity and the mechanisms through which insolation changes that result from Earth's orbital geometry are transmitted to the sedimentary record are discussed.

Geological setting and section/cores

The As Pontes Basin developed along a NW-SE-oriented dextral strike-slip fault system associated with the convergence between the Iberian and European plates (Santanach et al., 2005). The northern basin margin is structurally complex, characterized by a vertical stack of

numerous southward directed thrusts sheets coeval with N-S directed extensional faults derived from the major fault system (Fig. 1). The basin is divided into two fault-bounded sub-basins and the basin infill consists of a 400 m thick coal-bearing sedimentary record. A detailed basin stratigraphy is based on high-resolution basin-wide correlations, using the core database of the mining company. The bedrock of the catchment area consists mostly of Paleozoic slate and Precambrian meta-graywackes. Small-sized alluvial fan deposits accumulated in the proximal areas, and interfinger basinwards with metric and decametric-scale peat deposits (Fig. 2). Shifts of the facies belts led to the organization of the sedimentary fill into basin-wide decameter-scale sequences. Such sequences consist of a coal-rich clayey lower unit overlain by a clastic unit, which was mainly fed from alluvial fans along the northern basin margin (Fig. 2, Fig. 3). This cyclic stacking pattern is interrupted by a major clastic episode (Middle Sandstone Unit) in the middle of the sequence, which marks the complete connection between the two sub-basins during the late stage of the basin fill. The Middle Sandstone Unit onlaps on the structural high bounding the western and eastern sub-basins, and is associated with a rearrangement of the alluvial network following the connection of the sub-basins (Ferrús, 1998). Cyclic aggradation of the coal/clastic sequences is resumed after this episode. Finally, basin overfilling is marked by a coarsening trend, representing alluvial progradation due to a reduction of the accommodation space.

The paleobotanical record suggests a semitropical swamp forest environment (Cavagnetto, 2002), where warm and humid conditions prevailed in a continental non-ombrotrophic peatland. Faunal remains are scarce, but the occurrence of the fossil rodent *Issiodoromys minor* (López-Martínez et al., 1993) at the base of the West section provides a biochronological constraint, suggesting a correspondence with the MP24 mammal reference level (upper Rupelian; Gradstein et al., 2012). A magnetostratigraphic study of the complete record provided a preliminary correlation to the polarity time scale (Huerta et al., 1997). For our study

we used the West section of Huerta et al. (1997) and six cores located in the center of the western sub-basin of the As Pontes basin (see Fig. 1 for localities).

Magnetostratigraphic age model

The former magnetostratigraphy-based age model of Huerta et al. (1997) for the West section was revisited (Fig. 3). Their magnetostratigraphic age model is largely adopted here, except for the lowermost part of the section. The correlation of the basal normal magnetozone with chron C10n is not followed as it results in unrealistic changes in sedimentation rate. In addition, we were reluctant to use the lower two samples for magnetostratigraphic purposes, because the directional data deviate significantly from the expected geocentric dipole. As a result, we propose a revised correlation of the lower part of the section in which the reversed magnetozone R1 corresponds to chron C10r, and the normal magnetozone N1 with chron C10n. This correlation is reinforced by the occurrence of *Issiodoromys minor* in this part of the composite section, which fits well with the age range of the MP24 mammal reference level (López-Martínez et al., 1993; Gradstein et al., 2012). The refined magnetostratigraphy ranges from the top of chron C10r (around 29 Ma in the Rupelian) to chron C6Aar.2n in the early Miocene (*ca.* 21.7 Ma, East section not shown). The topmost sediments of the western sub-basin correlate with chron C6Cn.3n, just below the Oligocene-Miocene boundary (Fig. 3). The resultant sedimentation rates are in general low, averaging ~3 cm/kyr.

The new magnetostratigraphic age model proved critical for our cyclostratigraphic analysis and our attempt to establish the phase-relationship of potential orbitally-driven cycles with the astronomical parameters. For this purpose we established a correlation between core MP208 core and the West section, where magnetostratigraphic data are available, by means of detailed lithological correlations of coal-beds (Fig. 4). This correlation allowed us to apply the magnetostratigraphic age model to core MP208. This model was constructed using the Age

Scale tool of the Analyseries 2.08 software (Paillard et al., 1996) and the tie-points marked in Figure 4.

Cyclostratigraphy

Six cores of the Western sub-basin were selected for cyclostratigraphic analysis. Their location in the basin center was considered optimal for minimizing noise produced by tectonics and alluvial autogenic processes. Numerical values, ranging from proximal (1) to distal (8) and summarized in figure 2, were attributed to a suite of 36 different sedimentary facies described from the cores (Fig. 2; Table 1). The sedimentary model is based on criteria formulated by Sáez et al., (2002; 2003), who studied the sedimentology and the geochemistry of the basin and classified the different facies. The description of the lithofacies in the cores provided by previous studies was fully included in our model. Sampling resolution arrived at 39.1 cm following interpolation to obtain an evenly spaced depth-series. The magnetostratigraphic age model (sedimentation rates 2.5-3.5 cm/kyr) reveals that the sampling resolution fluctuates between 15.6 and 11.14 kyr in the time domain. Such values are below the Nyquist limit for precession and obliquity, but above the detection limit for all eccentricity cycles (Herbert, 1994; Meyers et al., 2008).

Spectral analysis, phase relations and astronomical tuning

Spectral analysis focused on the lower part of the basin fill in order to exclude the thick Middle Sandstone Unit from the time series, which represents a unique and at the same time aberrant interval in the record. This unit is associated with a sharp increase in sedimentation rates, and does not appear to follow the characteristic sequential arrangement of coal units. Spectral analyses of core records were carried out in the depth domain using the Analyseries software (Paillard et al., 1996) with default parameters for the Blackman-Tukey method. Subsequently, in order to correctly handle red noise, the records were also analyzed using the REDFIT software, which is based on the conventional AR(1) red noise model (Schulz and Mudelsee,

149 2000), with a rectangular window, 4000 simulations, and default HIFAC and OFAC values. The
150 spectral analyses indicate that significant peaks in the depth domain with periods between
151 15.1 m and 7.54 m occurred in all cores (Supplementary Information). A shifting average
152 sedimentation rate of 2.5-3.5 cm/kyr as inferred from the magnetostratigraphic age model,
153 implies that these peaks centered around 12 m fall within the range of the long orbital
154 eccentricity cycle of 405-kyr.

155 Analyseries was also used to apply a Gaussian band-pass filter (frequency: 0.0827 cycles/m;
156 bandwidth: 0.05) to the MP208 core data in the stratigraphic domain to extract the cyclicity
157 with a period around of 12 m (Fig. 4). We used a wide filter, in order to include all the potential
158 cycles taken the variability in sedimentation rates into account. In addition, the use of a wide
159 filter prevents the generation of artificial amplitude modulations in the range of eccentricity
160 (Zeeden et al., 2015). On the other hand, a 405-kyr centered filter was applied to the MP208
161 core in the (magnetostratigraphic) time domain. A correlation between the maxima of these
162 filters was performed, and extended to the 405-kyr eccentricity curve (Fig. 4). We used the
163 La2004 solution for eccentricity (Laskar et al., 2004), which for this time interval is stable and
164 identical to the La2011a solution (Laskar et al., 2011). The only tuning option in which the
165 magnetostratigraphic calibration is respected reveals a phase relationship in which the clastic
166 peaks correlate with maxima in the eccentricity curve (Fig. 4).

167 The same Gaussian band-pass filter was applied to the rest of the core data, improving the
168 correlation between the cores, and enabling an astronomical tuning to the 405-kyr eccentricity
169 component for all the cores (Fig. 5). To confirm orbital forcing at a 405-kyr-scale, independent
170 of the magnetostratigraphic age model, the astronomically-tuned age model to 405-kyr
171 eccentricity was applied to the raw data for spectral analysis. The spectra reveal peaks in the
172 100-kyr band (Fig. 6), thus providing independent evidence that the 405-kyr cycle age model is
173 meaningful and that the cycles are astronomically-forced. The statistical confidence of the 100-

kyr peak is at the 95% level in two out of the five core records, and at 90 % in the other three. The enhancement of peaks in the 100-kyr cycle range after the age model refinement indicates that the facies shifts were related to eccentricity cycles. This confirms that the regular decametric clastic units are associated with 405-kyr maxima, while coal units correspond to 405-kyr eccentricity minima. Although the spectral analyses reveal 100-kyr eccentricity-forced cycles, these cycles are not consistently present throughout the entire time-series. Low sedimentation rates and low resolution in the core description data, could explain the apparent lack of sensitiveness to the 100-kyr cycle in parts of the record.

Apart from the 405-kyr eccentricity cycle forcing, the astronomical correlation highlights that the three major basin-wide lignite units, indicated in Fig. 5 as H, A-B-C, and β horizons, occur during minima of the 2.4-Myr eccentricity cycle. These units contain the thickest coal seams, with isochronal limits that can be unequivocally traced across the basin, representing the main exploitable targets for the mining company.

It is noteworthy that these cycles are found in the distal part of a setting where tectonics and autogenic processes are potentially distorting the cyclicity. Episodes of tectonic deformation and uplifting can alter both the transport routing systems and the sediment fluxes (Armitage et al., 2013). The siliciclastic progradation of the Middle Sandstone Unit may well represent the sedimentary response to a tectonic reorganization, which temporarily disturbed the cyclic arrangement. Steady uplift rates, due to shortening accommodated by numerous minor thrusts (Santanach et al., 2005), could account for the low influence of tectonics on higher-frequency sedimentary architecture in the central parts of the basin.

Orbital forcing: climatic stability and coal accumulation.

Sharp basin-wide alternations of coal seams and siliciclastic sediments occur on a 405-kyr pacing, which suggests that coal accumulation is, on first order, dictated by favourable climatic conditions related to orbital eccentricity. The recurrent progradation of the sandstone units is

associated with an increase in sedimentation rate (Fig.2). The lack of a central lake with fluctuating base level implies that these sedimentary cycles are not accommodation-forced (Valero et al., 2015). Altogether this suggests that the cycles on this time scale are driven by changes in sediment input rate. Periods of 405-kyr eccentricity maxima mark pulses of increasing clastic supply and alluvial progradation, while at times of eccentricity minima clastic supply is reduced, favouring swamp development and peat accumulation.

Eccentricity itself does not provide significant insolation differences as to modify climatic patterns, but is a modulator of precession (Berger et al., 1992; Laskar et al., 2004). During eccentricity maxima, precession extremes can lead to insolation differences of about 20% (Laskar et al., 2004; Abels et al., 2013). Favourable conditions for peat formation would occur at times of eccentricity maxima in case the periodic development of swampy peats would be controlled by maxima in the range of seasonal insolation associated with climatic precession. The reason for this is that eccentricity determines the precession amplitude and thus the range of seasonal insolation and the climatic response. However, this is in contradiction with the observation that the major coal seams occur preferentially at times of eccentricity minima. Consequently, the lack of peatlands during eccentricity maxima suggests that other factors controlled coal accumulation. Prolonged intervals marked by low-amplitude insolation changes during combined eccentricity minima of the 100-kyr and 405-kyr cycles span several tenths of thousands of years, sustaining relatively stable climatic periods that avoid extreme seasonal signals. We propose that these stable climatic conditions during eccentricity minima promoted that peatlands and their adjacent ecosystems fixed soils efficiently, thereby decreasing erosion of the surrounding reliefs (Corenblit et al., 2011). In turn, the resultant reduction in clastic sediment supply favoured peat expansion in the basin. Conversely, during eccentricity maxima, and therefore high-amplitude precession, extreme maxima in seasonality during precession minima (for the Northern Hemisphere) will lead to the shrinking and fall of ecosystems and peatland decline.

Under stable climatic conditions and enhanced vegetation cover, the basin slope tends to reach dynamic equilibrium, particularly in a very low-gradient continental basin. Geomorphologic stability also contributes to reduce erosional rates, and subsequently sediment input (Whipple, 2001; Castelltort and Van Der Driessche, 2003). These periods of stability are more pronounced during the 2.4-Myr eccentricity minima, especially when such minima are combined with minimum eccentricity associated with the 405-kyr and 100-kyr cycles. During these orbital configurations, climatic stability can persist for about 50-60-kyr. The astronomical correlation shows that it is during these periods that the thicker peat layers that cover almost the entire basin accumulated.

Coal beds constitute an important sink for carbon storage. In this case, coal deposition and thus the carbon storage phase is associated with eccentricity minima. In contrast, in the neighbouring Ebro Basin, it has been shown that lake expansion and enhanced carbonate accumulation occurred during eccentricity maxima during the same time interval (Valero et al., 2014). As carbonate accumulation in lakes constitutes another efficient carbon sink (Sobek et al., 2009), the anti-phase behaviour of the respective carbon sinks within the same climatic belt and in nearby continental basins is noteworthy. The different sedimentary response of these basins to the same climatic changes likely depends on the different characteristics of the basins. This difference in response to climate changes as a function of basin characteristics is remarkable, as is the potential for nearby basins to buffer changes in carbon storage and, thus, the global carbon cycle, associated with eccentricity cycles, even when these basins are located within the same climatic belt.

Conclusions

The good to excellent correlation between the coal-alluvial sequences in the As Pontes Basin and the 405-kyr and 2.4-Myr eccentricity cycles suggests that these sequences are controlled by orbital climate forcing. Orbital rhythms were transmitted to the sediment record by the coupling between stable and favourable climate conditions, equilibrium landscapes, and the enhanced vegetation cover resilience. This suggests that even in small-sized tectonically active settings, the climatic signature can be detected, even when it is not driven by changes in the water balance, as in lakes. If the relationship between peatlands and long-term orbital forcing is shared with other mid-latitude basins, a wide-range of sensitive environments needs to be considered as potential carbon sinks. Depending on the overall response of basins to climatic changes as a function of their physiognomy it may constitute a long-term agent of global cooling.

Acknowledgments.

This is a contribution to the ESF Research Networking programme EARTHTIME-EU. This research was funded by the Spanish projects CGL2010-17479 and CGL2014-55900-P and the Research Group of "Geodinàmica i Anàlisi de Conques" (2009GGR 1198). LV thanks the University of Barcelona for the financial support (APIF-UB) and Christina Riesselman and the University of Otago in New Zealand for providing a place to write the first parts of this article.

References

Abels, H. A., Clyde, W.C., Gingerich, P.D., Hilgen, F.J., Fricke, H.C., Bowen, G.J., and Lourens, L.J., 2012, Terrestrial carbon isotope excursions and biotic change during Palaeogene hyperthermals: Nature Geoscience, v. 5, no. 5, p. 326–329, doi: 10.1038/ngeo1427.

Abels, H. A., Kraus, M.J., and Gingerich, P.D., 2013, Precession-scale cyclicity in the fluvial lower Eocene Willwood Formation of the Bighorn Basin, Wyoming (USA): Sedimentology, v.60, p. 1467-1483, doi: 10.1111/sed.12039.

Armitage, J.J., Dunkley Jones, T., Duller, R. A., Whittaker, A.C., and Allen, P. A., 2013, Temporal buffering of climate-driven sediment flux cycles by transient catchment response: Earth and Planetary Science Letters, v. 369-370, p. 200–210, doi: 10.1016/j.epsl.2013.03.020.

Berger, A, Loutre, M.F., and Laskar, J., 1992, Stability of the Astronomical Frequencies Over the Earth's History for Paleoclimate Studies: Science, v. 255, p. 560–566, doi: 10.1126/science.255.5044.560.

Bosmans, J.H.C., Drijfhout, S.S., Tuenter, E., Hilgen, F.J., Lourens, L.J., 2014, Response of the North African summer monsoon to precession and obliquity forcings in the EC-Earth GCM: Climate Dynamics, 1-19, doi: 10.1007/s00382-014-2260-z.

Briggs, J., Large, D. J., Snape, C., Drage, T., Whittles, D., Cooper, M., Macquaker, J.H.S, Spiro, B. F., 2007. Influence of climate and hydrology on carbon in an early Miocene peatland. Earth and Planetary Science Letters, 253(3), 445-454.

Castelltort, S., and Van Den Driessche, J., 2003, How plausible are high-frequency sediment supply-driven cycles in the stratigraphic record?: Sedimentary Geology, v. 157, p. 3–13, doi: 10.1016/S0037-0738(03)00066-6.

Cavagnetto, C., 2002. La palynoflore du Bassin d'As Pontes en Galice dans le Nord Ouest de l'Espagne á la limite Rupélien-Chattien (Oligocéne): Palaeontographica Abteilung B, p. 161-204.

Corenblit, D., Baas, A.C.W., Bornette, G., Darrozes, J., Delmotte, S., Francis, R. a., Gurnell, A.M., Julien, F., Naiman, R.J., and Steiger, J., 2011, Feedbacks between geomorphology and biota controlling Earth surface processes and landforms: A review of foundation concepts and current understandings: Earth-Science Reviews, v. 106, no. 3-4, p. 307–331, doi: 10.1016/j.earscirev.2011.03.002.

Ferrús, B., 1998, Análisis de cuenca y relaciones tectónica-sedimentación en la cuenca de As Pontes (Galícia): PhD thesis, Universitat of Barcelona, 351 p.

294 Gradstein, F.M., Ogg, J.G., Schmitz, M., Ogg, G., 2012, The Geologic Time Scale 2012 2-Volume Set:
295 Amsterdam, Elsevier.

296 Herbert, T. D., 1994, Reading orbital signals distorted by sedimentation: models and examples, in de
297 Boer, P. L., and Smith, D. G., editors, Orbital Forcing and Cyclic Sequences: Oxford, Blackwell Scientific
298 Publications, International Association of Sedimentologists, Special Publication 19, p. 483–507.

299 Hilgen, F.J., Hinnov, L. a., Abdul Aziz, H., Abels, H. a., Batenburg, S., Bosmans, J.H.C., de Boer, B., Husing,
300 S.K., Kuiper, K.F., Lourens, L.J., Rivera, T., Tuenter, E., Van de Wal, R.S.W., Wotzlaw, J.-F., et al., 2014,
301 Stratigraphic continuity and fragmentary sedimentation: the success of cyclostratigraphy as part of
302 integrated stratigraphy: Geological Society, London, Special Publications, doi: 10.1144/SP404.12.

303 Huerta, Á., Parés, J. M., Cabrera, L., Ferrús i Pinyol, B., & Sáez, A. (1997). Magnetocronología de las
304 sucesiones cenozoicas de la cuenca de As Pontes (La Coruña, Noroeste de España). Acta geológica
305 hispánica, 32(3-4), 127-145.

306 Kashiwaya, K., Ochiai, S., Sakai, H., and Kawai, T., 2001, Orbit-related long-term climate cycles revealed
307 in a 12-Myr continental record from Lake Baikal: Nature, v. 410, no. 6824, p. 71–74.

308 Large, D.J., Jones, T.F., Briggs, J., Macquaker, J.H.S., and Spiro, B.F., 2004, Orbital tuning and correlation
309 of 1.7 m.y. of continuous carbon storage in an early Miocene peatland: Geology, v. 32, no. 10, p. 873–
310 876, doi: 10.1130/G20824.1.

311 Large, D.J., Jones, T.F., Somerfield, C., Gorringe, M.C., Spiro, B., Macquaker, J.H.S., and Atkin, B.P., 2003,
312 High-resolution terrestrial record of orbital climate forcing in coal: Geology, v. 31, no. 4, p. 303, doi:
313 10.1130/0091-7613(2003)031<0303:HRTROO>2.0.CO;2.

314 Laskar, J., Robutel, P., Joutel, F., Gastineau, M., Correia, A.C.M., and Levrard, B., 2004, A long-term
315 numerical solution for the insolation: Astronomy & Astrophysics, v. 285, p. 261–285, doi: 10.1051/0004-
316 6361.

317 Laskar, J., Fienga, A., Gastineau, M., & Manche, H. (2011). La2010: a new orbital solution for the long-
318 term motion of the Earth. Astronomy & Astrophysics, 532, A89.

López-Martínez, N., Fernandez Marrón, T., Peláez-Campomanes, P., and De la Peña Zarzuelo, A., 1993: Revista Sociedad Geologica España, v. 6, p. 16–28.

Machlus, M.L., Olsen, P.E., Christie-Blick, N., and Hemming, S.R., 2008, Spectral analysis of the lower Eocene Wilkins Peak Member, Green River Formation, Wyoming: Support for Milankovitch cyclicity: Earth and Planetary Science Letters, v. 268, no. 1-2, p. 64–75, doi: 10.1016/j.epsl.2007.12.024.

Meyers, S. R., Sageman, B. B., & Pagani, M. (2008). Resolving Milankovitch: Consideration of signal and noise. American Journal of Science, 308(6), 770-786.

Miall, A. D., 2014, Fluvial Depositional Systems: New York, Springer, doi: 10.1007/978-3-319-00666-6

Olsen, P.E., and Kent, D. V., 1999, Long-period Milankovitch cycles from the Late Triassic and Early Jurassic of eastern North America and their implications for the calibration of the Early Mesozoic time-scale and the long-term behaviour of the planets: Philosophical Transactions of the Royal Society A: Mathematical, Physical and Engineering Sciences, v. 357, no. 1757, p. 1761–1786, doi: 10.1098/rsta.1999.0400.

Paillard, D., Labeyrie, L., Yiou, P., 1996. Macintosh program performs time-series analysis. Eos, Transactions American Geophysical Union, v.77, p.379

Sáez, A., and Cabrera, L., 2002, Sedimentological and palaeohydrological responses to tectonics and climate in a small, closed, lacustrine system: Oligocene As Pontes Basin (Spain): Sedimentology, v. 49, p. 1073–1094, doi: 10.1046/j.1365-3091.2002.00490.x.

Sáez, A., Inglès, M., Cabrera, L., and de las Heras, A., 2003, Tectonic-palaeoenvironmental forcing of clay-mineral assemblages in nonmarine settings: The Oligocene-Miocene As Pontes Basin (Spain): Sedimentary Geology, v. 159, p. 305–324, doi: 10.1016/S0037-0738(02)00333-0.

Santanach, P., Ferrús, B., Cabrera, L., and Sáez, A., 2005, Origin of a restraining bend in an evolving strike-slip system: The Cenozoic As Pontes basin (NW Spain): Geologica Acta, v. 3, p. 225–239.

Shanley, K.W., McCabe, P.J., 1994, Perspectives on the sequence stratigraphy of continental strata: American Association Petroleum Geologists Bulletin, v.78, p. 544–568

344 Schulz, M., and Mudelsee, M., 2002, REDFIT: estimating red-noise spectra directly from unevenly spaced
345 paleoclimatic time series: Computers & Geosciences, v. 28, no. 3, p. 421–426, doi: 10.1016/S0098-
346 3004(01)00044-9.

347 Valero, L., Garcés, M., Cabrera, L., Costa, E., and Sáez, A., 2014, 20 Myr of eccentricity paced lacustrine
348 cycles in the Cenozoic Ebro Basin: Earth and Planetary Science Letters, v. 408, p. 183–193, doi:
349 10.1016/j.epsl.2014.10.007.

350 Valero, L., Huerta, P., Garcés, M., Armenteros, I., Beamud, E., & Gómez-Paccard, M. (2015). Linking
351 sedimentation rates and large-scale architecture for facies prediction in nonmarine basins (Paleogene,
352 Almazán Basin, Spain). Basin Research. doi: 10.1111/bre.12145

353 van Vugt, N., Langereis, C.G., and Hilgen, F.J., 2001, Orbital forcing in Pliocene–Pleistocene
354 Mediterranean lacustrine deposits: dominant expression of eccentricity versus precession:
355 Palaeogeography, Palaeoclimatology, Palaeoecology, v. 172, no. 3-4, p. 193–205, doi: 10.1016/S0031-
356 0182(01)00270-X.

357 Van Vugt, N., Steenbrink, J., Langereis, C.G., Hilgen, F.J., and Meulenkamp, J.E., 1998,
358 Magnetostratigraphy-based astronomical tuning of the early Pliocene lacustrine sediments of Ptolemais
359 (NW Greece) and bed-to-bed correlation with the marine record: Earth and Planetary Science Letters, v.
360 164, no. 3-4, p. 535–551, doi: 10.1016/S0012-821X(98)00236-2.

361 Whipple, K.X., 2001, Fluvial landscape response time: How plausible is steady-state denudation?
362 American Journal of Science, v. 301, no. May, p. 313–325, doi: 10.2475/ajs.301.4-5.313.

363 Zachos, J.C., Shackleton, N.,J., Revenaugh, J.S., Pälike, H.,, Flower, B.P., 2001, Climate response to orbital
364 forcing across the Oligocene-Miocene boundary: Science, 292, 274-278.

365 Zeeden, C., S. R. Meyers, L. J. Lourens, and F. J. Hilgen (2015), Testing astronomically tuned age models,
366 Paleoceanography, 30, 369–383, doi:10.1002/2014PA002762.

367

368

Figure Captions
Click here to download Figure: EPSL_figure captions.docx

Figure 1. Location map of the As Pontes Basin, NW Spain. The map shows the principal structures and the locations of the bore holes and West Section.

Figure 2. Synthetic sedimentary facies model of the As Pontes Basin. Most of the terrigenous fraction was delivered from the North. Axial alluvial contributions became significant after the MSU deposition (see fig. 3). In the distal and restricted areas deposition of fines or coals occurred. The effects of the vegetation cover likely played an important role in the sedimentation dynamics of the basin. The main facies are indicated in numbers. The details of the facies distribution are further explained in Table 1.

Figure 3. A synthetic stratigraphic log of the basin (left) and stratigraphic record (right) in the western sub-basin combined with the magnetostratigraphic data is shown. A new magnetostratigraphic age model was built after revising the former study of Huerta et al. (1997). Marked changes occur in the lower part of their section, around chron C10n. The new correlation provides reliable sedimentation rates and is consistent with the *Issiodoromys minor* constraints.

Figure 4. Phase relationship determination. At the left the local magnetostratigraphy and the lithological log is shown. In the middle left, the facies record of Core MP208 is shown in the stratigraphic domain with the Gaussian band-pass filtered component in red superimposed (freq: 0.0827 cycles/m; bandwidth: 0.05). In the middle right, the borehole facies data of MP208 are shown in the time domain, using the magnetostratigraphic age model for conversion. Again the Gaussian band-pass filtered component of the 405-kyr cycle is shown. At the right, the eccentricity target curve (Laskar et al., 2004) is shown together with the filtered component isolating the 405-kyr eccentricity term. Red lines represent correlation lines that match maxima of the core data in the stratigraphic domain and maxima of the core data in the time domain, which are associated with clastic sediments, with successive 405-kyr eccentricity maxima. This is the unique correlation supported by the magnetochronologic age constraints.

Figure 5. The six cores used for the cyclostratigraphic analysis are shown from left to right. The facies variability is shown per core as thin black lines below the core headings. The lithology and polarity data is adapted from Huerta et al. (1997). Superimposed on these lines, the red curves mark the bandpass-filtered component centred at 12.07 m, with a bandwidth of 0.05 m^{-1}. The shifts from proximal to distal facies are correlated between all the cores, and finally to the West section. By means of magnetostratigraphy and the biochronological constraints, the West section is correlated to the GPTS of Gradstein et al. (2012). Horizontal (dashed) black lines indicate clastic pulses, which following the magnetostratigraphic age constraints are correlated to successive 405-kyr eccentricity maxima (Laskar et al., 2004). Horizontal grey shading indicates the extension of the distal facies from the cores to the West section. These coal-bearing seams are correlated to 405-kyr eccentricity minima. Bluish shading marks the stratigraphic intervals of the coal pits used with industrial purposes. These intervals correspond to 405-kyr eccentricity minima, within 2.4-Myr eccentricity minima.

Figure 6. Detail of the spectral analysis (using the REDFIT software) in the age domain for the interval underlying the Middle Sandstone Unit after applying a tuning based to the 405-kyr eccentricity cycle. Following the astronomical age model, the spectral analyses reveal significant peaks in the 100-kyr eccentricity frequency band, thus providing independent

evidence of a climatic forcing at a 405-kyr scale from the magnetostratigraphic age model. The high variability in sedimentation rates together with the intrinsic changes at a short eccentricity scale and below may account for a blurring of these cycles in some cores as MP222.

Figure 1_Location
Click here to download Figure: Fig_1_location.pdf

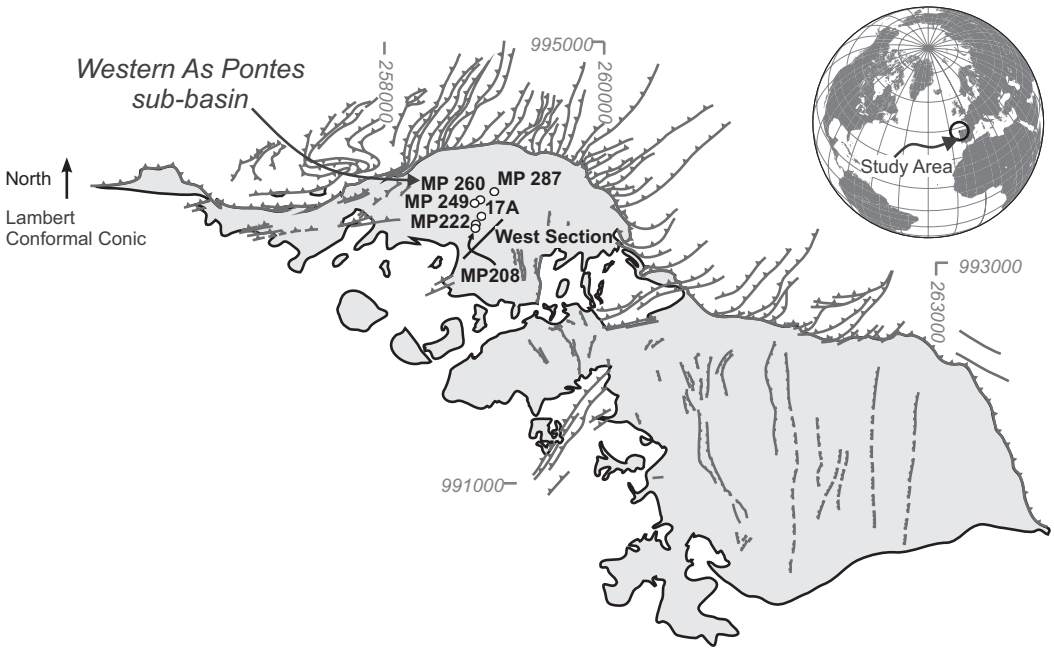

Figure 2_depos_model
Click here to download Figure: Fig_2_dep_model.pdf

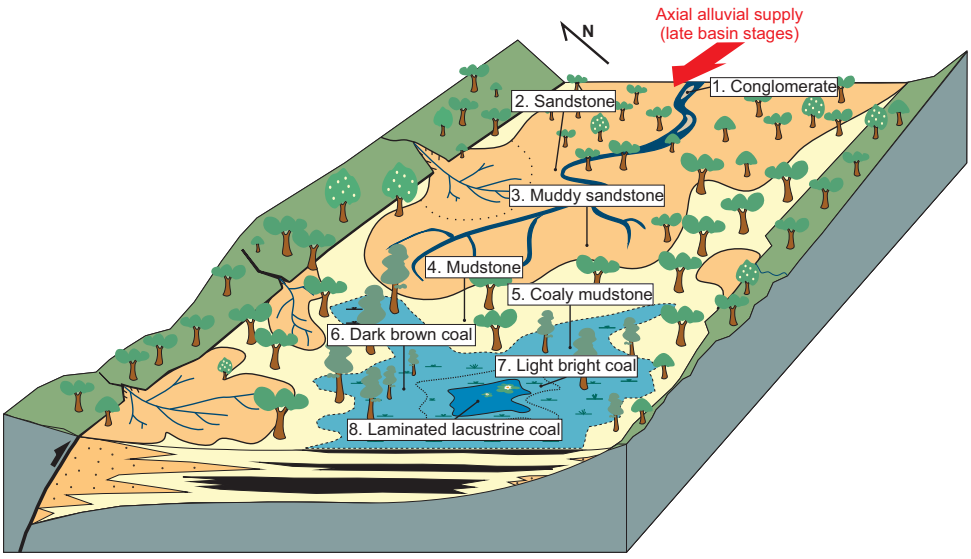

Figure 3_magnetostrat
Click here to download Figure: Fig_3_magneto.pdf

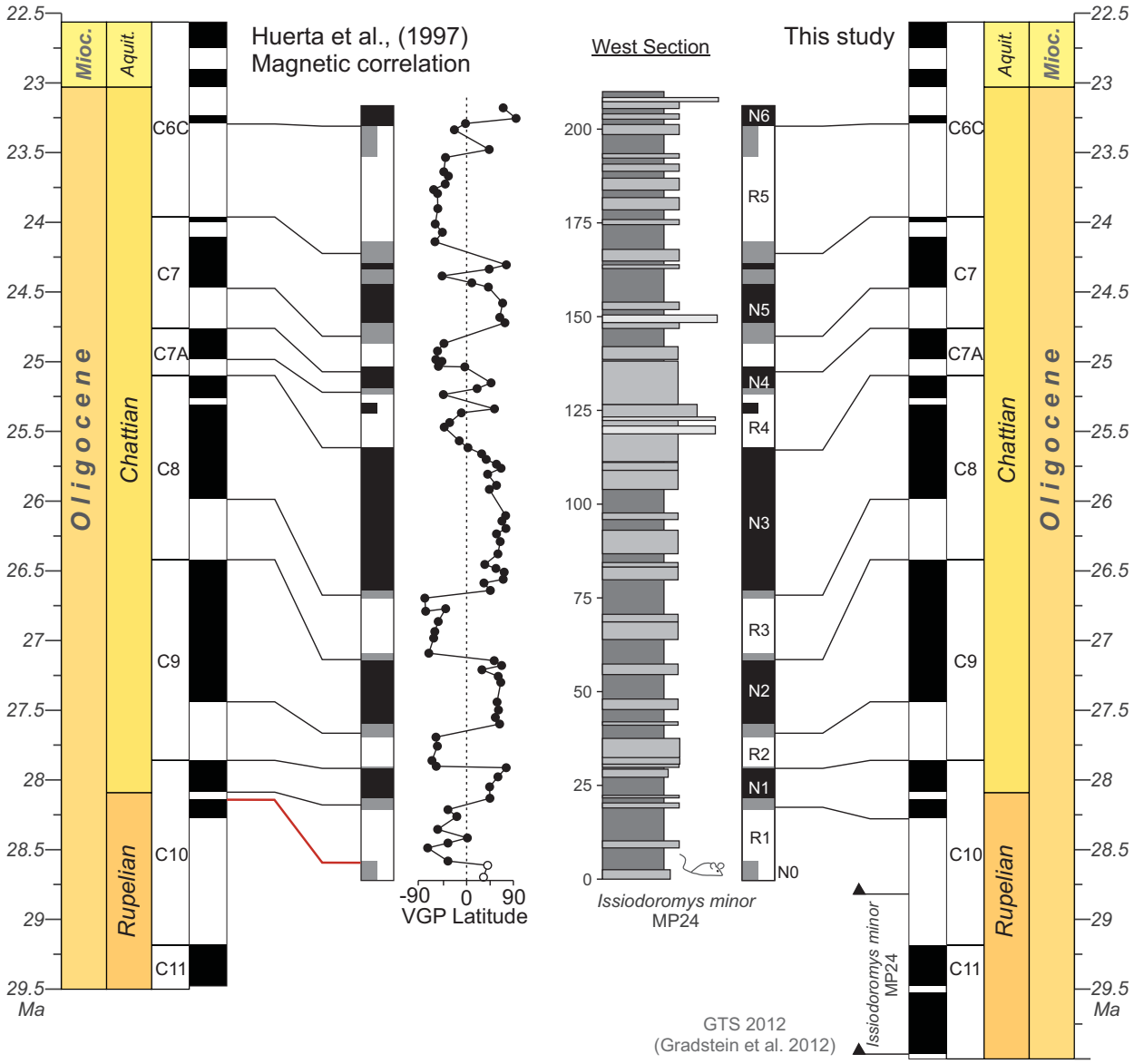

Figure 4_phase_relation

Click here to download Figure: Fig_4_phase relationship 405.pdf

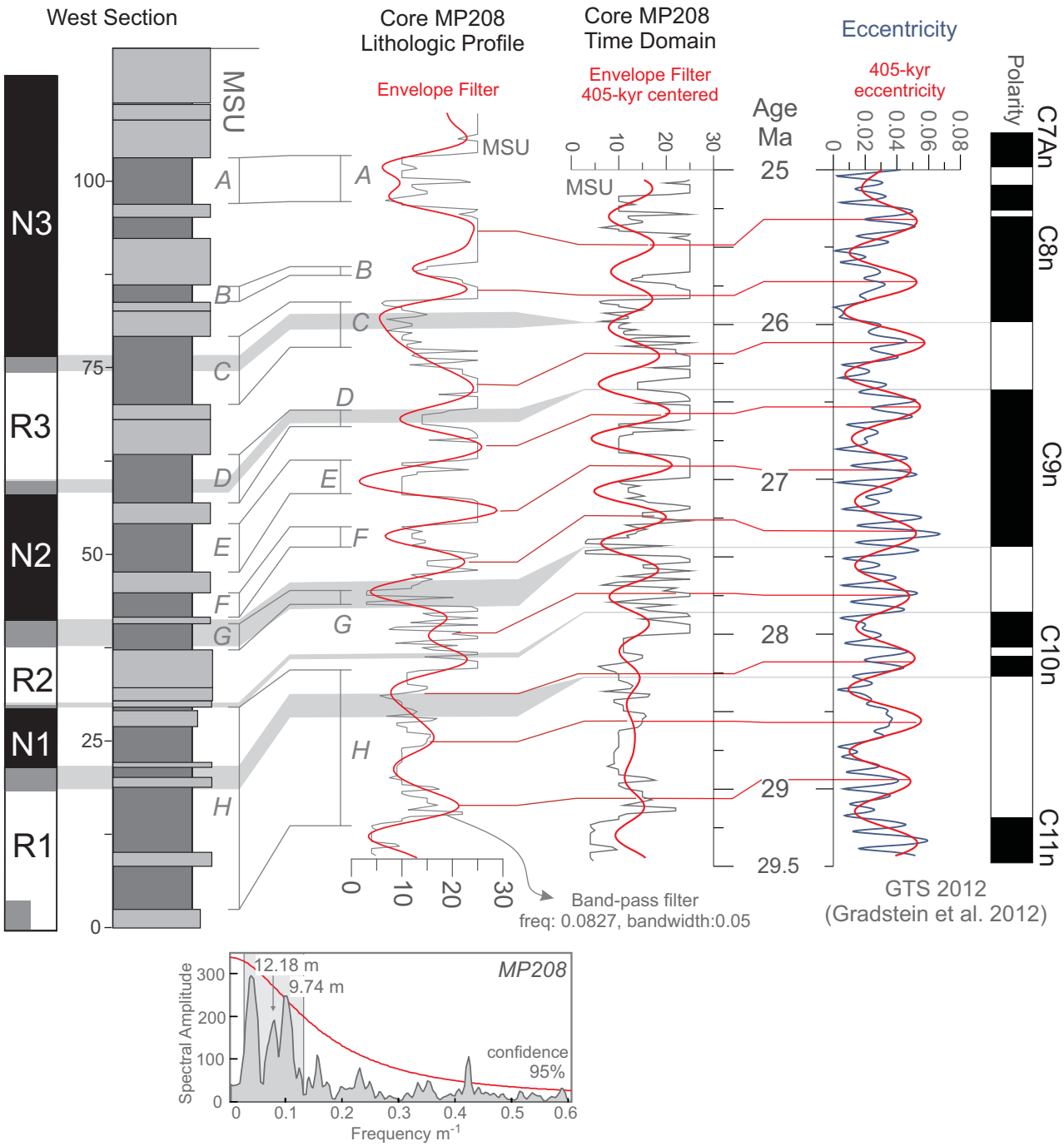

Figure 5_astrochrono

Click here to download Figure: Fig_5_correlation.pdf

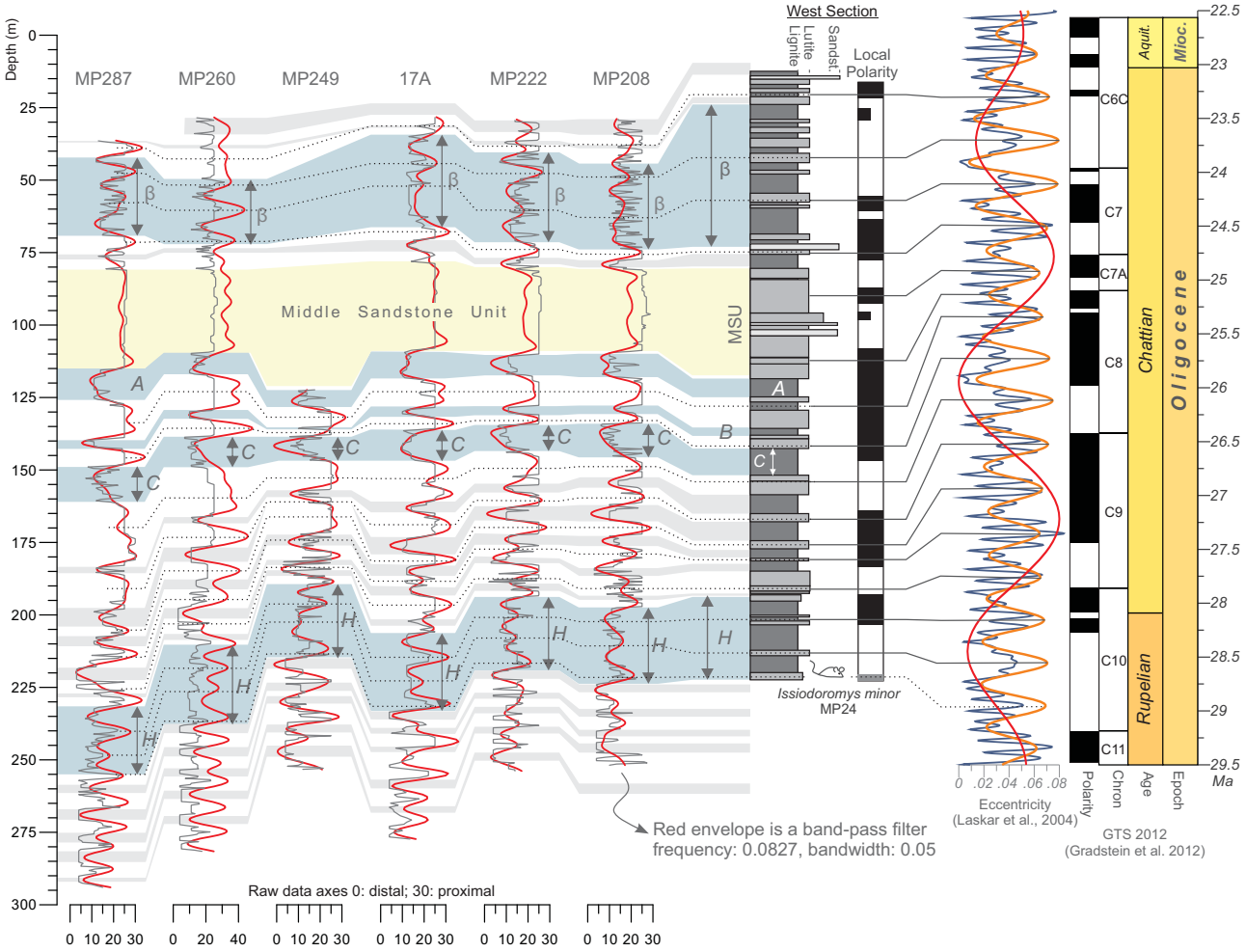

Figure 6_spectra

Click here to download Figure: Fig_6_ det_100ka.pdf

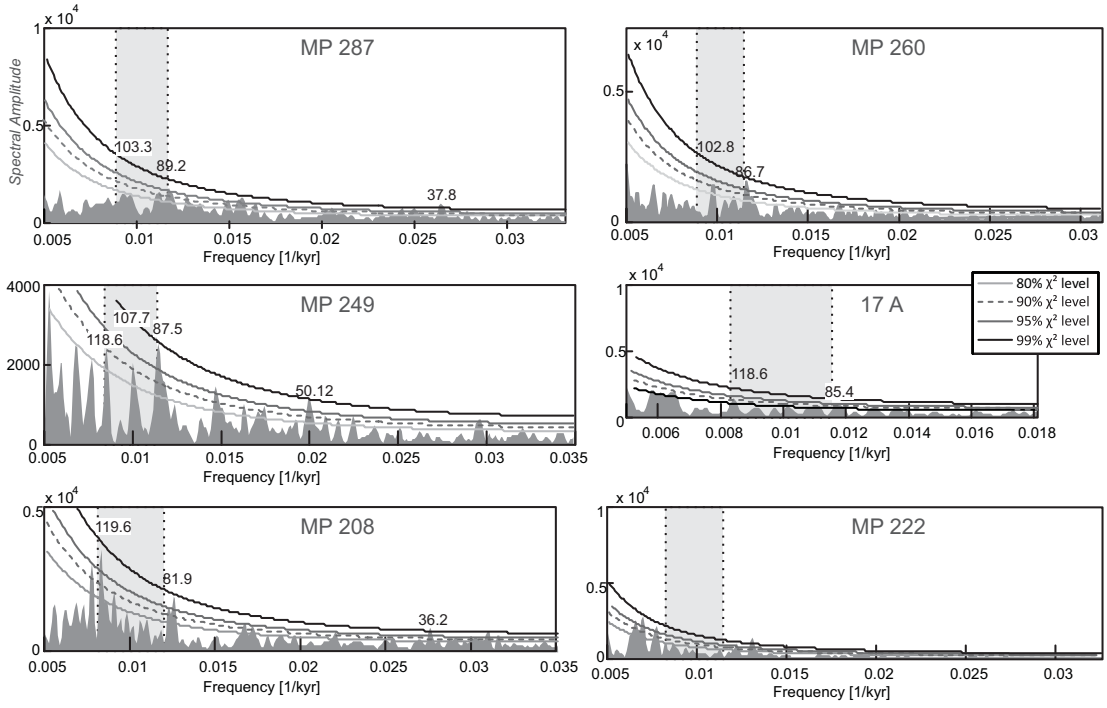

Table 1_facies rank

Click here to download Table: Table 1_Facies_rank.xlsx

Core description	Lithology	Location Fig. 2	Rank value
LAM	Laminites	8	1
LCTO	laminated lacustrine Lignite	8	2
ALC	laminated coaly lacustrine Mudstone	8	3
ALV	Green laminated Mudstone	8	4
MACICL	Green marls	8	5
PP	Light bright coal	7	6
PP..a	Light bright coal with very low mud content	7	6
PP.a	Light bright coal with low mud content	7	7
PP'a	Mud bearing Light bright coal	7	8
PPa	Muddy Light bright coal	7	9
L	Dark brown coal	6	10
L..a	Dark brown coal with very low mud	6	11
L.a	Dark brown coal with low mud content	6	12
L'a	Dark brown coal with mud	6	13
La	Muddy dark brown coal	6	14
LX	Xyloid Lignite	6	15
LX..a	Xyloid Lignite with very low mud	6	16
LX.a	Xyloid Lignite with low mud	6	17
LX'a	Xyloid Lignite with mud	6	18
LXa	Muddy Xyloid Lignite	6	19
L+A	Mudstones and Lignites	6	20
Ac	Coaly Mudstone	5	21
A'c	Mudstone with coal	5	22
A.c	Mudstone with low coal content	5	23
A..c	Mudstone with very low lignite content	5	24
A	Mudstone	4	25
A..ar	Mudstone with very low sand	3	26
A.ar	Mudstone with low sand	3	27
A'ar	Sandy Mudstone	3	28
Aar	Sandy Mudstone	3	29
S	Silt	3	30
AR'a	Sandstone with abundant mud	2	31
ANa	Muddy sandstone	2	32
AN.a	Sandstone with low mud content	2	33
AR..a	Sandstone with very low mud content	2	34
AN	Sandstone	2	35
AR'q	Quarzitic Sandstone	2	35
GRar	Sandy gravel	1	36
GRa	Muddy gravel	1	36
GR	Gravel	1	36
CG	Conglomerate	1	36
Q	Quartzite	0	x
P	Hercynian basement	0	x

CURRÍCULUM VITAE

LUIS VALERO MONTESA

Departament d'Estratigrafia, Paleontologia i Geociencies Marines
Facultat de Geologia. Universitat de Barcelona
Marti i Franques s/n, 08028, Barcelona, Spain
luisvalero@ub.edu

1. AREA PROFESIONAL Y DE INVESTIGACIÓN

1.1. Formación Académica

2010-2015 (previsto) Doctorado en Ciencias de la Tierra. Universitat de Barcelona
Supervisores: Dr. Miguel Garcés, Dr. Lluís Cabrera

2009-2010. Máster en Geologia. Universitat de Barcelona
Esp. Reservorios Sedimentarios.
Trabajo Final de Máster Matricula de Honor
Supervisores: Dr. Miguel Garcés, Dr. Lluís Cabrera

2002-2008. Licenciatura en Geologia. Universitat de Barcelona
Trabajo Final de Carrera Sobresaliente.
Supervisores: Dr. Miguel Garcés, Dr. Miguel Lopez-Blanco

1.2. Becas y Ayudas a la Investigación

2011–2014. Ajut al Personal Investigador en Formació. APIF-UB

2013. Beca de Movilidad. «European Science Foundation» ESF-EarthTime (EU)

2012. Beca de Movilidad para Estancias Internacionales. Programa APIF-UB. Universitat de Barcelona

2012. Beca de Movilidad. «National Science Foundation». NSF (USA)

1.3. Actividades Profesionales

Abril 2008. Análisis Paleomagnetico de muestras. Laboratori de Paleomagnetisme. «Institut de Ciències de la Terra Jaume Almera» (UB-CSIC).

2007-2008. Practicas en Empresa. Elaboración de bases de dades. «Institut Geològic de Catalunya».

1.4. Especialización de la Investigación. Códigos UNESCO

250601 Geología Regional. 250619 Estratigrafía. 250618. Sedimentología. 250704. Paleomagnetismo.

2.1. Participación en proyectos I+D+I Financiados en Convocatorias Públicas.

2011-2013. «Control climático (orbital) en medios sedimentarios continentales marinos y someros» Investigador Principal Miguel Garcés.

2.2. Publicaciones y Resultados Científicos.

2.2.1 Articulos Indexados en Journal Citation Index

Valero, L., Huerta, P., Garcés, M., Armenteros, I., Beamud, E., & Gómez-Paccard, M. (2015). Linking sedimentation rates and large-scale architecture for facies prediction in nonmarine basins (Paleogene, Almazán Basin, Spain). Basin Research. **Impact factor (2014): 2.732**

Valero, L., Garcés, M., Cabrera, L., Costa, E., & Sáez, A. (2014). 20-Myr of eccentricity paced lacustrine cycles in the Cenozoic Ebro Basin. Earth and Planetary Science Letters, 408, 183-193. **Impact Factor (2014): 4.734**

2.2.2 Libros o capítulos de libros.

Armenteros, I., Huerta, P., Muñoz, A., Garcés, M., Blanco, J.A., Valero, L., Corrochano, D., 2014. Transiciones fluvio-lacustres en el Neógeno de la Cuenca de Almazán: sedimentología y análisis secuencial. Edited by Idelfonso Armenteros. Sociedad Geológica de España. ISBN: 978-84-697-1189-7

Cabrera, L., Arbués, P., Cuevas, J.L., Garcés, M., López-Blanco, M., Marzo, M., Valero, L., 2011: Integrated analysis of the depositional fill in evolving -marine to continental- forelands: Advances in the eastern Ebro basin (Eocene-Early Miocene, NE Spain). Geoguías, vol 7, p 151-198. Soc. Geológica de España.

2.2.3. Presentaciones en congresos o conferencias.

Huerta, P., Valero, L., Garcés M., Armenteros I., Beamud E., Gómez-Paccard M., 2015. Sedimentation rates and large-scale fluvial architecture. Deciphering the basin external controls. 31th IAS Meeting of Sedimentology, 22nd-25th June 2015. Krakow (Poland).

Gibert, L., Brachert T., Bruch, A.A., Cruset, D., García Veigas, J., Giralt, S., Ibañez, J., Mertz, D., Scott, G., Valero, L., Vogel, H., Weber, M.E., 2015: Early Pleistocene climatic record from Paleo-lake Baza: implications for initial human dispersal into Europe. 6th International Limnology Congress, ILIC 2015, Reno (USA)

Povea de Castro, P., Cacho, I., Moreno, A., Pena, L., Valero, L., 2014. Major atmospheric changes in the tropical region during the Early Pleistocene (1.9 Ma) and oceanographic implications in Eastern Equatorial Pacific. UISPP congress, 1-7 Sept, 2014, Burgos (Spain).

Garcés, M., López-Blanco, M., Valero, L., Beamud, E., Pueyo-Morer, E., & Rodríguez-Pinto, A. (2014, May). Testing orbital forcing in the Eocene deltaic sequences of the South-Pyrenean Foreland Basins. In EGU General Assembly Conference Abstracts (Vol. 16, p. 10681).

Valero, L., Huerta, P., Garcés, M., Beamud, E., Gómez-Paccard, M., Armenteros, I., 2012: A Magnetostratigraphy for the Cenozoic record of the Almazán basin, Spain. VIII Congreso Geológico de España, Oviedo, (Spain), July 17th-19th., Geotemas 13, p89-92.

Valero, L., Garcés, M., Cabrera, L., 2012: Long-to-short term Milankovitch Forcing in a Foreland Basin: The Los Monegros lake system of the Ebro basin (late Oligocene-Miocene). AGU Fall meeting, 3rd–7th December, San Francisco CA (USA) GP13B-1119.

Valero, L., Garcés, M., Cabrera, L., 2011: Low frequency (2,4-Myr & 400-kyr) orbital control in a foreland basin (Ebro basin, Late Oligocene-Early Miocene). 28th IAS Meeting (International Association of Sedimentologists), 5th-8th July.

Valero, L., Garcés, M., Cabrera, L., 2010: Control orbital en secuencias lacustres oligoceno superior-miocenas en el sector central de la Cuenca del Ebro. MagIber VI, Puigcerdà (Spain), September 23th -26th

---

2.3. Experiencia Docente

2014-2015. Cartografia. Grau de Geologia, Universitat de Barcelona.16 hores.

2013-2014**.** Laboratori Estratigrafia 18 hores. Basin Analysis, Màster de Reservoris Sedimentaris, Universitat de Barcelona. 8 hores

2012-2013. Estratigrafia Grau de Geologia 2 hores. Laboratori Estratigrafia Grau de Geologia 2 hores. Estratigrafia Enginyeria Geològica 32 hores. Basin Analysis, Màster de Reservoris Sedimentaris, Universitat de Barcelona. 8 hores.

2011-2012. Cartografia, Grau de Geologia 16 hores. Basin Analysis, Màster de Reservoris Sedimentaris, Universitat de Barcelona, 16 hores.

2010-2011. Geologia, Llicenciatura de Ciències Ambientals 16 hores. Basin Analysis, Màster de Reservoris Sedimentaris, Universitat de Barcelona 16 hores.

Fotografia de Ariadna Salabarnada